Performance of a symmetrical converging-diverging tube differential pressure flow meter

by

LUC MWAMBA ILUNGA

BEng: Mining Engineering (University of Lubumbashi)

Thesis submitted in fulfilment of the requirements for the degree

Master of Technology: Civil Engineering

in the Faculty of Engineering

at the CAPE PENINSULA UNIVERSITY OF TECHNOLOGY

Supervisor: Prof. VG Fester

Cape Town

February 2014

CPUT Copyright Information

The thesis may not be published either in part (in scholarly, scientific or technical journals), or as whole (as a monograph), unless permission has been obtained from the university.

ABSTRACT

The current problems of orifice, nozzle and Venturi flow meters are that they are limited to turbulent flow and the permanent pressure drop produced in the pipeline. To improve these inadequacies, converging-diverging (C-D) tubes were manufactured, consisting of symmetrical converging and diverging cones, where the throat is the annular section between the two cones, with various angles and diameter ratios to improve the permanent pressure loss and flow measurement range.

The objective of this study was firstly to evaluate the permanent pressure loss, secondly to determine the discharge coefficient values for various C-D tubes and compare them with the existing differential pressure flow meter using Newtonian and non-Newtonian fluids, and finally to assess the performance of these differential pressure flow meters.

The tests were conducted on the multipurpose test rig in the slurry laboratory at the Cape Peninsula University of Technology. Newtonian and non-Newtonian fluids were used to conduct experiments in five different C-D tube flow meters with diameter ratios (β) of 0.5, 0.6 and 0.7, and with angles of the wall to the axis of the tube (θ) of 15°, 30° and 45°.

The results for each test are presented firstly in the form of static pressure at different flow rates. It was observed that the permanent pressure loss decreases with the flow rate and the length of the C-D tube. Secondly, the results are presented in terms of discharge coefficient versus Reynolds number. It was found that the C_d values at 15° drop earlier than at 30° and 45°; when viscous forces become predominant, the C_d increases with increasing beta ratio. The C_d was found to be independent of the Reynolds number for Re>2000 and also a function of angle and beta ratio.

Finally, the error analyses of discharge coefficients were assessed to determine the performance criteria. The standard variation was found to increase when the Reynolds number decreases. The average discharge coefficient values and their uncertainties were determined to select the most promising C-D tube geometry. An average C_d of 0.96, with an uncertainty of ±0.5 % for a range of Reynolds numbers greater than 2,000 was found.

The comparison between C-D tubes 0.6(15-15) and classical Venturi flow meters reveals that C-D 0.6(15-15) performs well in turbulent range and shows only a slight inaccuracy in laminar.

This thesis provides a simple geometrical differential pressure flow meter with a constant C_d value over a Reynolds number range of 2000 to 150 000.

DECLARATION

I, Luc Mwamba Ilunga, hereby declare that the content of this thesis represents my own unaided work, and that the thesis has not previously been submitted for academic examination towards any qualification. Furthermore, it represents my own opinions and not necessarily those of the Cape Peninsula University of Technology.

Signed

Dated this day of 2014

DEDICATION

To God Almighty, for always aligning my paths and being there for me even when I doubted myself.

To my father, Mr Sebatien Ilunga, for being a pillar of strength and support, and my joy, inspiration, and source of wisdom and encouragement through the many trials that I faced.

To my dearest mother, Mrs Georgette Ilunga, for supporting me spiritually, emotionally and for always struggling and sacrificing to make sure I am where I am today.

To my brothers, sisters and nephews, whom I love very dearly, thank you for being a blessing to me and may God grant you the desires of your heart.

To my friends, colleagues and family: thank you for being supportive.

ACKNOWLEDGEMENTS

- Prof Veruscha Fester – for her supervision, encouragement and continuous support throughout the course of this project.
- Aime Kabwe – for supporting me and challenging my thinking.
- Butteur Mulumba – for some interesting conversations on this project.
- MR Chowdhury – for his motivation.
- Richard du Toit – for his splendid laboratory supervisor role.
- The Flow Process and Rheology Centre staff and students for their continuous support in completing this project.
- The Cape Peninsula University of Technology and the Research Directorate – for the opportunity granted to further my studies at the institution.
- The National Research Foundation (NRF) – for financial support of the research.

TABLE OF CONTENTS

Experimental Work

LIST OF FIGURES

LIST OF TABLES

LIST OF APPENDICES

NOMENCLATURE

SYMBOL	DESCRIPTION	UNIT
A	Cross-section area of the pipe	m^2
D	Pipe diameter	mm
d	Throat diameter	mm
G	Gravitational acceleration	m/s^2
K	Fluid consistency coefficient	$Pa.s^n$
k	Pipe roughness	-
n	Flow behaviour index	-
P	Static pressure	Pa
Q	Volumetric flow rate	m^3/s
R	Plug radius	m
R	Pipe radius	m
Re	Reynolds number	-
Re_3	Slatter Reynolds number	-
Re_{M-R}	Metzner-Reed Reynolds number	-
U	Uncertainty	-
V	Mean velocity	m/s
V_{ann}	Annulus velocity	m/s
DP	Differential pressure	
ΔP_t	Traditional DP	Pa
ΔP_R	Recovered DP	Pa
ΔP_{PPL}	Permanent pressure loss	Pa
X	Experimental quantity	
$\overline{X}$	Mean value	
T	Theoretical quantity	

GREEK SYMBOLS

SYMBOL	DESCRIPTION	UNIT
P	Density	kg/m^3
B	Diameter ratio	
μ	Dynamic viscosity of the fluid	Pa.s
$\dot{\gamma}$	Shear rate	s^{-1}
f	Friction factor	-
T	Shear stress	Pa
τ_y	Yield stress	Pa
Θ	Angle of walls to the axis of an axisymmetric duct	°
Σ	Variance	

SUBSCRIPT

1	Upstream point of measurement
T	Throat point of measurement
B	Bingham
HB	Herschel-Bulkley
∞	Infinite
M-R	Metzner-Reed
VC	*Vena contracta*
Ann	Annulus
Max	Maximum
Min	Minimum

Introduction

1.1 Introduction

Over the past six decades, the importance of flow measurement in industry has grown, not just because of its widespread use, but also because of its applications in manufacturing processes. Over the years, performance requirements have become more stringent, with relentless pressure for improved reliability, accuracy, repeatability and range (Crabtree, 2009). Unless very high accuracy is required, or unless the application makes a non-intrusive device essential, differential pressure should be considered. Despite the predictions of its demise, there is little doubt that the differential pressure flow meter will remain a common method of flow measurement for many years to come (Webster, 1999).

One of the major advantages of the orifice plate, Venturi tube, or nozzle is that the measurement uncertainty can be predicted without the need for calibration, if it is manufactured and installed in accordance with one of the international standards covering these devices. The main disadvantage of these devices is their limited range, the permanent pressure drop they produce in the pipeline (which can result in higher pumping costs), and their sensitivity to the installation effect (which can be minimised using straight lengths of pipe before and after the flow meter) (Webster, 1999).

1.2 Problem statement

The development of an accurate and reliable differential pressure flow meter is required for industry.

1.3 Aim and objectives

The aim of this study is to provide a simple geometrical differential pressure flow meter with lower uncertainty for a wide measurement application.

The objectives of this study are to:

- analyse the pressure fluctuation to determine permanent pressure loss;
- evaluate different average discharge coefficient values at different Reynolds numbers; and
- assess the performance criteria such repeatability and accuracy of the discharge coefficient calculated.

Test studies used Newtonian and non-Newtonian fluids across various C-D tubes of 15, 30 and 45° angles with diameter ratios of 0.5, 0.6 and 0.7.

1.4 Methodology

A converging-diverging tube (C-D tube) shown in Figure 1.1 was designed, machined and mounted in a 46mm internal diameter pipe on a test rig.

To determine pressure, recovery point pressure transducers were used to measure the static pressures along the C-D tube, at P_1, P_2, P_t, P_4 and P_d respectively, which are the point pressure at location of inlet, middle of the converging section, the throat, middle of the diverging section and the outlet. The fluid was pumped through the pipes using a positive displacement pump. Figure 1.1 shows the position of the pressure taps across the C-D tube with the length L and symmetric converging and diverging angle θ.

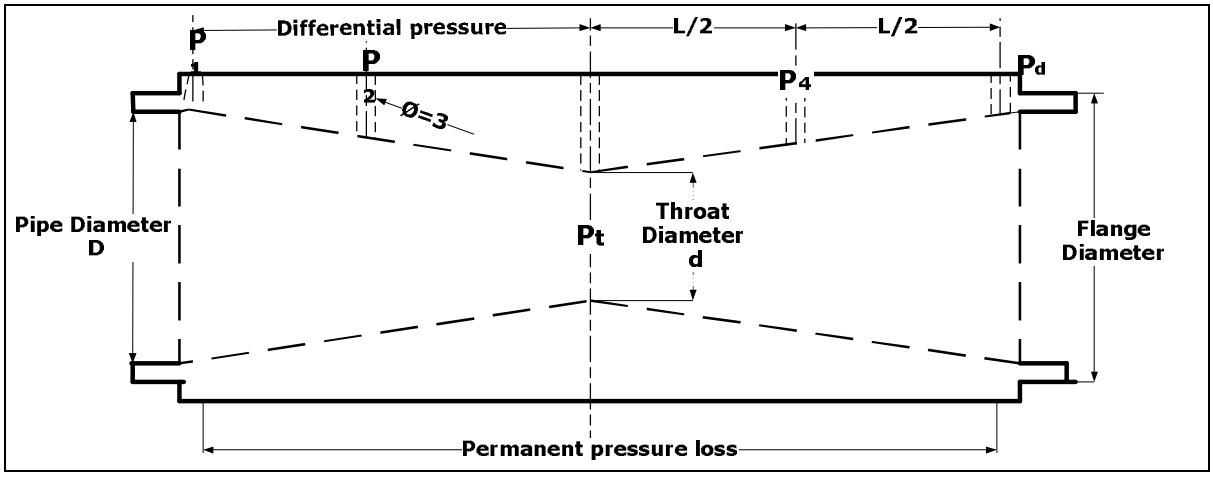

Figure 1.1: Schematic representation of C-D tube

The pressure drop for determining the discharge coefficient through a C-D tube was found with the arrangement of tap pressure in such a manner that the pressures sensed are indicative of the pressure 1D upstream of the upstream face C-D tube and the downstream at the lowest point of pressure which is the throat location.

1.5 Delineation of research

C-D tubes of diameter ratio $0.5 < \beta < 0.7$ have not been investigated. No other flow visualisation studies were conducted.

1.6 Significance of research

The purpose of this work is to provide a simple differential flow meter operating with an improved range of applications. The research will also contribute to an understanding of the effect of angle, diameter ratio and flow regime on permanent pressure loss, discharge coefficient and accuracy of the meter.

Literature Review

2.1 Introduction

This chapter provides the background information available in the literature on experimental and theoretical studies relevant to flow measurement.

Important concepts of flow measurement are presented. Because of the highly viscous character of the fluids used in this research, some rheological models are illustrated and the methods and procedures for characterisation of non-Newtonian fluids are presented.

2.2 Differential pressure flow meter (DP flow meter)

2.2.1 Definition

Differential pressure or head meters are used for measurement in completely filled pipes and include such primary devices as orifice plates, Venturi tubes, nozzles and a suitable differential pressure meter (Hite, 1950).

A differential pressure flow meter consists of two basic elements (Webster, 1999):

- An obstruction to cause a pressure drop in the flow is termed a "differential producer".
- A device for measuring the pressure drop across this obstruction is termed a "differential pressure transducer".

2.2.2 Principle of operation

In the 18th century, Bernoulli established the basic relationship between differential pressure and velocity head. Bernoulli's observation revealed that if an annular restriction is placed in a pipeline, then the velocity of the fluid through the restriction is increased. The increase in velocity at the restriction causes the static pressure to decrease at this section, and a pressure difference

is created across the element. The difference between the pressure upstream and pressure downstream of this obstruction is related to the rate of fluid flowing through the restriction and therefore through the pipe (Webster, 1999).

2.3 Permanent pressure loss

Meters such as differential pressure types have a pressure drop inside the meter section. The pressure measured upstream of the meter will be greater than the pressure just downstream of the meter. With movement downstream of the meter, the pressure recovers to a level not quite as high as the upstream pressure. The difference between the upstream pressure and downstream recovered pressure equals the permanent pressure loss (McCrometer, 1999)

2.3.1 Metering by permanent pressure loss

DP meters typically have equal inlet and exit cross-sectional areas. Therefore, as the fluid passes through the DP meter's primary element it flows first through a geometric constriction and then through a geometric expansion, thus producing a permanent pressure loss. Hence, every DP meter has imbedded within it three metering opportunities: a conventional converging geometry meter (using the traditional pressure, ΔP_t), an expanding geometry meter (using the recovered DP, ΔP_R), and a permanent pressure loss (using the permanent pressure loss, ΔP_{PPI}) (Steven, 2008).

The converging section is an effective device for converting pressure head to velocity head, while the diverging section converts velocity head to pressure head (Baylar et al., 2009)

A DP meter can be thought of as three flow meters in series in the same pipe location. As illustration, Figure 2.1 shows a sketch of a Venturi meter with DP transmitters to measure the three DPs of interest.

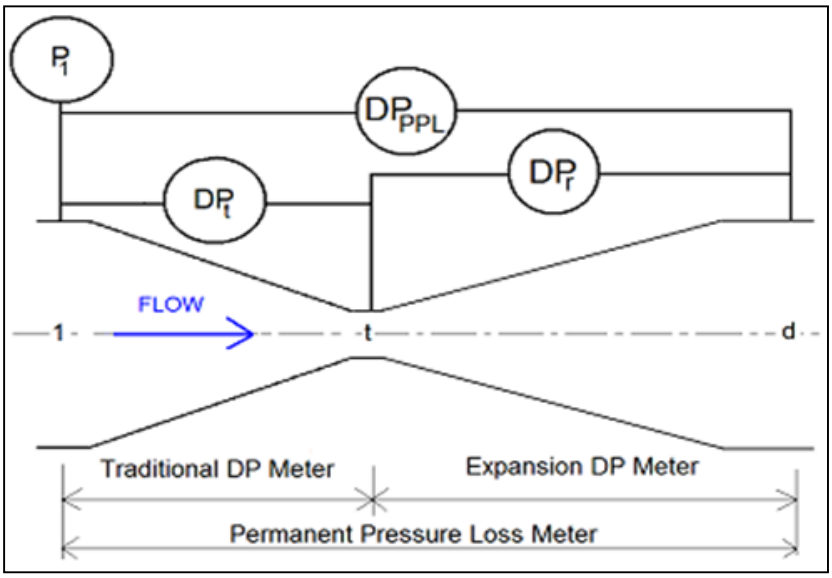

Figure 2.1: Venturi meter with 3 DP measurements

Figure 2.2 shows a sketch of the approximate pressure fluctuations through a DP meter (Steven, 2008), where P_1 , P_d and P_t are the inlet, downstream and throat pressure respectively.

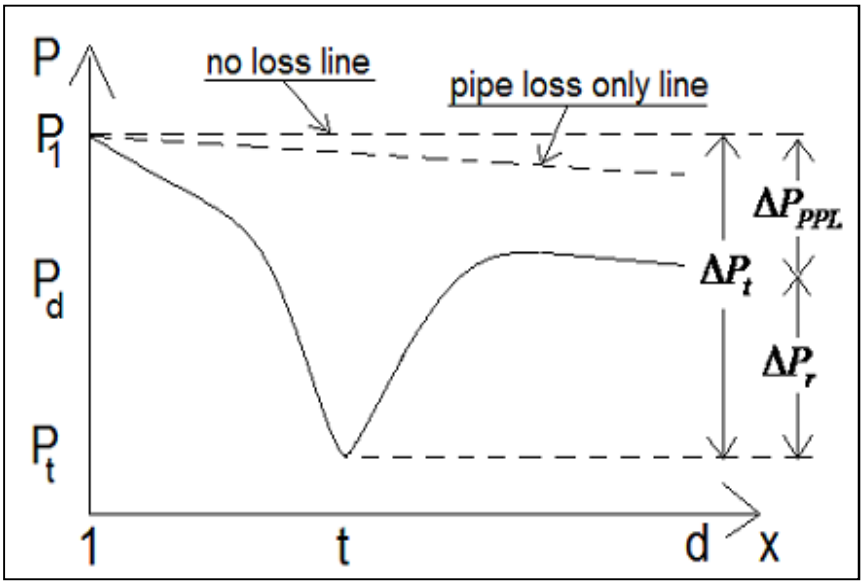

Figure 2.2: D.P meter pressure fluctuations

Figure 2.2 presents a fundamental DP meter rule that the sum of the "recovered" DP (the downstream to minimum area or "throat" DP) and PPL is the upstream to throat DP. This can be expressed as (Steven, 2008):

$$\Delta P_t = \Delta P_r + \Delta P_{PPL} \qquad \text{Equation 2.1}$$

$$\frac{\Delta P_r}{\Delta P_t} + \frac{\Delta P_{PPL}}{\Delta P_t} = 1 \qquad \text{Equation 2.2}$$

Measuring any two of these DPs allows the calculation of the third DP and therefore only two DP transmitters are required to have all three equations available. Naturally, with ΔP_t being the largest value, it is the easiest to measure accurately (Steven, 2008). The smaller value of ΔP_t and ΔP_{PPL} may have a higher measurement uncertainty. However, in the majority of applications, all three DPs are of a magnitude measurable to low uncertainty by standard DP transmitters (Steven, 2008).

According to Bertani et al. (2010), there are several flow tube designs that provide even better pressure recovery than the classical Venturi. The best known of these proprietary designs is the universal Venturi. The various flow tube designs vary in their contours, tap locations, generated Δp and unrecovered head loss. These flow tubes usually cost less than the classical and short-form Venturis, because of their short lay length.

2.3.2 Low permanent pressure loss

Much has been written about the low permanent pressure loss of proprietary flow tubes when expressed as a percentage of the differential produced. However, there is a paucity of research on the necessity, in most cases, of increasing initial differential pressures to meet operating range requirements with a corresponding increase in actual head loss (Ifft, 2010).

The percentage of the differential derived from Equation 2.2 can be written as followed (Coulson & Richardson, 1999):

$$\%\Delta P = \frac{\Delta P_{PPL}}{\Delta P_t} \times 100 \qquad \text{Equation 2.3}$$

Permanent pressure loss is just one of the characteristics to consider when evaluating a flow meter (McCrometer, 1999).

2.4 Discharge coefficient and performance measures

Measures of flow meter element performance represent the difference between how the ideal flow meter would perform and how the real one actually performs (Spitzer, 2005). Flow meter performance is described by the dimensionless numbers of discharge coefficient and Reynolds number (Nystrom & Stacy, 2008). Then greater focus is placed on discharge coefficient analysis.

2.4.1 Definition

In practice, the actual flow rate of a fluid through a differential pressure meter has proved to be somewhat different from the theoretical value calculated in an ideal equation. Therefore, when high accuracy has been required, it has been necessary to multiply the theoretical flow rate by an empirically coefficient called the discharge coefficient (C_d). The discharge coefficient is determined by the use of physical measurement of the amount of fluid passing through a tube over a specified period of time (Halmi and Associates, 1985).

It has been found that relatively high accuracy can be obtained in this manner and that an empirically determined C_d compensates for the following physical characteristics (Halmi and Associates, 1985):

- The effects of the Reynolds number as the fluid velocity changes.
- The effects of energy losses in the device.

- The effects of shear forces produced by the fluid as it passes the taps, causing the formation of vortices.

2.4.2 Determination of discharge coefficient

When a fluid flows through the differential pressure flow meter, the fluid is constricted, and thus the velocity of the fluid increases with a decrease in pressure. The ratio of the throat diameter, d, to the diameter of the pipe, D, is called diameter ratio and denoted by β, and given by Arun et al. (2010) as:

$$\beta = \frac{d}{D} \qquad \text{Equation 2.4}$$

By conservation of mass, for incompressible flow across the cross-sections between the cross section at the inlet (1) and at the throat (t), as shown in Figure 2.2,

$$Q_1 = A_1V_1 = A_tV_t = Q_t \qquad \text{Equation 2.5}$$

Reverting to the Bernoulli equation, with $V_1 = A_tV_t/A_1$, the equation becomes

$$\frac{P_1}{\rho} + \frac{1}{2}\left(\frac{A_tV_t}{A_1}\right)^2 = \frac{P_t}{\rho} + \frac{V_t^2}{2} \qquad \text{Equation 2.6}$$

resulting in

$$\frac{\Delta P_t}{\rho} = \frac{V_t^2}{2}\left[1 - \left(\frac{A_t}{A_1}\right)^2\right] \qquad \text{Equation 2.7}$$

Now the real rate of discharge is calculated by:

$$Q = C_d A_t V_t = \frac{C_d A_t}{\sqrt{1-(A_t/A_1)^2}}\sqrt{\frac{2\Delta P_c}{\rho}}$$ Equation 2.8

knowing that:

$$\beta = \frac{d}{D} \text{ or } \beta^4 = \left(\frac{A_t}{A_1}\right)^2$$ Equation 2.9

Then, the discharge coefficient is:

$$C_d = \frac{Q}{A_t}\sqrt{\frac{\rho(1-\beta^4)}{2\Delta P_c}}$$ Equation 2.10

For a discharge coefficient closer to unity, the performance approaches the theoretical values. This is due to the flow stability in the meter, which results from its smooth geometry (Laribi et al., 2001).

2.5 Errors, standard deviations and uncertainties

Errors in measurements are due to the following:

- Random errors are due to the imperfection of the measuring device, which affects the precision. Precision here is defined as the repeatability or reproducibility of values obtained during measurements several times, and it can be assessed by statistical analysis. Precision can be improved by increasing the number of specimens being tested (Taylor, 1997). Random errors are always written in form of +/- and are calculated as uncertainty.
- Systematic errors are procedural errors made by the experimenter. They cause the measured value to deviate from the "accepted" value in the same direction. Unlike random errors, systematic errors are not revealed by repeating the measurements several times. Hence, systematic errors

cannot be assessed by statistical analysis based on repeated measurements (Taylor, 1997). Typical examples of systematic error causes include miscalibration of instruments. In this case, the measured values might have good precision but poor accuracy. Systematic errors are calculated as percentage errors.

Random errors were assessed using statistical equations. These equations included calculations of the standard error also known as standard deviation of mean. The standard deviation of the mean (SDOM) is an evaluation of the margin of error incorporated in the mean (Taylor, 1997). The large percentage uncertainty and percentage error indicate that both systematic and random errors contributed significantly to the error in the measurements.

2.5.1 Mean, standard deviation and uncertainty

When a measurement is repeated several times, the measured values are grouped around some central value. This grouping or distribution can be described with two numbers: the mean, which measures the central value, and the standard deviation, which describes the spread or deviation of measured values about the mean (Taylor, 1997).

For a set of N-measured values for some quantity X, the mean of X is represented by the symbol $\overline{X}$ and is calculated by the following formula:

$$\overline{X} = \frac{1}{N}\sum_{i=1}^{N} X_i = \frac{1}{N}(X_1 + X_2 + X_3 + \cdots + X_{N-1} + X_N) \qquad \text{Equation 2.11}$$

where X_i is the i - th measured value of X.

The standard deviation of the measured values is given by the formula:

$$\sigma_X = \sqrt{\frac{1}{N-1}\sum_{i=1}^{N}(X_i - \overline{X})^2}$$ Equation 2.12

The variance σ_X^2 is a measure of how far each value in the data set is from the mean (Taylor, 1997).

The uncertainty in a stated measurement is the interval of confidence around the measured value so that the measured value is certain not to lie outside this stated interval (Spitzer, 2005).

Uncertainties may also be stated along with a probability. In this case the measured value has the stated probability of lying within the confidence interval (Figliola & Beasley, 2011).

Equation 2.13 is used to evaluate the uncertainties that occurred during the flow measurements. Results of uncertainty (U) at 95% confidence were expressed as follows:

$$U = 2\sigma\sqrt{\frac{N}{N-1}}$$ Equation 2.13

2.5.2 Percentage difference and percentage error

Percentage difference errors are applied when comparing two experimental quantities, X_1 and X_2 of the same measure and neither of which can be considered the "true" value. The percentage difference is expressed as follows:

$$\%\ \text{Difference} = \frac{|X_1 - X_2|}{\frac{1}{2}(X_1 + X_2)} \times 100$$ Equation 2.14

Percentage errors are applied when comparing an experimental quantity, X, with a theoretical quantity, T, which is considered the "true" value. The percentage error can be expressed as follows:

$$\%\text{Error} = \left|\frac{T - X}{T}\right| \times 100 \qquad \text{Equation 2.15}$$

2.6 Repeatability

Repeatability is what characterises the ability of an instrument to give identical indications or responses for repeated applications of the same value of the quantity measured under the same conditions (Davis, 2001).

This also refers to how stable the measurement will be over time (Spitzer, 2005).

Good repeatability does not guarantee accuracy. If there is no indication of a proper accuracy statement on equipment but only a repeatability statement, one has to be cautious (Davis, 2001).

An understanding of the error components in the flow meter is a key factor in flow meter performance.

2.7 Precision and accuracy

The precision of a flow meter is a measure of the reliability of the meter, or how reproducible the meter is. Accuracy is a measure of how closely the meter results agree with a true or accepted value (Figliola & Beasley, 2011).

Accuracy is the degree of conformity of a measured or calculated quantity to its actual value, while precision is the degree to which further measurements or calculations show the same or similar results (Figliola & Beasley, 2011).

Flow tube performance is much affected by calibration. The inaccuracy of the discharge coefficient in a classical Venturi, at Reynolds numbers exceeding 75 000, is 0.5%. The inaccuracy of a classical Venturi at Re > 20,000 is between 0.7 and 1.5%. Flow tubes are often supplied with discharge coefficient graphs

because the discharge coefficient changes as the Reynolds number drops. The variation in the discharge coefficient of a Venturi caused by pipe roughness is less than 1% because there is continuous contact between the fluid and the internal pipe surface.

2.8 Classification of fluids

Fluids can be classified into two major categories, namely Newtonian fluids or non-Newtonian fluids, according to the external applied pressure or effects produced under the action of a shear stress (Chhabra & Richardson, 1999). There are" compressible" and "incompressible" fluids, but in this thesis, only incompressible fluids will be treated. The flow characteristics of single-phase liquids, solutions and pseudo-homogeneous mixtures (such as slurries), which may be treated as a continuum if they are stable in the absence of turbulent eddies, are considered, depending on their response to externally imposed shearing action (Chhabra & Richardson, 1999).

2.8.1 Newtonian fluids

Newtonian fluids, by definition, have a linear relationship between the shear stress and the shear rate, with a zero intercept as shown on the rheogram in Figure 2.4. The higher the viscosity of the fluid, the steeper the slope becomes (Steffe, 1996).

Physically, the shear rate is the velocity gradient or the rate of angular deformation of the fluid (Liu, 2003). Mathematically, a Newtonian fluid can be expressed by the following relationship:

$$\tau = \mu_n \dot{\gamma} \qquad \text{Equation 2.16}$$

where, τ is the shear stress, μ_n the viscosity and $\dot{\gamma}$ the shear rate.

In the rheogram, the viscosity can be defined as the constant of proportionality appropriate for Newtonian fluid. Using units of N, m^2, m, m/s for force, area, length and velocity, gives viscosity as Pa.s, which is 1 poiseuille or 1000 centipoises. “Dynamic viscosity” and “coefficient of viscosity” are synonyms for the term “viscosity”, referring to Newtonian fluids (Steffe, 1996).

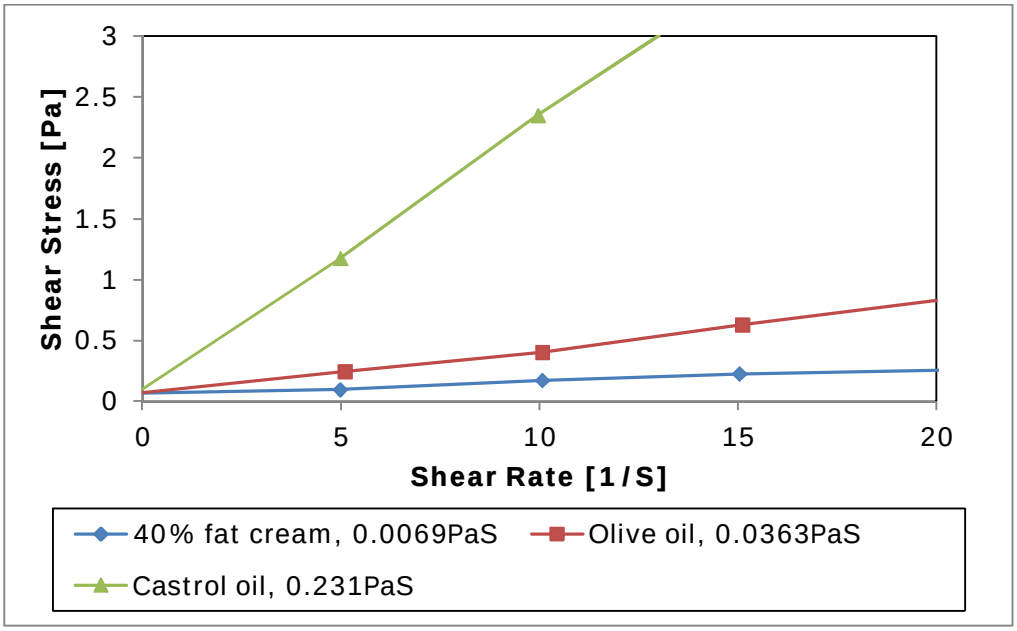

Figure 2.3: Rheogram for typical Newtonian fluids

2.8.2 Non Newtonian fluids

All fluids which do not exhibit a linear relationship between shear stress and shear rate are called non-Newtonian fluids. A general relationship to describe the behaviour of non-Newtonian fluids is the Herschel-Bulkley model or yield pseudoplastic model (Steffe, 1996):

$$\tau_0 = \tau_y + K(\dot{\gamma})^n \qquad \text{Equation 2.17}$$

where K is the consistency coefficient, n is the flow behaviour index, and τ_0 is the yield stress.

Equation 2.17 is very convenient because Newtonian, power law (shear-thinning when $0<n<1$ or shear-thickening when $1<n<\infty$) and Bingham plastic behaviour may be considered as special cases.

Figure 2.4 shows the qualitative flow curves on linear scales for these three types of fluid behaviour, and includes the linear relation typical of Newtonian fluids.

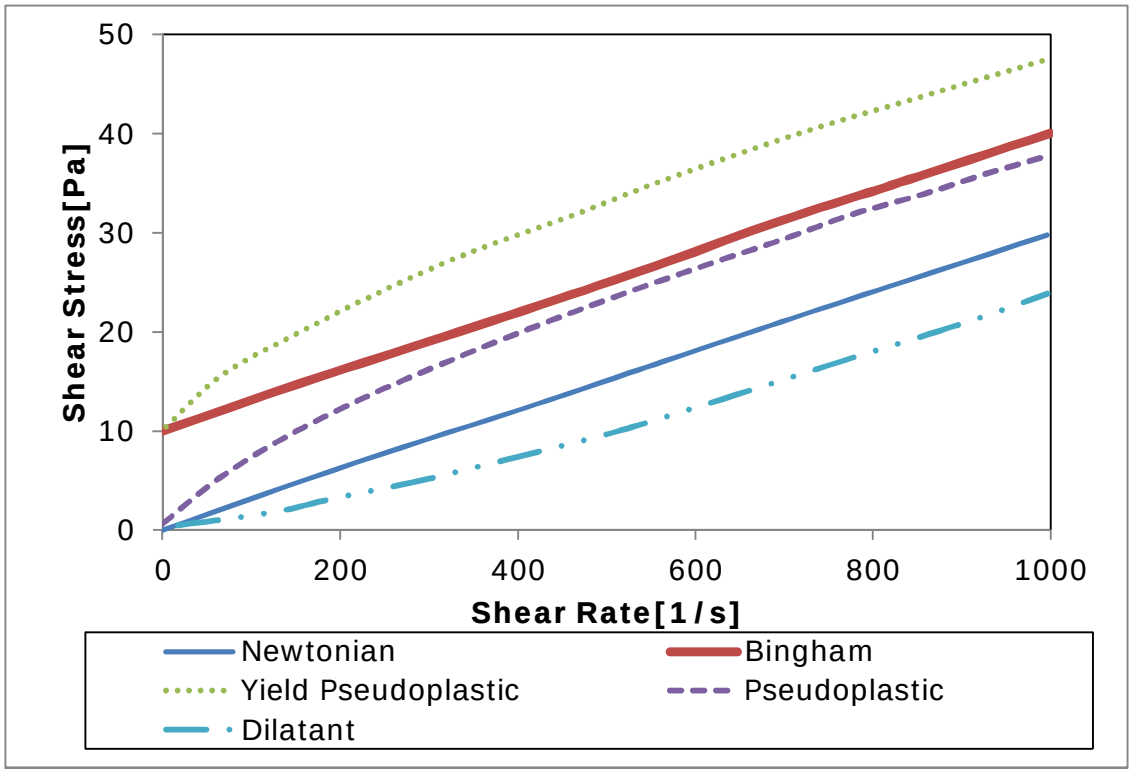

Figure 2.4: Rheogram for Herschel Buckley model

An important characteristic of Herschel-Bulkley and Bingham plastic behaviour is the presence of the yield stress, which represents the finite stress required to achieve the flow. Below the yield stress, a material exhibits solid-like characteristics: it stores energy at small strains and does not level out under the influence of gravity to form a flat surface (Steffe, 1996).

2.9 Rheometry

Rheometry encompasses the collection of physical data from the tests on a representative sample of fluid under investigation, for the purpose of establishing the relationship between shear stress and shear rate, both qualitatively (identification of the applicable rheological model) and quantitatively (the actual values of the rheological constants in the model) (Chhabra & Richardson, 1999)

The instrument used to measure viscous properties is called a viscometer or rheometer. There are two principal types of rheometers: rotational and tube viscometers.

2.9.1 Rotational viscometer

The rotational viscometer usually consists of a concentric bob and cup, one of which is rotated to produce shear in the test fluid, found in the gap between the bob and the cup. The shear stress is determined by measuring the torque on one of the elements (Chhabra & Richardson, 1999).

2.9.2 Tube viscometer

A tube viscometer is a device which forces a sample of fluid to flow at a measured rate in laminar motion under a measured pressure gradient in a precision-bore capillary tube of known diameter and length (Govier & Aziz, 1972). Because of their inherent similarity to many process flows, which typically involve pipes, capillary viscometers are widely employed in engineering

applications and are often converted or adapted to produce slit or annular flows (Chhabra & Richardson, 1999).

The determination of pseudo shear rate is based on the principle of linear momentum equation for steady flow in a horizontal circular duct (z=downstream dimension) gives us, for radius r.

$$\frac{dP}{dz} = \frac{2\tau}{r} \qquad \text{Equation 2.18}$$

$$\tau = -\frac{r}{2}\left(\frac{dP}{dz}\right) \qquad \text{Equation 2.19}$$

Resisting shear stress at the wall

$$\tau_0 = \frac{D}{4}\left(\frac{dP}{dz}\right) \qquad \text{Equation 2.20}$$

Equating Equation 2.19 and 2.16 and integrating over a circular section gives

$$\int_0^{u_{max}} du = \frac{-1}{2\mu}\frac{dP}{dz}\int_{D/2}^{0} r dr \qquad \text{Equation 2.21}$$

From which

$$u_{max} = \frac{D^2}{16\mu}\left(-\frac{dP}{dz}\right) \qquad \text{Equation 2.22}$$

Mean duct velocity $V = \frac{u_{max}}{2}$ for laminar flow in duct of circular section gives

$$V = \frac{1}{2} \times \frac{D^2}{16\mu}\left(-\frac{dP}{dz}\right) \qquad \text{Equation 2.23}$$

Substituting for $^{dP}/_{dz}$ from Equation 2.20

$$V = \frac{1}{2} \times \frac{D^2}{16\mu} \times \frac{\tau_0}{D/4} = \frac{D\tau_0}{8\mu} \quad \text{or} \quad \tau_0 = \mu\left(\frac{8V}{D}\right)$$ Equation 2.24

For flow in a horizontal duct of circular section

Data from a tube viscometer are plotted as τ_0 versus 8V/D on a pseudo-shear diagram from which the rheological parameters can be obtained. The flow curve obtained is called a pseudo-shear diagram. To obtain a true rheogram, Mooney (1931) and Rabinowitsch (1929) developed a relation:

$$\dot{\gamma}_w = \left[\frac{3n' + 1}{4n'}\right]\frac{8V}{D}$$ Equation 2.25

where

$$n' = \frac{d(\ln \tau_w)}{d\left(\ln \frac{8V}{D}\right)}$$ Equation 2.26

$$n = n'$$ Equation 2.27

For a series of N data points in the laminar region, fixed values of τ_y, K and n can be used in Equation 2.28 to calculate pseudo shear rates $(8V/D)_{calc}$ for each τ_0 value (Slatter, 1994).

$$\frac{32Q}{\pi D^2} = \frac{8V}{D} = \frac{4n}{K^{\frac{1}{n}}\tau_0^2}\left(\tau_0 - \tau_y\right)^{\frac{1+n}{n}}\left[\frac{\left(\tau_0 - \tau_y\right)^2}{1 + 3n} + \frac{\left(\tau_0 - \tau_y\right)^2}{1 + 2n} + \frac{\tau_y^2}{1 + n}\right]$$ Equation 2.28

where it is known that $\tau_0 = \frac{D\Delta P}{4L}$ and Q=VA

A realistic value of τ_y is then adjusted by minimising the error function. E is the root square difference between observed data and calculated ones (Neill, 1988):

$$E = \sqrt{\frac{\sum_{i=1}^{N}[(8V/D)_{i\,abs} - (8V/D)_{i\,calc}]^2}{N-1}}$$ Equation 2.29

K value for minimum error K_{min} is given by:

$$K_{min} = \frac{1}{\left[\frac{2\sum_{i=1}^{N}(8V/D)_i/_8}{\sum_{i=1}^{N}(\tau_0-\tau_y)^{\frac{1+n}{n}}\left[\frac{(\tau_0-\tau_y)^2}{1+3n}+\frac{2\tau_y(\tau_0-\tau_y)}{1+2n}+\frac{\tau_y^2}{1+n}\right]}\right]}$$ Equation 2.30

The main error sources in the tube viscometer arise from (Brown & Heywood, 1991):

- The wall slip effect, when the viscous laminar flow data do not coincide for different tubes diameters. The slip velocity must be calculated for each tube diameter and deduced from the measured main velocity.
- The entrance and exit losses. It is important that these losses be minimised. This is achieved by ensuring that the flow is fully developed before differential pressure readings are taken; usually at least 50D is allowed.

2.10 Non-Newtonian Reynolds number

There are various expressions for the Reynolds numbers for non-Newtonian fluids. The following are presented in this thesis:

2.10.1 Metzner & Reed generalised Reynolds number

It has been demonstrated that for laminar pipe flow of any given time-independent fluid, that 8V/D is some unique function of τ_0 only. According to Metzner and Reed (1955), this may be expressed as:

$$\tau_0 = \frac{D\Delta p}{4L} = K' \left(\frac{8V}{D}\right)^{n'} \qquad \text{Equation 2.31}$$

In most cases K' and n' are not constants, but vary with 8V/D. If the shear stress is plotted against 8V/D on a logarithm scale, Equation 2.31 is simply the equation of the tangent to the curve at a given value of 8V/D, n' being the slope of this tangent and K' the intercept on the ordinate at 8V/D equal to unity (Skelland, 1967). Metzner and Reed (1955) developed a generalised Reynolds number applicable to the pseudo-plastic model from the considerations above as:

$$Re_{M-R} = \frac{8\rho V^2}{K' \left(\frac{8V}{D}\right)^{n'}} \qquad \text{Equation 2.32}$$

After transformation, Equation 2.32 can be expressed as:

$$Re_{M-R} = \frac{\rho V^{2-n'} D^{n'}}{8^{n'-1} K'} \qquad \text{Equation 2.33}$$

Applying the Rabinowitsch-Mooney relation by replacing Equation 2.25 and Equation 2.27 into Equation2.32, it results in:

$$Re_{M-R} = \frac{8\rho V^2}{K(8V/D)^n}\left[\frac{4n}{3n+1}\right]$$ Equation 2.34

After transformation, the relation can be written as:

$$Re_{M-R} = \frac{\rho V^{2-n} D^2 (4n)}{8^{n-1} K(3n+1)}$$ Equation 2.35

2.10.2 Slatter Reynolds number

The Slatter Reynolds number directly takes the yield stress of non-Newtonian fluids and seeks to express the ratio of inertial forces to viscous shear forces in the sheared portion of the flow (Slatter, 1994)

The Slatter Reynolds number is given by:

$$Re_3 = \frac{8V_{ann}^2 \rho}{\tau_y + K\left(\frac{8V_{ann}}{D_{shear}}\right)^n}$$ Equation 2.36

For a fluid with a yield stress, there is a plug flow at the centre of the pipe in laminar flow, and the radius of the plug is:

$$r_{plug} = \frac{\tau_y}{\tau_0} R$$ Equation 2.37

The shear diameter is:

$$D_{shear} = D - D_{plug}$$ Equation 2.38

Again,

$$D_{plug} = 2r_{plug}$$ Equation 2.39

The mean velocity of the annulus is:

$$V_{ann} = \frac{Q_{ann}}{A_{ann}}$$ Equation 2.40

where,Q_{ann} is:

$$Q_{ann} = Q - Q_{plug}$$ Equation 2.41

$$Q_{plug} = U_{plug}.A_{plug}$$ Equation 2.42

$$U_{plug} = \frac{R}{\tau_0 K^{\frac{1}{n}}} \frac{n}{n+1} (\tau_0 - \tau_y) \frac{n+1}{n}$$ Equation 2.43

and

$$A_{plug} = \pi r_{plug}^2$$ Equation 2.44

The Slatter Reynolds number is valid for all time-independent non-Newtonian fluids in laminar flow up to and including the transition to turbulent flow. There is a discontinuity in the formulation in that in turbulent flow the plug ceases to

exist. In this case $V=V_{ann}$ the Equation 2.29 predicts laminar to turbulent transitions in the range of 2100 to 2300 (Paterson & Cooke, 2010).

2.11 Friction factor

Accurately predicting rheological parameters of fluids is essential for calculating the capacity and pressure requirements of the pipeline as these affect the economics of pipeline transportation. All the equations used in pipeline design require an understanding of the basics of flow regimes (Paterson & Cooke, 2010).

The Fanning friction factor for non-Newtonian fluids in laminar flow is given by the following relation (Chhabra & Richardson, 1999):

$$f = \frac{16}{Re_{MR}} \qquad \text{Equation 2.45}$$

Slatter and Pienaar (1999) developed a friction factor for non-Newtonian fluids with a yield stress:

$$f_{ann} = \frac{2\tau_0}{\rho V_{ann}^2} \qquad \text{Equation 2.46}$$

Turbulent flow is complex and consistent mathematical analysis has not been achieved. Predictions are obtained empirically from experiments. In turbulent flow, the friction factor is a function of the Reynolds number and pipe roughness k.

Equation 2.40, well known as the Colebrook and White equation, can be used to calculate the friction factor (Massey, 1998).

$$\frac{1}{\sqrt{f}} = -4\log\left[\frac{k}{3.7D} + \frac{1.26}{Re\sqrt{f}}\right] \qquad \text{Equation 2.47}$$

Equation 2.48, the Blasius equation, can be used in the case of a smooth wall pipe and Reynolds number 3000 and 100000, to determine the friction factor (Massey, 1998):

$$f = \frac{0.079}{(Re)^{0.25}} \qquad \text{Equation 2.48}$$

2.12 Previous work

In recent years, concentrated research work has been devoted to studying both experimentally and computationally operating conditions on the accuracy of differential pressure flow meters. Most of these studies evaluated the effect upon the discharge coefficient. A review of the effect of angle, beta ratio and rheology on the pressure drop and discharge coefficient, as well as the flow meter performance (repeatability, linearity and accuracy are the main points) has been given in this section for various differential pressure flow meters.

2.12.1 Orifice flow meter

Engineers have failed to predict the orifice flow rate for non-Newtonian fluids owing to the lack of data for orifice discharge coefficients observed at lower Reynolds number (Salas-Valerio & Steffe, 1990). The authors determined the orifice discharge coefficient for non-Newtonian fluids (cornstarch solutions from 5 to 10%) regarding their behaviour in terms of the orifice diameter, fluid velocity and fluid properties. It was found that C_d decreases as the consistency coefficient increases. It was also proposed that C_d may be expressed as an exponential function of the generalised Reynolds number at low Reynolds number.

The influence of parameters on the discharge coefficient such as accuracy and the effect of Reynolds number was noted by McNeil et al. (1999), who constructed a test facility to measure the flow rate, pressure drop and momentum effects of the orifice. The orifice had a diameter ratio β of 0.491 and tests were conducted with a Reynolds number ranging from 40 to around 400, using a solution of Luviskol® K90 in water as the working fluid. The pressure transducer was used to measure the pressure drops across the orifice plate.

The flow coefficients were also determined as the ratio of actual to the ideal volume flow rates. The laminar flow values were shown to have a strong dependence on the Reynolds number and to be considerably smaller than the turbulent flow value. However, over usable flow range, the flow coefficient could be correlated by the quadratic fit to the data within ±2%. The turbulent flow values all lay within ±1% of the mean.

The authors concluded that at low Reynolds numbers, the discharge coefficient is dependent on both the Reynolds number and the flow geometry; also the agreement tends to suggest that the flow resistance in similar geometries is similar in magnitude.

Singh et al. (2010) carried out flow simulations with water as the working fluid for different fluids and β ratios. The discharge coefficients of the orifice meter were calculated using the standard Equation 2.10. Statistical analysis for each case was also carried out to evaluate the mean value, standard deviation and standard error in discharge coefficients using Equations 2.12 and 2.13.

The predicted values of discharge coefficients match fairly well with experimental values over a wide range of Reynolds numbers. At lower β values (0.40 and 0.50), the discharge coefficient of an orifice meter decreases marginally with an increase in plate thickness. For a higher diameter ratio (0.60 and 0.70), the discharge coefficient increases slightly with an increase in plate thickness. The

bevel angle of the orifice plate has a marginal impact on the discharge coefficient of orifice plate for different plate thickness. The value of discharge coefficient at 45° bevel angle is higher than the corresponding at 30° bevel angle. Uncertainty in the discharge coefficient also increases with increase of plate thicknesses (0.65% for 3.5mm and 0.78% for 9.0mm).

The discharge coefficient for orifices depends on the boundary layer at the upstream tap and on the geometry of the orifice itself. Keyser and Friedman (2010) showed that orifices are more complicated to model than nozzles and Venturis because, fortunately, the latter are always geometrically similar.

2.12.2 Venturi flow meter

Because of the fully developed velocity profile at the upstream tap and the size of the boundary layer relative to the pipe diameter, its effect on the discharge coefficient may be neglected. By far, the major contribution of the boundary layer to the discharge coefficient occurs at the downstream tap for which the displacement thickness is used. The growth of the boundary layer for Venturis is based on that formed from the leading edge of a flat plate. For the purpose of deriving the discharge coefficient, Keyser and Friedman (2010) identified four intervals of Reynolds numbers based on distance from the leading edge:

- Region 1: Wholly laminar: $Re < 5 \times 10^5$.
- Region 2: Mostly laminar, but partly turbulent, with laminar thickness greater than the turbulent contribution: $5 \times 10^5 < Re < 7 \times 10^5$.
- Region 3: Partly laminar and partly turbulent, with the turbulent contribution greater than the laminar contribution. The start of this region is often called transition in the flow meter: $7 \times 10^5 < Re < 10^7$.
- Region 4: Fully developed turbulent boundary layer: $Re > 10^7$.

The authors showed that the distance taken from the leading edge is that at which a fully turbulent boundary layer would begin in order to equal the

momentum thickness at transition Reynolds number's distance. In cases of highly polished throats, this transition may be delayed to significantly higher values.

Shook and Masliyah (1974) contributed to both theoretical and experimental knowledge in respect of the behaviour of the Venturi when used with slurries. They also examined the role of wall friction effects for flow with negligible slip between the fluid and solid phases. They predicted and observed, in fairly extreme cases, discharge coefficients greater than unity.

Jitschin (2004) performed some experiments using a classical Venturi in gas flow. He found that the discharge coefficient C_d approaches the value 1 at large Reynolds number, which gives the result $C_d = 0.990 \pm 0.005$ (depending on wall roughness) at Reynolds number greater than 2×10^5. The discharge coefficient becomes significantly smaller than 1 with decreasing Reynolds numbers. The reason for this behaviour is, according to the author, an important increase of friction at the walls.

To obtain greater insight into the flow inside the Venturi tube, the author also measured the throughput in the classical Venturi tube operated in reverse direction, with 8° conical converging and 21° conical diffuser. In the reverse direction, the discharge coefficients are substantially smaller than in the normal direction, particularly at small Reynolds numbers. This behaviour is to be expected in the reverse direction, since the entrance section of the Venturi tube is considerably longer, leading to considerably more wall friction.

Reader-Harris et al. (2001) conducted an investigation on the discharge coefficient with a standard and non-standard convergent angle. They manufactured 21 Venturi tubes with a diameter ratio ranging from 0.4 to 0.75. Fifteen were standard, with an angle of 21°, with diameters ranging from 50mm

to 200mm and diameter ratios from 0.4 to 0.75. Six were non-standard, with convergent angles which were either 10.5° or 31.5°, and a diameter of 100mm.

The Venturi tubes were calibrated in water. For each Venturi tube, the data in water lay on a straight line and with a small scatter. The gradients were small: when fitted against the pipe diameter Reynolds number the majority had a positive gradient, but since several had a negative gradient, it seemed appropriate to represent the discharge coefficient of each Venturi tube by its mean value. Over the range of the data the average increase in discharge coefficient with Reynolds number was 0.0007.

A maximum deviation of 0.57% in mean discharge coefficient was found for two standard Venturi tubes made from the same drawings. The Reynolds number range of $1.2\times 10^5 < Re < 2\times 10^5$ over which the data were used to calculate the mean, where C_d was approximately constant. From these data, a fitting Equation 2.49, with an uncertainty of 0.74 % (based on two standard deviations), was arrived at.

$$C_d = 0.9878 + 0.0123\beta \qquad \text{Equation 2.49}$$

The effect of the converging angle by comparing the non-standard and standard Venturi using Equation 2.49 was also shown. They found that the discharge coefficient of Venturi with a converging angle of 10.5° is smaller than that with the standard angle, owing to the additional pressure loss in the Venturi tubes with a convergent angle of 31.5° are also smaller than those with the standard angle. This may be due to separation at the downstream end of the converging section.

Laribi and co-authors (2001) investigated the effect of disturbed flow conditions on the flow meter performance; the Venturi meter was first installed in the fully developed flow condition at some 100 pipe diameters downstream of the pipe entrance.

The flow rate error and discharge coefficient shift were determined to see the effect of the installation effects on the meter reading. According to ISO 5167 standards, the flow rate was determined from differential pressure measured through the Venturi meter. The discharge coefficient was determined as the ratio of measured flow rate to the true flow rate measured from the constant volume tank. The percentage shift in the discharge coefficient was determined from Equation 2.50,

$$\Delta C_d = \left(\frac{C_{d0} - C_d}{C_{d0}}\right) \times 100\% \qquad \text{Equation 2.50}$$

where C_{d0} represents the discharge coefficient measured under standard conditions (clean meter with no obstacles at fully developed flow condition) and C_d being the discharge coefficient measured under non-standard operating conditions.

For the effect of flow conditions on percentage change of the discharge coefficient, a general trend is that the C_d shift is much higher for lower Reynolds numbers and tends to decrease as the Reynolds number increases. It can be seen how unstable the C_d value at lower Reynolds numbers is for any obstruction in the flow meter.

Miller and co-authors conducted a study to evaluate the effects of an emulsion mixture through a Venturi flow meter (Miller et al., 2009). The primary focus of the study was to determine heavy oil fluid flows with viscosity ranging from 0.003 to 0.3Pa.s. The testing consisted of an emulsion mixture flow loop, where the mixture was pumped through the system at different velocities to determine the effect of viscosity on the discharge coefficient. The Reynolds numbers varied between 400 and 24,000. The authors derived an equation that could be used to evaluate the discharge coefficient:

$$C_d = B + A \times \log(Re) \qquad \text{Equation 2.51}$$

Although this equation can be used to evaluate the discharge coefficient and consequently the flow through a Venturi flow meter, there is still significant uncertainty in respect of the values of A and B, depending on the viscosity of the fluid used. The authors were able to determine that the resulting relative errors for Re>2000, ranged from 2 to 4%, while the uncertainty grew from 400<Re<2000 to as much as 6%.

It provided an accurate description of the performance of pressure drop measurement devices when used with viscous fluids (multiphase). The dependence on viscosity is addressed within the coefficient of discharge.

2.12.3 Other flow meters

Literature shows that the use of Venturi flow meters can be extended to various applications such as gas flows (Reader-Harris et al., 2001) and gas-solid two-phase flow (Wu & Xie, 2008) if the Venturi tube design is optimised. The cone flow element, because of its conditioning effect, helps in the adoption of a short metering length. Cone element angles were selected on the basis of classical Venturi design with a diameter ratio β varying from 0.4 to 0.8. (Sapra et al., 2011).

For the investigation of the performance characteristics of 100mm line size cone flow elements, a magnetic flow meter was used as reference standard for flow measurement in the vertical test section. The authors conducted a series of experiments using water.

The value of the discharge coefficient was obtained for a range of flow rates for all beta ratios with Equations 2.11, 2.12 and 2.13.

Sapra and co-authors (2011) analysed the behaviour of discharge coefficient as a function of Reynolds number and upstream disturbance; a quantitative

analysis was carried out to ascertain the extent of error in measurement. The quantitative analysis data are presented in Table 2.2.

Table 2.1: Uncertainty in the discharge coefficient for 100mm cone flow element (Sapra et al., 2011)

β ratio	Mean C_d	Standard deviation (σ)	Percentage Uncertainty +/- (U%)	Experimental range of Reynolds number (Re)
0.408	0.730	0.0043	0.4557	27000 – 200500
0.510	0.729	0.0042	0.4570	30700 – 170000
0.608	0.728	0.0030	0.3115	59300 – 185000
0.705	0.701	0.0017	0.1871	22700 – 189000
0.803	0.697	0.0035	0.3798	28300 – 196500

It is significant to observe that using the correct discharge coefficient is vital. The varying discharge coefficient is an essential parameter for accurate measurement of low Reynolds number flows (Hollingshead et al., 2011).

Hollingshead and co-authors (2011) provided an improved understanding of differential flow meters operating at low Reynolds numbers and investigated experimental measurements to characterise the behaviour of Venturi, orifice, V-cone and wedge meters from very low to high Reynolds numbers. Water was used to obtain results at higher Reynolds numbers. As a test of consistency, both water and heavy oil were run at a Reynolds number of 20,000

The correction factor equations plotted for each meter type are shown in Figure 2.5.

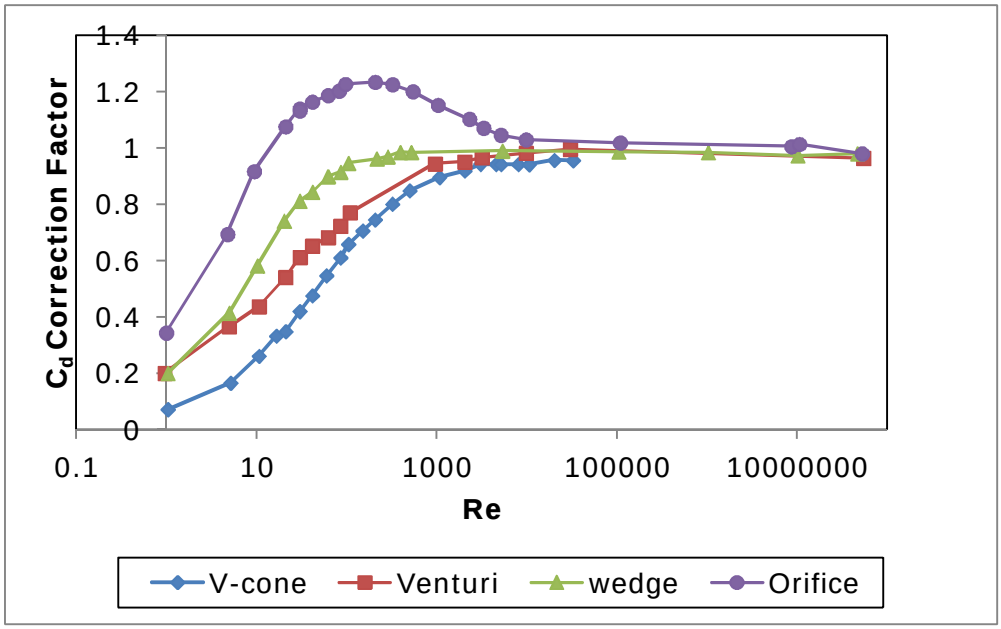

Figure 2.5: Average C_d factors (Hollingshead et al., 2011)

The calibration is mostly done with cold water. Therefore, there is a need for accurate low Reynolds number flow measurement for various pressure drop flow meter devices.

The authors indicated that at low Reynolds numbers, the discharge coefficients decrease rapidly with decreasing Reynolds numbers for Venturi, V-cone, and wedge flow meters. The orifice plate meter did not follow the general trend of the other meters, but rather as the Reynolds number decreased, the discharge coefficient increased to a maximum before sharply dropping off with a further decrease in the Reynolds number.

Fyrippi and co-authors (2004) investigated two aspects: the first was concerned with the accuracy of the flow meter when operating with non-Newtonian liquids, the second was with the nature of fluid flow and how it related to the observed flow meter accuracy. It was found that the Coriolis flow meter was unaffected by the fluid rheology, the electromagnetic flow meter exhibited an additional

uncertainty of about 1% during transition, while the ultrasonic flow meter exhibited inaccuracies up to 18%. The inaccuracies are because the flow velocity profiles of non-Newtonian fluids are different from those of Newtonian fluids.

2.13 Conclusion

This chapter presented a summary of previous research work conducted on differential pressure flow meters. It has been shown from the literature that the Reynolds number and discharge coefficient merit acute observation in analysing the capabilities of flow meters. The review reports that the majority of the data available in the open literature are in a limited range of applications and cannot provide accurate measurement at a lower Reynolds number (Re=10000). Some equations have been established to predict the orifice flow rate for non-Newtonian fluids using discharge coefficient as a function of the generalised Reynolds number, diameter, velocity, fluid properties, or flow geometry.

2.14 Identification of research topic

Literature shows that changing the convergent angle showed a significant impact on the discharge coefficient uncertainty and the application range of the commercially available flow meters. The influence of angle and diameter ratio on the discharge coefficient of the flow meter to address the limited range of flow measurements offered by the classical Venturi flow meter was therefore studied in this work.

Experimental Work

3.1 Introduction

The test rig was designed and developed to measure pressure loss coefficients data in both turbulent and laminar flows for Newtonian and non-Newtonian fluids for various types of pipe fittings. This chapter discusses the overall test facility and the components within the facility. A detailed procedure for the calibration of the measuring instruments is also outlined in this section.

The objective of this experimental work was to measure the static pressure data through different converging-diverging tubes. An important aspect of the experiment was that identical slurries would be used to test all the C-D tubes of different β ratios and θ angles.

3.2 Test rig

The test facility used for conducting the experiment in this study is shown in Figure 3.1. The corresponding schematic of this test facility is shown in Figure 3.2. The experimental test rig consists of five lines of PVC pipes with diameters ranging from 46mm to 100mm internal diameter (ID). Each line is 25m long, to allow a fully developed flow before and after each fitting. Test fluids were mixed in a 1.7m^3 rubber-lined mixing tank. The testing fluids were circulated in a continuous loop using a positive displacement pump. A heat exchanger was used to maintain the slurry temperature. The heat exchanger was followed by two valves coupled in parallel that directed the flow either to the upper part of the rig (which contained smaller pipes of 52, 63 and 2 x 46mm) or the lower part (which contained the larger pipe, 100mm ID). Each of the two routes was fitted with a flow meter (a KROHNE of 40mm ID [5 l/s] and a SAFMAG of 100mm ID [80 l/s]). After the flow meter, the fluids could enter any of the five test sections. An on/off diaphragm valve was situated at both ends of each test pipe for isolation, so that only one line was tested at a time. The same was done at the end of each test section. After a fluid passed through a test section it was

collected via a common pipe and directed to the mixing tank. Another KROHNE flow meter [11 l/s] of 65mm ID was installed on the common pipe to ensure accurate flow rate measurements over a wide range. At the outlet it was possible to divert the fluid through a weigh tank used for calibration purposes.

Figure 3.1: Experimental test rig

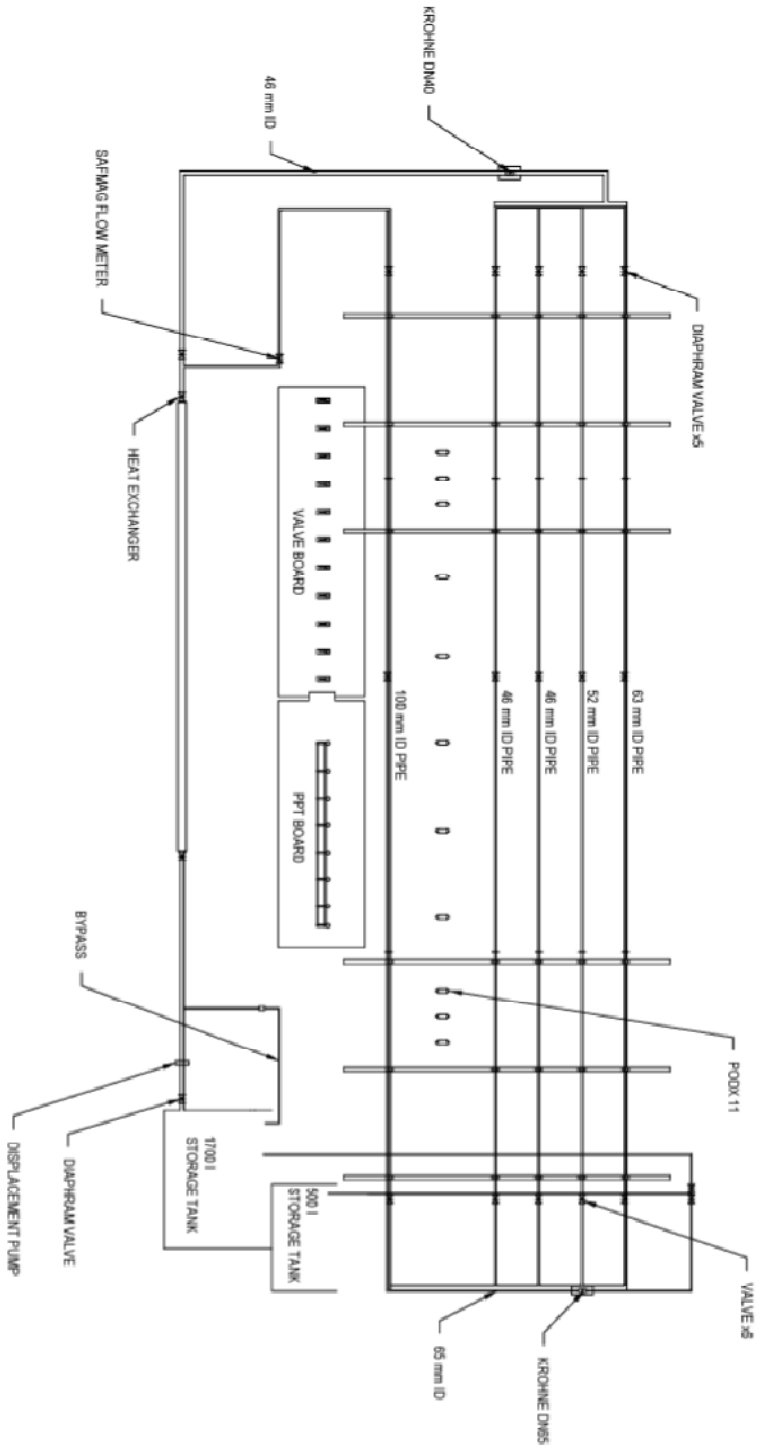

Figure 3.2: Experimental test rig

3.3 Instrumentation

This section presents all the instruments connected to the rig or used to collect experimental data.

3.3.1 Pressure transducers

Two types of pressure transducers were used to measure the pressure: the point pressure transducer (PPT) and differential pressure transducer (DP Cell).

The PPT was used to measure the static pressure at a given point in the line test. The pressure gradients were measured with a pressure transducer of the type PHPWO1V1-AKAYY-OY [GP] version 25.0 Fuji Electric with a maximum range of 500 kPa and a precision of 0.25%. The output of this instrument was a DC current ranging from 4 to 20 mA, proportional to the pressure applied. The range and span of this instrument were adjusted with a hand-held communicator (HHC).

The Differential Pressure Transducers (DP cell) were used to measure the difference of static pressure between two points.

Two DP cells of the type IKKW53VI-AKCYYAA [DP], version 25.0 Fuji Electric, were used to measure differential pressures. The maximum ranges were 6 kPa and 130 kPa respectively. They had the same characteristics as the PPT, that is, a precision of 0.25%, and could be adjusted with a hand-held communicator (HHC).

3.3.2 Hand-held communicator (HHC)

A Fuji electric hand-held communicator, type FXY 10AY A3, was used. This portable instrument was connected to the PPT or DP cell to change parameters such as data display, range, span, time constant, units, calibration, etc. It was mainly used to change the ranges and to calibrate the transducers.

3.3.3 Data acquisition unit (DAU)

A Hewlett Packard (HP) data acquisition unit of the type HP34970A was connected to a computer. This instrument received, through various channels, analogue signals from different parts of the rig (DP cell, PTT, temperature probes, load cell) and converted them to digital signals compatible with a PC.

3.3.4 Computer

All processes were controlled by a central PC, a Celeron 300. This was coupled with the DAU as an interface and was used to capture and process the experimental data automatically. Test programs were written in Visual Basic 6.0.

3.3.5 Flow meters

Three flow meters, two installed vertically and one horizontally on the test rig, were used:

- A KROHNE IFC 010D-DN40 of 40mm internal diameter with a maximum flow rate 5 l/s.
- A KROHNE OPTIFLUX 4000-DN65 of 65mm internal diameter with a maximum flow rate 11 l/s.
- A SAFMAG 100A2NESSR0032 of 110mm internal diameter.

3.3.6 Weigh tank and load cell

The weigh tank, similar to the bucket and stopwatch method, was used to determine the mass slurry distribution between the two vessels. The operation of the weigh tank is quite simple. The output voltage of the load cell varied linearly with the applied force, and was proportional to the input voltage. The resistors were connected to a power supply independent of the input voltage. An accurate calibration of the load cell is essential.

3.3.7 Pump

A progressive cavity positive displacement pump (B9602-C1 EN8N1T), driven by a 15KW electric motor, was used to circulate the fluid in the test loop. The pump

was connected to a Yaskawa VSD (variable speed drive) of type (V1000) to obtain the desirable flow rates.

3.3.8 Heat exchanger

A double pipe heat exchanger was installed at the inlet of the rig to keep the test fluids at a constant temperature.

3.3.9 Temperature probes

Two temperature probes were installed to measure the temperature before and after a fluid had entered a test section. They were located at the exit point of the heat exchanger and before the diversion point between the weigh tank and the mixing tank. This information was used to regulate the temperature of the test fluid, using the heat exchanger, and by either reducing or increasing the flow rate of water.

3.3.10 Mixer

A mixer, driven by a 3kW electrical motor, was fitted to the storage tank to mix the test fluids at the preparation stage. At times, the mixer was run during a test to keep the fluid particles suspended.

3.3.11 Valves board

A switchboard made of small ball valves, as shown in Figure 3.3, was used to select a particular test section and its direct pressure readings to specific transducers, so that different test modes could be possible.

Connections of pressure lines on the valves board were made of nylon of 3mm ID filled with water. Deviation valves (D_1, D_2... D_{11}) were on-off valves giving access to pressure transducers. Pressure lines [(PL1...PL4) and (1,2...11)] were connected to the test sections' pressure tappings via solid pods filled with water. The purpose of the pods was to collect any solid particles that might come from the test fluid, preventing them from entering the pressure lines. Each pod had a

valve on the top and bottom. The top valve was for flushing away any air bubbles, while the bottom valve was used for flushing away solid particles.

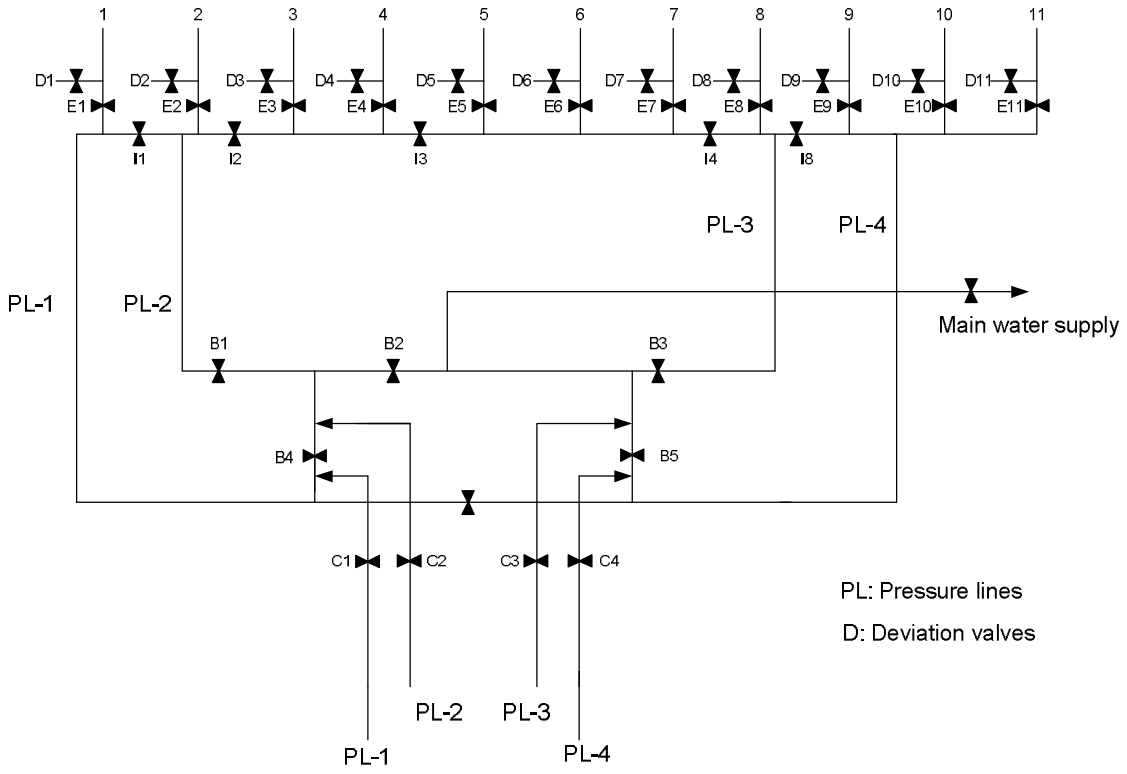

Figure 3.3: Pressure lines board of valves test rig

3.4 Experimental procedures

A strict set of test procedures was established to ensure the collection of repeatable and accurate data for each C-D tube's flow meter. The procedure consists of calibration of different instruments. This is followed by the measuring procedures for relative density, running determination of viscous properties, and discharge coefficient values.

3.4.1 Calibration of measuring instruments

3.4.1.1 Introduction

A calibration applies a known input value to a measurement system for the purpose of observing the system output value. It establishes the relationship between the input and output values.

The static calibration curve describes the static input-output relationship for a measurement system and forms the logic by which the indicated output can be interpreted during an actual measurement. A correlation will have the form y=f(x) and is determined by applying physical reasoning and curve-fitting techniques to the calibration curve. The correlation can be used in later measurements to ascertain the unknown input value based on the output value, the value indicated by measurement system (Figliola & Beasley, 2011).

3.4.1.2 Load cell

The load cell on which the weight tank was mounted was calibrated against calibration weights. These weights were measured on a high-precision electronic scale. The weights were loaded and the load cell voltage was recorded for each known weight. The load cell calibration is as follows:

- Switch on the computer and load the calibration program.
- Select channel 120 on the DAU (Data Acquisition Unit), assigned to capture the voltage induced on the load cell.
- Put blocks of standard loads on the load cell in its centre of mass.
- Record the weight from zero to close to maximum range of the load cell on the PC via DAU as well as its voltage.
- Plot the standard weight versus the voltage and determine the slope and intercept of the linear relationship as shown in Figure 3.4.

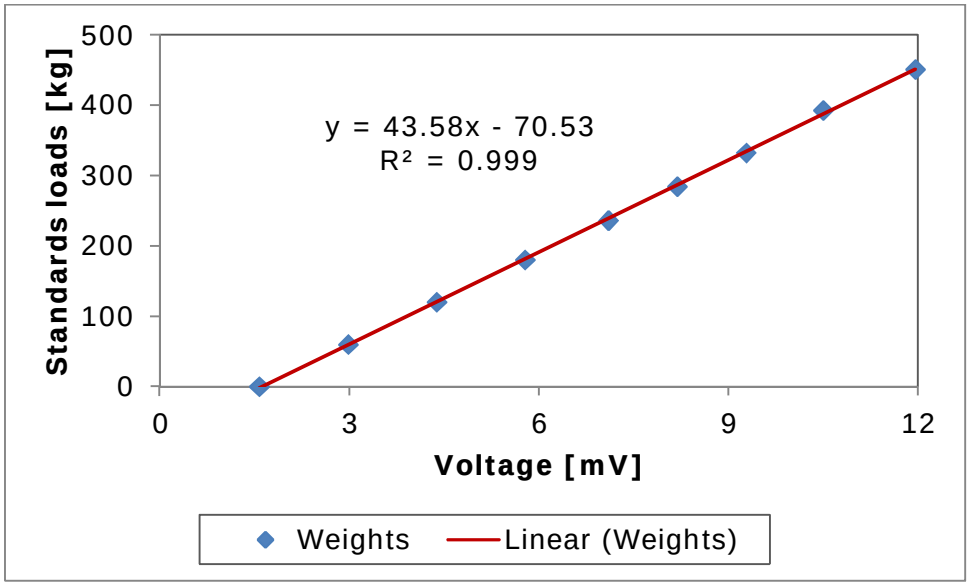

Figure 3.4: Load cell calibration curve

3.4.1.3 Flow meter

Flow meter calibration is a conceptually simple matter of performing adjustments to the flow meter so that it measures flow within predetermined accuracy constraints (Spitzer, 2005).

The calibration was as follows:

- Switch on the computer and flow meter calibration program.
- Select channel 118 and 204 on the DAU respectively for the DN40 and DN65 KROHNE flow meter assigned to capture the voltage induced on the weight tank.
- Pump the fluid through the rig and close the valve to divert the flow through the KROHNE flow meter and weight tank.
- Start the computer program. Stop it when the tank is almost full
- Empty the weight tank by opening the valve at the bottom of the tank.
- Record on the PC via the DAU the weight tank as well as the voltages.
- Vary the speed of pump to change the flow rate of fluid through the rig and repeat the procedure to acquire a set of data of differing flow rates.

- Plot the flow rate versus voltage and determine the slope and the intercept of the linear relationship.

Figure 3.5 shows the calibration curves for the KROHNE flow meter of 40mm with its calibration constant.

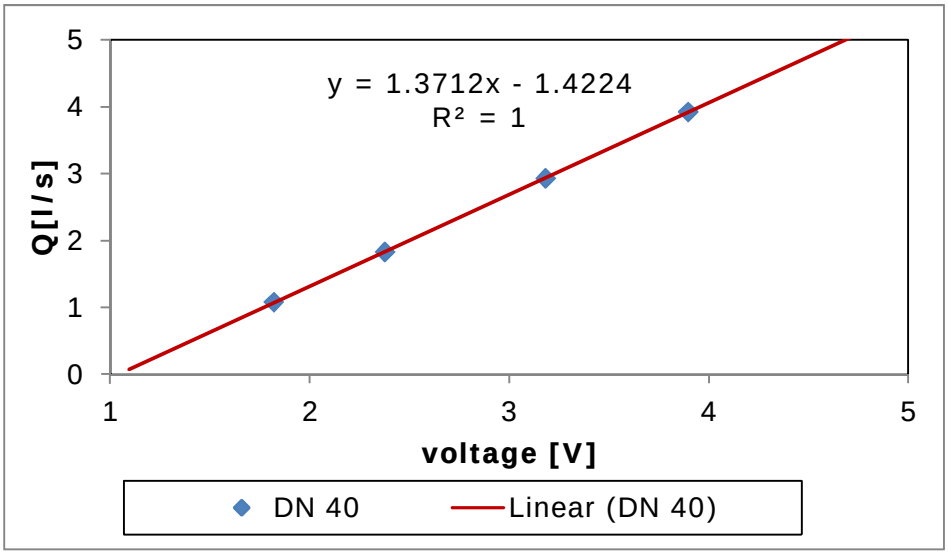

Figure 3.5: KROHNE DN 40 calibration constants

Figure 3.6 shows the calibration curve of different fluids in the KROHNE flow meter of 65mm pipe diameter with its calibration constant.

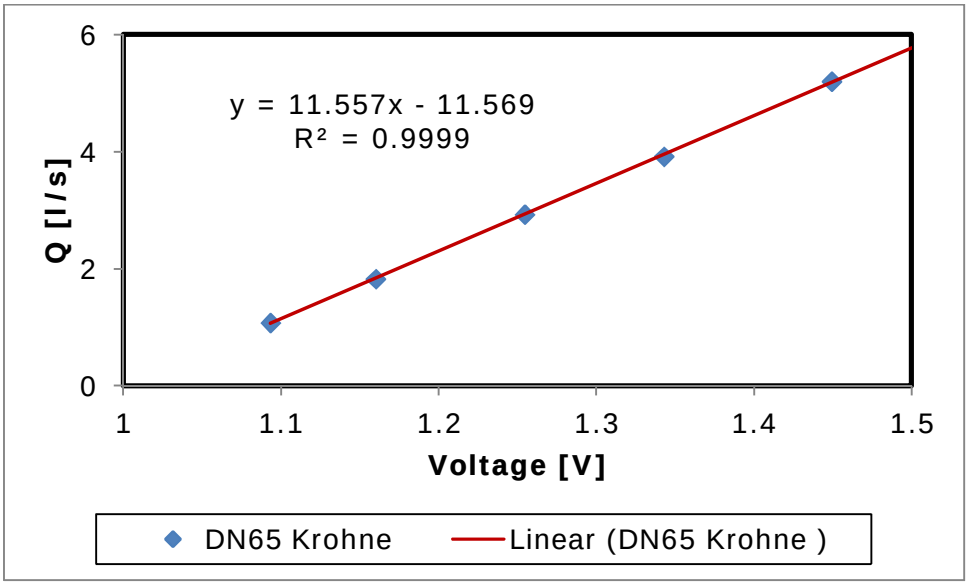

Figure 3.6: KROHNE DN 65 calibration constants

3.4.1.5 Transducer

The point pressure and differential pressure were calibrated using the hand-held communicator (HHC). A known pressure was applied directly to the transducers using a hydraulic pump connected to a digital manometer.

The calibration procedure was as follows:

- Open the calibration program and switch on the DAU to channel 101.
- Open the transducer's cap and set it to zero.
- Open the pipe valves leading to the transducers and expose them to the atmosphere, to release any pressure induced by the system.
- Connect the hand-held communicator to the transducers and switch it on.
- Set the hand-held communicator to the desired pressure range, either 0 – 40 kPa or 0-130 kPa, and set it on data recording mode.
- Read the pressure recorded by the handheld communicator and the voltage recorded by DAU. This is considered as the zero mark.
- Apply pressure on the transducers and record both the pressure and the voltage reading on the hand-held communicator and the DAU, respectively.

- Continue to increase the pressure on the transducers, recording the pressure and voltage readings to acquire at least six different readings.
- Plot the pressure readings against the voltage reading to determine the linear relationship between them. The slope and the intercept of this linear relationship are used to relate the pressure applied by the test fluid in the rig to the voltage recorded by the DAU.

The linear relationship of the pressure versus the voltage for PPT calibration is given in Figure 3.7:

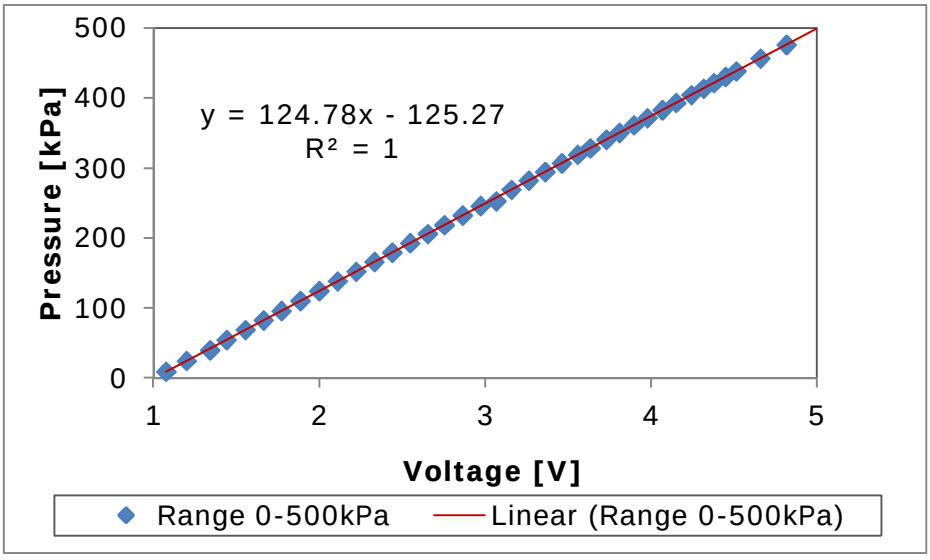

Figure 3.7: Calibration curve of pressure transducer

The calibration of the DP cell was conducted in a similar manner. The only difference was the channels used on the DAU to record the voltage produced by the pressure in the system, channel 115 and 116 of the DAU, were used to calibrate the DP cells for a pressure drop range of 130 kPa. The linear relationship of the pressure versus the voltage for the 130 kPa differential transducer is shown in Figure 3.8

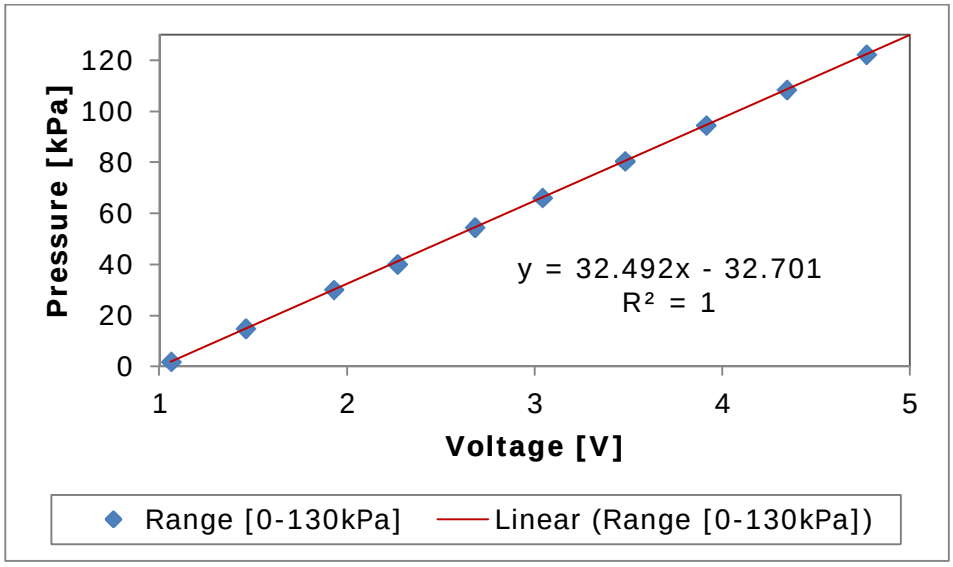

Figure 3.8: Calibration of DP cell

3.4.2 Measurement of the fluid relative density

The slurry density (ρ) and the relative density (RD) were determined carefully for each fluid tested. The following procedure was followed:

- Three clean, dry 250 ml volumetric flasks were weighed (M_1).
- A slurry sample was taken from a tapping in the pipe wall of any of the five pipes and was weighed (M_2).
- The volumetric flasks were filed to the 250 ml level with clear water and weighed again (M_3).
- The volumetric flasks were emptied, filled with clear water and weighed again (M_4).
- The relative density RD = ρ/ρ_W

$$RD = \frac{\text{Mass of fluid}}{\text{Mass of equal volume of water}} = \frac{M_2 - M_1}{(M_4 - M_1) - (M_3 - M_2)} \qquad \text{Equation 3.1}$$

3.4.3 Experimental procedures

The aim of a test on the 46mm line on the fittings rig was to obtain a set of static pressures across five different points of the C-D tube. These sets of points were transformed into differential pressure to assess a set of discharge coefficient versus Reynolds number. This section explains step by step the operation mode of the fitting test rig. The operation was as follows:

3.4.3.1General mode

- Switch on the computer and open the desired of test operation that is, HGL manual mode, the straight pipe test.
- Switch on the mixer to mix the slurry.
- Open fully the by-pass valve, positioned immediately after the pump, to ensure that there is no build-up of pressure in the rig if the wrong valves are open or if all outlet valves are closed.
- Switch on the pump and set it at the desired speed to achieve a certain flow rate.
- Open all the diaphragm valves in the system to circulate the test fluid left in the rig.
- Close the by-pass valve and let the pump run for an hour to thoroughly mix the test fluid.
- As the testing C-D tube line is operating. Then close all other valves of the rig except the one that is leading the fluid into the 46mm ID pipe which contains the C-D tube.
- Flush the pressure pods and pressure line board and fill them with tap water, ensuring that there are no bubbles in the tubes.
- Decide on the required pressure tappings on the test section and record their distances in the appropriate columns of the spreadsheet

on the computer program.

- Open the valves of the tappings leading to the pressure pods.
- Use the hand-held communicator to set the pressure range to be used during the test.
- Set the computer program to the determined pressure range and chosen pipe diameter, and indicate the type of fluid to be tested.
- Connect the pressure tapping to the transducers by operating or closing the appropriate valves on the pressure lines board.
- Take a sample of the fluid and conduct RD tests, and record the information on the computer program.
- Start the test.
- Change the flow rate of the fluid by increasing or decreasing the pump speed.
- Perform the flow stability control test and take a reading only if the flow has stabilised.

The test liquid was circulated from the tank using a positive displacement pump to the test section. The flow rate was controlled by a by-pass valve and measured with two different flow meters. The liquid discharge from the test section was provided with pressure taps at various points of the upstream and downstream sections of pipe. The static pressure at different points was measured by using the PPT. The fluid's temperature was maintained between 25°C and 30°C.

3.4.3.2 Straight pipe test

The results obtained in the straight pipe section are presented here for both water and non-Newtonian fluids. The straight pipe results are important for establishing the credibility of the test rig, as well as for rheological characterisation of non-Newtonian fluids.

3.4.3.2.1 Clear water test

Water tests were conducted in the straight pipe to establish the credibility and accuracy of the test equipment. The experiment to determine the friction factor is compared to Equation 2.47, an accepted design formula for turbulent flow (Finnemore & Franzini, 2009).

Water test comparison with Colebrook-White Equation (Figure 3.9) shows the comparison of the experimentally obtained shear stress (τ_0) with the calculated shear stress using the friction factor obtained from Equation 2.47, the pipe roughness k was found to be 15µm (which value is acceptable for smooth wall pipes) by iterations of solving the Equation 2.47 (Finnemore & Franzini, 2009).

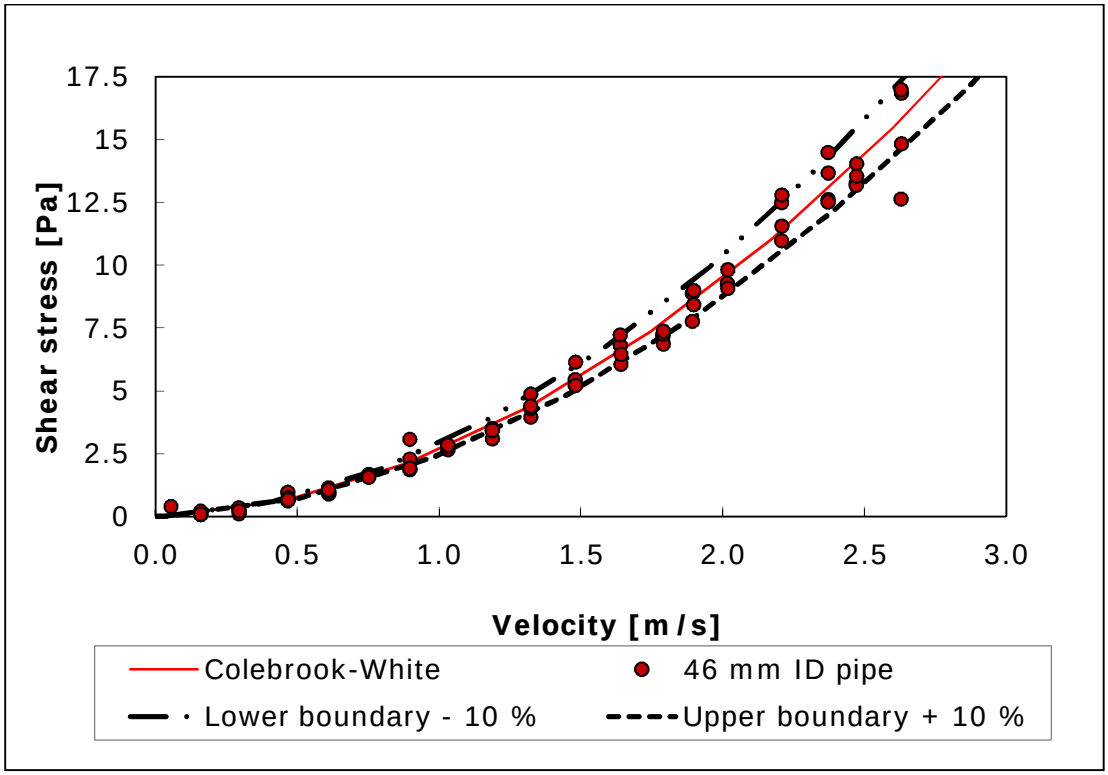

Figure 3.9: Water test comparison with Colebrook-White equation

It can be seen that 89% of the data falls within +/- 10% of the theoretical prediction for the 46mm ID pipe as illustrated in Figure 3.9. The closeness of experimental data and Equation 2.47 relates the validity and the degree of the

experimental technique and equipment used in this experimental study. This shows the accuracy for turbulent flow conditions.

3.4.3.2.2 Non-Newtonian fluids

The straight pipe test can be conducted simultaneously on the downstream and upstream pipes of the C-D tube test section. It was used to determine the viscous properties of the fluids. The test consisted of measuring pressure drop over a straight part of the test section at least 50D away from the bend or test fitting. The pressure drops were measured simultaneously with two DP cells. This test was conducted in at least three different diameters, 46, 52 and 63mm inner diameter, to ensure that there was no slip effect.

The procedure is as follows, referring to Figure 3.3:

Choose the straight pipe section on which the pressure drop will be measured and record the tapping distance.

- On pressure lines board close the isolating valves I1, I3 and I4.
- Open the E valves according to the test sections chosen. All deviation valves and the other E valves must be closed.
- Close the by-pass valves B2, B4, B5, and B6.
- Use the pressure line PL-1 and PL-2 to measure the pressure drop upstream of the test tube by opening the connecting valves C1 and C2.
- Ensure that the pressure line PL-1 is connected to the high side of the DP cell and PL-2 to the low side of the DP cell.
- Use the pressure line PL-3 and PL-4 to measure the pressure drop downstream of the test fitting by opening the connecting valves C3 and C4.

3.4.3.3 Hydraulic grade line

The pressure grade line test was conducted by reading the static pressure using only one point pressure transducer for all eleven tapping points. The procedure was as follows, referring to the pressure lines board (Figure 3.3):

- The exit valve E1 is open to read the pressure on tapping 1.
- E2 to E11 are closed.
- The deviation valves (D1 to D11) are closed. The isolation valves are open.
- The bypass valves (B1 to B6) are closed, as well as the connecting ball valves, except C1.
- C1 is connected to the PPT 1.
- Record the pressure reading.
- Close valve E1 and open E2.
- Read the pressure, close E2 and open E3.
- Continue the procedure until E11 is open.

3.5 C-D Tubes flow meter tested

3.5.1 C-D Tubes flow meter sizing

Five different sized shapes in converging and diverging zones were machined from Perspex at the mechanical engineering workshop of the Cape Peninsula University of Technology. The dimensions for the C-D tubes are presented in Table 3.1. For illustration purposes, a photograph is also shown in Figure 3.10. A drawing with the converging and diverging shapes of these tubes is presented in Figure 3.12 to 3.16.

Table 3.1: Converging-diverging tubes sizing

Ratio	Cone	Pipe	Throat	conical section	C-D tube
β	Angle	Diameter	Diameter	Length	Length
d/D	Θ [°]	D[mm]	d [mm]	L[mm]	2L[mm]
0.5	45°	46	23	28	56
0.5	30°	46	23	43	86
0.5	15°	46	23	88	176
0.6	15°	46	28	70	140
0.7	15°	46	32	52	104

Figure 3.10: Various C-D tubes

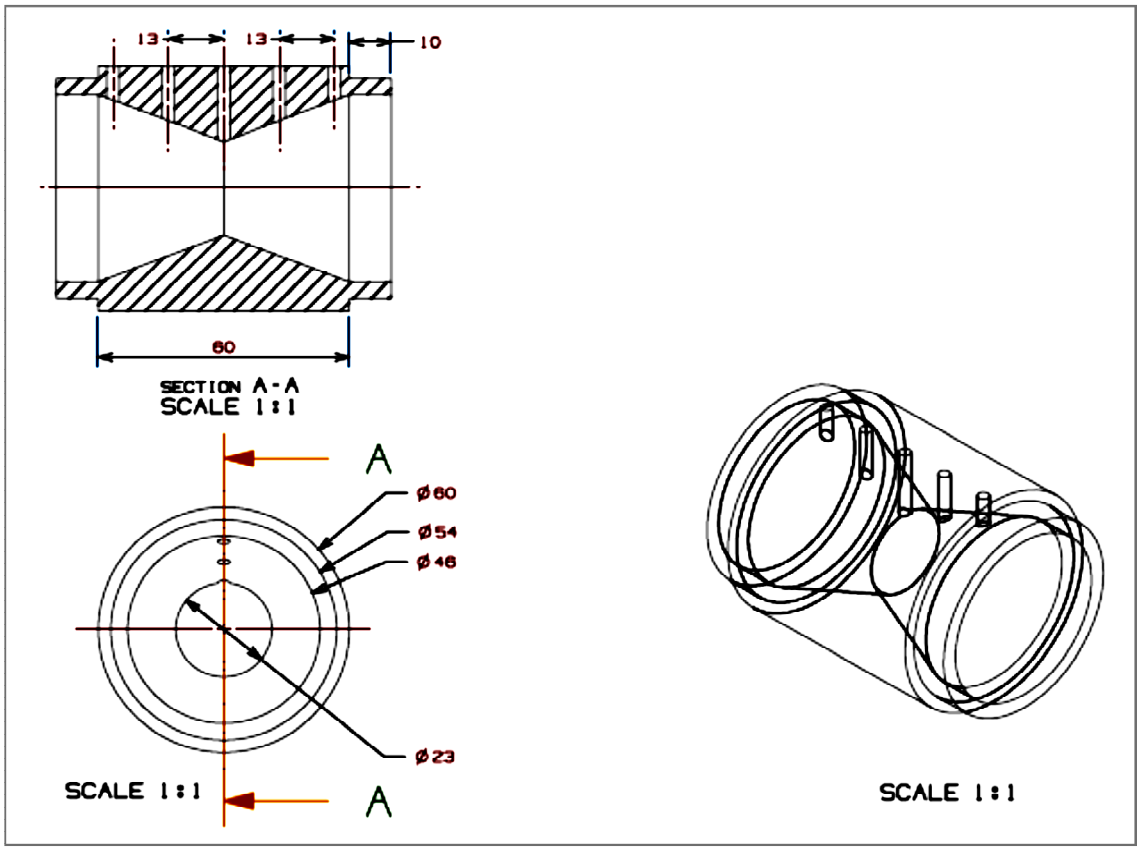

Figure 3.11: Drawing of C-D tube with ß =0.5; θ =45°

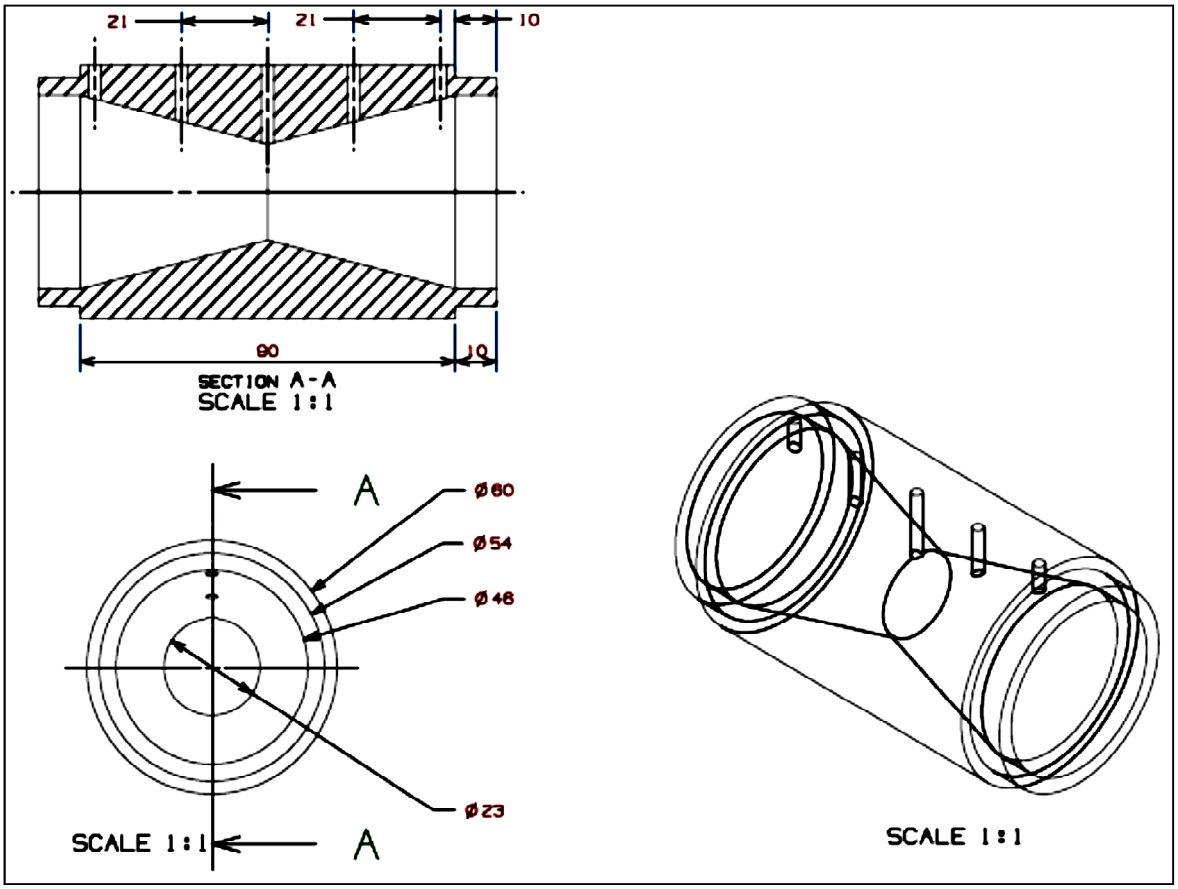

Figure 3.12: Drawing of C-D tube with ß =0.5; θ=30°

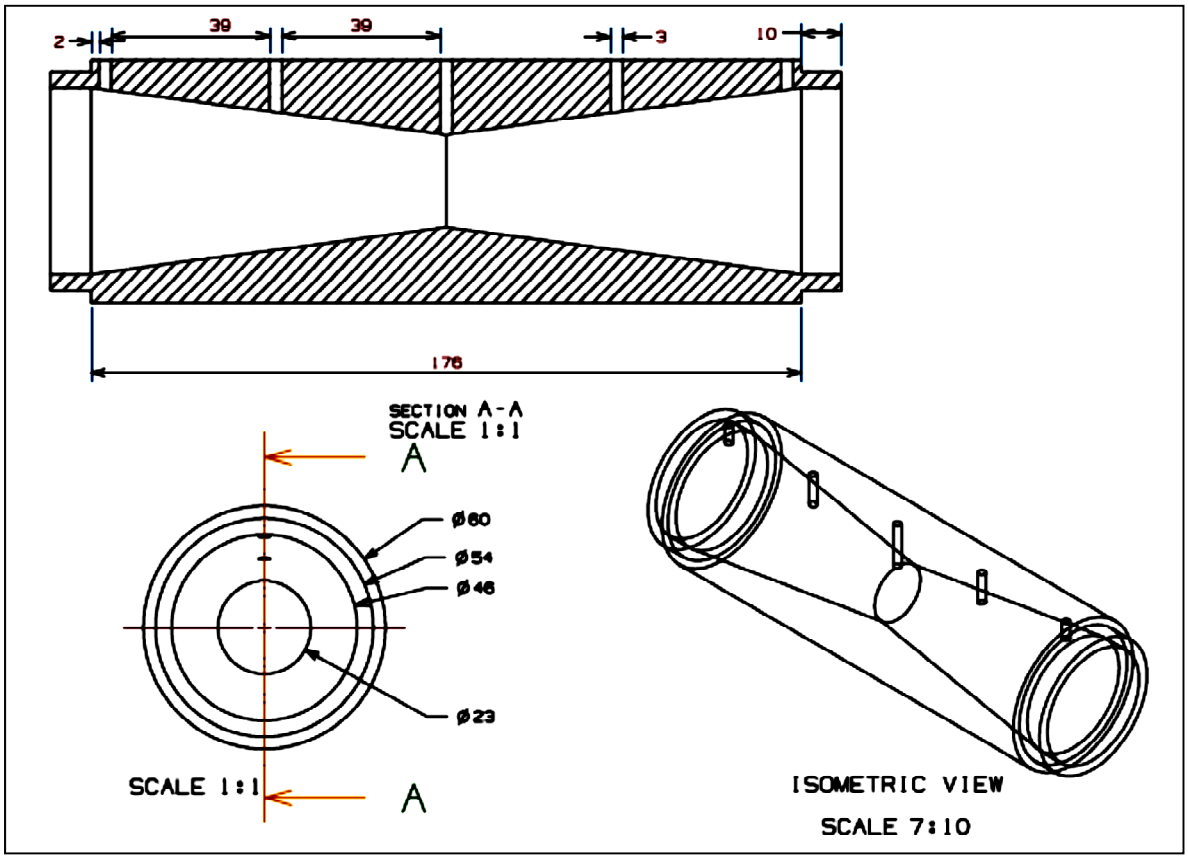

Figure 3.13: Drawing of C-D tube with β=0.5; θ=15°

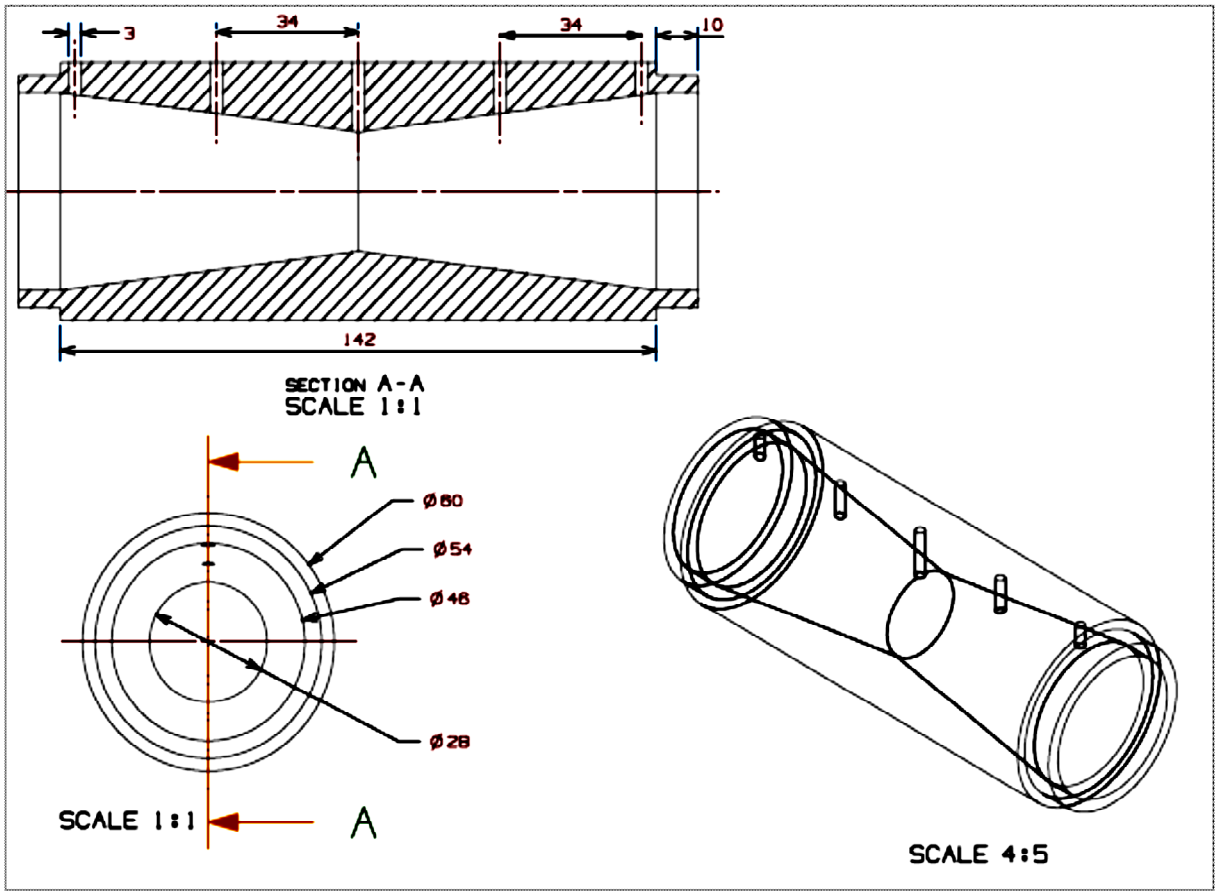

Figure 3.14: Drawing of C-D tube with β=0.6; θ=15°

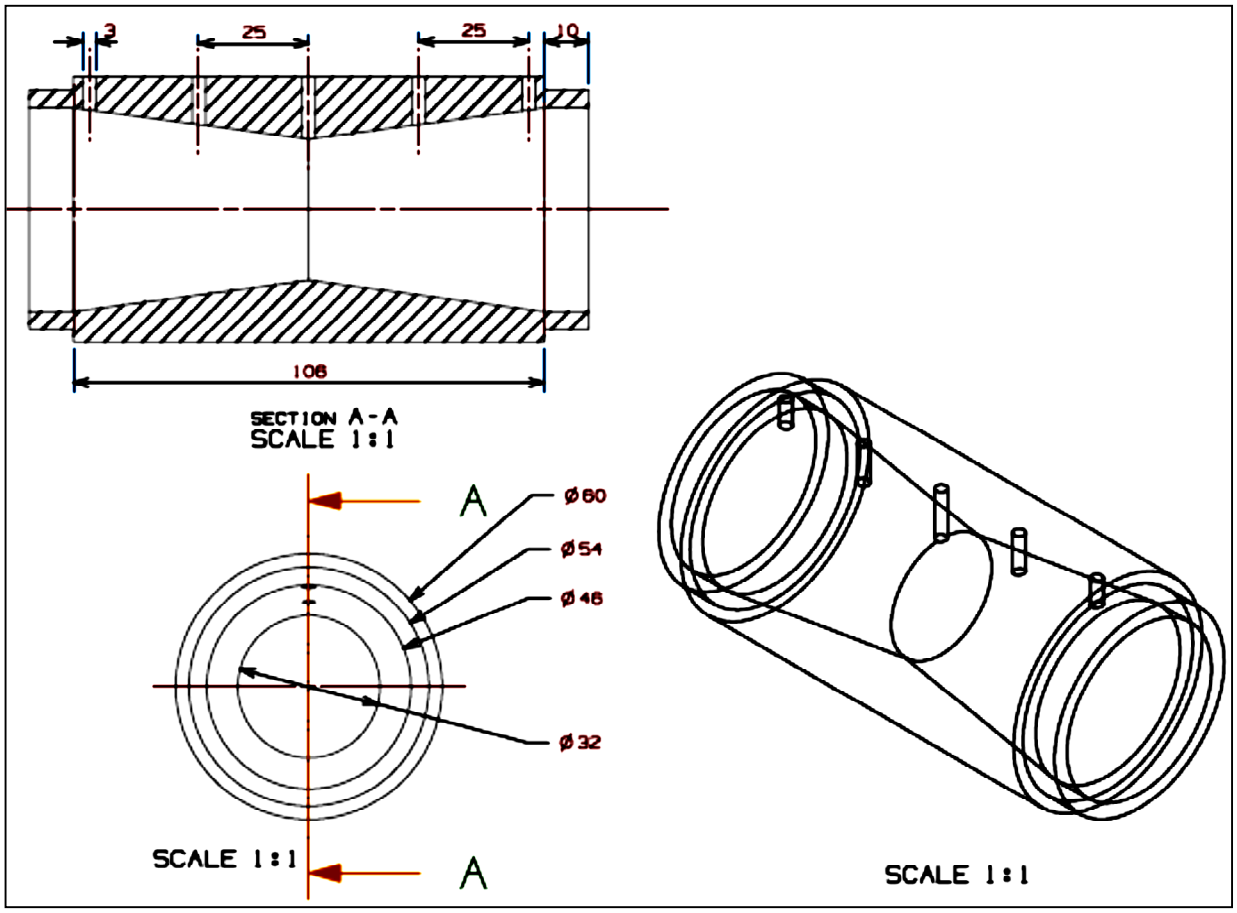

Figure 3.15: Drawing of C-D tube β=0.7; θ=15°

3.6 Venturi ISO 5167 sizing

Table 3.2 presents the details for the classical Venturi tube according to the standard ISO 5167.

Table 3.2: Dimensions of Venturi ISO 5767 in stainless steel

Tag	**Venturi**	
Nominal Size	1 1/2”	
D	46.00	mm
d	23.00	mm
L1	46	mm
L2	62	mm
L3	23	mm
L4	188	mm
Total length without flanges	319	mm
Total mass	14	kg
β ratio	0.5	
Converging angle (°)[Full]	21.00	°
Diverging angle (°)[Full]	7.00	°
Fabricated Venturi (F)	M	
Machined Venturi (M)		
Wall thickness (mm) [Entrance]	6	mm
Density (Pipe & Cones)	8000	kg/m^3
Density (Throat)	8000	kg/m^3
Flange mass (kg each)	4.5	kg
Flange length [mm each]	8	mm
Volume of Venturi tube	1	litres

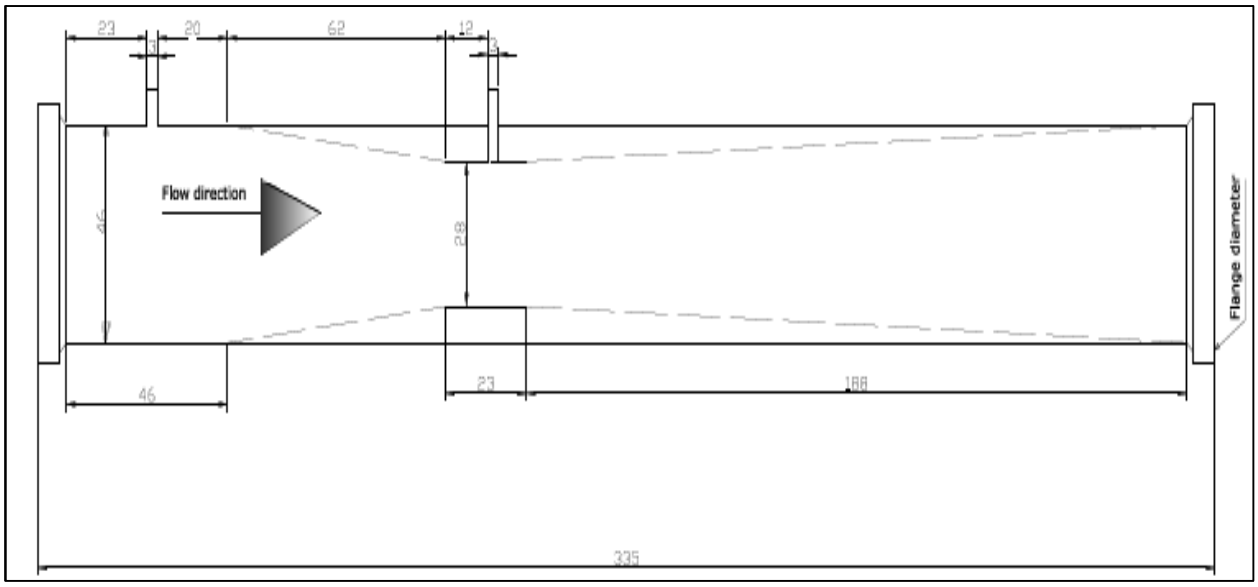

Figure 3.16: Drawing of Venturi tube ISO 5167

3.7 Material tested

In order to perform the tests, fluids were selected to represent a wide range of rheological behaviour associated with industrial slurries. Newtonian fluid (water) was used for the calibration of the fitting test rig and non-Newtonian fluids (CMC and solutions of xanthan gum and CMC at different concentrations) were tested to understand the flow measurement behaviour, which will be useful for practical applications in industries. A detailed description of these fluids is given below:

3.7.1 Water

The Cape Town municipal water, with a pH of 8.7, was tested in straight pipes to establish credibility, accuracy and precision of the procedure and apparatus. It was also used in the mixture to make up other fluids.

3.7.2 Carboxylmethyl cellulose (CMC)

CMC is a polyanionic cellulose ether. It has good solubility in both hot and cold water. It is used in drilling mud, in detergents as a soil-suspending agent, in resin emulsion paints, adhesives, and printing inks, as a protective colloid general and as a stabiliser in foods (Mahadevan, 1964). The flow properties of CMC solutions proved to be constant throughout the test work.

3.7.3 Xanthan gum (XG)

Xanthan gum is classed as “semi-flexible” (Rodd et al., 2000). XG is soluble in water and transparent, making it ideal for obtaining Laser Doppler Anemometry measurements. The XG used during this investigation was Ziboxan F80-xanthan gum (food grade).

Ziboxan F80 is a normal powder XG produced by fermentation of a carbohydrate with *Xanthomonas campestris*. Its solutions are neutral, and suitable for use in food and food preparations as a stabiliser, thickener or emulsifier.

3.8 Conclusion

This chapter has reviewed the sequence that was followed in collecting experimental data. A description of the experimental test rig and its equipment, experimental procedures such as test and calibration, and the test used to evaluate the properties of fluids were also described. The water test results correlated well to the Colebrook and White equation. Discussion of the results obtained will be presented in the next chapter.

Analysis of Results

4.1 Introduction

Because of the different non-Newtonian fluids used in this experimental work, the rheological characterisation has been done for each fluid to obtain the rheological constants K (fluid consistency index) and n (flow consistency index).

The coefficients of discharge were calculated based on the pressure drop and the flow rate.

Therefore, the purpose of this chapter is to present the:

- rheological constants obtained for the fluids under investigation,
- pressure variation in the meters, and
- discharge coefficients versus Reynolds number and their statistical approaches.

4.2 Determination of rheological constants

The non–Newtonian fluids tested were CMC at various concentrations and the mixture of CMC 2% and xanthan gum (XG) solutions. Rheological constants obtained for non-Newtonian fluids are presented for CMC 2% concentration by mass (63.46 kg of CMC for 170 l volume water and 629 g XG in 170 l of CMC 2% at two different days). The objective of this section is to explain how the rheological constants were obtained.

4.2.1 Fitting the pseudo plastic model

The power law model was fitted to wall shear stress (τ_0) against pseudo shear rate (8V/D) data to determine the rheological constants n and K of CMC 2%, and the mixture of CMC 2% and XG.

A pseudo shear diagram of CMC at various concentrations and a mixture of CMC 2% and XG is given in Figure 4.1.

Figure 4.1 illustrates that the addition of XG simultaneously increases the viscosity and shear stresses of the solution. The same solution has been tested on two different days; it can be seen that the rheological parameters are not constant, owing to the hydrating properties of XG. However, the rheological parameters were checked during and after the test period and were not affected for the duration of the tests. This was done by repeating pressure drop measurements at specific flow rates during the test in a random manner. These were always found to be repeatable. It was only when left overnight that the rheological properties changed significantly.

Table 4.1 gives the different rheological constants used in this study for the fluid tested. It was observed that K increases, when n decreases with the concentration and increase in density of the solution.

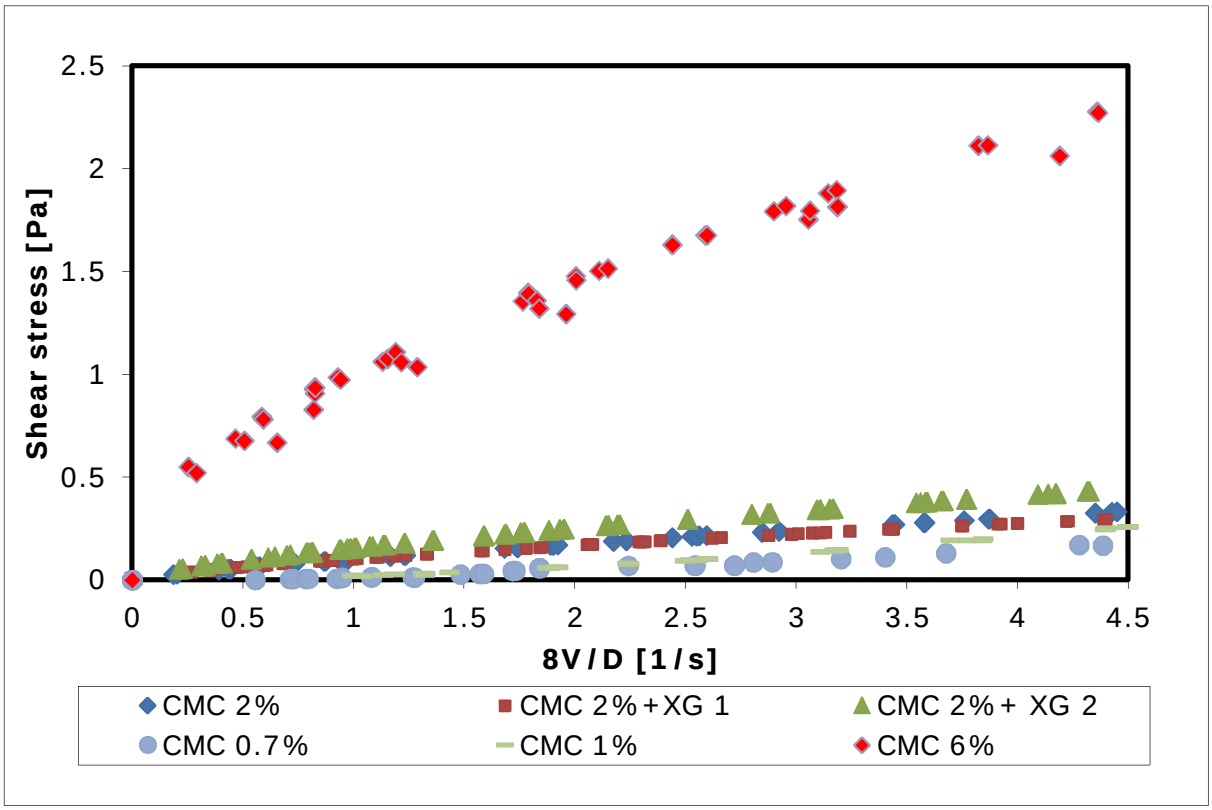

Figure 4.1: Pseudo shear diagram of various fluids used

The Rabinowitsch-Mooney relation Equation 2.25 and Equation 2.27 were used for the transformation of the rheological constants to the true values.

Table 4.1: Rheological constants of testing fluids

	CMC 0.7%	CMC 1%	CMC 2% +XG day 1	CMC 2% +XG day 2	CMC 6%
K [Pa.s^n]	0.074	0.082	0.103	0.323	2.20
n	0.740	0.726	0.710	0.675	0.594
Density [kg/m^3]	1000	1007	1013	1015	1031

4.2.2 Friction factor versus Metzner and Reed generalised Reynolds number

The calculated friction factor was compared with the theoretical friction factor, Equation 2.45, for laminar and Equation 2.48 for turbulent flow.

Figure 4.2 shows a friction factor chart for a CMC solution at different concentrations and a mixture of CMC 2% with XG respectively. It was found that 82% of reliable experimental friction factor data fell within ± 20% of the calculated friction factor; this confirms the validity and degree of accuracy of the test equipment and the experimental techniques applied during this work.

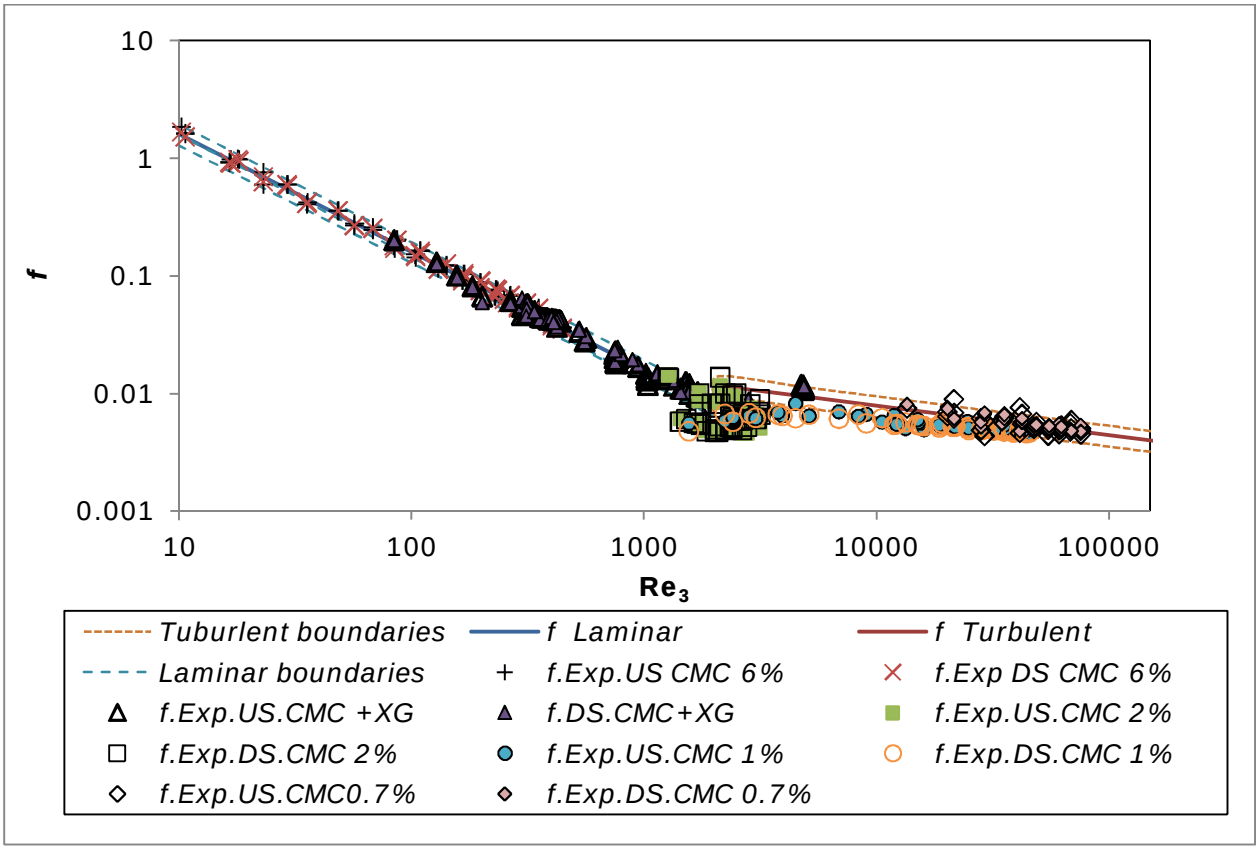

Figure 4.2: Friction factor comparison for various solutions of fluids used

4.3 Permanent pressure loss evaluation

The pressure variation profile through different C-D tubes and venturi tube are presented in this section.

Figures 4.3(a) to 4.3(f) show figures of approximate pressure fluctuations at 2.00l/s through different C-D tubes at different angles, 15°, 30° and 45° and beta ratio of 0.5, 0.6 and 0.7, as well as for a classical Venturi meter ISO 5167, with beta ratio 0.6.

For each pipe, the non-dimensionalised axial distances and the distances from the first point of the differential pressure meter were recorded as illustrated in Figures 4.3(a) to 4.3 (f). Five points were used to record the static pressure for

the C-D tubes as shown in Figure 1.1 and two points for the Venturi meter as illustrated in Figure 3.15. The negative points for the non-dimensionalised axial distance refer to the points before the throat.

From Figure 4.3, it can be seen that the pressure profile shows that there is no pressure recovery for C-D tubes at 45°. At constant beta ratio, the decrease of angle augments the pressure recovery and there is almost full pressure recovery at 15°. At a constant angle of 15° and a different beta ratio, the pressure recovery is more pronounced at the smallest angle, but there is no significant difference of pressure recovery among them. The Venturi meter shows a recovery in pressure for a long diverging section.

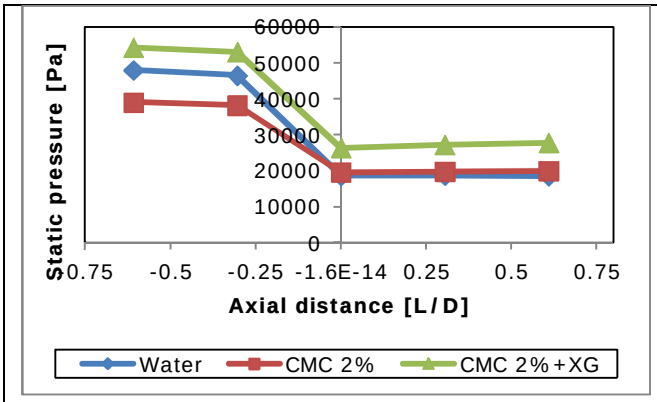

a. C-D tube with β=0.5; θ=45° and L= 1.21D

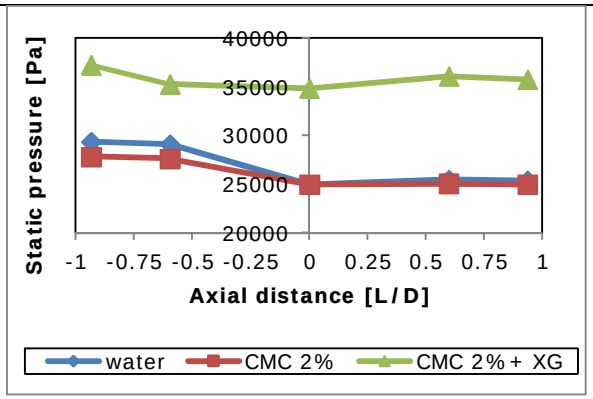

b. C-D tube with β=0.5; θ=30° and L=1.9D

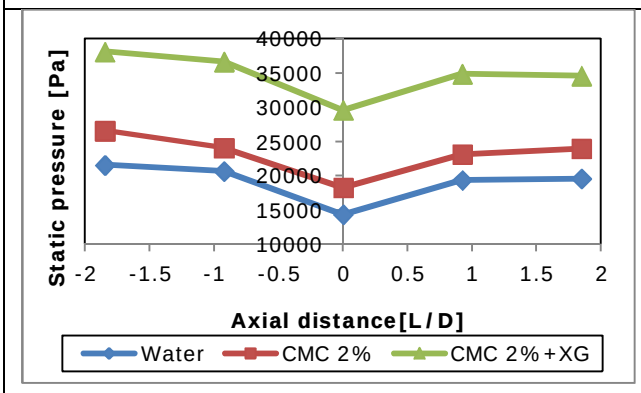

c. C-D tube with β=0.5; θ=15° and L=3.8D

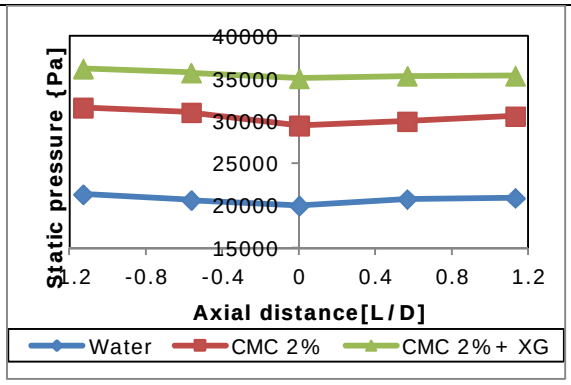

d. C-D tube with β=0.7; θ=15° and L=2.3D

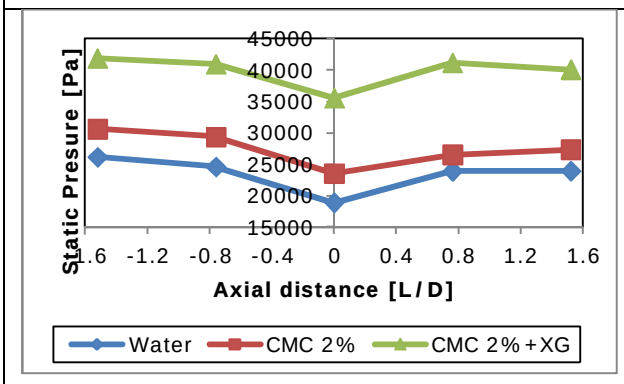

e. C-D tube with β=0.6; θ=15° and L=3.04D

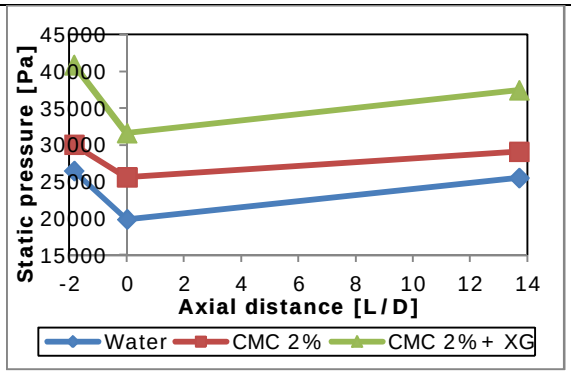

f. Classical Venturi meter with β=0.6; andL=7.28D

Figure 4.3: Pressure fluctuations for various DP flow meters used

To quantify the illustration shown in Figure 4.3, a typical method to measure the permanent pressure loss in a differential pressure flow meter is to state a

percentage of the differential pressure created at a given flow rate, which is expressed in Equation 2.3 with the results given in Table 4.2.

Table 4.2: Percentage of differential pressure for different C-D tubes

C-D tube flow meter	ΔP%
β=0.5; θ=45° and L=1.21D	99
β=0.5; θ=30° and L=1.90D	85
β=0.5; θ=15° and L=3.80D	32
β=0.6; θ=15° and L=3.04D	37
β=0.7; θ=15° and L=2.30	39

The percentage pressure drop increases when the length of the C-D tube decreases. It can be seen that there is almost no pressure recovery in the 45^{o} angle at beta ratio of 0.5.

Table 4.2 shows that at constant beta ratio of 0.5, the permanent pressure drop increases with the increase of 3 different angles (15°, 30° and 45°.) For this particular study, there is a good agreement at 15° in the 0.5 (15-15) with a percentage pressure drop of 32%. But at a constant angle, the permanent pressure drop increases with the increase of beta ratio ranging from 0.5 to 0.7. Again at small beta ratio, there is less permanent pressure drop. But the evaluation and selection of the perfect differential pressure flow meter depends on many factors and the permanent pressure drop is only one of them.

4.4 Evaluation of discharge coefficient

Over the course of this study, the discharge coefficient data were determined for various Reynolds numbers across the five C-D tubes and Venturi tube under consideration using water, CMC 2%, and the mixture of CMC 2% and XG. The tests conducted used 10 readings for each Reynolds number ranging from 380 to 150000.

4.4.1 Analysis of repeatability

Figures 4.4 to 4.9 illustrate how much the deviation of C_d data is from the average. The analysis covered 10 tests run at each Reynolds number for water.

Equation 2.12 is used to quantify the deviation of the C_d data; smaller deviations express the characteristic of good repeatability.

4.4.1.1 C-D tube with β=0.5 and θ=45°

Figure 4.4 shows how much deviation exists from the average C_d value for a C-D tube with β=0.5 and θ=45° using water.

Table 4.3 shows the standard deviation of C_d values as a function of Reynolds number and fluids used for a C-D tube with β=0.5 and θ=45°.

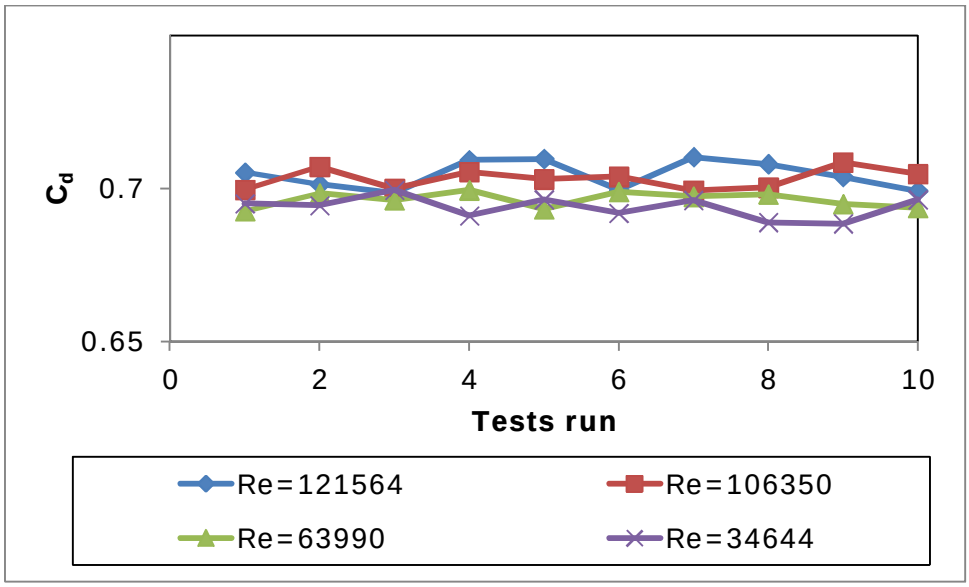

Figure 4.4: Variation of C_d values for C-D tube β=0.5 and θ=45° using water

Table 4.3: Standard deviation for C-D tube β=0.5 and θ=45°

Water experimental Re	**121563**	**106350**	**63990**	**34644**
Standard deviation	0.004	0.003	0.003	0.004
CMC experimental Re	**23595**	**10341**	**4212**	
Standard deviation	0.005	0.004	0.003	
CMC+XG experimental Re	**2759**	**1696**	**758**	**309**
Standard deviation	0.006	0.005	0.005	0.010

4.4.1.2 C-D tube with β=0.5 and θ=30°

Figure 4.5 shows the variation of C_d data for C-D tube β=0.5 and θ=30° with water.

Table 4.4 presents variation at different Reynolds numbers for C-D tube β=0.5 and θ=30° with different fluids.

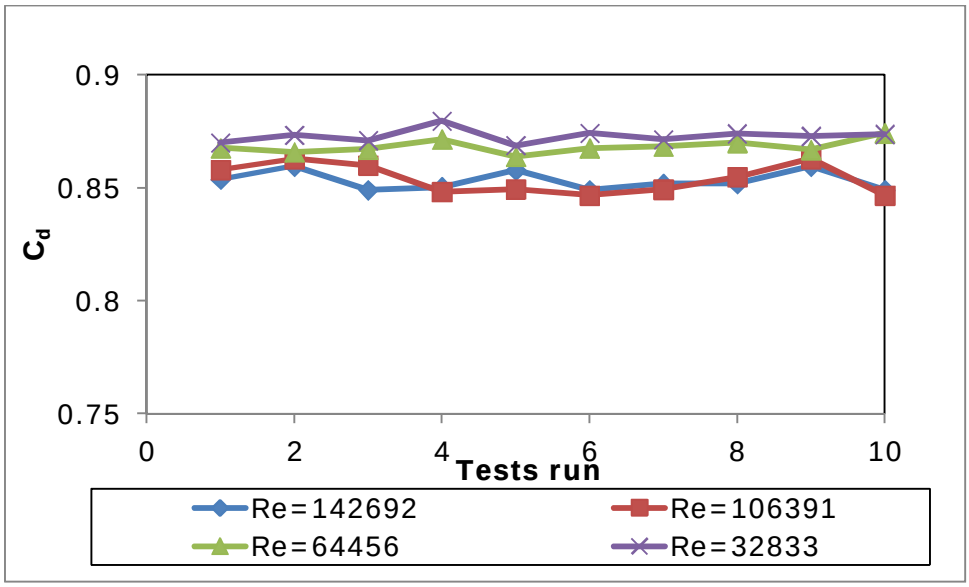

Figure 4.5: Variation of C_d values for C-D tube β=0.5 and θ=30° using water

Table 4.4: Standard deviation for C-D tube β=0.5 and θ=30°

Water experimental Re	**142693**	**106391**	**64456**	**32834**
Standard deviation	0.004	0.007	0.003	0.003
CMC experimental Re	**22441**	**10485**	**4292**	
Standard deviation	0.006	0.008	0.011	
CMC + XG experimental Re	**2450**	**1595**	**756**	**382**
Standard deviation	0.010	0.012	0.011	0.011

4.4.1.3 C-D tube with β=0.5 and θ=15°

Figure 4.6 shows the variation of C_d values in a C-D tube β=0.5 and θ=15° with water.

Table 4.5 presents the standard deviation as a function of the Reynolds number and different fluids used for C-D tube β=0.5 and θ=15°.

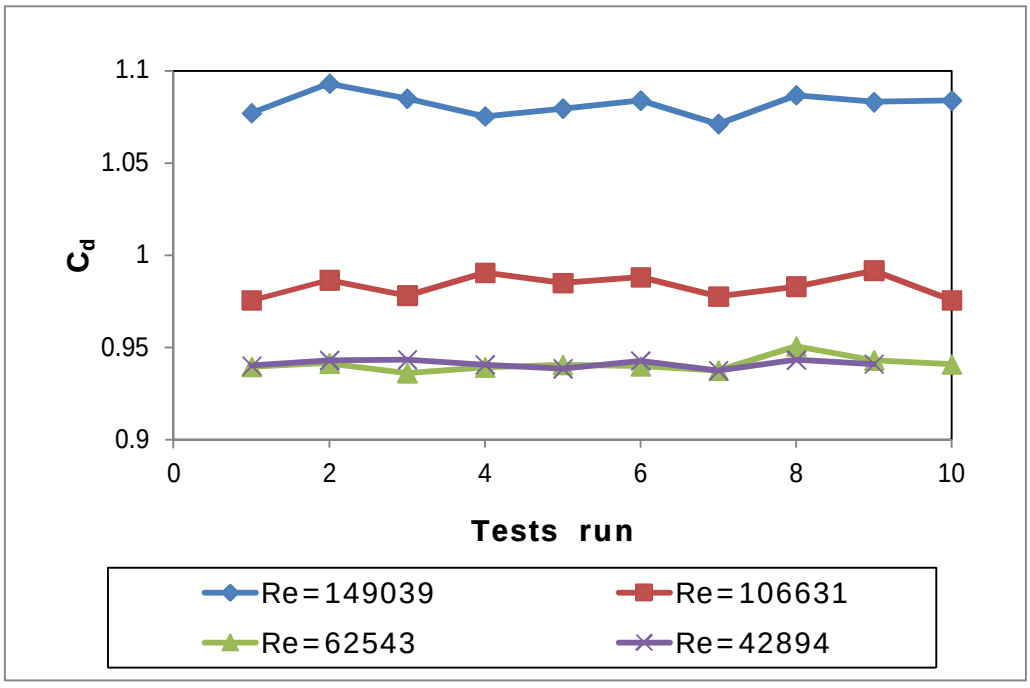

Figure 4.6: Variation of C_d values for C-D tube β=0.5 and θ=15° using water

Table 4.5: Standard deviation for C-D tube β=0.5 and θ=15°

Water experimental Re	**149040**	**106631**	**62543**	**42894**
Standard deviation	0.006	0.006	0.004	0.002
CMC experimental Re	**35354**	**17923**	**9014**	**4786**
Standard deviation	0.005	0.005	0.006	0.005
CMC +XG experimental Re	**2570**	**1473**	**915**	**403**
Standard deviation	0.009	0.011	0.008	0.009

4.4.1.4 C-D tube with β=0.6 and θ=15°

Figure 4.7 illustrates the variation of C_d values in C-D β=0.6 and θ=15° using water.

Standard deviations as a function of the Reynolds number with different fluids for C-D β=0.6 and θ=15° are presented in Table 4.6.

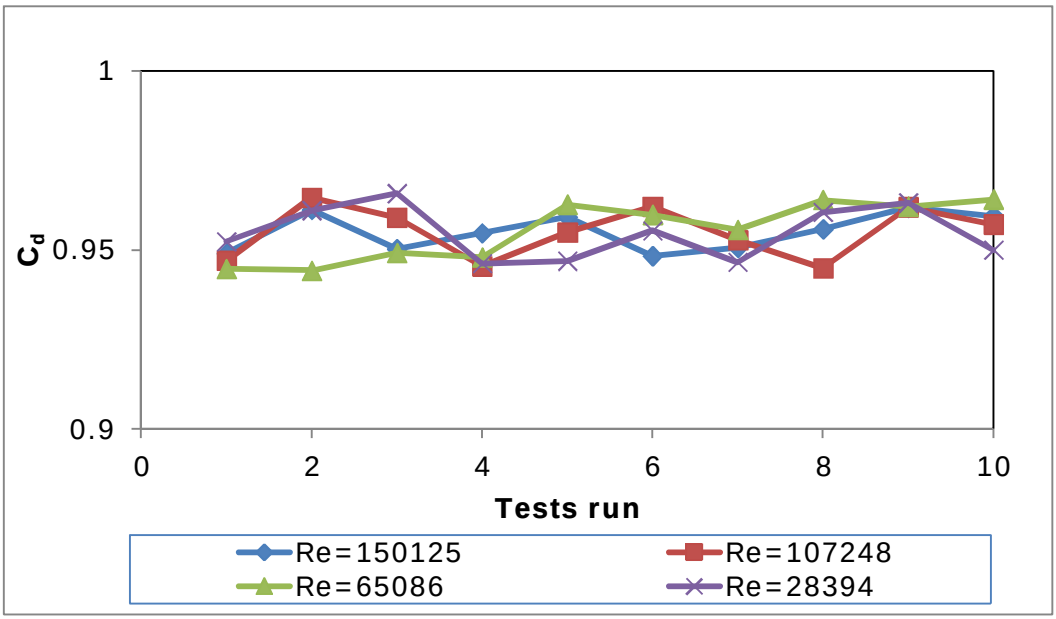

Figure 4.7: Variation of C_d values for C-D tube β=0.6 and θ=15° using water

Table 4.6: Standard deviation for C-D tube β=0.6 and θ=15°

Water experimental Re	**150125**	**107249**	**65086**	**28394**
Standard deviation	0.005	0.007	0.008	0.007
CMC experimental Re	**14549**	**6250**	**4297**	**1274**
Standard deviation	0.016	0.025	0.011	0.009
CMC +XG experimental Re	**2397**	**1531**	**794**	**323**
Standard deviation	0.011	0.011	0.011	0.009

4.4.1.5 C-D tube with β=0.7 and θ=15°

Figure 4.8 shows the variation of C_d values observed with water testing fluid for C-D tube β=0.7 and θ=15°.

Table 4.7 presents the standard deviation at different Reynolds numbers for C-D tube β=0.7 and θ=15° with different fluids.

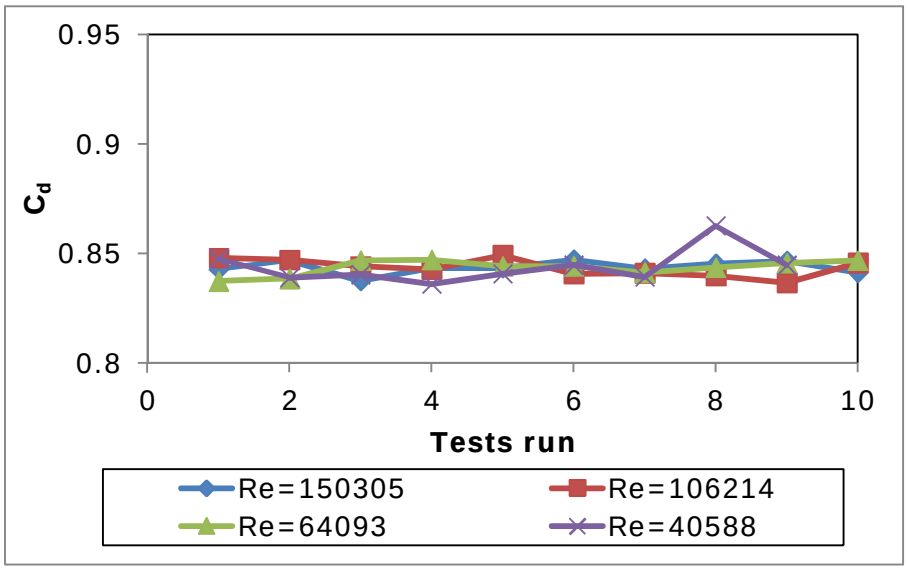

Figure 4.8: Variation of C_d values for C-D tube β=0.7 and θ=15° using water

Table 4.7: Standard deviation for C-D tube β=0.7 and θ=15°

Water experimental Re	**150305**	**106214**	**64093**	**40589**
Standard deviation	0.003	0.004	0.003	0.008
CMC experimental Re	**29837**	**16276**	**4822**	
Standard deviation	0.005	0.006	0.006	
CMC +XG experimental Re	**2689**	**1450**	**824**	**334**
Standard deviation	0.008	0.008	0.011	0.009

4.4.1.6 Classical Venturi with β=0.6

Figure 4.9 shows how much variation exists from the average C_d in the classical Venturi with β=0.6 for water.

The standard deviation at various Reynolds numbers for a classical Venturi tube with different fluids used is presented in Table 4.8.

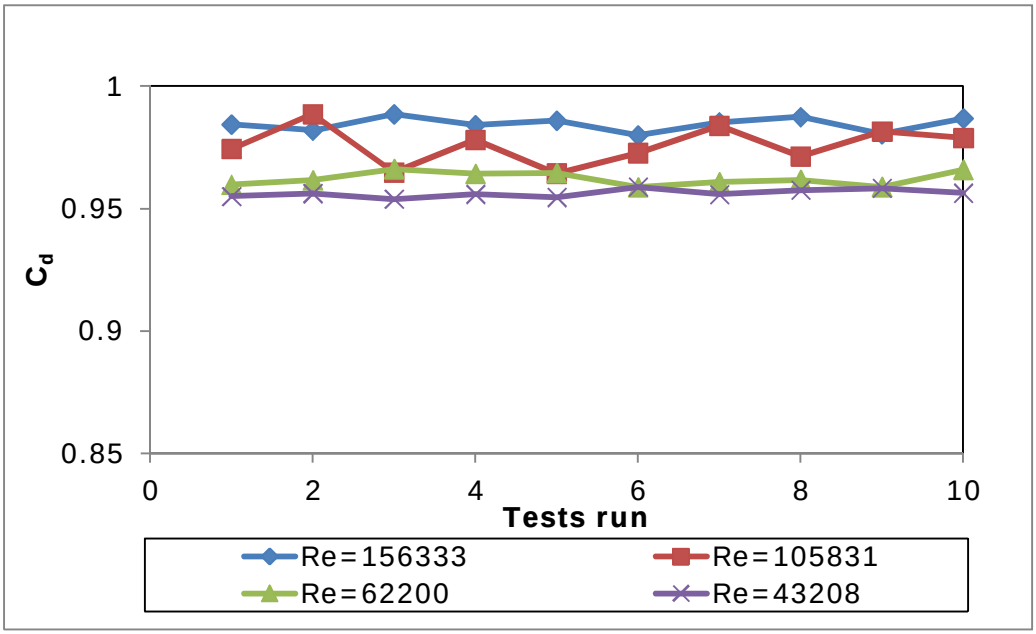

Figure 4.9: Variation of C_d values for classical Venturi using water

Table 4.8: Standard deviation for classical Venturi

Water experimental Re	**156333**	**105831**	**62200**	**43208**
Standard Deviation	0.003	0.008	0.003	0.002
CMC experimental Re	**34093**	**19796**	**9731**	**4000**
Standard Deviation	0.005	0.006	0.003	0.009
CMC +XG experimental Re	**3129**	**1761**	**688**	**180**
Standard Deviation	0.020	0.020	0.018	0.014

4.4.2 Analysis of mean discharge coefficient versus Reynolds number

The results are presented in terms of the discharge coefficient as a function of the Reynolds number on semi-log graphs.

Figure 4.10 to 4.15 show the discharge coefficient data, the average values and the range of uncertainty.

Table 4.9 to 4.14 present uncertainties in discharge coefficient for different fluids and tubes used at various Reynolds number.

4.4.2.1 C-D tube with β=0.5 and θ=45°

Figure 4.10 shows the discharge coefficient data for a C-D tube with diameter ratio, β=0.5, symmetrical converging-diverging angle θ=45° and a length of 1.61D.

It was observed from Fig. 4.10 that the trend for discharge coefficient data increases with the Reynolds number in the range of Re<750; the discharge coefficient became nearly constant at an average value of 0.7 at Reynolds number above 750.

The maximum uncertainty of ±3.01% for C_d value was found at Re=309, and a minimum uncertainty of ±0.76% for C_d value at Re=63990 with water, as presented in Table 4.9.

Table 4.9: Uncertainty in C_d for C-D tube β=0.5 and θ=45°

Water experimental Re	121563	106350	63990	34644
Mean C_d	0.704	0.703	0.696	0.694
Uncertainty +/- (U %)	1.31%	0.89%	0.76%	1.09%
CMC experimental Re	23595	10341	4212	
Mean C_d	0.724	0.707	0.715	
Uncertainty +/- (U %)	1.38%	1.28%	0.90%	
CMC+XG experimental Re	2759	1696	758	309
Mean C_d	0.708	0.714	0.700	0.667
Uncertainty +/- (U %)	1.91%	1.37%	1.40%	3.01%

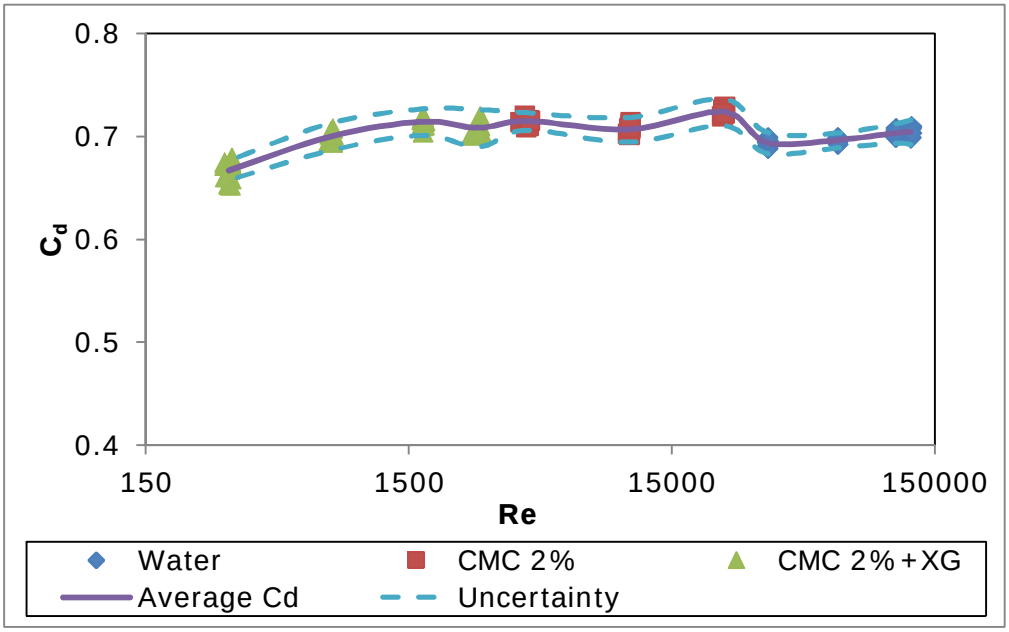

Figure 4.10: Discharge coefficient data versus Reynolds number for β=0.5 and θ=45°

4.4.2.2 C-D tube with β=0.5 and θ=30°

Discharge coefficient data for C-D tube β=0.5; θ=30° and the length of 1.90D are presented in Figure 4.11.

Two zones can be observed from the experimental data. For Re<22440, the C_d value increases from 0.799 to a peak of 0.896. From Re>22440, the C_d value decreases from the peak to the average value of 0.853.

Table 4.10 shows that a maximum uncertainty of ±3.08% was obtained at Re=1595 and the minimum of ±0.72% at Re=64456. These values of uncertainty represent the range of uncertainty values obtained for this C-D tube geometry.

Table 4.10: Uncertainty in the C_d for C-D tube β=0.5 and θ=30°

Water experimental Re	**142693**	**106391**	**64456**	**32834**
Mean C_d	0.853	0.854	0.868	0.873
Uncertainty +/- (U %)	1.06%	1.63%	0.72%	0.83%
CMC experimental Re	**22441**	**10485**	**4292**	
Mean C_d	0.896	0.861	0.860	
Uncertainty +/- (U %)	1.49%	2.03%	2.67%	
CMC + XG experimental Re	**2450**	**1595**	**756**	**382**
Mean C_d	0.844	0.844	0.824	0.799
Uncertainty +/- (U %)	2.38%	3.08%	2.72%	2.85%

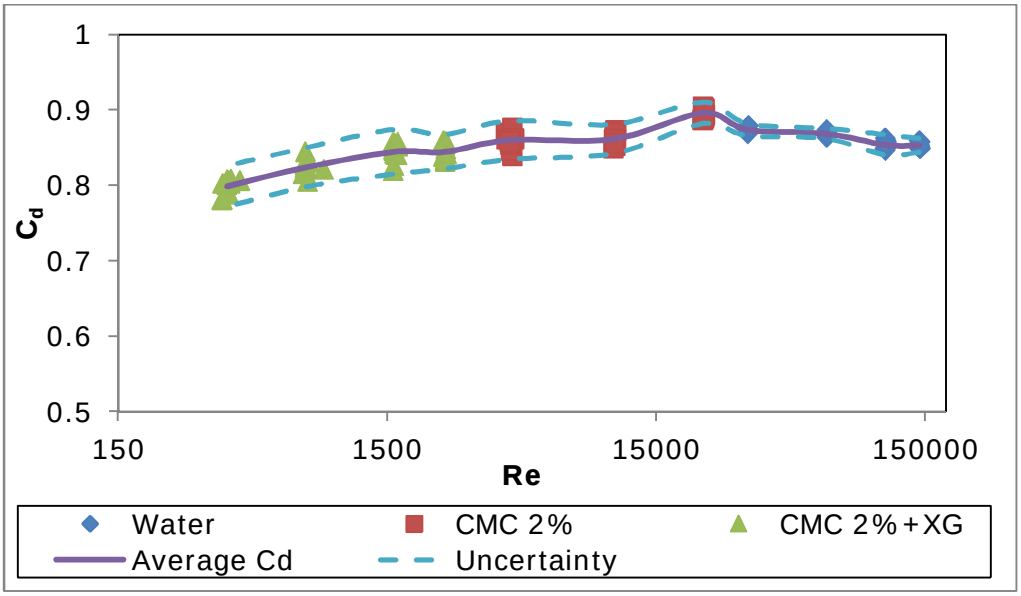

Figure 4.11: Discharge coefficient data versus Reynolds number for C-D tube β=0.5 and θ=30°

4.4.2.3 C-D tube with β=0.5 and θ=15°

The discharge coefficient data for the longest C-D tube with 3.8D length, and diameter ratio β=0.5 and θ=15°, are presented in Figure 4.12.

The figure shows three different trends in discharge coefficient variation for these regions:

- For Re<2600, the C_d value increased with Reynolds number from 0.828 to 0.923.
- 42800<Re>2600, the C_d value became nearly constant with an average value of about 0.960.
- For Re>42800, the C_d value increased with Reynolds number from 0.941 to 1.082.

The maximum uncertainty of ± 2.50% at Re=1473 and a minimum of ± 0.43% at Re= 42894 are shown in Table 4.11.

Table 4.11: Uncertainty in C_d for C-D tube β=0.5 and θ=15°

Water experimental Re	**149040**	**106631**	**62543**	**42894**
Mean C_d	1.082	0.983	0.941	0.941
Uncertainty +/- (U %)	3.65%	1.24%	0.89%	0.43%
CMC experimental Re	**35354**	**17923**	**9014**	**4786**
Mean C_d	0.969	0.972	0.909	0.956
Uncertainty +/- (U %)	1.09%	1.03%	1.28%	1.17%
CMC+XG experimental Re	**2570**	**1473**	**915**	**403**
Mean C_d	0.955	0.922	0.909	0.828
Uncertainty +/- (U %)	2.01%	2.50%	1.81%	2.36%

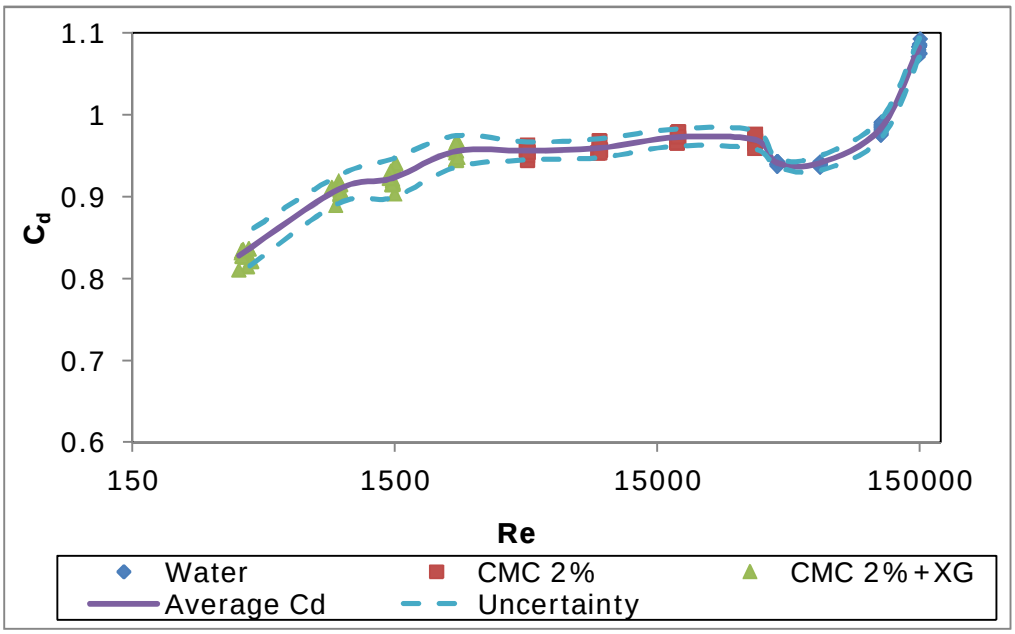

Figure 4.12: Discharge coefficient data versus Reynolds number for C-D tube β=0.5 and θ=15°

4.4.2.4 C-D tube with β=0.7 and θ=15°

Figure 4.13 shows discharge coefficient data for a C-D tube with diameter ratio, β=0.7, symmetrical converging-diverging angle, θ=15°, and length of 2.3D.

It is observed in Figure 4.13 that the discharge coefficient increases with the Reynolds number in the range of Re<2600 from 0.645 to 0.889. The discharge coefficient became nearly constant with the average value of about 0.890 in the range of 2600<Re<40500. From Re>40500, the value of the discharge coefficient drops and becomes nearly constant at an average value of 0.840.

Table 4.12 presents the maximum uncertainty of ±3.04% at Re=824 and a minimum of ±0.74% at 150305.

Table 4.12: Uncertainty in C_d for C-D tube β=0.7 and θ=15°

Water experimental Re	**150305**	**106214**	**64093**	**40589**
Mean C_d	0.844	0.844	0.844	0.845
Uncertainty +/- (U %)	0.74%	1.01%	0.87%	1.96%
CMC experimental Re	**29837**	**16276**	**9286**	**4822**
Mean C_d	0.888	0.891	0.892	0.901
Uncertainty +/- (U %)	1.10%	1.41%	1.38%	1.29%
CMC+ XG experimental Re	**2689**	**1450**	**824**	**334**
Mean C_d	0.889	0.848	0.769	0.645
Uncertainty +/- (U %)	1.79%	2.06%	3.04%	2.79%

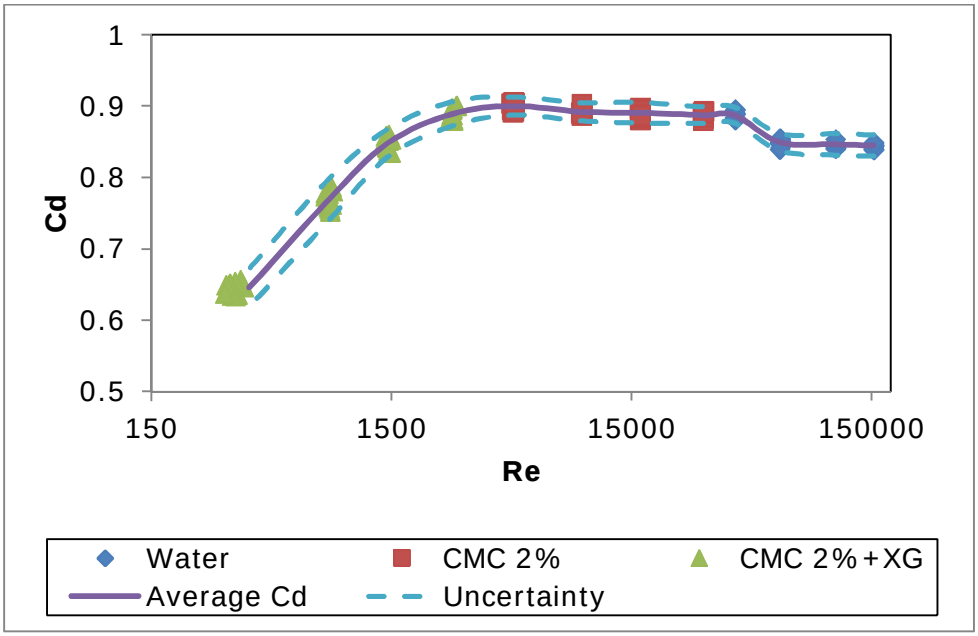

Figure 4.13: Discharge coefficient data versus Reynolds number for C-D tube β=0.7 and θ=15°

4.4.2.5 C-D tube with β=0.6 and θ=15°

Discharge coefficient data for C-D tube β=0.6; θ=15° and the length of 3.04D are presented in Figure 4.14.

It can be observed that for Re<15000, the C_d is dependent on the Reynolds number decreasing from 0.955 to 0.766. Above Re of about 15000, the C_d becomes constant at an average value of 0.955.

A maximum uncertainty of ±5.62% at Re=6250, and a minimum of 1.13% at 150125, are presented in Table 4.13.

Table 4.13: Uncertainty in C_d for C-D tube β=0.6 and θ=15°

Water experimental Re	**150125**	**107248**	**65086**	**28393**
Mean C_d	0.955	0.955	0.955	0.955
Uncertainty +/- (U %)	1.13%	1.60%	1.80%	1.64%
CMC experimental Re	**14549**	**6250**	**4297**	**1274**
Mean C_d	0.951	0.949	0.938	0.938
Uncertainty +/- (U %)	3.58%	5.62%	2.48%	1.96%
CMC+XG experimental	**2397**	**1531**	**794**	**323**
Mean C_d	0.932	0.925	0.868	0.766
Uncertainty +/- (U %)	1.20%	1.15%	1.28%	1.22%

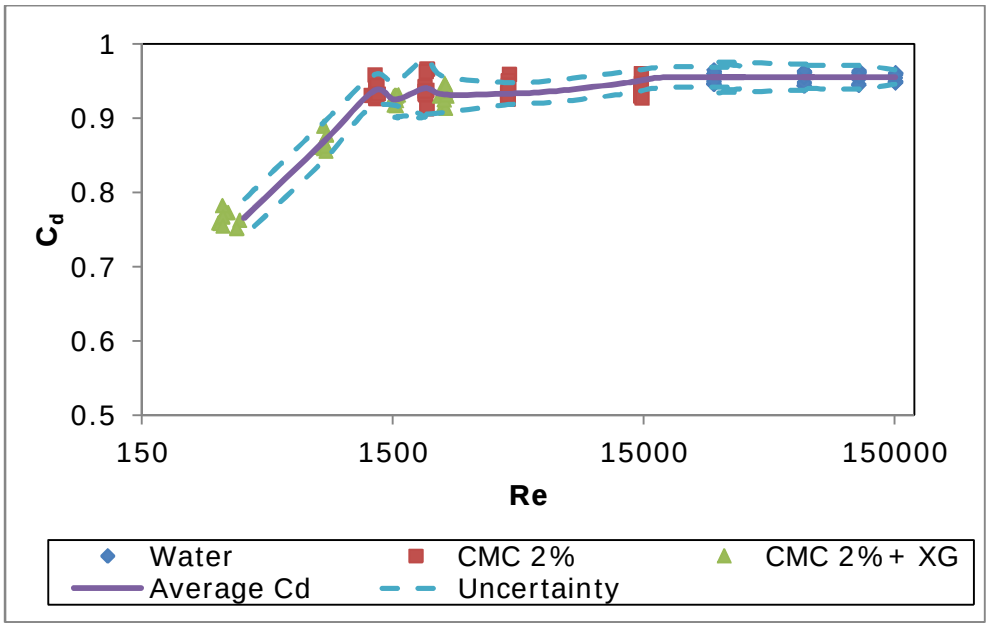

Figure 4.14: Discharge coefficient data versus Reynolds number for C-D tube β=0.6 and θ=15°

4.4.2.6 Classical Venturi with β=0.6

Figure 4.15 shows the discharge coefficient experimental data across the classical Venturi tube with a length of 7.28D.

Discharge coefficient data decrease with Reynolds number from a value of 0.984 to 0.818 for Reynolds number ranging between 380 and 150,000. A significant range of uncertainty in discharge coefficient values is observed for Re<3000. Maximum uncertainty of ±4.63% at Re=1761 and minimum of ±0.35% at Re=43208, are presented in Table 4.14.

Table 4.14: Uncertainty in C_d for classical Venturi

Water experimental Re	**156333**	**105831**	**62200**	**43208**
Mean C_d	0.984	0.976	0.962	0.956
Uncertainty +/- (U %)	0.63%	1.70%	0.58%	0.35%
CMC experimental Re	**34093**	**19796**	**9731**	**4000**
Mean C_d	0.956	0.955	0.947	0.929
Uncertainty +/- (U %)	1.00%	1.29%	0.66%	1.95%
CMC+XG experimental Re	**3129**	**1761**	**688**	**180**
Mean C_d	0.920	0.903	0.885	0.818
Uncertainty +/- (U %)	4.56%	4.63%	4.19%	3.59%

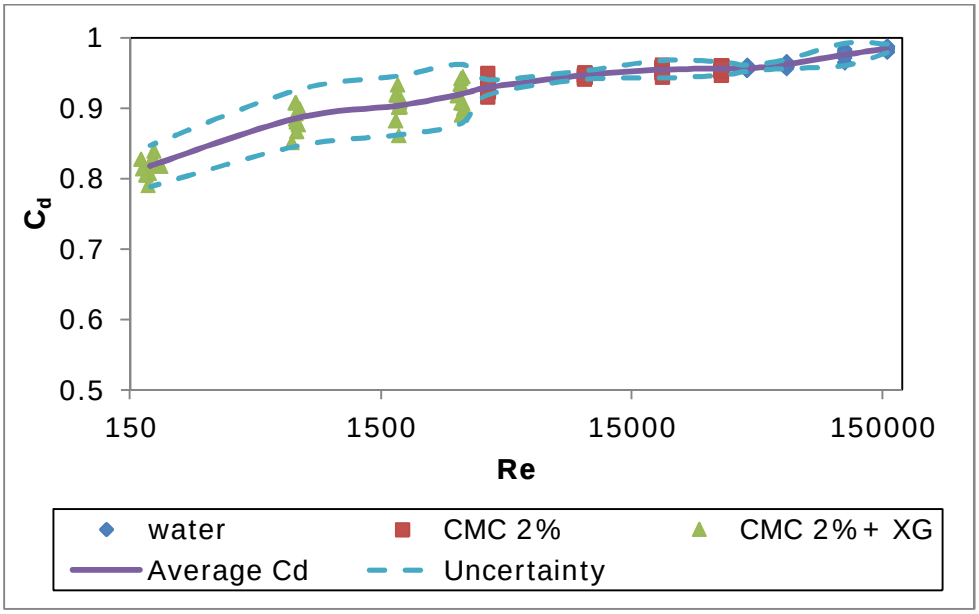

Figure 4.15: Discharge coefficient data versus Reynolds number for classical Venturi β=0.6

4.5. Conclusion

This chapter presented and discussed the results generated from experimental investigations carried out through different geometries of C-D tubes and classical Venturi.

The efficiency of the equipment has been validated with 82% of data within ±20% reliable friction factor data.

The pressure profiles have shown that when the angle of the converging and diverging sections decreases, the symmetry in the pressure profile between the converging and diverging sections becomes significant.

The evaluation of permanent pressure losses has shown that the permanent pressure loss decreases with the angle of the C-D tube. The smaller angle was found to have a percentage pressure drop of less than 40%, while a C-D tube with an angle greater than 30° had a percentage pressure drop greater than 85%.

C-D tube performance was described by the dimensionless numbers of discharge coefficient and Reynolds number. To achieve the flow measurement uncertainty, a quantitative analysis of error in determination of C_d values was carried out.

The repeatability of discharge coefficient 10 times at each low rate was evaluated with the standard deviation σ_x. It was seen that σ_x at a low Reynolds number is slightly higher and reduces with an increase in the Reynolds number.

The next chapter will compare the more efficient C-D tube, the Venturi tube and other existing differential pressure flow meters, as found in the literature.

Discussion of Results

5.1 Introduction

In this chapter, trends in data from the present study are discussed and compared with the results from previous studies.

5.2 Trend in permanent pressure loss data

Figure 5.1 shows the comparison between the permanent pressure loss data of a C-D tube (Table 4.2) with a smaller angle and existing differential flow meter data from Miller et al. (2009).

C-D tubes with smaller angles performed much better than the nozzle, V-cone and orifice flow meters. This correlates with Miller et al. (2009), who showed that the permanent pressure increases with the exit angle.

The present data were not in agreement with Miller et al. (2009) in terms of the diameter ratio parameter. The permanent pressure loss for C-D tubes increases with diameter ratio parameter in contrast with the existing differential flow meter.

It can be seen that the longer the diverging section, the better the permanent pressure loss.

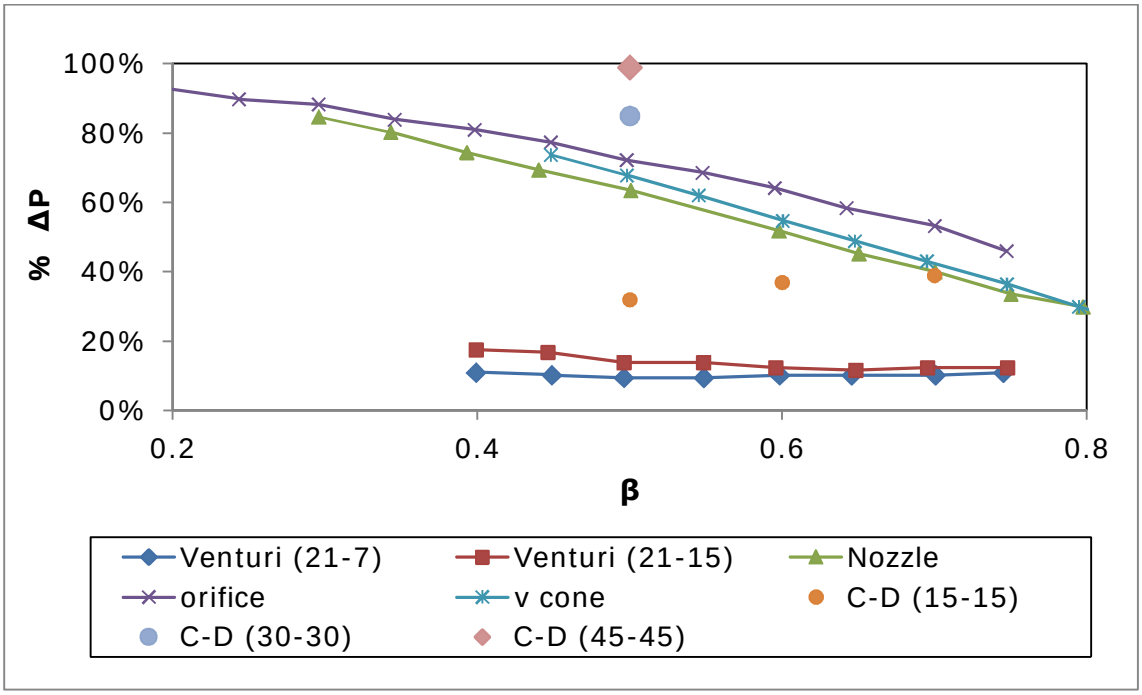

Figure 5.1: Comparison between C-D tube flow meters and the existing DP flow meters

5.3 Average discharge coefficient data comparison for various DP flow meters used

Figure 5.2 presents the average C_d values for different flow meters used at various Reynolds numbers between 380 and 150000. The mean value of the coefficient of discharge (C_d) was calculated using Equation 2.11. It can be seen that the C_d values at 15° drop earlier than those at 30° and 45° when viscous forces become predominant, and they increase with increasing beta ratio. C_d is independent on Re for Re > 3000 and depends on angles and beta ratio.

In agreement with Reader-Harris et al. (2001), from an analysis of data for non-standard Venturi, the discharge coefficient of C-D with a convergent angle greater than the classical Venturi was found to be smaller in the case of C-D 0.5 (30-30) and C-D 0.5 (45-45). This is similar for C-D tubes with a convergent

angle smaller than the classical Venturi in the case of the C-D tube of 15° with different β ratios. According to Laribi et al. (2001), the performance flow meter requires C_d closer to unity. It can be seen that C-D 0.5 (15-15), C-D 0.6 (5-15) and Venturi tube are more efficient in this context.

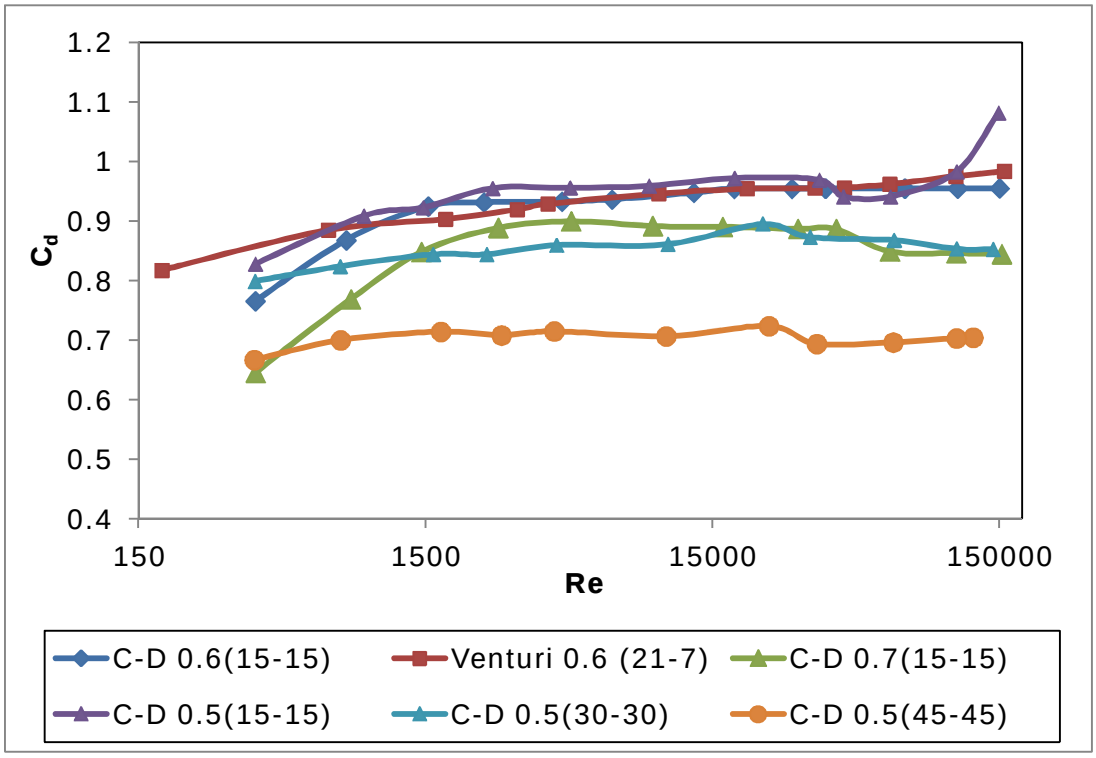

Figure 5.2: Average C_d versus Reynolds number in various C-D tubes

The evaluation of the mean C_d ±1% uncertainty allowed the identification of the Reynolds number range of applicability for each C-D tube. Table 5.1 presents the mean discharge coefficient obtained for each C-D tube and the Reynolds number range where C_d is independent of the Reynolds number.

From Table 5.1, it is seen that C-D tube β=0.6 with θ=15° presents a wide range of application.

Table 5.1: Mean C_d and its range of application

C-D tube	Mean C_d ±1% uncertainty	Range of application (Re)
β=0.5 with θ=45°	0.704	34,644 to 121,563
β=0.5 with θ=30°	0.853	106,391 to 142,693
β=0.5 with θ=15°	0.983	17,923 to 106,631
β=0.6 with θ=15°	0.955	6,228 to 150,125
β=0.7 with θ=15°	0.844	40,589 to 150,305

5.4 Trend in discharge coefficient data

The comparison of the results obtained in the current experimental investigation with the data found in the literature is one of the assessments of performance criteria of this work. The percentage error and percentage difference were calculated to estimate the difference between the data.

5.4.1 Comparison between two different data sets of C-D 0.6(15-15) and Classical Venturi tube

Figure 5.3 presents two different sets of experimental data collected during years 2012 and 2013 to confirm the performance of the C-D tube flow meter.

The one set of results obtained in 2012 shows an average C_d of 0.957 and the results from 2013 show a C_d of 0.99, which indicate that the C-D tube is

sensitive to installation effects. It is, however, very clear in both sets that C_d is independent of the Reynolds number for C-D tube compared to the venturi.

It can be seen that the data for the mixture of XG and CMC experiment decrease more rapidly than for the CMC only. This is similar to results emanating from Miller et al. (2009), when a flow of heavy oil and water through the Venturi meters tested, was found to decrease rapidly because of the fluid properties.

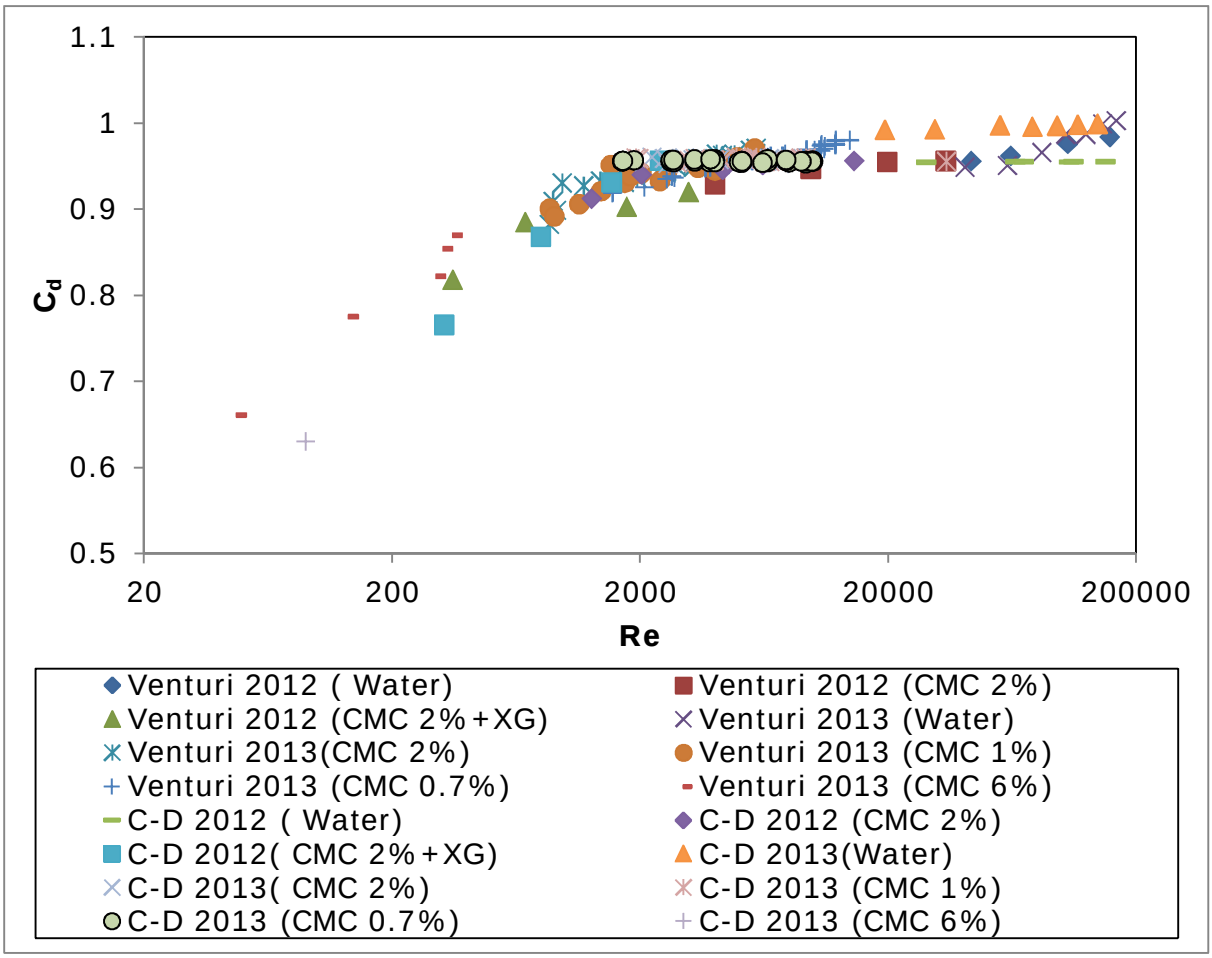

Figure 5.3: Comparison between two sets data of C-D 0.6 (15-15) and classical Venturi tube

5.4.2 Comparison with Reader-Harris and co-authors (2001)

Figure 5.4 presents the results for the standard Venturi tubes, where in two Venturi tubes having the same diameter ratio and different diameters, the maximum difference in mean discharge was found to be 0.57%

Using Equation 2.14, the percentage difference between the experimental work obtained in a venturi by Reader-Harris et al. (2001) and this work was 1.9%.

In agreement with ISO (2003), when 50mm ≤ D ≤ 250mm, 0.4≤ β ≤ 0.75 and $2\times10^5 \leq Re_D \leq 1\times10^6$, under these conditions the value of C_d is 0.995 with an uncertainty of ±1%.

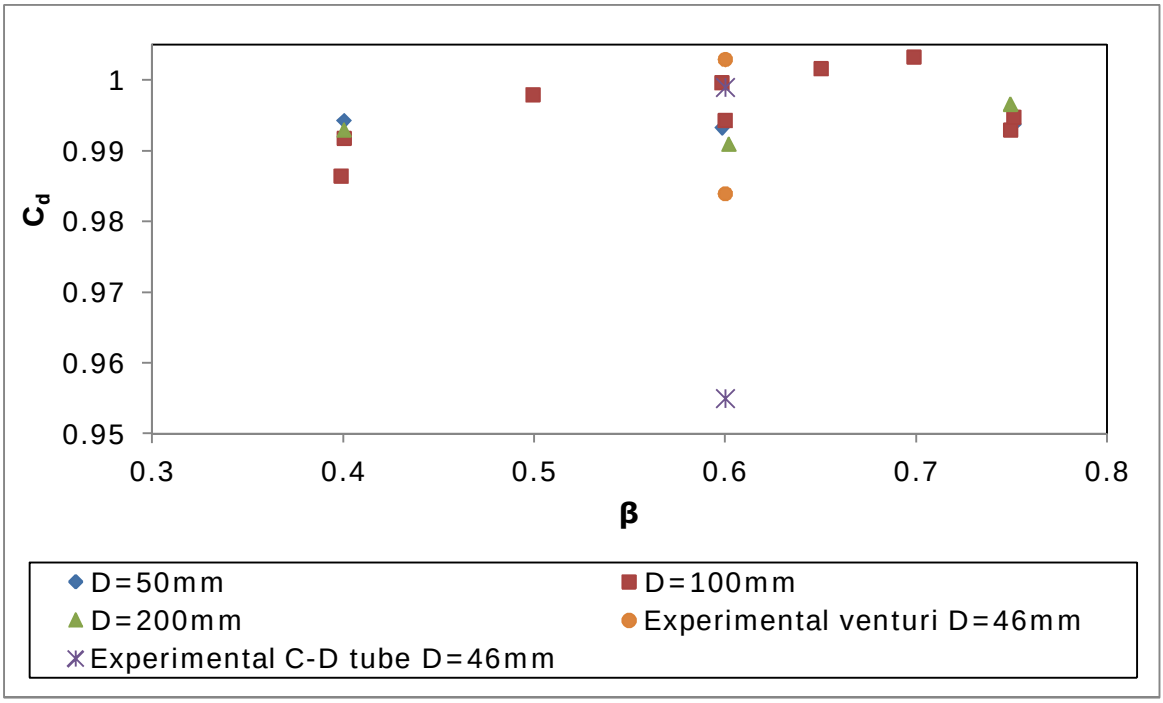

Figure 5.4: Average C_d for various pipe diameters versus diameter ratio

Figure 5.5 shows discharge coefficient data found in the range of $1.2\times10^5 < Re < 2\times 10^5$ for Venturi tubes with standard and non-standard convergent angles and the present work data compared with Equation 2.49.

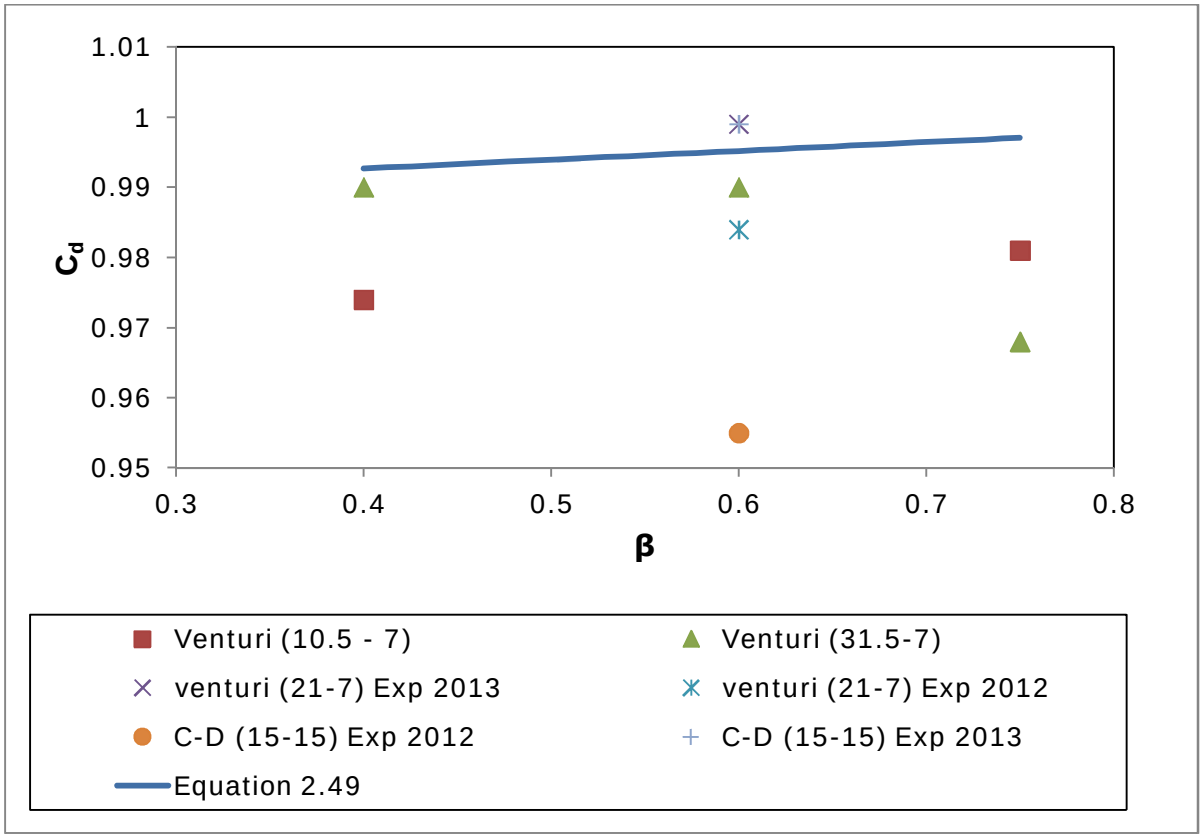

Figure 5.5: Comparison between experimental data: Reader-Harris et al. (2001) data and Equation 2.49

Table 5.2 presents the percentage errors obtained using Equation 2.14 between the discharge coefficient data found in this work and those found by Harris-Reader et al. (2001). Appreciable percentage errors were found between Equation 2.49 and the experimental data with the Venturi tube and C-D 0.6(15-15) of the 2013 experiments. This shows the reliability of the experimental results.

Table 5.2: Percentage error between experimental data and Equation 2.49

β	Experimental				Harris-Reader et al., 2001	
	C-D Tube (15-15)	C-D Tube (15-15)	Venturi (21-7)	Venturi (21-7)	Venturi (10.5-7)	Venturi (31.5-7)
	2012	2013	2012	2013		
0.40					1.89%	0.27%
0.60	4.04%	0.38%	1.12%	0.38%		0.52%
0.75					1.61%	2.91%

5.4.3 Comparison with Hollingshead et al. (2011)

Figure 5.6 presents the comparison between experimental data obtained through C-D tube, Venturi tube and the data of Venturi from Hollingshead et al. (2011). The Venturi smooth and Venturi sharp tubes are similar to the geometry of the CD tube. In these Venturi, the inlet smoothly transitioned to the throat with a parabolic cone and the other had what might be described as a segmented cone with two break points as it reduced from inlet to the throat. In terms of geometry, Hollingshead's Venturi had a much smaller length of straight pipe for the throat than the classical Venturi, but was still longer than the annular throat used in the C-D tube. Comparison of the results gives insight into the effect of this arrangement of the C-D tube throat on the discharge coefficient. It can be seen that C_d values of C-D tubes do agree with the CFD data of Venturi from Hollingshead et al. (2011) for Reynolds number greater than 2000. This demonstrates the accuracy of the experimental work conducted in this study and that the pressure measurements are not greatly affected by the throat arrangement of the C-D tube. This is of great encouragement as the annular throat design is significant in reducing the length of the flow meter.

The result for C_d is presented at various ranges of Reynolds numbers. The reason is that it is difficult to see the inconsistencies over the wide range of Re = 1 to 50,000,000. An average C_d value obtained for the C-D tube is 0.957±0.5% in the range of Re>1000, compared with C_d values of 0.96±1% for Hollingshead smooth Venturi in the range of Re = 5,000 to 75,000 and 0.96±1% in the range of Re = 10,000 to 50,000,000 for a sharp Venturi.

Below a Reynolds number of 1000, the C_d values showed strong dependence on the Reynolds number and decreased significantly for C-D tube and smooth and sharp Venturi tested by Hollingshead. The primary difference between the two modelled venturi was their respective inlet geometries. In one case the inlet smoothly transitioned to the throat using a parabolic cone and the other had what might be described as a segmented cone having two break points as it reduced from inlet to the throat.

Trends from the C-D tube in this range were found to be in parallel to Hollingshead's results. Hollingshead suggested CFD studies to be better suited to determine accurate discharge coefficients at low Reynolds numbers owing to the inconsistencies of experimental measurements because of low pressure drop, and this could be the reason for discrepancies observed.

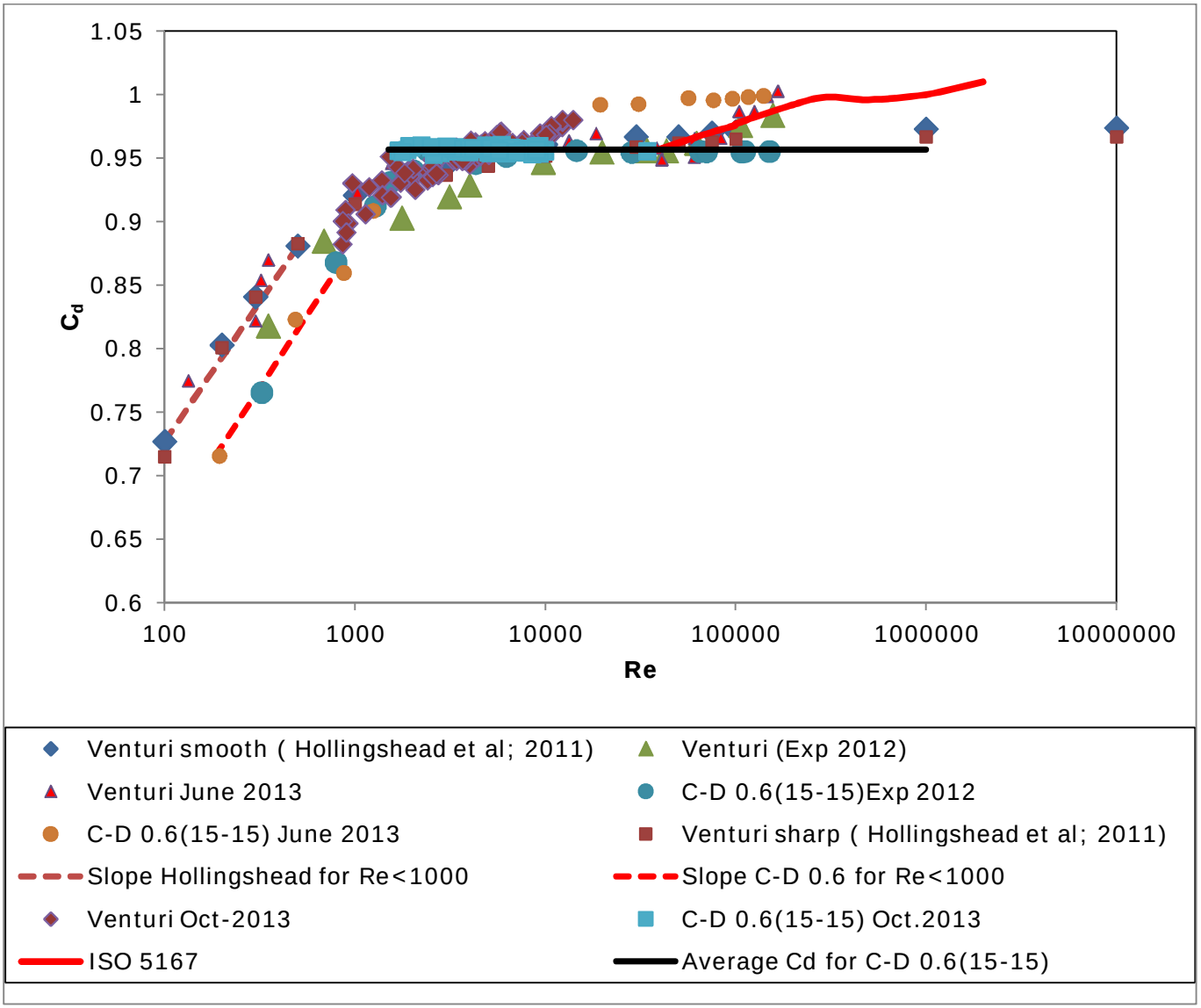

Figure 5.6: Comparison between present data and Hollingshead et al. (2011)

5.6. Conclusions

The aim of this work was to discuss the experimental data and to compare it with the data obtained in the literature.

A summary of the conclusions follows:

The discharge coefficient increased with a decreasing converging and diverging angle at the same diameter ratio. For the same converging-diverging angle, the discharge coefficient increased with a decreasing diameter ratio.

A greater and smaller converging angle than that of the classical Venturi, gives smaller C_d values in agreement with Reader-Harris et al. (2001).

The discharge coefficient trend of the experimental C-D tube was found to be independent of the Reynolds number for the range of Re > 2,000. Venturi are usually designed to work at high Re (Re>100,000) and predictive trends (ISO 5167) are found quite easily when working in this range, but not at lower Reynolds numbers.

The discharge coefficients obtained for a C-D tube with $\beta=0.6$ and $\theta=15°$ has shown good agreement with Hollingshead et al. (2011) for Re greater than 1000 and and a similar trend at Re less than 1000.

The trend of discharge coefficients of the various experiments conducted with the C-D tube 0.6 and the work of Hollingshead and Miller et al. (2009) showed that the differences are most prominent in the region where C_d depends on Re and it also depends on the fluid used.

Conclusion and Recommendations

6.1 Introduction

The C-D tube flow meter is a differential pressure flow meter similar to the Venturi tube. The objective of this work was to evaluate if a simpler geometry than that of the classical venturi would enable a wider range of application where C_d remains independent of the Re. This section gives a summary of work done, its main contribution to the topic, and recommendations for future research. Newtonian and non-Newtonian fluids were used to measure pressure profiles in five C-D tubes with diameter ratios of β=0.5, 0.6 and 0.7, and with angles of 15°, 30° and 45° and compare results with that obtained with a classical venturi.

6.2 Conclusions

Symmetrical pressure profiles of converging and diverging sections were found with smaller angles. This optimum pressure profile allows lower permanent pressure loss.

The performance criteria were found from an error analysis of the dimensionless numbers; discharge coefficient as a function of the Reynolds number. It was seen that the standard deviation at a low Reynolds number is slightly higher and reduces with an increase in the Reynolds number.

The average C_d and their uncertainties at various Reynolds numbers showed that a C-D tube 0.6(15-15) with average C_d of 0.957 with 0.5% uncertainty covered a range of applications in Reynolds number greater than 2000.

The C-D tube of β=0.6 gave the best performance and was therefore compared with a classical Venturi ISO 5167 with a diameter ratio of β=0.6. This comparison revealed that the C-D tube was able to deliver constant flow at a Reynolds number range of 10000 to 150000 where results from a classical venturi are Reynolds number dependent.

6.3. Contributions

This study provides a simple geometrical differential pressure flow meter with a constant C_d from the Reynolds number greater than 2,000 up to 150,000 compared to the classical Venturi that shows a strong dependence on Reynolds number. It was also shown that a straight section of pipe was not required for the throat and that the annular section did not affect the pressure measurements.

6.4. Future research recommendations

The C-D tubes suffer from installation effects and this issue must be investigated to ensure a robust industrial device with optimum performance.

The future research work should also include visualisation of flow patterns using advanced imaging or modelling such as Computational Fluid Dynamics. Small adjustments to the best performing C-D tube in this thesis may be required to define an optimum design and CFD could be used to do this.

References

Arun, N., Malavarayan, S. & Kaushik, M. 2010. CFD analysis on discharge coefficient during non-Newtonian flows through orifice meter. *International Journal of Engineering Science and Technology*, 2(7):3151-3164.

ASME. 2004. Measurement of fluid flow in pipe using orifice, nozzle and Venturi MFC-3MO. American Society of Mechanical Engineers Standard, ASME MFC-3M-2004. Part 1 & 2. New York: ASME International.

Baylar, A., Aydin, M.C., Unsal, M. & Ozkan, F. 2009. Numerical modeling of Venturi flows for determining air injection rates using FLUENT V6.2. *Mathematical and Computational Applications*, 14(2):97-108.

Baylar, A., Ozkan, F. & Ozturk, M. 2005. Influence of Venturi cone angles on jet aeration systems. *Proceedings of the Institution of Civil Engineers (ICE) Water Management Conference*, 158(1):9-16. London: Institution of Civil Engineers, Thomas Telford.

Bertani, C., De Salve, M., Malandrone, M., Monni, G. & Panella, B. 2010. State-of-art and selection of techniques in multiphase flow measurement. Report RdS/2010/67. Turin: Italian National Agency for New Technologies, Energy and Sustainable Economic Development; Rome: ENEA.

Brown, N.P. & Heywood, N.I. (eds). 1991. *Slurry handling: design of solid-liquid systems*. London: Elsevier Applied Science.

Cascetta, F. 1995. Short history of the flowmetering. *ISA Transactions*, 34:229-243, October.

Chan, Y.C., Chen, Y.H., Kang, S.C. & Lee, T.H. 2008. Development of virtual equipment for a hydraulic mechanics experiment. *Tsinghua Science & Technology*, 13(S1):261-265.

Chhabra, R.P. & Richardson, J.F. 1999. *Non-Newtonian flow in the process industries: fundamentals and engineering applications*. Oxford: Butterworth-Heinemann.

Coulson, J.M & Richardson, J.F. 1999. *Chemical engineering: vol. 1: fluid flow, heat transfer and mass transfer*. 6th ed. Oxford: Butterworth-Heinemann.

Crabtree, M.A. 2009. Industrial flow measurement. Unpublished Master of Science thesis, University of Huddersfield.

Davis, J. 2001. Understanding flowmeter. *InTech*: 42-44, August.

Figliola, R.S. & Beasley, D.E. 2011. *Theory and design for mechanical measurements*. 5th ed. Hoboken, NJ: John Wiley.

Finnemore, E.J. & Franzini, J.B. 2009. *Fluid mechanics with engineering applications*. 10th ed. Boston, MA: McGraw-Hill.

Fleischman, W.H. 1999. Plates perforated with Venturi-like orifices. Patent US5918637.

Fyrripi, I., Owen, I. & Escudier, M.P. 2004. Flowmetering of non-Newtonian liquids. *Flow Measurement and Instrumentation*, 15(3):131-138.

Govier, G.W. & Aziz, K. 1972. *The flow of complex mixtures in pipes*. New York: Van Nostrand Reinhold.

Halmi, D. and Associates. 1985. Flow metering device with recessed pressure taps. Patent US4528847.

Hite, H.O. 1950. Primary devices and meters for waste flow measurements. *Sewage and Industrial Wastes*, 22(10):1357-1363, October.

Hollingshead, C.L., Johnson, M.C., Barfuss, S.L. & Spall, R.E. 2011. Discharge coefficient performance of Venturi, standard concentric orifice plate, V-cone and wedge flow meters at low Reynolds numbers. *Journal of Petroleum Science and Engineering*, 78(3-4):559-566, September.

Ifft, S.A. 2010. Permanent pressure loss comparison among various flowmeter technologies. White paper. Hemet, CA: McCrometer Inc. International.

International Organization for Standardization. 1980. Measurement of fluid flow by means of orifice plates, nozzles and Venturi tubes inserted in circular cross-section conduits running full. ISO-5167-1980(E). Geneva: ISO.

International Organization for Standardization. 2003. Measurement of fluid flow by means of pressure differential devices. ISO EN 5167. Geneva: ISO.

Jitschin, W. 2004. Gas flow measurement by the thin orifice and the

classical Venturi tube. *Vacuum*, 76(1), 89-100.

Keyser, D.R. & Friedman, J.R. 2010. Extrapolation and curve-fitting of calibration data for differential pressure flow meters. *Journal of Engineering for Gas Turbines and Power*, 132(2):4

Laribi, B., Wauters, P. & Aichouni, M. 2001. Experimental study of the decay of swirling turbulent pipe flow and its effect on orifice meter performance. *Proceedings of the Fluids Engineering Division Summer Meeting (FEDSM2001) 2001, ASME Fluids Engineering Conference, New Orleans, LA, 29 May – 1 June 2001,* 1:93-96. Paper no. FEDSM2001-18039. New York: ASME.

Liu, H. 2003. *Pipeline engineering*. Boca Raton, FL: Lewis Publishers.

Mahadevan, V. 1964. Report of the literature review committee: Annual review of the literature on fats, oils, and detergents. *Journal of American Oil Chemists' Society*, 41(8):559-584, August.

Massey, B.S. 1998. *Mechanics of fluids*. 7th ed. Cheltenham: Stanley Thornes.

McCrometer. 1999. Permanent pressure loss. *Flow Measurement News*, 5(1), March 3. http://www.mccrometer.com/library/pdf/24508-37.pdf [20 November 2013].

McNeil, D.A., Addlesee, J. & Stuart, A. 1999. An experimental study of viscous flows in contractions. *Journal of Loss Prevention in the Process Industries*, 12(4):249-258, July.

Metzner, A.B. & Reed, J.C. 1955. Flow of non-Newtonian fluids – correction of the laminar, transition and turbulent-flow regions. *AIChE Journal*, 1(4):434-440, December.

Miller, G.J., Pinguet, B.G., Theuveny, B. & Mosknes, P.O. 2009. The influence of liquid viscosity on multiphase flow meters. Glasgow: TUV NEL.

Miller, R.W. 1989. *Flow measurement engineering handbook.* 2nd ed. New York: McGraw-Hill.

Mooney, M. 1931. Explicit formulas for slip and fluidity. *Journal of rheology,* 2, 210.

Neill, R.I.G. 1988. The rheology and flow behaviour of high concentration mineral slurries. Unpublished MSc Dissertation. University of Cape Town.

Nystrom, J.B. & Stacy, P.S. 2008. Performance of nozzle, Venturi, and orifice meters relative to extrapolation criteria. *Proceedings of ASME2008 Power Conference, Lake Buena Vista, FL, 22-24 July 2008.* POWER2008 – Paper no. 60112. New York: ASME: 509-513.

Paterson & Cooke. 2010. The design of slurry pipeline systems. 15th Annual Four Day Course presented at the Breakwater Lodge, Victoria and Alfred Waterfront, Cape Town, 23 – 26 February 2010.

Rabinowitsch, B. 1929. Über die viskosität und elastizität von solen. *Zeitschrift für physikalische Chemie*, 145, 1-26.

Reader-Harris, M.J., Brunton, W.C., Gibson, J.J., Hodges, D. & Nicholson, I.G. 2001. Discharge coefficients of Venturi tubes with standard and non-standard convergent angles. *Flow Measurement and Instrumentation*, 12(20):135-145, April.

Rodd, A.B., Dunstan, D.E. & Boger, D.V., 2000. Characterization of xanthan gum solutions using dynamic light scattering and rheology. *Carbohydrate Polymers*, 42:159-174.

Salas-Valerio, W.F. & Steffe, J.F. 1990. Orifice discharge coefficient for power-law fluids. *Journal of Food Process Engineering*, 18(2):89-98, February.

Sapra, M.K., Bajaj, M., Kundu, S.N. & Sharma, B.S.V.G. 2011. Experimental and CFD investigation of 100mm size cone flow elements. *Flow Measurement and Instrumentation*, 22(5):469-474.

Shook, C.A. & Masliyah, J.H. 1974. Flow of slurry through a Venturi meter. *Canadian Journal of Chemical Engineering*, 52(2):228-233, April.

Singh, R.K., Singh, S.N. & Seshadri, V. 2010. Performance evaluation of orifice plate assemblies under non-standard conditions using CFD. *Indian Journal of Engineering and Materials Sciences*, 17(6):397-406, December.

Skelland, A.H.P. 1967. *Non-Newtonian flow and heat transfer.* New York: John Wiley.

Slatter, P.T. 1994. Transitional and turbulent flow of non-Newtonian slurries in pipes. Unpublished PhD (Civil Engineering) thesis, University of Cape Town.

Slatter, P.T & Pienaar, V.G. 1999. Establishing dynamic similarity for non-Newtonian fittings loss. *Proceedings of the British Hydromechanics*

Research Group 14th International Conference on Slurry Handling and Pipeline Transport: Hydrotransport 14, Maastricht, The Netherlands, 8 – 10 September 1999. Cranfield, Befordshire: BHR Group: 245-254.

Spitzer, D.W. 2005. *Industrial flow measurement*. 3rd ed. Raleigh, NC: ISA.

Steffe, J.F. 1996. *Rheological methods in food process engineering*. 2nd ed. East Lansing, MI: Freeman Press.

Steven, R. 2008. Diagnostic methodologies for generic differential pressure flow meters. *Proceedings of the 26th International North Sea Flow Measurement Workshop, St Andrews, Scotland, 21 – 24 October 2008*. London: Energy Institute: 143-0174.

Taylor, J.R. 1997. *An introduction to error analysis: the study of uncertainties in physical measurements*. 2nd ed. Sausalito, CA: University Science Books.

Webster, J.G. (ed.). 1999. *The measurement, instrumentation, and sensors handbook*. Boca Raton, FL: CRC Press, IEEE.

Wu, Z. & Xie, F. 2008. Optimization of Venturi tube design for pipeline pulverized coal flow measurements. *Frontiers of Energy and Power Engineering in China*, 2(4):369-373.

Appendices

Appendix A

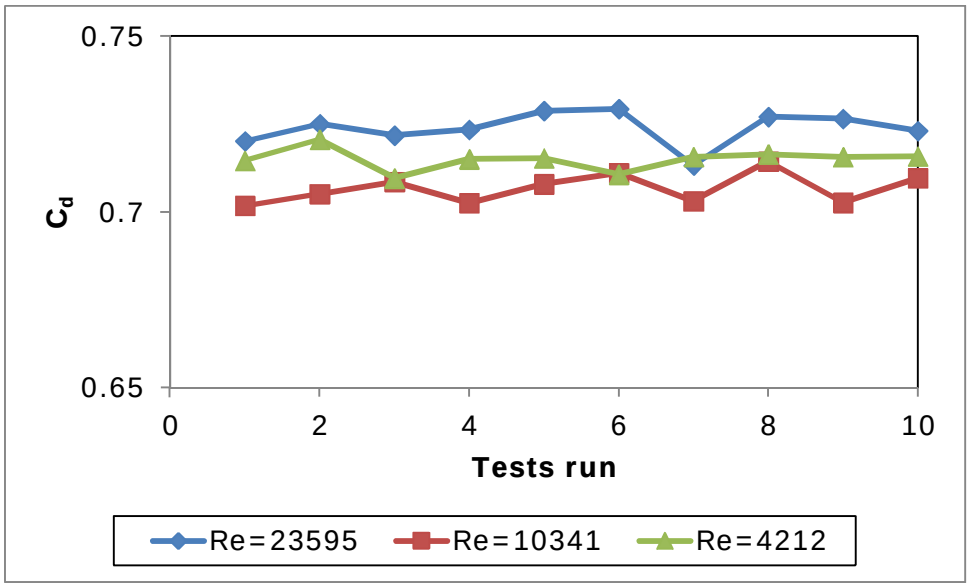

Figure A.1: Variation of C_d values for C-D tube with β=0.5 and θ=30° using CMC

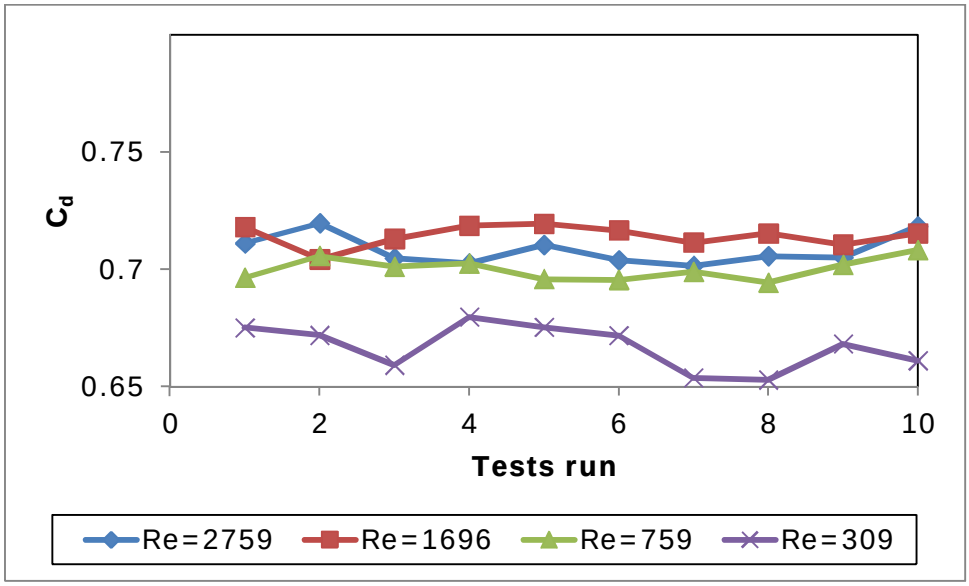

Figure A.2: Variation of C_d for C-D tube β=0.5 and θ=45° using CMC +XG

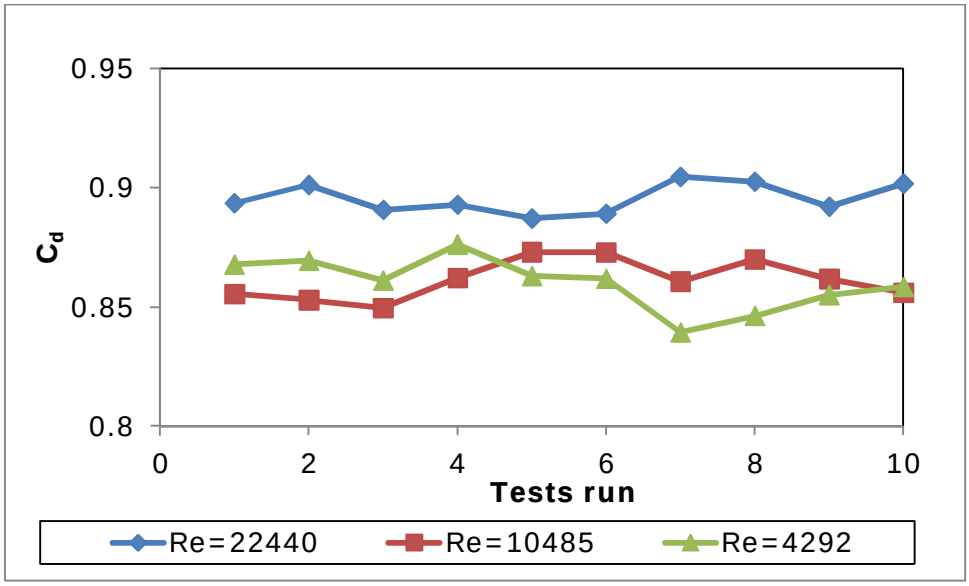

Figure A.3: Variation of C_d values for C-D tube β=0.5 and θ=30° using CMC

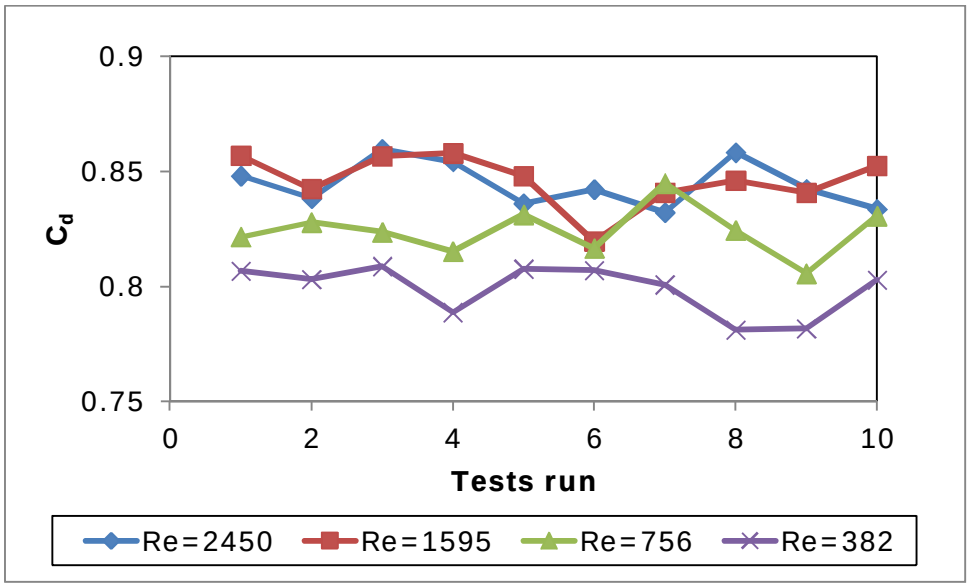

Figure A.4: Variation of C_d values for C-D tube β=0.5 and θ=30° using CMC + XG

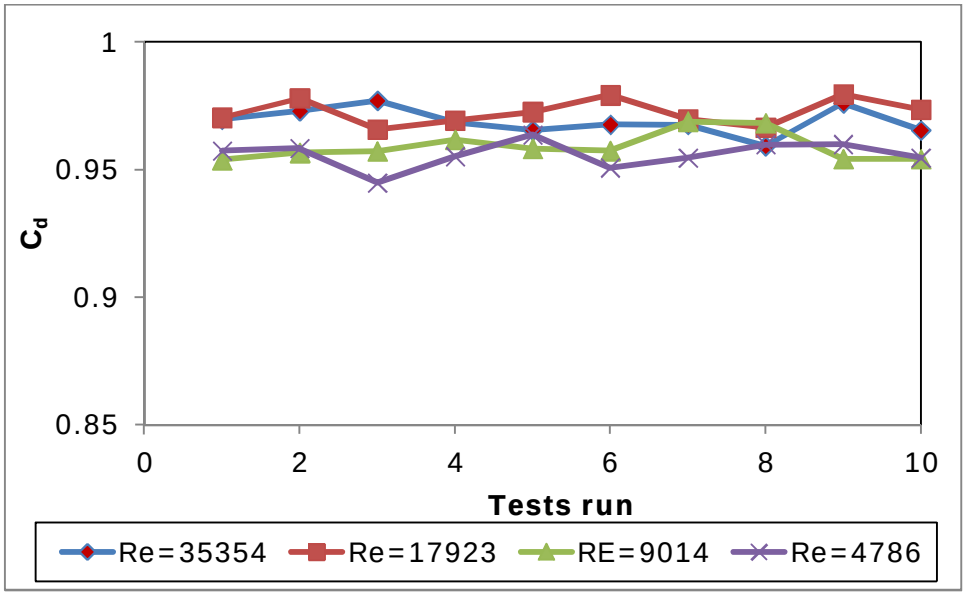

Figure A.5: Variation of C_d values for C-D tube β=0.5 and θ=15° using CMC

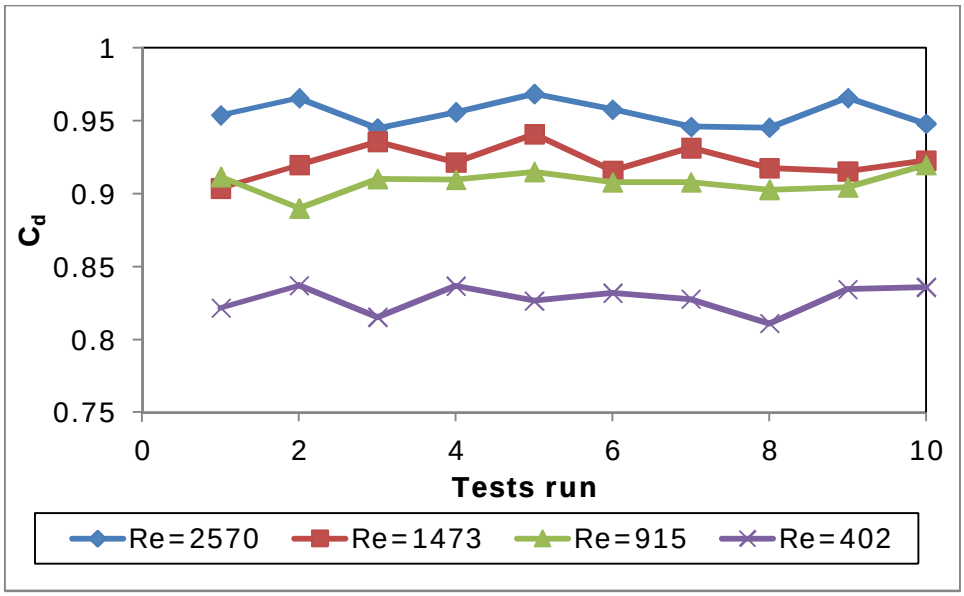

Figure A.6: Variation of C_d values for C-D tube β=0.5 and θ=15° using CMC+XG

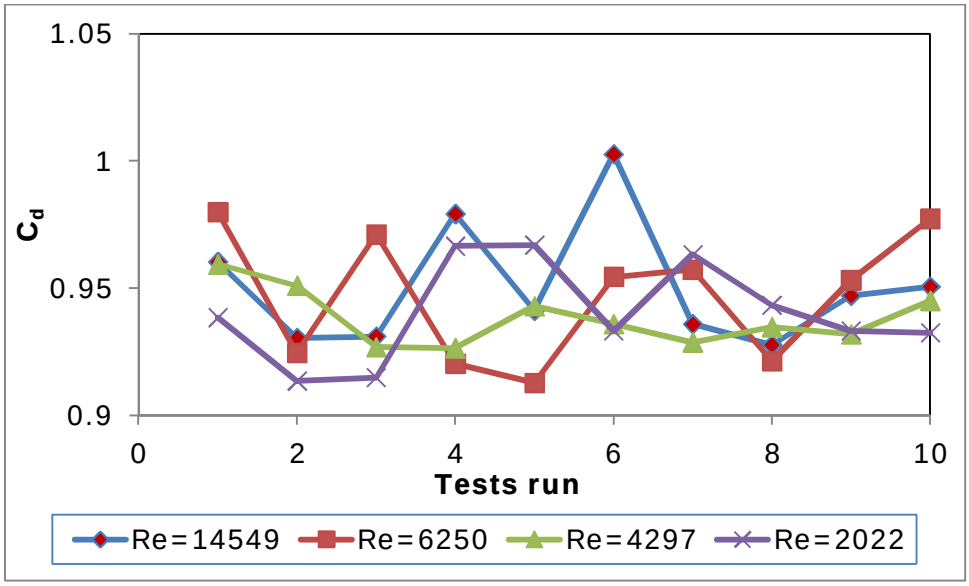

Figure A.7: Variation of C_d values for C-D tube β=0.6 and θ=15° using CMC

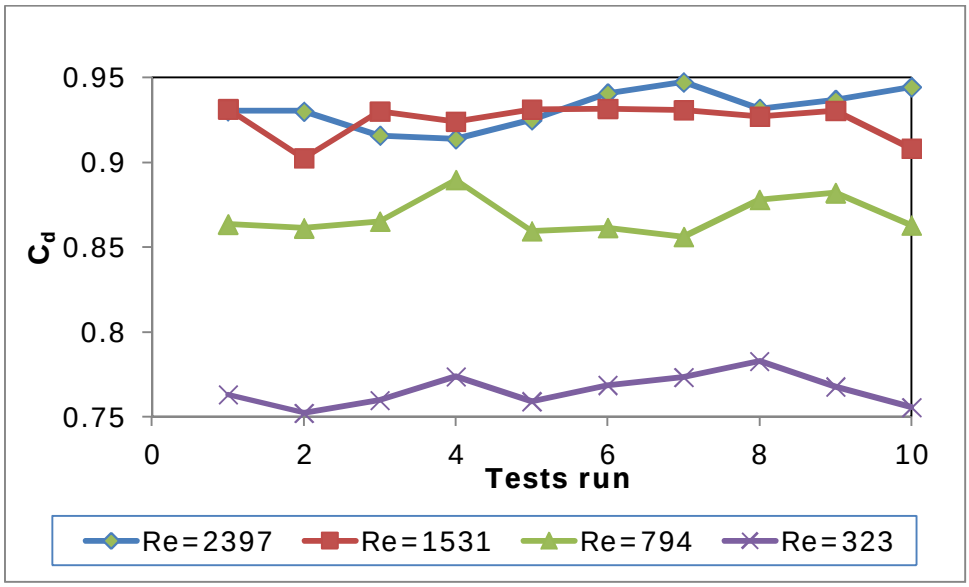

Figure A.8: Variation of C_d values for C-D tube β=0.6 and θ=15° using CMC+XG

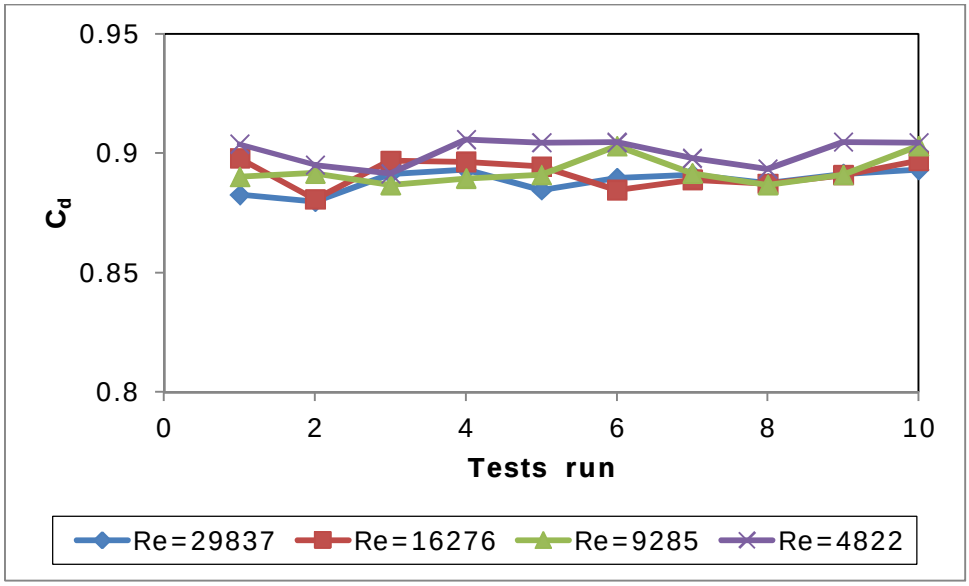

Figure A.9: Variation of C_d values for C-D tube β=0.7 and θ=15° using CMC

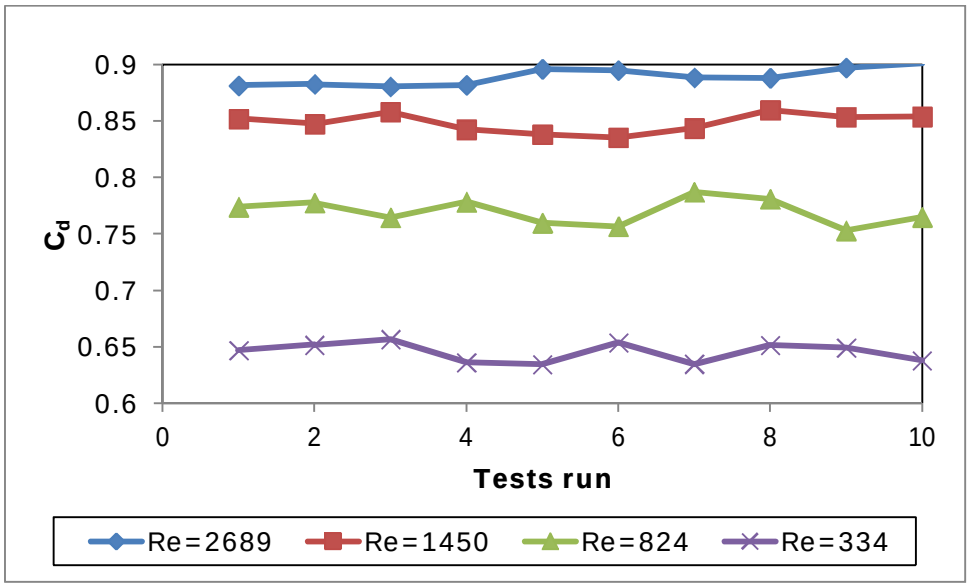

Figure A.10: Variation of C_d values for C-D tube β=0.7 and θ=15° using CMC+XG

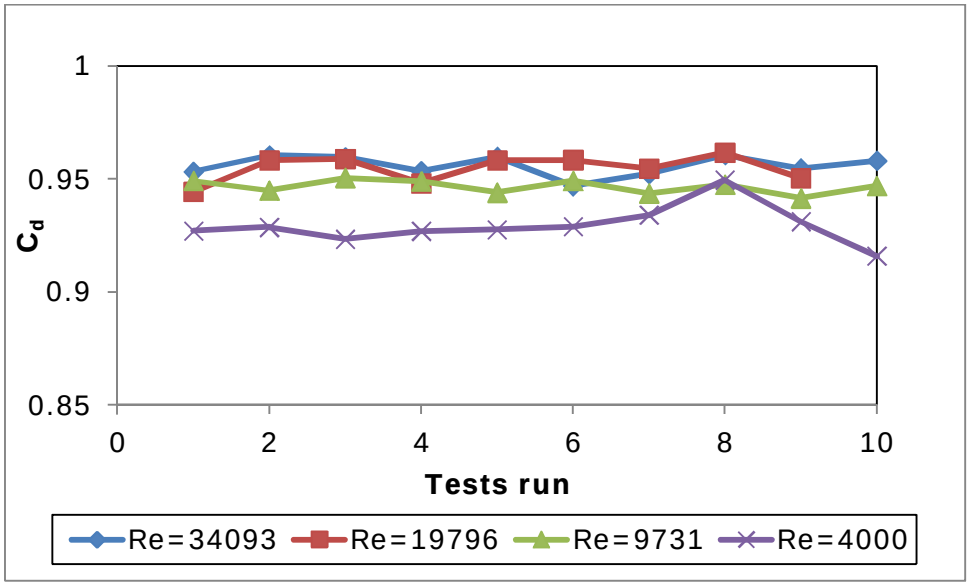

Figure A.11: Variation of C_d values for classical Venturi β=0.6 using CMC

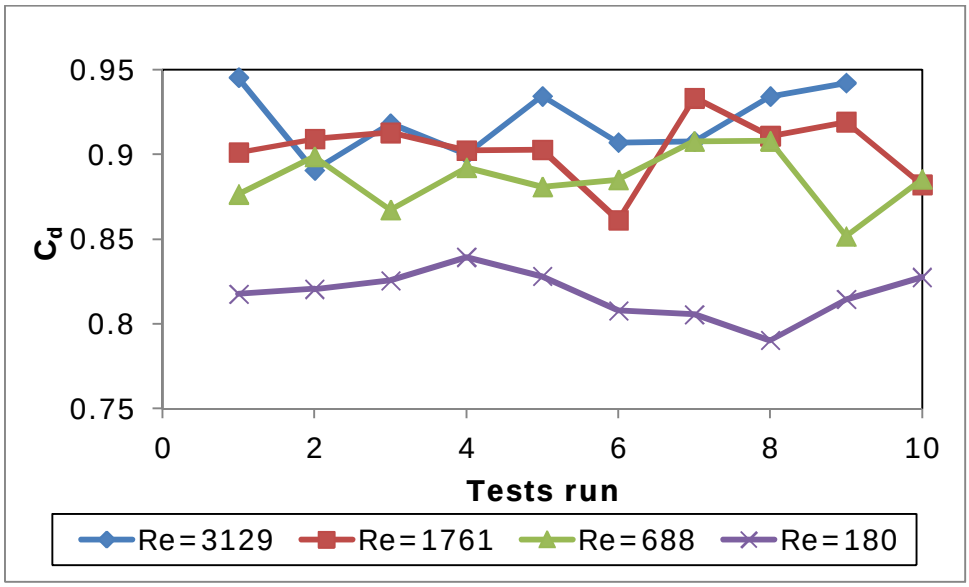

Figure A.12: Variation of C_d values for classical Venturi β=0.6 using CMC+XG

Appendix B

Table B.1: C-D 0.5(45-45) with Water

				Date:	03/10/2012	Test done by Luc							
				Venturi angle [°]:	45								
				Venturi length [m]:	0.062	Area[m2]							
				Throat diameter[m]:	0.023	0.00042							
				Pipe Diameter [m]:	0.046	0.00166							
				Diameter ratio	0.5								
				Material Type:	Water								
				Density[kg/m3]:	999.87								
				Concentration:	1								
				ty:	0								
				K:	0.001			1/n	n/(n+1)	(n+1)/n	K1/n		
				n:	1			1	0.5	2	0.001		
					Flange	Contracting		Throat	Expanding				
				Axial distances	-0.078	-0.028	-0.014	0	0.014	0.028			
				Non-dimensionalised distar	-1.695652	-0.6087	-0.3043	0	0.30435	0.6087			
				Distances[m]:	6.85	6.9	6.914	6.928	6.942	6.956			
Run #	**d(D&D/2**	**d(Flange**	**Re3**	**Pod 3**	**Pod 4**	**Pod 5**	**Pod 6**	**Pod 7**	**Pod 8**	**Average Q [l/s]**	**Dp cont**	**Dpflange**	
1	0.709	0.705	120263	115875	114725	108752	13491	9780	9720	4.35	101234	102384	
2	0.703	0.701	120406	116133	115749	108708	12372	9260	9357	4.35	103377	103761	
3	0.700	0.699	121180	116139	115613	108930	10200	9147	12192	4.38	105413	105940	
4	0.710	0.709	122184	115823	115522	108770	11358	9706	11545	4.41	104163	104464	
5	0.711	0.710	121807	115973	115589	108930	12264	9852	12529	4.40	103325	103708	
6	0.701	0.700	121497	116143	115659	108958	9935	9165	11938	4.39	105724	106209	
7	0.711	0.710	122111	116003	115908	109084	11947	9870	11612	4.41	103961	104056	
8	0.709	0.708	121954	115827	115509	109136	11363	10064	11413	4.41	104147	104464	
9	0.705	0.704	122034	116021	115591	108808	10189	9352	11599	4.41	105401	105832	
10	0.700	0.699	121654	115825	115588	108977	9261	9665	11815	4.40	106328	106565	
11	0.704	0.704	122111	115972	115870	108939	9931	9057	11508	4.41	105940	106041	
Mean	**0.706**	**0.704**											
Stdev	**0.004**	**0.004**											
uncertai	**0.012**	**0.012**											
1	0.699	0.700	106254	94476	94604	88824	13267	13290	15124	3.84	81337	81209	
2	0.708	0.707	106222	94278	94044	88322	14833	13431	14484	3.84	79210	79444	
3	0.701	0.700	106257	94233	94012	88842	13098	13877	15145	3.84	80914	81135	
4	0.706	0.705	106417	94342	94249	88716	14226	13265	15017	3.85	80023	80116	
5	0.704	0.703	106403	94192	94066	88930	13545	13002	15242	3.84	80522	80648	
6	0.706	0.704	106114	94502	94124	89042	14487	13492	14875	3.83	79637	80015	
7	0.701	0.699	106372	94438	94171	88915	12993	13283	14977	3.84	81177	81445	
8	0.701	0.700	106484	94321	94092	88985	12928	14086	14619	3.85	81164	81393	
9	0.710	0.709	106414	94328	94002	88880	14919	14244	14575	3.85	79083	79409	
10	0.706	0.705	106564	94266	94031	89178	13772	13511	14805	3.85	80259	80495	
Mean	**0.704**	**0.703**											
Stdev	**0.004**	**0.003**											
uncertai	**0.010**	**0.009**											
	0.699	0.693	64101	48580	48047	46551	18428	18828	18483	2.32	29619	30152	
	0.708	0.698	64056	48484	47677	46495	18872	18392	18178	2.31	28805	29611	
	0.706	0.696	64052	48256	47421	46360	18461	18771	18655	2.31	28960	29795	
	0.710	0.700	64059	48330	47456	46458	18802	18830	18487	2.31	28655	29528	
	0.696	0.693	64024	48241	48011	46419	18217	18658	18388	2.31	29794	30024	
	0.700	0.699	63934	48254	48156	46416	18796	18673	18563	2.31	29360	29458	
	0.699	0.697	63909	48377	48204	46443	18810	18622	18469	2.31	29394	29567	
	0.699	0.698	63902	48228	48147	46544	18729	18632	18575	2.31	29419	29499	
	0.696	0.695	63951	48268	48139	46494	18454	19070	18650	2.31	29685	29814	
	0.695	0.694	63909	48336	48264	46589	18456	19011	19080	2.31	29809	29880	
Mean	**0.701**	**0.696**											
Stdev	**0.005**	**0.003**											
uncertai	**0.015**	**0.007**											

Run 37	0.727	0.695	34411	34394	33655	33831	25765	25790	25497	1.24	7890	8629
Run 38	0.729	0.695	34467	34386	33590	33754	25714	25566	25457	1.25	7876	8672
Run 40	0.733	0.699	34726	34260	33492	33558	25582	25368	25149	1.25	7909	8678
Run 41	0.721	0.691	34563	34150	33447	33576	25345	25525	25191	1.25	8102	8805
Run 42	0.727	0.696	34621	34186	33462	33491	25485	25407	25228	1.25	7977	8701
Run 43	0.721	0.692	34673	34167	33471	33461	25328	25155	25064	1.25	8144	8839
Run 44	0.726	0.696	34873	34144	33433	33490	25310	25484	25081	1.26	8123	8834
Run 45	0.720	0.689	34730	34215	33455	33389	25268	25326	25052	1.25	8186	8947
Run 47	0.719	0.689	34678	34221	33471	33373	25289	25339	25154	1.25	8181	8931
Run 48	0.727	0.696	34698	34089	33373	33340	25350	25275	25114	1.25	8023	8739
Mean	**0.725**	**0.694**										
Stdev	**0.004**	**0.004**										
uncertai	**0.012**	**0.010**										

Table B.2: C-D 0.5(45-45) with CMC 2%

			Date:	08/10/2012	**Test done by Luc**							
			Venturi angle [°]:	45								
			Venturi length [m]:	0.062	Area[m2]							
			Throat diameter[m]:	0.023	0.00042							
			Pipe Diameter [m]:	0.046	0.00166							
			Diameter ratio	0.5								
			Material Type:	CMC								
			Density[kg/m3]:	1012								
			Concentration:	2%								
			ty:	0								
			K:	0.096		**1/n**	**n/(n+1)**	**(n+1)/n**	**K1/n**			
			n:	0.716		1.26582	0.44134	2.26582	0.00517			
					Contracting		**Throat**	**Expanding**				
	Axial distances			-0.078	-0.028	-0.014	0	0.014	0.028			
	Venturi plane											
	Non-dimensionalised dista			-1.696	-0.609	-0.304	0	0.304	0.609			
	Distances[m]:			6.85	6.9	6.914	6.928	6.942	6.956			
Run #	**Cd(D&D**	**Cd(Flan**	**Re3**	**Pod 3**	**Pod 4**	**Pod 5**	**Pod 6**	**Pod 7**	**Pod 8**	**Average [l/s]**	**DPcont**	**DPFlang**
Run 1	0.721	0.720	23225	90158	89892	85926	18014	16569	21046	3.70	71878	72144
Run 2	0.728	0.725	23669	89619	88950	85324	16176	16391	18117	3.76	72774	73444
Run 3	0.729	0.722	23422	90097	88702	85903	17263	15535	17355	3.73	71438	72834
Run 4	0.726	0.723	23727	89583	88973	85895	15514	15802	17108	3.77	73459	74068
Run 5	0.732	0.729	23754	89831	89125	86085	16711	14989	17458	3.77	72415	73121
Run 6	0.733	0.729	23817	89869	89077	86015	16528	15026	16879	3.78	72548	73341
Run 7	0.714	0.713	23549	89904	89791	86022	14667	17249	19498	3.74	75124	75237
Run 8	0.726	0.727	23621	89696	89882	86112	16914	16411	17850	3.75	72968	72782
Run 10	0.729	0.726	23505	88945	88515	86607	16632	14824	17270	3.74	71882	72313
Run 11	0.728	0.723	23661	89835	88866	85942	16031	15074	16629	3.76	72835	73805
Mean	**0.727**	**0.724**										
Stdev	**0.006**	**0.005**										
uncertai	**0.015**	**0.013**										

Run 13	0.706	0.702	10308	39640	39394	38539	19799	20032	20142	1.89	19595	19841
Run 14	0.714	0.705	10354	39405	38927	38350	19608	20026	19809	1.90	19318	19796
Run 15	0.714	0.709	10374	39274	38963	37979	19606	19775	19882	1.90	19356	19667
Run 16	0.709	0.703	10310	39340	38979	38016	19539	19816	19984	1.89	19441	19801
Run 17	0.713	0.708	10308	39284	39009	38264	19787	19815	19970	1.89	19222	19497
Run 18	0.719	0.711	10421	39233	38781	38159	19558	19601	20217	1.91	19223	19675
Run 19	0.704	0.703	10195	39168	39137	38057	19758	19698	19886	1.87	19380	19410
Run 20	0.718	0.714	10408	39178	38954	38424	19721	19586	20263	1.91	19233	19457
Run 21	0.713	0.703	10363	39323	38757	38082	19357	19929	19868	1.90	19400	19966
Run 22	0.714	0.710	10370	39138	38920	38027	19543	19624	19985	1.90	19378	19595
Mean	**0.712**	**0.707**										
Stdev	**0.005**	**0.004**										
uncertai	**0.014**	**0.012**										
Run 24	0.716	0.715	3973	28977	28962	28828	25019	25350	25495	0.86	3943	3958
Run 26	0.729	0.721	4122	29280	29188	28984	25144	25075	24532	0.89	4043	4136
Run 27	0.726	0.710	4182	28816	28619	28458	24447	24381	24196	0.90	4172	4369
Run 28	0.732	0.715	4218	28577	28374	28277	24214	24110	23933	0.90	4161	4363
Run 29	0.733	0.715	4233	28437	28223	28113	24051	23926	23790	0.91	4172	4387
Run 30	0.731	0.711	4259	28344	28094	28007	23854	23801	23639	0.91	4239	4489
Run 31	0.730	0.716	4267	28228	28054	27946	23789	23743	23537	0.91	4265	4440
Run 32	0.730	0.716	4273	28163	27995	27913	23722	23677	23518	0.91	4274	4441
Run 33	0.737	0.716	4288	28163	27906	27849	23686	23594	23456	0.92	4220	4477
Run 34	0.738	0.716	4305	28115	27847	27752	23612	23523	23367	0.92	4234	4503
Mean	**0.730**	**0.715**										
Stdev	**0.006**	**0.003**										
uncertai	**0.017**	**0.009**										

Table B.3:C-D 0.5 (45-45) with CMC + XG

			Date:	18/10/2012	Test done by Luc							
			Venturi angle [°]:	45								
			Venturi length [m]:	0.062	Area[m2]							
			Throat diameter[m]:	0.023	0.000							
			Pipe Diameter [m]:	0.046	0.002							
			Diameter ratio	0.500								
			Material Type:	CMC +Xanthan								
			Density[kg/m3]:	1013								
			Concentration:	2%								
			ty:	0.000								
			K:	0.103		**1/n**	**n/(n+1)**	**(n+1)/n**	**K1/n**			
			n:	0.710		1.404	0.416	2.404	0.047			
					Contracting		**Throat**	**Expanding**				
			Axial distan	-0.078	-0.028	-0.014	0.000	0.014	0.028	4.638		
			Venturi plane									
		Non-dimensionalised dist		-1.696	-0.609	-0.304	0.000	0.304	0.609	100.826		
			Distances[r	-0.078	-0.028	-0.014	0.000	0.014	0.028	4.638		

Run #	**Cd(D&D**	**Cd(Flan**	**Re3**	**Pod 3**	**Pod 4**	**Pod 5**	**Pod 6**	**Pod 7**	**Pod 8**	**Pod 9**	**Average [l/s]**	**DP contr**	**DP Flang**
Run 1	0.724	0.711	2778	55476	54472	53139	26779	26841	30705	32239	2.302	27692	28697
Run 2	0.728	0.720	2790	54059	53393	52116	25853	26189	26445	31723	2.310	27540	28206
Run 3	0.713	0.705	2764	54316	53643	52373	25311	25564	25979	32488	2.294	28332	29005
Run 5	0.715	0.703	2797	54629	53577	52589	24919	25220	25601	31501	2.314	28658	29710
Run 7	0.721	0.710	2781	57061	56208	55383	28251	28920	28279	32301	2.305	27957	28811
Run 8	0.717	0.704	2803	54096	53022	52238	24385	25051	25364	32559	2.319	28636	29710
Run 9	0.708	0.701	2584	53744	53287	52439	27381	31547	31787	36680	2.177	25906	26362
Run 10	0.715	0.706	2799	54701	53975	52793	25220	25726	27722	31763	2.316	28755	29480
Run 11	0.726	0.705	2736	55181	53563	51325	26661	26407	27069	33205	2.276	26902	28520
Run 12	0.709	0.718		56764	57462	55498	29017	30329	28930	32967	2.287	28445	27747
Mean	**0.718**	**0.708**											
Stdev	**0.007**	**0.006**											
uncert	**0.019**	**0.018**											

Run 14	0.732	0.718	1682	41987	41494	41158	29072	29545	35342	30946	1.560	12422	12915
Run 15	0.717	0.704	1690	41748	41275	40613	28219	28296	29475	30612	1.566	13056	13530
Run 16	0.724	0.713	1683	41471	41060	40548	28366	28950	29128	30654	1.560	12694	13105
Run 17	0.732	0.719	1688	41412	40948	40673	28453	28511	28824	30655	1.564	12496	12959
Run 18	0.734	0.719	1703	41160	40627	40165	28043	28765	28810	30231	1.575	12584	13117
Run 20	0.731	0.717	1677	41904	41386	40671	28997	29360	29508	30733	1.556	12389	12907
Run 21	0.725	0.711	1717	41594	41083	40579	28012	29169	29236	30362	1.585	13071	13581
Run 22	0.726	0.715	1714	41210	40821	40158	27806	28530	28894	30272	1.583	13014	13404
Run 23	0.731	0.711	1692	41754	41034	40448	28438	28819	29030	30700	1.567	12596	13316
Run 24	0.724	0.715	1717	41482	41177	40531	28043	28534	29035	30561	1.585	13134	13439
Mean	**0.728**	**0.714**	**1696**										
Stdev	**0.005**	**0.005**	**15.332**										
uncert	**0.015**	**0.013**	**0.018**										
Run 26	0.734	0.696	767	35517	35117	34957	31460	31768	31919	31595	0.848	3657	4057
Run 27	0.738	0.706	757	35578	35245	35170	31706	32067	32276	32072	0.839	3539	3872
Run 28	0.729	0.701	754	35890	35597	35420	31993	32239	32421	32076	0.837	3605	3898
Run 29	0.731	0.702	748	35643	35344	35214	31806	32139	32359	32095	0.832	3539	3837
Run 30	0.725	0.696	744	35856	35551	35395	31977	32228	32399	32027	0.828	3574	3879
Run 31	0.709	0.696	742	35398	35253	35089	31539	31693	32073	31666	0.826	3715	3860
Run 32	0.719	0.699	766	35329	35108	34880	31310	31546	31727	31431	0.847	3798	4019
Run 33	0.731	0.694	766	35258	34856	34619	31185	31466	31660	31333	0.847	3671	4073
Run 34	0.744	0.702	772	35188	34741	34602	31157	31322	31500	31139	0.852	3584	4031
Run 35	0.742	0.708	768	34964	34619	34516	31033	31347	31548	31094	0.849	3586	3931
Mean	**0.730**	**0.700**											
Stdev	**0.011**	**0.005**											
uncert	**0.029**	**0.013**											
Run 37	0.776	0.675	298	34656	34414	34335	33664	33677	54344	33128	0.406	750	992
Run 38	0.760	0.672	297	34913	34695	34600	33912	33937	37204	33409	0.406	782	1001
Run 39	0.691	0.659	316	34915	34813	34772	33774	34072	34941	33574	0.426	1039	1141
Run 40	0.741	0.680	317	35146	34974	34985	34064	34266	34674	33694	0.427	910	1082
Run 41	0.715	0.675	315	35221	35105	35087	34137	34315	34613	33719	0.425	968	1084
Run 42	0.710	0.672	317	35269	35153	35095	34162	34291	34556	33751	0.427	991	1107
Run 43	0.712	0.654	309	35513	35337	35285	34393	34599	34781	34100	0.418	944	1120
Run 44	0.750	0.653	314	35652	35374	35288	34501	34561	34720	34037	0.423	873	1152
Run 45	0.765	0.668	312	35643	35384	35383	34553	34722	34853	34212	0.422	831	1089
Run 46	0.689	0.661	299	35819	35736	35746	34774	35151	35246	34618	0.408	962	1045
Mean	**0.731**	**0.667**											
Stdev	**0.032**	**0.010**											
uncert	**0.087**	**0.029**											

Table B.4: C-D 0.5(30-30) with Water

			Date:	02/10/2012	Test done by Luc									
			Venturi angle [°]:	30										
			Venturi length [m]:	0.086	Area[m2]									
			Throat diameter[m]:	0.023	0.00042									
			Pipe Diameter [m]:	0.046	0.00166									
			Diameter ratio	0.5										
			Material Type:	Water										
			Density[kg/m3]:	999.87										
			Concentration:	1										
			ty:	0										
			K:	0.001		1/n	n/(n+1)	(n+1)/n	K1/n					
			n:	1		1	0.5	2	0.001					
					Contracting		Throat		Expanding					
	Axial distances			-0.093	-0.043	-0.0215	0	0.0215	0.043	4.653				
	Venturi plane													
	Non-dimensionalised dista			-2.021739	-0.9348	-0.5972	0	0.59722	0.93478	101.152				
	Distances[m]:			6.85	6.9	6.9215	6.943	6.9645	6.986	11.596				
Run #	**Cd(D&D**	**Cd(Flan**	**Re3**	**Pod 3**	**Pod 4**	**Pod 5**	**Pod 6**	**Pod 7**	**Pod 8**	**Pod 9**	**Average**	**Dpcont**	**Dpflange**	
											[l/s]			
Run 3	0.85359	0.85379	142413	111596.96	111644	97180.9	12970.7	21409.4	26549.4	45716	5.1458	98673.1	98626.3	
Run 4	0.86094	0.85959	142071	111387.56	111085	97136.5	14553.7	22268.1	26131.6	45820.4	5.13346	96531.1	96833.9	
Run 5	0.84297	0.84912	143337	109942.29	111421	97901.2	8928.85	23111	28128	46293.8	5.17919	102492	101013	
Run 8	0.85792	0.85037	142364	112469.82	110729	96262.2	13115.3	23273.2	25692.3	45948	5.14404	97613.2	99354.5	
Run 9	0.8595	0.85783	143012	112733.44	112352	98453.1	14207.8	21041.5	27205.5	46312.7	5.16747	98143.7	98525.6	
Run 10	0.85779	0.84901	143173	112553.45	110503	97771.2	11746	22613.8	26760.6	45620.5	5.17326	98756.5	100807	
Run 11	0.85743	0.85182	142800	112279.7	110982	96368.3	12657.2	21694.7	26709.3	46054.9	5.15979	98324.7	99622.5	
Run 14	0.85965	0.85181	142514	112685.88	110884	98358.3	13458.6	21354.2	25782.6	45987	5.14946	97425.4	99227.2	
Mean	**0.8562**	**0.8529**	**142710**											
stdev	**0.0058**	**0.0039**	**440.99**											
uncertai	**0.0135**	**0.0092**	**0.0062**											
Run 16	0.86032	0.85799	107136	75040.68	74742.2	67784.7	19769.1	23917	26756.8	37539.3	3.87113	54973	55271.6	
Run 17	0.86736	0.86287	106177	74519.039	73965	68084.9	20844	25708	27306.5	37872.1	3.83649	53120.9	53675	
Run 19	0.85906	0.86	106864	74555.109	74675.5	66815.4	19820	26181.5	27453.7	37321	3.86131	54855.4	54735.1	
Run 20	0.85147	0.84827	105943	74317.977	73903.7	66990	19024.2	25430	26937.2	37249.5	3.82805	54879.5	55293.8	
Run 21	0.85008	0.84946	106034	74536.648	74456.1	67599	19303	25743.3	27478	37906.6	3.83133	55153.2	55233.7	
Run 22	0.85494	0.8467	106313	73802.297	72729.4	67096.5	17914.4	25962.2	27172.8	37232.8	3.8414	54815	55887.9	
Run 25	0.84914	0.84929	106553	73663.078	73683.2	66353.7	17864.9	23599	26718.1	37155.2	3.8501	55818.3	55798.2	
Run 26	0.86182	0.85486	106403	73601.961	72718.8	66312.1	18683.3	25596.8	26390.2	36970.4	3.84468	54035.5	54918.7	
Mean	**0.8568**	**0.8537**	**106428**											
stdev	**0.006**	**0.0057**	**383.01**											
uncertai	**0.014**	**0.0133**	**0.0072**											
Run 29	0.88543	0.86758	64554.3	41574.742	40791.6	38536	21948.8	24681.9	24438.4	28253.1	2.33254	18842.9	19626	
Run 31	0.88505	0.86579	64547.3	41244.32	40396.4	38215.1	21541.3	24461.2	24148.5	27997.3	2.33229	18855	19703	
Run 32	0.88398	0.86712	64404.4	41145.023	40406.4	38153.5	21589.5	24367.7	23812.4	27582	2.32712	18816.9	19555.6	
Run 33	0.88709	0.87152	64554.3	40725.977	40049	37792.7	21276.9	24022.3	23799.6	27537.8	2.33254	18772.1	19449	
Run 34	0.88151	0.86388	64362.5	40692.426	39913.2	37761.4	21015.3	23987.1	23703.4	27504.9	2.32561	18897.9	19677.1	
Run 35	0.8835	0.86752	64404.4	40650.008	39949.3	37821.6	21112.1	23965.3	23759.7	27467.3	2.32712	18837.3	19537.9	
Run 36	0.88786	0.86843	64474.1	40681.328	39835.7	37663.3	21142.4	23778	23613.7	27273.5	2.32964	18693.2	19538.9	
Run 37	0.88727	0.86997	64383.5	40437.164	39687.3	37545.6	21021.8	23661.6	23549.7	27232.6	2.32637	18665.5	19415.4	
Run 38	0.88456	0.86691	64515.9	40490.699	39714.9	37546.8	20857.5	23763.7	23560.3	27277.8	2.33116	18857.4	19633.2	
Run 39	0.89065	0.87425	64355.6	40301.965	39601.1	37368.3	21093.2	23486.6	23314.3	26999.3	2.32536	18507.8	19208.8	
Mean	**0.8857**	**0.8683**	**64456**											
stdev	**0.0026**	**0.003**	**82.321**											
uncertai	**0.0059**	**0.0068**	**0.0026**											

Run 41	0.93924	0.86994	32774.1	31245.572	30530.5	30322.2	26214.2	26710.9	26547.2	27560.5	1.18423	4316.26	5031.33
Run 42	0.93454	0.87335	32830.4	30960.9	30326.4	30118.5	25951.6	26417.3	26292.2	27324.1	1.18626	4374.77	5009.28
Run 43	0.93119	0.871	32880.4	30704.793	30072.9	29851.4	25653.1	26163.1	26035.9	27069.1	1.18807	4419.79	5051.7
Run 44	0.93669	0.87959	32881.3	30396.811	29811.2	29587.6	25443	25972.3	25852.2	26869.7	1.1881	4368.23	4953.8
Run 45	0.92746	0.86878	32706.7	30055.561	29439.9	29189.9	25031.5	25543	25425.4	26417.7	1.18179	4408.46	5024.09
Run 46	0.93315	0.87432	32827.5	29759.398	29149.1	28880.7	24762.1	25287.7	25180.4	26195.5	1.18616	4387.09	4997.35
Run 47	0.93067	0.87136	32827.9	29584.805	28963.9	28686.3	24553.3	25085.4	24978.8	26021.2	1.18617	4410.55	5031.46
Run 48	0.92836	0.87406	32876.7	29434.367	28864.9	28532	24419.1	24992.8	24914.6	25892.7	1.18793	4445.76	5015.24
Run 49	0.93045	0.87295	32863.9	29302.074	28700.3	28427.5	24278	24852.6	24752.9	25745.9	1.18747	4422.32	5024.09
Run 50	0.92984	0.8738	32828.3	29150.266	28565.4	28281.7	24146.8	24702.6	24626	25608.8	1.18619	4418.57	5003.46
Run 52	0.93827	0.87933	32873.8	28892.473	28289.6	28067.3	23938	24475.1	24359.9	25378.7	1.18783	4351.61	4954.5
Mean	**0.9327**	**0.8735**	**32834**										
stdev	**0.004**	**0.0034**	**53.492**										
uncertai	**0.0086**	**0.0079**	**0.0033**										

Table B.5: C-D 0.5(30-30) with CMC 2%

			Date:	08/10/2012	Test done by Luc									
			Venturi	30										
			Venturi	0.086	Area[m2]									
			Throat d	0.023	0.00042									
			Pipe Dia	0.046	0.00166									
			Diamete	0.5										
			Material	CMC										
			Density[	1012										
			Concent	2%										
			ty:	0										
			K:	0.096		**1/n**	**n/(n+1)**	**(n+1)/n**	**K1/n**					
			n:	0.716		1.26582	0.44134	2.26582	0.00517					
					Contracting		**Throat**	**Expanding**						
	Axial distances			-0.093	-0.043	-0.0215	0	0.0215	0.043	4.653				
	Venturi plane													
	Non-dimensionalised dista			-2.021739	-0.9348	-0.5972	0	0.59722	0.93478	101.152				
	Distances[m]:			6.85	6.9	6.9215	6.943	6.9645	6.986	11.596				
Run #	**Cd(D&D**	**Cd(Flan**	**Re3**	**Pod 3**	**Pod 4**	**Pod 5**	**Pod 6**	**Pod 7**	**Pod 8**	**Pod 9**	**Average [l/s]**	**Dpcont**	**ΔPflange**	
Run 2	0.90025	0.89352	22625	71498.156	70824.5	64342.1	26314.6	29233.2	31580.2	37741	3.62182	44509.9	45183.5	
Run 3	0.90925	0.90114	22583.1	71194.617	70407.7	65401.5	26908.1	28364.7	30687.3	37924.4	3.61628	43499.6	44286.5	
Run 4	0.91504	0.8907	22490.8	71752.875	69389.9	65011.4	26728.3	28523	30890.6	37724.7	3.60406	42661.7	45024.6	
Run 5	0.91135	0.89294	22456.6	71949.234	70162.7	64659.1	27262.9	27516.5	30369.2	37781.1	3.59952	42899.8	44686.3	
Run 6	0.91128	0.88705	22256.1	71556.828	69215.9	63905.2	26941.5	27261.7	29982.2	37720.4	3.57294	42274.4	44615.3	
Run 7	0.90943	0.8891	22445.2	70958.055	68966.7	64454	25922.5	27639.5	30789.5	37692.4	3.59801	43044.2	45035.5	
Run 8	0.9053	0.90455	22297.9	70162.266	70090.9	63924.7	27123.2	28759.6	31724.9	37666.3	3.57848	42967.7	43039.1	
Run 9	0.90106	0.90252	22402.4	69908.391	70050.2	64834.9	26340.1	28152	30797	38132.9	3.59234	43710.1	43568.2	
Run 10	0.90081	0.8921	22345.4	70202.344	69347.3	63491.4	25797.4	28475	30458.1	37753.2	3.58478	43549.9	44404.9	
Run 11	0.91572	0.90172	22504.2	70796.656	69462.6	64309.9	26822.5	28583.4	30348.7	38206	3.60582	42640	43974.1	
Mean	**0.9079**	**0.8955**												
Stdev	**0.0058**	**0.0063**												
uncertai	**0.0128**	**0.0141**												
Run 14	0.86791	0.85536	10457.9	39423.551	39028.4	37365.8	25653.8	26088.5	26815.5	28659.7	1.91402	13374.6	13769.8	
Run 15	0.87311	0.85288	10504.1	39654.434	39015.3	37231	25703.3	25909.3	26758.1	28714.6	1.921	13312.1	13951.2	
Run 16	0.86662	0.84955	10344.4	39364.203	38829.4	37227.3	25654.8	26012.6	26423.2	28543.3	1.89685	13174.6	13709.4	
Run 17	0.87777	0.86212	10572.9	39436.32	38948.6	37472.3	25634.4	26034.8	26663.1	28726.7	1.93141	13314.3	13801.9	
Run 18	0.88984	0.87302	10559.2	39504.387	39001.5	37444.7	26073.9	25859.3	26662.5	28796.8	1.92933	12927.5	13430.5	
Run 19	0.89405	0.87284	10564.5	39466.137	38835.8	37506.8	26018.8	26470.3	27090.2	28559.9	1.93014	12816.9	13447.3	
Run 20	0.86794	0.86069	10445.8	39335.91	39110.2	37219.8	25762.1	26208	26737.3	28653	1.9122	13348.1	13573.9	
Run 21	0.88035	0.86997	10493.5	39213.207	38899.4	37558.1	25827.1	26186.5	26652.5	28872.6	1.91941	13072.3	13386.1	
Run 22	0.86918	0.86169	10435.2	39237.891	39005.9	37372.6	25718.4	26021.7	26796.9	28567.3	1.91059	13287.5	13519.5	
Run 23	0.89073	0.85593	10470.8	39667.172	38611.4	37412.7	25887.4	26041.6	26883.8	28936.7	1.91598	12724	13779.8	
Mean	**0.8778**	**0.8614**												
Stdev	**0.0105**	**0.0083**												
uncertai	**0.024**	**0.0193**												
Run 25	0.91329	0.86778	4218.62	28799.996	28510.1	28340.6	25816.5	25734.6	25916.3	26101	0.90386	2693.52	2983.45	
Run 26	0.9156	0.86937	4133	28659.664	28376.8	28242.8	25786.2	25829.7	25805.9	26291.3	0.88867	2590.61	2873.47	
Run 27	0.90344	0.8611	4160.52	28875.984	28604.9	28342.7	25914.7	26062.1	25860	26244.7	0.89356	2690.16	2961.25	
Run 29	0.92109	0.87626	4359.24	28114.457	27821	27640.1	25025.5	25015.8	24962.7	25337.6	0.92869	2795.53	3088.94	
Run 30	0.90858	0.86301	4400.36	27927.545	27611.3	27417	24693.3	24869.2	24740	25138.5	0.93592	2917.97	3234.27	
Run 31	0.90608	0.86186	4415	27855.443	27545	27330.5	24594.7	24531.9	24459.9	25064.9	0.93849	2950.29	3260.76	
Run 32	0.87985	0.83936	4360.51	27690.58	27387.7	27133.8	24322.5	24375	24317.6	24802.9	0.92891	3065.22	3368.08	
Run 33	0.88688	0.84622	4316.06	27619.291	27327.4	27180.3	24361.3	24477.2	24453.4	24944	0.92108	2966.17	3258.04	
Run 34	0.88643	0.85499	4283.79	27638.717	27419.1	27228.2	24486.5	24832.9	24556.6	25050.3	0.91539	2932.56	3152.21	
Run 35	0.91315	0.85835	4273.55	27813.701	27451	27244.8	24698.4	24872.8	24701	25116.9	0.91358	2752.53	3115.27	
Mean	**0.9034**	**0.8598**												
Stdev	**0.0142**	**0.0109**												
uncertai	**0.0313**	**0.0254**												

Table B.6: C-D 0.5 (30-30) with CMC 2% + XG

			Date:	19/10/2012	Test done by Luc									
			Venturi angle [°]:	30										
			Venturi length [m]:	0.086	Area[m2]									
			Throat diameter[m]:	0.023	0.00042									
			Pipe Diameter [m]:	0.046	0.00166									
			Diameter ratio	0.5										
			Material Type:	CMC+xanthan										
			Density[kg/m3]:	1013										
			Concentration:	2%										
			ty:	0										
			K:	0.323		**1/n**	**n/(n+1)**	**(n+1)/n**	**K1/n**					
			n:	0.675		1.62075	0.38157	2.62075	0.19179					
					Contracting		**Throat**	**Expanding**						
	Axial distances			-0.093	-0.043	-0.0215	0	0.0215	0.043	4.653				
	Venturi plane													
	Non-dimensionalised dista			-2.021739	-0.9348	-0.5972	0	0.59722	0.93478	101.152				
	Distances[m]:			6.85	6.9	6.9215	6.943	6.9645	6.986	11.596				
Run #	**Cd(D&D**	**Cd(Flan**	**Re3**	**Pod 3**	**Pod 4**	**Pod 5**	**Pod 6**	**Pod 7**	**Pod 8**	**Pod 9**	**Average [l/s]**	**Dpcont**	**DPFlang**	
Run 4	0.8674	0.84808	2461.37	69750.18	67849.7	35007.9	26614.4	47217.4	41912.8	40938.8	3.36167	41235.3	43135.8	
Run 5	0.86249	0.83834	2414.3	70576.75	68206	35555.9	27648.4	47595.3	41883.8	41932.8	3.31506	40557.6	42928.3	
Run 6	0.88612	0.85973	2415.06	71128.461	68732.3	37129.5	30291.2	47524	42244.6	41320	3.31582	38441.1	40837.3	
Run 8	0.8601	0.85423	2447.48	70731.195	70157.7	38182.3	28560.7	47100.7	42615.8	42311.4	3.34794	41597	42170.5	
Run 9	0.86261	0.83612	2465.84	72140.867	69449.3	37525.3	27645.2	47031.4	42430	41566.4	3.36608	41804.1	44495.6	
Run 10	0.85912	0.84218	2483.73	71103.766	69374	29993.2	26786.1	47248	40906.4	41169	3.38372	42587.9	44317.7	
Run 11	0.85682	0.83217	2452.58	71319.57	68791.5	34888.6	26749.9	46951.2	42744.6	40823.6	3.35298	42041.6	44569.7	
Run 12	0.87745	0.85826	2466.48	71086.586	69258.5	35995.3	28841.3	47325.1	41810.6	41485.3	3.36671	40417.2	42245.3	
Run 13	0.87314	0.84241	2450.03	71799.758	68796.7	37518.2	28371.9	46307.4	43142.7	41245.8	3.35046	40424.8	43427.8	
Run 14	0.85697	0.83367	2450.28	72176.633	69797.6	38155.2	27827.5	47058.8	42405	42014.7	3.35071	41970.1	44349.1	
Run 15	0.86742	0.84274	2447.48	70557.172	68126.6	36164.2	27229.1	46225.7	41503.5	40657.9	3.34794	40897.5	43328.1	
Mean	**0.8663**	**0.8444**												
Stdev	**0.0093**	**0.0096**												
uncertai	**0.0214**	**0.0227**												
Run 20	0.86382	0.85689	1563.98	52812.848	52462.2	34985.1	30882.2	42211.2	39130.3	38528.1	2.42186	21580	21930.7	
Run 21	0.86525	0.84241	1589.01	54852.016	53642.5	35344.1	31633.8	41371.2	38465.4	36737.4	2.44983	22008.7	23218.2	
Run 22	0.8958	0.85664	1583.14	54524.078	52614.1	34458	32190.7	42659.9	39007.1	37282.9	2.44328	20423.4	22333.4	
Run 23	0.89396	0.85796	1632.45	53849.32	52012.3	33655.1	30574.9	41211.4	37968.9	38419.7	2.49808	21437.5	23274.5	
Run 25	0.90436	0.84796	1575.69	54053.578	51317.8	35104.3	31415.7	41087.9	39030.6	37402.3	2.43496	19902.1	22637.9	
Run 26	0.84709	0.81969	1571.29	55495.512	53960	35315.7	31366.8	42013.2	39440.2	37810.8	2.43005	22593.1	24128.7	
Run 27	0.87137	0.84087	1608.7	55104.492	53472.6	35402.8	31382.3	41869.7	37814.7	35992.3	2.47175	22090.3	23722.2	
Run 28	0.87293	0.84601	1581.55	55074.406	53686	35161.8	32209.6	40913.4	38209	37637.4	2.44151	21476.4	22864.8	
Run 29	0.88269	0.84074	1623.12	54799.867	52569.5	34278.4	30762.2	40837.2	35700.1	36154.2	2.48775	21807.3	24037.7	
Run 30	0.88323	0.85251	1634.05	55146.945	53533.5	36309.2	31540.9	41307.8	36567.4	36268.6	2.49984	21992.6	23606	
Run 31	0.84593	0.82639	1578.96	55576.922	54485	36550.8	31670.1	41946.9	39803.1	37864.7	2.43862	22814.8	23906.8	
Mean	**0.8751**	**0.8444**												
Stdev	**0.0191**	**0.0124**												
uncertai	**0.0436**	**0.0294**												

Run 33	0.85821	0.82156	866.607	44613.504	43764.3	36194.8	34455.2	38215.4	37059.8	35237.1	1.58034	9309.14	10158.3
Run 34	0.86922	0.82787	738.16	41965.488	41228.8	35291.9	34032.8	37076.8	36056.7	34151.1	1.40725	7195.97	7932.67
Run 35	0.87491	0.82367	738.149	41063.645	40152.5	34139.6	33050	36144.5	35435.7	33910	1.40724	7102.54	8013.67
Run 36	0.88385	0.8153	727.122	41472.418	40279.1	34505.5	33469.5	36528.3	35651.7	34041.7	1.39201	6809.64	8002.96
Run 37	0.90243	0.83124	740.677	41561.852	40363.5	34648.3	33654.6	36770	35755.7	34327.8	1.41072	6708.97	7907.3
Run 38	0.87897	0.81667	741.751	41568.645	40446.2	34480.9	33359.5	36561.2	35661.3	34175.9	1.4122	7086.69	8209.17
Run 39	0.92108	0.84483	740.883	41501.254	40285.7	34541.1	33843.1	36525.9	35578.5	34254.8	1.41101	6442.61	7658.11
Run 40	0.89212	0.82449	745.087	41698.422	40515.9	34494.7	33591.7	36455.7	35561	34164.1	1.41679	6924.19	8106.69
Run 41	0.85448	0.8056	755.73	41000.684	40037.5	33557.9	32333.5	35350.2	34429.7	32968.1	1.43139	7704.01	8667.17
Mean	**0.8817**	**0.8242**											
Stdev	**0.0212**	**0.0106**											
uncertai	**0.0481**	**0.0258**											
Run 44	0.8986	0.80668	422.576	36746.566	36022.6	33533.9	33017.3	34597.9	34284.9	32952.2	0.94018	3005.34	3729.3
Run 45	0.90442	0.80315	388.961	37539.699	36834.2	34653.8	34202.5	35518.1	35175.9	33868.9	0.88549	2631.66	3337.16
Run 46	0.92045	0.80882	390.905	37912.543	37157.4	35105	34598.2	35884.9	35487.5	34134.5	0.88869	2559.18	3314.31
Run 47	0.90332	0.78878	385.215	37885.801	37075.4	34981.3	34474	35747	35450.2	34186.9	0.87932	2601.42	3411.77
Run 49	0.98709	0.8077	378.205	38054.535	37007.5	35243.1	34886	36260.3	35819.5	34489.3	0.86772	2121.52	3168.55
Run 50	0.97515	0.8071	381.336	38126.23	37114.8	35377.8	34915	36114.3	35698	34267.3	0.8729	2199.84	3211.25
Run 51	0.95383	0.80081	377.512	38335.609	37386.9	35554.7	35120.9	36233	35943.8	34474.2	0.86656	2266	3214.71
Run 52	0.9443	0.78122	361.843	38486.891	37484.2	35662.4	35309.7	36631.5	36385.8	35141.5	0.84041	2174.48	3177.15
Run 53	0.92861	0.78176	364.489	39213.902	38280	36411	36007.6	36977.6	36590.1	35213.9	0.84485	2272.43	3206.32
Run 54	0.96258	0.80292	364.605	38644.406	37719.3	35985.6	35603.4	36771.7	36456.4	35138.2	0.84504	2115.84	3040.99
Mean	**0.9378**	**0.7989**											
Stdev	**0.0316**	**0.0108**											
uncertai	**0.0673**	**0.027**											

Table B.7: C-D 0.5 (15-15) with Water

			Date:	04/10/2012	Test done by Luc								
			Venturi angle [°]:	15									
			Venturi length [m]:	0.176	Area[m2]								
			Throat diameter[m]:	0.023	0.00042								
			Pipe Diameter [m]:	0.046	0.00167								
			Diameter ratio	0.5	0.19697								
			Material Type:	Water									
			Density[kg/m3]:	999.87									
			Concentration:	1									
			ty:	0									
			K:	0.001		1/n	n/(n+1)	(n+1)/n	K1/n				
			n:	1		1	0.5	2	0.001				
					Contracting		Throat	Expanding					
	Axial distances			-0.135	-0.085	-0.0425	0	0.0425	0.085	0.135			
	Venturi plane												
	Non-dimensionalised dista			-2.934783	-1.8478	-0.9239	0	0.92391	1.84783	2.93478			
	Distances[m]:			6.85	6.9	6.9425	6.985	7.0275	7.07	7.12			
Run #	Cd(D&D	Cd(Flan	Re3	Pod 3	Pod 4	Pod 5	Pod 6	Pod 7	Pod 8	Pod 9	Average	Dpcont	ΔPflange
											[l/s]		
Run 3	1.07142	1.07698	148235	61980.148	62675.1	56496	-4750.7	34720.6	41856.1	38888	5.35619	67425.8	66730.9
Run 5	1.07112	1.09295	150442	61979.887	64728.4	57915.9	-4758.7	31114.5	41901.7	39514.8	5.43593	69487.1	66738.6
Run 6	1.07118	1.08479	149773	62415.531	64133	49589.1	-4729.8	31092.5	42052.4	40351.5	5.41174	68862.8	67145.3
Run 7	1.0698	1.07523	150041	63791.07	64489.2	48462.3	-4799.2	32365.3	40971.1	40165.4	5.42144	69288.4	68590.2
Run 9	1.03463	1.07953	148389	61816.535	67718.8	49703.1	-4737	31168.3	41939.6	39151.6	5.36173	72455.7	66553.5
Run 10	1.04824	1.08376	148497	61385.023	65942.5	57750.3	-4747.2	32739.1	41738.9	39191.7	5.36564	70689.7	66132.2
Run 11	1.05692	1.07116	147587	62130.18	63944.9	57899.5	-4739	34560.1	41284.8	39588.3	5.33276	68683.9	66869.2
Run 12	1.07506	1.08666	149449	61885.039	63331.1	56424.1	-4740.1	35943.7	44199.6	40415.4	5.40003	68071.2	66625.1
Run 13	1.06399	1.08303	148689	61649.879	64046.9	58255.3	-4742.7	33571.6	43128.4	40034.6	5.37256	68789.6	66392.6
Run 14	1.07163	1.08383	149295	62058.98	63589.6	48884.6	-4776.8	33183.7	43477	39806.5	5.39449	68366.4	66835.8
Mean	**1.0634**	**1.0818**											
stdev	**0.013**	**0.0062**											
uncertai	**0.0245**	**0.0115**											
Run 15													
Run 16	0.97895	0.97565	106421	42989.223	42706.9	37134.7	1080.34	27982.6	32383.3	30693.1	3.84531	41626.6	41908.9
Run 17	0.98729	0.98654	106644	43037.605	42974.9	36363.4	1876.26	27784.7	32466.1	30374.8	3.85337	41098.7	41161.3
Run 18	0.98745	0.9782	106675	43184.176	42403.2	37316.6	1293.88	28032.7	32450.7	30359.5	3.85451	41109.4	41890.3
Run 19	0.99766	0.99047	106571	42956.484	42371.1	36599.2	2177.7	27670.5	32542.5	30370.9	3.85073	40193.4	40778.8
Run 21	0.98345	0.98499	106494	42526.371	42655.9	36235	1351.78	27800.1	32560.5	30232.5	3.84795	41304.1	41174.6
Run 22	0.99376	0.98814	106682	42648.801	42185.7	36425.8	1591.18	27556.3	32423.7	30005.4	3.85476	40594.5	41057.6
Run 23	0.99094	0.9776	106602	43237.574	42117.8	36549.7	1353.63	27814.4	32445.9	30190.2	3.85186	40764.1	41883.9
Run 24	0.98692	0.98308	106724	42827.262	42505.3	36119.4	1313.86	27731.6	32341.6	30170	3.85627	41191.4	41513.4
Run 25	1.00142	0.99174	106954	42906.172	42118.3	36591.9	1938.52	27666.6	32258	29976.4	3.86458	40179.8	40967.7
Run 26	0.98802	0.97568	106637	43110.145	42065	36729.6	1032.92	27895	32366.1	30161.4	3.85312	41032.1	42077.2
Run 27	0.98849	0.98065	106536	42892.422	42236	37098.6	1319.94	27843.8	32302.3	30126	3.84947	40916.1	41572.5
mean	**0.9895**	**0.983**											
stdev	**0.0063**	**0.0058**											
uncertai	**0.0127**	**0.0119**											
Run 29	0.94936	0.93949	62563.5	26212.311	25889.1	23938.5	10591.6	21748.5	22651.1	22243.1	2.26061	15297.5	15620.8
Run 30	0.9479	0.94143	62566.9	25977.391	25765.9	23833.3	10419.5	21679.3	22579.4	22139.4	2.26073	15346.5	15557.9
Run 31	0.94641	0.93619	62563.5	26011.816	25674.2	23780.9	10280.9	21641.2	22521.3	22096.3	2.26061	15393.2	15730.9
Run 32	0.94845	0.9393	62570.5	25965.887	25665.8	23780.9	10335.5	21590.2	22486.8	22092	2.26086	15330.4	15630.4
Run 35	0.94886	0.94058	62633.2	25968.959	25697.6	23773.5	10349.7	21569	22416.4	22064.4	2.26313	15347.9	15619.2
Run 36	0.94682	0.93977	62518.2	25939.006	25708	23730.1	10350.4	21533.9	22389.8	22068.8	2.25897	15357.6	15588.6
Run 37	0.94548	0.93752	62406.6	25959.109	25697.3	23724.4	10351.2	21558.7	22388.7	22075.9	2.25494	15346.1	15607.9
Run 38	0.95772	0.95072	62647.2	25905.17	25682.3	23689	10610.5	21481.2	22348.6	22078.4	2.26363	15071.8	15294.6
Run 39	0.94981	0.94307	62413.6	25893.242	25675	23687.7	10465.1	21450.4	22289.6	22009.3	2.25519	15209.9	15428.1
Mean	**0.949**	**0.9409**											
Stdev	**0.0036**	**0.0042**											
uncertai	**0.0075**	**0.0089**											

Run 43	0.94808	0.93999	42747.9	21760.727	21637	20739.1	14475.9	19497.8	19671.5	19777.7	1.54461	7161.16	7284.85
Run 44	0.95193	0.94304	42922.5	21753.227	21617.5	20761.4	14456	19426.9	19674.3	19778	1.55092	7161.46	7297.18
Run 45	0.95123	0.94336	42887.8	21723.289	21603.3	20753.3	14443	19438.6	19657.6	19746	1.54966	7160.36	7280.3
Run 46	0.95043	0.94075	42849.7	21717.326	21569.2	20686.9	14409.4	19464.8	19611.5	19744.2	1.54829	7159.8	7307.89
Run 48	0.94624	0.93851	42807.9	21640.09	21520.8	20653.1	14311.7	19358.3	19581.5	19704	1.54678	7209.14	7328.39
Run 49	0.95112	0.94281	43066.1	21638.84	21511	20625.4	14289.2	19367	19568.6	19659.9	1.55611	7221.77	7349.62
Run 50	0.94556	0.93747	42903.1	21631.49	21505.9	20613.3	14254.1	19325.6	19552.3	19651.5	1.55022	7251.72	7377.34
Run 51	0.94963	0.94327	42970.1	21591.568	21494.1	20587.8	14281.9	19321.8	19538.8	19672.8	1.55264	7212.21	7309.7
Mean	**0.9493**	**0.9412**											
Stdvev	**0.0024**	**0.0023**											
uncertai	**0.005**	**0.0049**											

Table B.8: C-D 0.5(15-15) with CMC 2%

			Date:	06/10/2012	Test done by Luc								
			Venturi angle [°]:	15									
			Venturi length [m]:	0.176	Area[m2]								
			Throat diameter[m]:	0.023	0.00042								
			Pipe Diameter [m]:	0.046	0.00167								
			Diameter ratio	0.5									
			Material Type:	CMC									
			Density[kg/m3]:	1012									
			Concentration:	2%									
			ty:	0									
			K:	0.096		**1/n**	**n/(n+1)**	**(n+1)/n**	**K1/n**				
			n:	0.716		1.26582	0.44134	2.26582	0.00517				
					Contracting		**Throat**		**Expanding**				
	Axial distances			-0.135	-0.085	-0.0425	0	0.0425	0.085	0.135			
	Venturi plane												
	Non-dimensionalised dista			-2.934783	-1.8478	-0.9239	0	0.92391	1.84783	2.93478			
	Distances[m]:			6.85	6.9	6.9425	6.985	7.0275	7.07	7.12			
Run #	**Cd(D&D**	**Cd(Flan**	**Re3**	**Pod 3**	**Pod 4**	**Pod 5**	**Pod 6**	**Pod 7**	**Pod 8**	**Pod 9**	**Average [l/s]**	**Dpcont**	**ΔPflange**
Run 2	1.00332	0.96963	35456.2	77149.227	71859.2	66382.6	-2963.2	28401.6	45102.3	45935.4	5.25011	74822.4	80112.4
Run 3	1.0099	0.97291	35422.2	76346.859	70634	60089.1	-3099.2	26864.8	42001.9	46962.9	5.24596	73733.2	79446.1
Run 4	0.99761	0.97697	35451	75944.555	72714.5	64923.4	-2948.2	33679.9	48794.7	47247	5.24948	75662.7	78892.8
Run 5	0.99093	0.96851	35401.6	77638.5	74056.2	66661.9	-2454.2	32711.6	46903.3	46423.1	5.24344	76510.4	80092.7
Run 6	0.99664	0.96539	35274	77340.867	72393.9	61350.6	-2791.6	22776.1	38545.3	46799.9	5.22782	75185.5	80132.5
Run 7	1.01396	0.96764	35365.6	77418.719	70267.3	63031.5	-2682.8	23652.3	41492.8	46669.3	5.23903	72950.1	80101.6
Run 8	1.0228	0.96757	35336.8	77743.313	69336.1	58893.6	-2262.6	27918.9	42464	46667.2	5.2355	71598.7	80005.9
Run 9	0.98856	0.95917	35248.3	78878.523	74130.5	60295.4	-2197.5	26506.7	40129.3	46744.6	5.22467	76328	81076
Run 10	0.98254	0.97598	35304.9	76192.297	75146.9	66024.9	-2323.7	25772.3	35718	46697.2	5.23159	77470.6	78516
Run 6	0.99664	0.96539	35274	77340.867	72393.9	61350.6	-2791.6	22776.1	38545.3	46799.9	5.22782	75185.5	80132.5
Mean	1.00069	0.96931											
Stdev	0.01301	0.00549											
uncetair	0.02601	0.01132											
Run 15	0.95461	0.9703	18013.6	39478.32	40344.1	30749.2	13357	26188.3	28306.2	29969.7	2.99998	26987.1	26121.3
Run 16	0.96373	0.9779	17848.1	39565.406	40315.6	31303.9	14237.9	24803.9	28331.9	29552.1	2.97718	26077.7	25327.5
Run 17	0.97137	0.96574	17843.5	40286.996	39986.6	30230.6	14328.5	25051.7	29030.3	29834.1	2.97655	25658.2	25958.5
Run 18	0.96447	0.96921	17938.6	39586.336	39842.7	28835.4	13586.4	24632.5	28748.1	30466	2.98965	26256.4	26000
Run 19	0.98281	0.97255	18010	40294.195	39754.2	28791.8	14302.3	24736.4	27891.2	29797.8	2.99948	25452	25991.9
Run 20	0.97642	0.97913	17952.3	39722.77	39864.4	30071.5	14214.4	24472.5	27474.1	30137.9	2.99154	25650	25508.4
Run 21	0.95913	0.96964	17902	39674.133	40245	30027.7	13784.6	24379.1	26463.4	29641.2	2.98462	26460.3	25889.5
Run 22	0.99053	0.96638	17757.7	40519.113	39280.4	30427.3	14800.9	25281.9	27418.1	29882.8	2.96471	24479.5	25718.2
Run 23	0.98134	0.9795	18035.6	39919.738	39823.3	29520.3	14234.8	23319.5	26921	29733.2	3.00301	25588.5	25684.9
Run 24	0.96002	0.97347	17932.2	39877.801	40604.2	29125.7	14119.6	24571.4	28077.6	29561.7	2.98877	26484.6	25758.2
Mean	0.97044	0.97238											
Stdev	0.01192	0.00505											
uncertai	0.02457	0.01039											
Run 25													

Run 26	0.96723	0.95374	8878.08	27707.941	27475.3	24106.6	19312.4	24722.3	43822.6	23061.7	1.67173	8162.84	8395.51
Run 27	0.96757	0.95656	9001.27	27352.658	27159.5	24168.9	18814.4	23273	26324.2	23022.7	1.69088	8345.05	8538.23
Run 28	0.98442	0.95715	9064.86	27060.215	26588.9	23799.2	18432.6	23022.1	24382.7	23264.5	1.70074	8156.25	8627.58
Run 29	0.98421	0.96174	9018.12	26851.258	26468.7	23956.8	18378.5	23207.8	23872.8	23270.2	1.69349	8090.2	8472.77
Run 30	0.96668	0.95823	9064.18	26811.172	26661.4	23991.7	18204.1	23506	23974.3	23025.2	1.70064	8457.34	8607.09
Run 31	0.96808	0.95732	9100.73	26661.139	26469.2	24301.7	17980.2	22980.9	23623.4	23049.1	1.70631	8489.09	8680.99
Run 32	0.96892	0.96882	8995.59	26208.545	26206.9	24080.3	17893.7	22784.6	23420.5	22764.3	1.69	8313.16	8314.82
Run 33	0.9684	0.96815	9060.13	26353.186	26348.9	24011.8	17927.9	22684.5	23628.6	23004.2	1.70001	8421.01	8425.3
Run 34	0.9696	0.95416	8908.82	26459.004	26192.6	24063.2	18023	22756.3	23297.9	22851	1.67651	8169.65	8436.04
Run 35	0.97227	0.95417	9048.86	26540.654	26221.5	24267.6	17884.4	22661.2	23193.9	22641.6	1.69826	8337.02	8656.22
Mean	0.97174	0.959											
Stdev	0.00681	0.00553											
uncertai	0.01401	0.01153											
Run 37	0.97333	0.95736	4747.33	25809.199	25712.8	24536	22848.6	25091.8	25018.6	24161.8	0.99651	2864.28	2960.64
Run 38	0.97623	0.95823	4759.92	25651.697	25543.2	24330	22683.5	25046.2	25208.3	24134.3	0.99869	2859.73	2968.18
Run 39	0.95812	0.9448	4797.1	25616.883	25531.5	24210.7	22524.2	24955.6	25147	24023.8	1.00513	3007.31	3092.73
Run 40	0.97239	0.95514	4787.08	25593.029	25487	23779.6	22577.3	24842.2	24996.5	24038.4	1.0034	2909.64	3015.7
Run 41	0.97813	0.96361	4807.54	25534.676	25446.7	23445.7	22550.8	24905.5	25049.2	24027.4	1.00694	2895.93	2983.86
Run 42	0.98037	0.95067	4796.06	25610.227	25428	22908	22556.7	24760	24942.3	24016.2	1.00495	2871.36	3053.55
Run 43	0.97175	0.95462	4784.24	25604.398	25499	22979.6	22588.4	24845.8	24970.7	23968.3	1.00291	2910.63	3016.01
Run 44	0.96676	0.95977	4785.62	25601.221	25558.2	23036.3	22616.1	24770.2	25067.5	23973.5	1.00315	2942.13	2985.11
Run 45	0.96822	0.9599	4769.57	25514.15	25463.4	23048	22546.4	24616.9	24788.1	24072.1	1.00037	2917.03	2967.79
Run 46	0.96527	0.95461	4828.71	25525.248	25458	23018.5	22462.7	24583.6	24696.7	23979.8	1.0106		
Mean	0.97106	0.95587											
stdev	0.00665	0.0053											
uncertai	0.0137	0.01108											

Table B.9: C-D 0.5 (15-15) with CMC +XG

			Date:	20/10/2012	Test done by Luc								
			Venturi angle [°]:	15									
			Venturi length [m]:	0.176	Area[m2]								
			Throat diameter[m]:	0.023	0.00042								
			Pipe Diameter [m]:	0.046	0.00167								
			Diameter ratio	0.5	0.19697								
			Material Type:	CMC+XG									
			Density[kg/m3]:	1015									
			Concentration:	2%									
			ty:	0									
			K:	323		**1/n**	**n/(n+1)**	**(n+1)/n**	**K1/n**				
			n:	0.675		1.61551	0.38233	2.61551	0.20152				
					Contracting		**Throat**	**Expanding**					
	Axial distances			-0.135	-0.085	-0.0425	0	0.0425	0.085	0.135			
	Venturi plane												
	Non-dimensionalised dista			-2.934783	-1.8478	-0.9239	0	0.92391	1.84783	2.93478			
	Distances[m]:			6.85	6.9	6.9425	6.985	7.0275	7.07	7.12			
Run #	**Cd(D&D**	**Cd(Flan**	**Re3**	**Pod 3**	**Pod 4**	**Pod 5**	**Pod 6**	**Pod 7**	**Pod 8**	**Pod 9**	**Average**	**Dpcont**	**ΔPflange**
											[l/s]		
Run 2	1.01006	0.95398	2559.99	53166.582	49073.6	46121.2	15251.4	41768	41554.2	36029.7	3.55354	33822.1	37915.1
Run 2	0.98003	0.96562	2601.57	53205.387	52099.6	46560.5	15324.9	41964.3	40935.6	36845	3.59524	36774.6	37880.5
Run 3	1.00838	0.94485	2572.66	54091.438	49341.2	45389.3	15162.9	41452.9	40488.6	35218.2	3.56626	34178.3	38928.6
Run 5	1.00522	0.95598	2573.91	53787.91	50150.7	43566.5	15733.2	42319.1	40156.5	35130.2	3.56752	34417.5	38054.7
Run 6	0.97676	0.96866	2584.34	52792.867	52177.5	45989.2	15510.8	41457	39315.8	34435.5	3.57798	36666.6	37282
Run 7	0.93181	0.95786	2532.33	52437.34	54536.2	47022.8	15415.8	42558.4	40530.1	36317.5	3.5257	39120.4	37021.6
Run 8	0.97372	0.94601	2557.48	54461.391	52301.6	47238.8	15959.5	40590.4	40934.7	36236.1	3.55102	36342.1	38501.9
Run 9	0.94922	0.94546	2557.36	53832.547	53527.9	44942.7	15288.2	40609.4	40066.8	35073.8	3.55089	38239.7	38544.4
Run 10	0.94464	0.96587	2560.11	52533.16	54214.2	46652.4	15542.7	41431.1	41027.3	35854.4	3.55367	38671.4	36990.4
Run 11	0.96573	0.94815	2601.57	54848.117	53430.7	46649.8	15558.9	40947.8	39282.3	35536.3	3.59524	37871.8	39289.2
mean	**0.9746**	**0.9552**											
stdev	**0.0275**	**0.0091**											
uncertai	**0.0565**	**0.0191**											

Run 14	0.67791	0.90377	1496.99	45124.207	60222.9	40527.6	25701.5	38253.1	37662.6	34262.2	2.40952	34521.4	19422.7
Run 16	0.92154	0.91974	1469.29	44317.867	44246.4	41320.2	26064.1	39672.7	38804.1	35132.1	2.37714	18182.3	18253.8
Run 17	0.9761	0.93584	1498.07	46295.219	44830.1	41342.1	28161.8	39633.6	38848.1	35282.3	2.41077	16668.3	18133.4
Run 18	0.96895	0.92146	1469.5	46031.602	44292.2	40565	27842.2	41043.3	40316.8	36249.6	2.37739	16450	18189.4
Run 19	0.89722	0.94094	1510.3	43865	45676.8	41785.5	25715	39644.3	38620	33902.6	2.42501	19961.8	18150
Run 20	0.70506	0.91581	1473.48	45013.133	57717	43670.2	26526.3	39403.4	39412.9	36115.1	2.38205	31190.8	18486.9
Run 21	0.94103	0.93152	1443.65	45761.652	45412.8	42444.5	28414.8	40198.7	39646.6	36407.7	2.34703	16998	17346.9
Run 22	0.94494	0.91765	1476.82	44931.469	43880	41848.3	26458.3	40390.9	39793.6	36270.8	2.38596	17421.7	18473.2
Run 23	0.94702	0.91531	1460.47	44983.469	43780.4	40860.9	26712.6	40358.3	39970	36001.4	2.36681	17067.8	18270.9
Run 24	0.93526	0.92294	1426.55	44249.438	43795	40727.5	26880.8	38959.6	39054.3	36214.2	2.32687	16914.1	17368.6
mean	**0.8915**	**0.9225**											
Stdev	**0.1079**	**0.0109**											
uncertai	**0.2421**	**0.0237**											
Run 26	0.97458	0.91168	861.227	42204.113	41133.4	39828.7	33633.2	38092.7	37651.5	34537.8	1.61461	7500.18	8570.91
Run 27	0.92571	0.89012	892.388	40318.32	39604.4	37887.9	30852.3	35987.2	35733.1	32878.5	1.65671	8752.04	9465.99
Run 28	0.95154	0.9104	911.458	39382.652	38593.3	37087.9	30052.2	35186.9	34813.2	31952.6	1.68227	8541	9330.4
Run 29	0.96063	0.90978	923.862	38838.543	37856.4	36568.2	29310.7	34591.5	34459.2	31755.7	1.69882	8545.71	9527.86
Run 30	0.94719	0.91522	931.032	38362.789	37730.9	36090.5	28842	34400.1	34017.7	31402.5	1.70835	8888.89	9520.78
Run 31	0.94959	0.90797	930.886	38370.41	37541.2	35876	28699.2	34091.3	33850.2	31283.6	1.70816	8842.04	9671.23
Run 32	0.98212	0.90801	927.524	38221.93	36825	35801.2	28602.1	33926.9	33765.6	31142	1.70369	8222.9	9619.79
Run 33	0.94749	0.90294	926.423	38280.84	37389	35753.8	28569.3	34064.2	33848.1	31492.7	1.70222	8819.7	9711.56
Run 34	0.95391	0.90452	923.874	38224.141	37251.8	35974.8	28585.1	33990.3	33742.3	31359.4	1.69883	8666.76	9639.06
Run 35	0.96512	0.91983	915.33	38211.371	37368.5	35553.6	29015.1	34427.4	34260	31634.8	1.68744	8353.4	9196.32
Run 36	0.95883	0.9148	921.36	38893.176	38050.9	36899.4	29506.6	34840.2	34601.6	32040.2	1.69548	8544.31	9386.56
mean	**0.9561**	**0.9087**											
stdev	**0.0151**	**0.0078**											
uncertai	**0.0315**	**0.0172**											
Run 38	1.08763	0.82162	426.48	37706.629	36069.3	35563.2	33893	34794.3	34757.2	33191	0.97063	2176.31	3813.6
Run 39	0.97737	0.8372	416.138	37734.383	36790.5	36536.9	34189.6	35564.2	35463	33754.9	0.95353	2600.88	3544.75
Run 40	0.93804	0.81539	411.649	37610.539	36711.5	36142.4	33931.9	35170	34928.9	33308.3	0.94607	2779.57	3678.65
Run 41	0.928	0.83683	417.292	37202.488	36537	35900.6	33640.4	35018.1	34943.3	33142.5	0.95545	2896.62	3562.09
Run 42	0.94671	0.82667	406.878	37350.289	36514.4	36009.8	33831.2	35119	34995.4	33202.9	0.93812	2683.22	3519.08
Run 43	0.93604	0.83199	390.001	37435.977	36749.9	36146	34168.5	35832.9	35916.3	34274.5	0.90978	2581.37	3267.46
Run 44	0.98395	0.82772	392.206	38542.215	37569.2	37078	35213.9	36334.7	36169.2	34474.3	0.9135	2355.3	3328.29
Run 45	1.00179	0.81111	381.224	38636.785	37491	36906.7	35310.4	36379.4	36097.2	34068.2	0.89491	2180.59	3326.34
Run 46	0.95094	0.83452	391.072	38719.984	37970.5	37087.1	35459.4	36228.9	36262.9	34675.5	0.91159	2511.11	3260.57
Run 47	0.87812	0.83598	395.907	38276.871	37967	36842.8	34969.3	36119.3	35933.7	34091.1	0.91974	2997.71	3307.55
mean	**0.9629**	**0.8279**											
stdev	**0.0557**	**0.0093**											
uncertai	**0.1156**	**0.0224**											

Table B.10: CMC 0.7 (15-15) with water

			Date:	01/10/2012	Test done by Luc								
			Venturi angle [°]:	15									
			Venturi length [m]:	0.104	Area[m2]								
			Throat diameter[m]:	0.0322	0.00082								
			Pipe Diameter [m]:	0.046	0.00167								
			Diameter ratio	0.7	0.38607								
			Material Type:	Water									
			Density [kg/m3]:	999.87									
			Concentration:	1									
			ty:	0									
			K:	0.001		**1/n**	**n/(n+1)**	**(n+1)/n**	**K1/n**				
			n:	1		1	0.5	2	0.001				
					Contracting		**Throat**	**Expanding**					
	Axial distances			-0.102	-0.052	-0.026	0	0.026	0.052	0.102			
	Venturi plane												
	Non-dimensionalised dista			-2.217391	-1.1304	-0.5652	0	0.56522	1.13043	2.21739			
	Distances[m]:			6.85	6.9	6.926	6.952	6.978	7.004	7.054			
Run #	**Cd(D&D**	**Cd(Flan**	**Re3**	**Pod 3**	**Pod 4**	**Pod 5**	**Pod 6**	**Pod 7**	**Pod 8**	**Pod 9**	**Average**	**DPcont**	**ΔPFlang**
											[l/s]		
Run 2	0.9866	0.84399	152419	55397.074	48896.2	49551.5	31157.8	46279.1	50212.7	41870.2	5.50736	17738.4	24239.3
Run 2	0.96883	0.84216	152726	55689.246	49715.6	49972.2	31246.4	45766.5	50285.8	41592.6	5.51845	18469.2	24442.8
Run 4	0.9569	0.83947	153305	55690.074	49979.6	50136.3	30903.5	45733.6	50618.1	41775	5.53936	19076.1	24786.6
Run 6	0.96687	0.84381	152956	55680.633	49859.9	49933.1	31259.9	46179.3	50079.3	41998.4	5.52676	18600.1	24420.8
Run 7	0.97951	0.84562	153029	55504.805	49305.5	50092.5	31165	45685.7	50230.4	41742.8	5.52941	18140.5	24339.8
Run 8	0.96882	0.83872	153186	55663.043	49451.4	50335.3	30870.5	46788.4	50164.7	41737.4	5.53508	18580.9	24792.5
Run 9	0.96506	0.86133	153186	55356.594	50574.7	50342.5	31848.6	45389.6	50141	41818.9	5.53508	18726.1	23508
Run 10	1.00855	0.83908	152656	55519.516	47946.7	51195.4	30919.1	46347.7	50170.5	41824.6	5.51593	17027.6	24600.4
Run 11	0.98009	0.84517	153036	55682.711	49435.3	50535.1	31314.9	45739.3	50146.3	41738.2	5.52966	18120.5	24367.8
Run 12	0.94713	0.84881	153193	55381.277	50615.9	50433.2	31172.5	45676.5	50138.2	42055.8	5.53533	19443.4	24208.8
Mean	**0.9728**	**0.8448**											
stdev	**0.0161**	**0.0063**											
uncertai	**0.0332**	**0.0149**											
Run 15	0.99802	0.84406	105912	38453.488	35121.7	36619.4	26751.6	33707.8	35672.6	31569.2	3.82692	8370.03	11701.8
Run 16	0.9593	0.84049	105881	38577.168	35836.6	36338.5	26782.6	34325	35852.1	31407.5	3.82578	9054.04	11794.6
Run 18	0.94298	0.84375	105947	38266.293	35930	36685.9	26548.2	33994.3	35549.5	31479.5	3.82818	9381.8	11718.1
Run 19	0.97274	0.84627	105793	38411.473	35587.7	36641.2	26796.7	34028	35687.1	31400.4	3.82263	8791.02	11614.8
Run 20	0.94182	0.86076	105912	38134	36280.4	36987.7	26881.8	34082.3	35463.9	31582.9	3.82692	9398.62	11252.2
Run 21	0.91324	0.84254	106184	38340.645	36583.5	36848.8	26535.9	34190.7	35666.1	31286.2	3.83674	10047.6	11804.7
Run 23	0.97454	0.84072	106180	38511.41	35479.2	36956.5	26656.4	33885.3	35494.3	31300.6	3.83662	8822.77	11855
Run 24	0.99476	0.84408	105943	38319.391	35041.1	36755.8	26611.1	33893.6	35758.7	31591.8	3.82805	8430.02	11708.3
Run 25	0.94331	0.84843	106107	38214.414	35993.6	36806	26589.9	33966.1	35595.2	31148.6	3.83397	9403.72	11624.5
Run 27	0.96572	0.85349	106090	38373.586	35859.7	37113	26890.5	34061.7	35601.6	31382.7	3.83334	8969.27	11483.1
Mean	**0.9606**	**0.8465**											
Stdev	**0.0261**	**0.0063**											
Uncertai	**0.0544**	**0.015**											
Run 29	0.943	0.85384	61939.4	25629.643	24925.1	26905.3	21718.6	24557.5	24997.9	23391.9	2.23806	3206.44	3911.03
Run 30	0.94207	0.83943	62099.8	25768.314	24930.3	26634.5	21700.8	24104.5	24594.5	23011.8	2.24385	3229.48	4067.49
Run 32	0.91083	0.85281	62413.6	25384.223	24893.2	26622.6	21403.4	24009.3	24363.5	22775.5	2.25519	3489.78	3980.81
Run 33	0.90198	0.84791	62242.7	25337.9	24872.1	26587.2	21333	23969	24325.1	22722.1	2.24902	3539.1	4004.94
Run 34	0.98259	0.84863	62479.8	25296.037	24272.4	26578.4	21267.4	23929.2	24273.3	22697.8	2.25758	3005.06	4028.67
Run 35	0.96447	0.84921	62357.8	25279.111	24378.5	26644.5	21271.7	23907.6	24244.7	22632.3	2.25317	3106.86	4007.45
Run 36	0.97262	0.85392	62399.6	25273.992	24364.5	26627.6	21305.4	23897.4	24289.3	22659.2	2.25469	3059.11	3968.63
Run 37	0.93587	0.85118	62399.6	25263.57	24573.3	26671.4	21269.3	23891.9	24282.3	22641.4	2.25469	3304.04	3994.28
Run 38	0.93743	0.85451	62410.1	25284.533	24614.2	26742.4	21320.1	23922.6	24308.6	22694.3	2.25506	3294.17	3964.47
Run 39	0.94527	0.84199	62521.6	25311.549	24465	26763	21213.7	23954.1	24316	22680.9	2.25909	3251.33	4097.85
Mean	**0.9436**	**0.8493**											
stdev	**0.0252**	**0.0051**											
uncertai	**0.0534**	**0.0121**											

Run 42	0.98504	0.8905	40326.6	21508.49	21230	23611.7	19984.4	20703	20864.8	20312.4	1.45712	1245.62	1524.14
Run 43	0.97819	0.88066	40504.4	21521.41	21223.5	23590.2	19949.2	20732.6	20876.1	20277	1.46355	1274.31	1572.18
Run 44	0.96775	0.89441	40454	21509.318	21287.6	23609.1	19988.9	20770.1	20863	20297.3	1.46172	1298.71	1520.42
Run 45	0.94278	0.88855	40514	21511.275	21338.6	23582.2	19966.2	20767.7	20871.9	20323.5	1.46389	1372.48	1545.12
Run 46	0.93901	0.89523	40535.5	21527.088	21388.3	23614.1	20003.3	20789.1	20889.1	20324	1.46467	1384.98	1523.76
Run 47	0.94589	0.88991	40530.1	21555.354	21378.3	23659.1	20013.7	20802.6	20924.9	20361.3	1.46447	1364.54	1541.62
Run 50	0.9427	0.88225	40383.6	21598.496	21405.2	23710.6	20041.3	20840.6	20956.8	20394.8	1.45918	1363.9	1557.18
Run 51	0.94032	0.8841	40471.8	21606.809	21426.1	23723.2	20049.4	20842.8	20957.7	20396.2	1.46237	1376.79	1557.45
Run 52	0.94958	0.88307	40476.7	21617.215	21406.1	23754.1	20055.7	20878.3	20989.1	20401.3	1.46255	1350.4	1561.47
Run 53	0.95973	0.8834	40362.1	21631.912	21394.9	23794.9	20080.4	20876.2	20976.3	20414.5	1.45841	1314.5	1551.49
Mean	**0.9551**	**0.8872**											
stdev	**0.0158**	**0.0049**											
uncertai	**0.0332**	**0.0112**											

Table B.11: C-D 0.7 (15-15) with CMC 2%

			Date:	07/10/2012	Test done by Luc								
			Venturi angle [°]:	15		0.13165							
			Venturi length [m]:	0.104	Area[m2]	0.055							
			Throat diameter[m]:	0.0322	0.00082								
			Pipe Diameter [m]:	0.046	0.00167								
			Diameter ratio	0.7	0.38607								
			Material Type:	CMC									
			Density[kg/m3]:	1012									
			Concentration:	2%									
			ty:	0									
			K:	0.096		**1/n**	**n/(n+1)**	**(n+1)/n**	**K1/n**				
			n:	0.716		1.26582	0.44134	2.26582	0.00517				
					Contracting		**Throat**	**Expanding**					
	Axial distances			-0.102	-0.052	-0.026	0	0.026	0.052	0.102			
	Venturi plane												
	Non-dimensionalised dista			-2.217391	-1.1304	-0.5652	0	0.56522	1.13043	2.21739			
	Distances[m]:			6.85	6.9	6.926	6.952	6.978	7.004	7.054			
Run #	**Cd(D&D**	**Cd(Flan**	**Re3**	**Pod 3**	**Pod 4**	**Pod 5**	**Pod 6**	**Pod 7**	**Pod 8**	**Pod 9**	**Average [l/s]**	**DPcont**	**ΔPFlang**
Run 3	0.89432	0.88251	29780.6	52774.449	52373.4	48768	37480.6	43795.1	45634.2	39988.7	4.54526	14892.9	15293.9
Run 4	0.89322	0.8797	29819.5	52765.293	52301.9	49067.9	37340.2	42680.1	45247.5	39993.6	4.55017	14961.7	15425.1
Run 5	0.89805	0.89123	29871.5	52575.191	52347.2	49067.5	37503.4	42092.2	44804	39926.6	4.55672	14843.9	15071.8
Run 6	0.89425	0.89303	29939.5	52151.16	52110.2	48598	37083.5	42573.8	44446.7	40159.1	4.56529	15026.7	15067.7
Run 8	0.89941	0.88454	29792.6	52690.828	52191.3	48796	37456.8	42716.3	46476.3	39909.7	4.54677	14734.5	15234.1
Run 9	0.89118	0.88955	29795.6	52215.898	52160.6	48507	37150.3	43402.7	46469.1	40101.7	4.54715	15010.3	15065.6
Run 10	0.91463	0.89102	29736.7	52896.605	52133.7	48788.3	37929.8	42273.3	46625.4	39662.9	4.53971	14203.9	14966.8
Mean	**0.8979**	**0.8874**											
Stdev	**0.0079**	**0.0051**											
uncertai	**0.0176**	**0.0115**											
Run 14	0.9022	0.8979	16313.7	39101.863	39049.9	37735.3	33638.3	36242.2	36767.3	33235.8	2.76402	5411.53	5463.54
Run 15	0.88912	0.88064	16285.8	39136.648	39029.1	37612.6	33472.9	35587.3	36616.8	33313.2	2.76012	5556.15	5663.75
Run 16	0.87625	0.89677	16253.5	38777.945	39035.9	37616.4	33334.1	35352.5	36381.7	33203.8	2.75558	5701.79	5443.88
Run 17	0.90972	0.89635	16233.7	39158.152	38999.5	37745.2	33720.1	34993.5	36113.7	33428	2.75281	5279.37	5438.02
Run 18	0.89724	0.89437	16212.1	39094.785	39060	37736.7	33644.7	34964.6	36151.1	33373.1	2.74979	5415.28	5450.09
Run 19	0.91029	0.88456	16252.6	39275.734	38963.9	38055.9	33681	35189.7	36290.8	33342.2	2.75545	5282.85	5594.69
Run 20	0.90286	0.8889	16347.9	38998.004	38826.3	37595.4	33404	35209.1	35841.6	33512.1	2.76881	5422.36	5594.03
Run 21	0.92814	0.88718	16330.8	39207.367	38723.4	37823.3	33601.3	35050.7	35756	33218	2.76642	5122.13	5606.06
Mean	**0.902**	**0.8908**											
Stdev	**0.0154**	**0.0064**											
uncertai	**0.0342**	**0.0144**											
Run 25	0.96412	0.89013	9258.99	31778.461	31456.7	31209.2	29598.6	29633.4	30150.4	28989	1.73079	1858.12	2179.83
Run 26	0.89994	0.89156	9323.85	31671.814	31631.1	30994.4	29473.7	29974.7	30043.5	29001.2	1.74081	2157.33	2198.09
Run 27	0.87887	0.88674	9281.34	31633.414	31673.1	30993.1	29428.1	29541.8	29753.7	29053	1.73424	2244.97	2205.32
Run 28	0.86715	0.88943	9310.29	31495.023	31609.7	31140.9	29291.7	29975.3	30071.8	29004.9	1.73871	2318	2203.32
Run 31	0.95164	0.8909	9252.41	31893.406	31624.8	30776.6	29719.9	30426.5	33066.8	29226	1.72977	1904.91	2173.51
Run 33	0.89712	0.90301	9287.73	31364.824	31392.8	30914	29235.8	30286.4	30259.4	28416.5	1.73523	2157.01	2129
Mean	**0.9098**	**0.892**											
stdev	**0.0393**	**0.0057**											
uncertai	**0.0865**	**0.0127**											

Run 39	0.91462	0.90375	4730.54	26499.021	26482.6	26324.3	25802.1	25846.4	25901.9	25396.8	0.99359	680.43	696.885
Run 40	1.04088	0.89503	4774.57	26320.719	26132.7	26090.7	25599.2	25601.1	25546	25161.3	1.00123	533.471	721.496
Run 41	1.05231	0.89138	4804.17	26121.34	25913.8	25932.6	25386.5	25424.4	25326.4	25018.5	1.00636	527.301	734.889
Run 42	1.02628	0.90565	4829.83	25967.15	25808.2	25769.7	25248.9	25265	25156.4	24809.8	1.0108	559.299	718.215
Run 43	1.07533	0.90439	4827.76	25889.357	25678.7	25660.3	25169.7	25191.8	25091.8	24766.9	1.01044	509.076	719.705
Run 44	1.01479	0.90454	4862.78	25767.742	25618.1	25572.9	25039.6	25116.7	25020.2	24701.6	1.01649	578.502	728.113
Run 45	1.03546	0.89785	4860.18	25765.965	25582.8	25549.2	25027.6	25067.8	24987.9	24650.1	1.01605	555.143	738.35
Run 46	1.01835	0.89334	4851.62	25686.363	25515	25495.9	24942.7	24996.7	24940.9	24585	1.01457	572.283	743.652
Run 47	0.98986	0.90469	4851.62	25634.787	25515.4	25467	24909.7	25008.3	24921.1	24597	1.01457	605.699	725.117
Mean	**1.0187**	**0.9001**											
stdev	**0.0459**	**0.0057**											
uncertai	**0.0901**	**0.0126**											

Table B.12: C-D 0.7 (15-15) With CMC 2% +XG

			Date:	19/10/2012	Test done by Luc								
			Venturi angle [°]:	15									
			Venturi length [m]:	0.104	Area[m2]								
			Throat diameter[m]:	0.0322	0.00082								
			Pipe Diameter [m]:	0.046	0.00167								
			Diameter ratio	0.7	0.38607								
			Material Type:	CMC+xanthan									
			Density[kg/m3]:	1015									
			Concentration:	2%									
			ty:	0									
			K:	0.323		**1/n**	**n/(n+1)**	**(n+1)/n**	**K1/n**				
			n:	0.675		1.62075	0.38157	2.62075	0.19179				
					Contracting		**Throat**	**Expanding**					
	Axial distances			-0.102	-0.052	-0.026	0	0.026	0.052	0.102			
	Venturi plane												
	Non-dimensionalised dista			-2.217391	-1.1304	-0.5652	0	0.56522	1.13043	2.21739			
	Distances[m]:			6.85	6.9	6.926	6.952	6.978	7.004	7.054			
Run #	**Cd(D&D**	**Cd(Flan**	**Re3**	**Pod 3**	**Pod 4**	**Pod 5**	**Pod 6**	**Pod 7**	**Pod 8**	**Pod 9**	**Average [l/s]**	**DPcont**	**ΔPFlang**
Run 2	0.98115	0.88112	2682.55	52671.551	50838.7	49375.3	43199.8	48855.7	47439.2	42306.9	3.56727	7638.93	9471.75
Run 2	1.01969	0.88248	2692.64	52855.961	50472.9	49004.8	43362	49135.6	47622.9	42293.6	3.57697	7110.93	9493.95
Run 3	1.00235	0.8803	2698.15	52851.098	50662.5	49054	43281.6	48322.3	47888.7	42877.3	3.58226	7380.83	9569.45
Run 4	0.9923	0.88172	2629.5	51925.129	49991	48743.3	42735.5	48757.7	47554.4	42606.1	3.51612	7255.49	9189.66
Run 5	0.97242	0.89586	2676.65	52059.273	50677.7	48993.6	42925.7	48410.8	47831.9	42329.3	3.5616	7752.02	9133.57
Run 6	0.97028	0.89486	2671.94	51268.441	49904.3	48733.6	42137.8	48621.4	47208.9	42388.4	3.55707	7766.46	9130.61
Run 7	1.02327	0.88839	2664.22	52462.309	50190.5	48769.2	43236.8	47530.8	47668.1	42059.5	3.54963	6953.7	9225.53
Run 8	1.08165	0.88798	2692.51	52770.699	49713.8	49035.8	43394.6	48230.5	47336.2	42608.5	3.57685	6319.13	9376.05
Run 9	1.00303	0.89702	2679.93	51704.953	49877.9	49006.4	42579	48969.3	46884.4	42220.5	3.56475	7299	9126
Run 11	1.04417	0.90062	2797.2	49080.914	46614.7	45014.7	39449.3	44051.4	42841.7	37985.1	3.67687	7165.44	9631.64
Mean	**1.009**	**0.889**											
Stdev	**0.0346**	**0.0076**											
uncertai	**0.0687**	**0.017**											
Run 12													
Run 13	1.39352	0.85178	1456.68	42630.203	40004.8	39649.3	38438.9	40498	39520.4	35816.6	2.29399	1565.97	4191.35
Run 14	1.2786	0.84725	1386.46	42510.695	40298.4	38951.5	38566.5	41971	41015.7	37598.8	2.21349	1731.88	3944.2
Run 15	1.37266	0.85798	1421.29	42488.484	40059.3	38940.2	38501.8	39300.3	39068.7	36047.6	2.25355	1557.53	3986.68
Run 17	1.18707	0.84233	1441.22	43112.07	41016.8	41727.7	38891.8	40703.3	40225.4	36420.3	2.27635	2125	4220.29
Run 18	1.00242	0.83808	1455.69	43507.52	42205.6	41320	39182.3	39979.9	39323.2	35922.9	2.29286	3023.34	4325.21
Run 19	0.99844	0.83534	1485.97	43482.703	42137	40531.2	38997.4	39259	38177.1	34769.5	2.32725	3139.6	4485.28
Run 20	1.04845	0.84347	1437.36	43718.719	42239.6	42124.4	39526.1	40724.7	40640.5	36328.9	2.27195	2713.47	4192.59
Run 21	1.07095	0.85956	1460.33	43811.48	42341.7	41715.9	39680.7	40568.3	39625.7	35461.3	2.29815	2660.99	4130.8
Run 22	1.09746	0.85354	1489.76	43581.848	41878.1	40861.2	39269.9	39049.9	38303.6	34948.4	2.33153	2608.18	4311.9
Run 23	0.86142	0.85369	1465.1	43189.383	43114.2	42401.4	38981.8	40485.7	39737.2	35740.6	2.30357	4132.38	4207.6
Mean	**1.1311**	**0.8483**											
Stdev	**0.1734**	**0.0083**											
uncertai	**0.3066**	**0.0196**											

Run 25	0.82652	0.77384	795.873	38189.141	37927.7	37397.2	36070.5	36669	36832.1	34530.8	1.48174	1857.21	2118.69
Run 26	1.00194	0.77755	818.525	37496.707	36627.4	36258.6	35311.3	35652.5	35872.8	33738.7	1.51211	1316.18	2185.43
Run 27	1.13228	0.7646	794.941	37399.219	36220.6	35853.2	35232.7	35869	35921.5	34135.1	1.48048	987.938	2166.55
Run 28	1.31437	0.77834	798.15	38613.762	37248.2	36530.7	36510.8	36325.7	36312.4	34021.3	1.4848	737.445	2102.97
Run 29	1.16902	0.75967	819.946	38421.457	37095.4	36658.9	36126.1	36168.1	35988.9	33765.1	1.51401	969.273	2295.31
Run 30	0.99347	0.75675	828.209	37320.301	36335.2	35869.4	34973.5	35452	35417.6	33147	1.52503	1361.68	2346.83
Run 31	1.14231	0.78708	842.05	37050.078	35883	35265	34828	34882.7	34815.1	32606.7	1.54342	1054.93	2222.04
Run 32	1.13577	0.78088	850.668	36436.52	35228.5	34753.2	34145.6	34402.9	34388.2	32454.6	1.55482	1082.95	2290.97
Run 33	1.04329	0.75288	832.782	35899.895	34754.5	34245.5	33509.9	33825.4	33953.9	32026.5	1.53111	1244.62	2389.96
Run 34	1.21512	0.76484	835.842	36699.414	35293.7	34854.7	34371.3	34797.1	34937.3	32890.8	1.53518	922.371	2328.12
Run 35	1.08505	0.76223	843.415	36449.559	35246.7	34690.4	34074.7	34316.8	34201.3	32464	1.54522	1171.95	2374.85
Mean	**1.0963**	**0.769**											
Stdev	**0.1293**	**0.0111**											
uncertai	**0.2358**	**0.0289**											
Run 36													
Run 37	1.48462	0.64686	363.623	34928.988	34137.6	34134.6	33952.2	34125.3	34304	32460.4	0.84099	185.43	976.773
Run 38	1.30916	0.65174	356.829	35433.703	34729.5	34763.7	34497.4	34644.9	34690.3	32932.5	0.8296	232.047	936.289
Run 39	#NUM!	0.65684	352.293	35812.793	34822.9	35129.2	34907.9	35053.1	34979.2	33225.7	0.82196	-84.961	904.918
Run 41	#NUM!	0.63643	341.336	36369.672	35288.4	35320.4	35448.8	35540.5	35368.7	33718.9	0.80339	-160.42	920.852
Run 42	2.88964	0.63465	335.326	36877.035	36018	35935.4	35974.5	35968.7	35809.3	34324.3	0.79314	43.5352	902.539
Run 43	1.9078	0.65379	334.208	36862.879	36115.9	35923.6	36016.5	36180.7	35923.1	34455.7	0.79123	99.3945	846.359
Run 44	#NUM!	0.6349	324.337	36940.387	35885.6	35619	36081	36182.3	35956.6	34655.4	0.77426	-195.39	859.395
Run 45	#NUM!	0.65143	317.74	37238.523	35551	35661.1	36446.1	36474.4	36218.8	34782.4	0.76284	-895.06	792.434
Run 46	#NUM!	0.64936	306.924	37637.871	36528.9	36035	36879.3	35872.1	36593.4	34747.5	0.74397	-350.48	758.535
Run 47	#NUM!	0.6379	303.544	37935.855	36717.9	36287.3	37162.3	37267	37148.1	35544.2	0.73804	-444.46	773.531
Mean		**0.6454**											
Stdev		**0.0086**											
uncertainty		**0.0265**											

Table B.13: C-D 0.6(15-15) with water

			Date:	27/09/2012	Test done by Luc								
			Venturi angle [°]:	15									
			Venturi length [m]:	0.14	Area[m2]								
			Throat diameter[m]:	0.0276	0.0006								
			Pipe Diameter [m]:	0.046	0.00167								
			Diameter ratio	0.6	0.28364								
			Material Type:	Water									
			Density [kg/m3]:	999.87									
			Concentration:	1									
			ty:	0									
			K:	0.001		1/n	n/(n+1)	(n+1)/n	K1/n				
			n:	1		1	0.5	2	0.001				
					Contracting		Throat	Expanding					
	Axial distances			-0.12	-0.07	-0.035	0	0.035	0.07	4.67			
	Venturi plane												
	Non-dimensionalised dista			-2.608696	-1.5217	-0.7609	0	0.76087	1.52174	101.522			
	Distances[m]:			6.85	6.9	6.935	6.97	7.005	7.04	11.64			
Run #	**Cd(D&D**	**Cd(Flan**	**Re3**	**Pod 3**	**Pod 4**	**Pod 5**	**Pod 6**	**Pod 7**	**Pod 8**	**Pod 9**	**Average [l/s]**	**Dpcont**	**ΔPFlang**
Run 2	0.96436	0.94906	150066	57004.156	55763.4	47565.1	17573.3	41912.5	41060.3	40894.7	5.42233	38190.1	39430.8
Run 3	0.96801	0.96119	150575	56169.02	55625.7	48526.1	17465.8	41337.6	41427.2	40918	5.44072	38159.9	38703.2
Run 4	0.95548	0.95028	150115	56798.66	56371.2	48295.5	17443.1	42285.2	41358.4	41006	5.42409	38928.1	39355.6
Run 5	0.95518	0.95469	149958	56159.02	56118.9	48776.3	17247.3	42353	41295.8	41024.4	5.41842	38871.7	38911.7
Run 6	0.96114	0.95919	150226	56259.945	56102.9	48437.5	17574.4	42085.2	41883.3	41056.4	5.42812	38528.5	38685.5
Run 7	0.96211	0.94825	150083	56867.301	55736.9	47973	17359.6	42257	41381.7	40931.2	5.42296	38377.3	39507.7
Run 8	0.95165	0.95058	150069	56459.641	56371.5	48462.2	17152.6	42594.3	41493.3	40811.5	5.42245	39218.8	39307
Run 9	0.95459	0.95577	150034	56057.102	56153.2	48120.4	17193.6	41891.9	42068.8	40926.8	5.42119	38959.6	38863.5
Run 10	0.94959	0.96184	150104	55588.441	56585.6	48231.6	17178.1	42152	41558.6	41132.1	5.42371	39407.4	38410.3
Run 11	0.95215	0.95948	150191	55977.531	56574.8	48386.2	17333.8	42244.9	41565.2	41095.8	5.42686	39240.9	38643.7
Run 12	0.9586	0.9594	149954	55852.723	55916.6	47528.3	17324	42427.4	41567.5	40870.9	5.4183	38592.7	38528.7
Mean	**0.9575**	**0.9554**											
stdev	**0.0058**	**0.0051**											
% uncer	**0.0121**	**0.0107**											
Run 14	0.94205	0.94707	107338	39533.238	39749.5	35272	19274.7	31909.2	33952.1	30913.9	3.87844	20474.9	20258.6
Run 15	0.97184	0.96461	107523	39516.043	39225.7	35112.6	19920.4	32360.3	32501.7	30877.8	3.88512	19305.3	19595.6
Run 16	0.96864	0.959	107327	39196.797	38805.7	33549	19443.1	31663.1	31848.3	30394.7	3.87806	19362.6	19753.7
Run 18	0.95151	0.94542	106982	39330.23	39072.4	35129.6	19135.5	32282.1	32426.7	30915	3.86559	19937	20194.8
Run 19	0.9595	0.95485	106825	38945.988	38755.3	35139.6	19206.3	31997.4	32010.4	31037.7	3.85992	19549	19739.7
Run 20	0.95993	0.96207	107146	39274.063	39361.3	35191.5	19712.6	31837.4	32086	30795.6	3.87151	19648.7	19561.5
Run 21	0.95043	0.95273	107338	39253.402	39350.5	35405.9	19234.9	32142.3	32073.4	31199.9	3.87844	20115.6	20018.5
Run 22	0.95816	0.94486	107188	39372.652	38812.9	34817.9	19076	32274.1	32346.4	30989	3.87303	19736.9	20296.7
Run 23	0.95333	0.96196	107481	38890.949	39249	34539.2	19202.6	32380.9	31957.5	31167.6	3.88361	20046.4	19688.4
Run 24	0.96212	0.95716	107338	39219.715	39015.7	34639.6	19386	32202.3	31961.8	31047.8	3.87844	19629.7	19833.7
Mean	**0.9578**	**0.955**											
stdev	**0.0088**	**0.0073**											
% uncer	**0.0185**	**0.0152**											
Run 28	0.94702	0.94472	64868.1	26380.973	26344.9	24978.9	18945.4	24284.4	24461.6	23452	2.34388	7399.57	7435.6
Run 29	0.95277	0.94423	65018	26452.047	26318.5	24774.5	18974.2	24085.1	24119.3	23239.8	2.3493	7344.33	7477.86
Run 30	0.95611	0.94918	65108.7	26326.154	26219	24684.9	18905.4	23952.4	23948.5	23175.6	2.35257	7313.54	7420.74
Run 31	0.95509	0.94795	65094.7	26254.596	26143.8	24583.7	18817.8	23860.1	23913.6	23091.7	2.35207	7326.02	7436.83
Run 32	0.96952	0.96268	65094.7	26179.873	26078.5	24520.8	18969	23902.1	23876.3	23096.3	2.35207	7109.51	7210.88
Run 33	0.96367	0.9598	65136.5	26179.691	26121.5	24512.3	18916.2	23849.7	23861.2	23068	2.35358	7205.33	7263.53
Run 34	0.96126	0.95565	65018	26155.885	26070.9	24542.8	18855.7	23867.3	23855.3	23062.8	2.3493	7215.19	7300.21
Run 35	0.97012	0.96395	65133.1	26152.525	26061.3	24510.4	18952.2	23811	23827.5	23055.1	2.35345	7109.13	7200.35
Run 36	0.96666	0.96212	65248.1	26123.418	26055.5	24495	18870	23807.1	23795.5	23025.2	2.35761	7185.49	7253.44
Run 37	0.96613	0.96412	65140.1	26082.518	26052.7	24471.8	18883.1	23747	23746.1	23027.3	2.35371	7169.56	7199.38
Mean	**0.9608**	**0.9554**											
stdev	**0.0078**	**0.0082**											
% uncer	**0.0162**	**0.0171**											

Table B.14: C-D 0.6 (15-15) with CMC 2%

			Date:	07/10/2012	Test done by Luc								
			Venturi angle [°]:	15									
			Venturi length [m]:	0.14	Area[m2]								
			Throat diameter[m]:	0.0276	0.0006								
			Pipe Diameter [m]:	0.046	0.00167								
			Diameter ratio	0.6	0.28364								
			Material Type:	CMC									
			Density[kg/m3]:	1012									
			Concentration:	2%									
			ty:	0									
			K:	0.096		**1/n**	**n/(n+1)**	**(n+1)/n**	**K1/n**				
			n:	0.716		1.65289	0.37695	2.65289	0.03388				
					Contracting		**Throat**		**Expanding**				
	Axial distances			-0.12	-0.07	-0.035	0	0.035	0.07	4.67			
	Venturi plane												
	Non-dimensionalised dista			-2.608696	-1.5217	-0.7609	0	0.76087	1.52174	101.522			
	Distances[m]:			6.85	6.9	6.935	6.97	7.005	7.04	11.64			
Run #	**Cd(D&D**	**Cd(Flan**	**Re3**	**Pod 3**	**Pod 4**	**Pod 5**	**Pod 6**	**Pod 7**	**Pod 8**	**Pod 9**	**Average**	**Dpcont**	**ΔPflange**
											[l/s]		
Run 1	0.95036	0.96032	14535.2	68314.773	69145.9	59107.5	28868.9	45978.8	55545.7	48124.4	5.45281	40277	39445.9
Run 2	0.94024	0.93049	14480.9	67838.578	66976.7	59035.3	26047.8	45641.5	53710.7	48341	5.4382	40928.9	41790.7
Run 3	0.95101	0.93107	14589.6	69400.609	67649.7	60240.9	27211.9	44614.3	55100.3	48277.1	5.46743	40437.8	42188.7
Run 4	0.99412	0.97921	14575	67465.164	66330.8	60660.1	29377.1	44129.2	53967.6	48385.5	5.46352	36953.7	38088.1
Run 5	0.94194	0.94122	14466.4	67019.375	66957.1	58555.5	26234.3	46138.2	55144.3	48211	5.43429	40722.8	40785
Run 6	0.9714	1.00263	14545.5	65956.266	68323.1	59113.3	29732.6	45636.4	54919.3	48641.6	5.45559	38590.4	36223.6
Run 7	0.94294	0.93589	14510.4	66983.883	66366.8	60074.9	25553.2	45499.3	54911.8	49030.4	5.44614	40813.6	41430.6
Run 9	0.93669	0.92776	14699	68000.703	67185.9	58180	25053.1	45236.5	54732.8	48275.2	5.49678	42132.8	42947.6
Run 10	0.94547	0.94708	14542.7	67697.992	67836.6	58765.2	27111.7	44236.2	54167	47883	5.45483	40725	40586.3
Mean	**0.9527**	**0.9506**											
stdev	**0.0185**	**0.0256**											
uncertai	**0.0389**	**0.0539**											
Run 14	0.98019	0.98967	5902.96	35688.289	35886.7	33425.9	25484.2	29416.9	31092.1	28859.8	2.85813	10402.5	10204.1
Run 15	0.97611	0.97986	6224.42	36552.832	36639.2	34573.6	25321	29622.5	30951.3	29194.3	2.96887	11318.2	11231.8
Run 16	0.9224	0.92459	6250.6	36953.172	37013.3	34128.5	24262.3	30246.9	31949.8	29646.2	2.97781	12751	12690.9
Run 17	0.96754	0.97113	6250.6	36884.941	36970.5	34693	25381.3	30484.9	31947.9	29208.9	2.97781	11589.2	11503.7
Run 18	0.94532	0.92035	6242.85	37334.898	36668.2	34524.2	24549.6	30360.6	31636.2	29491.4	2.97516	12118.6	12785.3
Run 19	0.92393	0.91284	6234.37	37041.766	36732.1	34946.3	24070.5	30653.3	31951.5	29451.9	2.97227	12661.6	12971.2
Run 20	0.96194	0.95444	6275.34	36827.102	36641	34252.5	24850.1	30660.7	31643.4	29592.4	2.98625	11790.9	11977
Run 21	0.96464	0.95727	6284.2	37074.91	36893.3	34254.7	25144.5	30671.1	32041.2	29365.3	2.98928	11748.8	11930.4
Run 22	0.93051	0.92138	6247.28	36988.516	36739.1	33688.4	24218.8	30452.6	31954.4	29215	2.97668	12520.3	12769.7
Run 23	0.97152	0.95313	6257.98	36984.344	36535.8	34157.6	25021.9	30026.3	31355.1	29668.8	2.98033	11513.9	11962.4
Run 24	0.98511	0.97729	6236.96	36858.875	36679.9	34213.9	25535.4	30308.2	31858.8	29483.6	2.97315	11144.5	11323.5
Run 25	0.94442	0.94003	6282.35	36776.652	36662	34571.4	24409.7	30267.7	32082.1	29394.7	2.98865	12252.3	12366.9
Run 26	0.98411	0.96123	6242.85	36953.852	36415.3	33995	25233.1	30693.3	32028.7	29518.3	2.97516	11182.2	11720.8
Run 27	0.97172	0.96115	6210.43	36825.457	36573.6	34222	25189.8	30097.5	31940.8	29606.9	2.96408	11383.8	11635.6
Run 28	0.92193	0.91359	6246.17	36829.887	36596.2	34619.9	23844.9	30583.6	31828.1	29479.6	2.9763	12751.3	12984.9
Run 29	0.97697	0.98771	6266.48	36701.344	36948.2	34090.6	25540.2	30364.1	32154.5	29346.6	2.98323	11408	11161.1
Mean	**0.958**	**0.9516**											
stdev	**0.023**	**0.0265**											
uncertai	**0.0481**	**0.0557**											
Run 31	0.99202	0.95938	4336.72	30064.867	29613.2	28845.1	23085.9	25990.7	26988.1	26073.1	2.29135	6527.34	6978.97
Run 32	0.94416	0.95098	4292.88	30627.963	30729.5	29577.3	23627.8	26270.7	27164.8	26042.3	2.27472	7101.65	7000.15
Run 33	0.94929	0.92685	4284.93	31187.311	30844	29281.4	23837.6	26520.5	27275	26317.2	2.27169	7006.38	7349.71
Run 34	0.92639	0.92649	4299.18	30922.756	30924.3	29453.1	23532.1	26514.3	27396	25905.2	2.27711	7392.15	7390.63
Run 35	0.96375	0.943	4322.43	30952.287	30646	29073	23762.9	26562	27296.4	26134.4	2.28593	6883.14	7189.42
Run 36	0.95376	0.9359	4296.53	30909.443	30641	29371.8	23673.1	26564.1	27476.2	25997.8	2.2761	6967.88	7236.32
Run 37	0.94914	0.92876	4278.3	30926.656	30616.5	29297.7	23623.4	26716.1	27507	26288.7	2.26917	6993.1	7303.3
Run 38	0.92214	0.93479	4281.94	30493.879	30693.4	29620.4	23275.7	26562.7	27431.1	26077.1	2.27056	7417.7	7218.15
Run 39	0.95314	0.93192	4285.92	30976.141	30655.8	29548.3	23703.7	26895.8	27705.3	26183.6	2.27207	6952.19	7272.49
Run 40	0.93863	0.94509	4292.22	30588.027	30685.8	29457.2	23501.9	26706.9	27158.2	26204.8	2.27446	7183.9	7086.13
mean	**0.9492**	**0.9383**											
stdev	**0.0196**	**0.011**											
uncertai	**0.0414**	**0.0235**											

Run 42	0.96379	0.93845	2032.66	28120.705	27993	27626.2	25659.6	27009	27213	26955.8	1.331	2333.39	2461.1
Run 43	0.95254	0.91357	2032.6	27987.586	27779.4	27451.2	25390.7	26912.7	26933.5	25911.1	1.33097	2388.71	2596.86
Run 44	0.94458	0.91485	2040.72	27588.797	27427.4	27003.7	24984.3	26453.3	26692.4	25614.4	1.33478	2443.06	2604.46
Run 45	1.00006	0.96657	2048.03	27430.422	27276	27099.3	25085.3	26561.2	26733.7	25614.8	1.33821	2190.71	2345.15
Run 46	1.00422	0.96691	2032.73	27724.975	27555.9	27235.6	25406.5	26913.5	27038.7	25903	1.33103	2149.38	2318.44
Run 47	0.93034	0.93329	2005.26	28139.424	28154.9	27579.2	25699	26772.5	27070.5	26148.1	1.31812	2455.94	2440.43
Run 48	0.97593	0.96328	2020.38	27998.262	27938.6	27488.4	25682.6	26665.9	26917	26131.2	1.32523	2256.02	2315.65
Run 49	0.94538	0.94337	2000.22	28048.182	28038.1	27563.8	25668.2	26759.9	26943.2	26161.8	1.31574	2369.86	2379.98
Run 50	0.95223	0.93331	2016.03	28054.975	27958.2	27546.4	25595.8	26560.5	26608.9	26115	1.32318	2362.38	2459.16
Run 51	0.95708	0.9325	2008.63	28057.053	27932.8	27504.2	25606.6	26337	26796.6	26264.6	1.3197	2326.21	2450.44
Run 52	0.96423	0.9371	2004.12	28072.713	27938.5	27597.8	25654.1	26405.2	26764.7	26211.9	1.31758	2284.45	2418.65
mean	**0.9628**	**0.9403**											
stdev	**0.0228**	**0.0186**											
uncertai	**0.0475**	**0.0396**											
Run 57	1.0067	0.93166	1223.35	26932.938	26759.9	26672.8	25727.1	25853.2	25807.1	25764.2	0.92492	1032.77	1205.82
Run 59	0.9754	0.93098	1259.19	26436.928	26324.9	26149.8	25178.3	25336.6	25325.3	25262.9	0.94426	1146.61	1258.63
Run 60	1.005	0.95915	1264.45	26271.234	26164.9	26015.6	25078.3	25216.3	25160.3	25126.2	0.94709	1086.54	1192.9
Run 61	1.00977	0.94131	1274.2	26199.27	26035.2	25914.7	24947	25064	24998.5	24989.2	0.95232	1088.21	1252.25
Run 62	0.98125	0.92741	1276.8	26056.57	25918.5	25782.2	24762.7	24958	24912.3	24926.6	0.95371	1155.75	1293.84
Run 63	1.00089	0.93833	1280.21	25984.619	25831	25728.9	24715.9	24906.8	24828.2	24822.1	0.95554	1115.11	1268.74
Run 64	0.99437	0.93005	1287.14	25921.824	25758.9	25663.6	24620.3	24779.5	24725.4	24743.6	0.95924	1138.56	1301.49
Run 65	0.99351	0.94434	1289.29	25851.092	25728.9	25589.6	24585.7	24687.2	24665.9	24675.5	0.96039	1143.26	1265.41
Run 66	0.98564	0.93347	1302.11	25807.844	25672.5	25517.9	24494.3	24639.6	24619.6	24626.2	0.96723	1178.19	1313.54
mean	**0.9947**	**0.9374**											
stdev	**0.012**	**0.0099**											
uncertai	**0.0241**	**0.0211**											

Table B.15:C-D 0.6(15-15) with CMC+XG

			Date:	19/10/2012	Test done by Luc								
			Venturi angle [°]:	15									
			Venturi length [m]:	0.14	Area[m2]								
			Throat diameter[m]:	0.0276	0.0006								
			Pipe Diameter [m]:	0.046	0.00167								
			Diameter ratio	0.6	0.28364								
			Material Type:	CMC+XG									
			Density[kg/m3]:	1015									
			Concentration:	2%									
			ty:	0									
			K:	0.323			**1/n**	**n/(n+1)**	**(n+1)/n**	**K1/n**			
			n:	0.675			1.62075	0.38157	2.62075	0.19179			
					Contracting		**Throat**	**Expanding**					
	Axial distances			-0.12	-0.07	-0.035	0	0.035	0.07	4.67			
	Venturi plane												
	Non-dimensionalised dista			-2.6086957	-1.5217	-0.7609	0	0.76087	1.52174	101.522			
	Distances[m]:			6.85	6.9	6.935	6.97	7.005	7.04	11.64			
Run #	**Cd(D&D**	**Cd(Flan**	**Re3**	**Pod 3**	**Pod 4**	**Pod 5**	**Pod 6**	**Pod 7**	**Pod 8**	**Pod 9**	**Average [l/s]**	**Dpcont**	**ΔPFlang**
Run 3	0.99729	0.93052	2292	50772.867	48915.1	47031.8	36418.5	46001.1	44513.5	38154.4	3.18366	12496.5	14354.3
Run 4	1.03016	0.93016	2447.96	46684.445	43765.9	42781.6	30884.2	42081.5	39940.1	36574.2	3.33887	12881.6	15800.2
Run 5	0.99996	0.91596	2357.73	47695.422	45211.4	42897.3	32262.8	42523.1	40867.2	36166.7	3.24942	12948.6	15432.6
Run 6	0.99315	0.91397	2420.54	47844.324	45379.2	43002.1	31743.7	41118.8	41121.3	36203.1	3.31178	13635.5	16100.6
Run 7	1.01271	0.92513	2391.81	47466.918	44910.9	42638.7	32021.6	41597.5	39582.7	36278.4	3.28331	12889.3	15445.3
Run 8	1.01098	0.94087	2394.73	47239.77	45236.8	43010.2	32280.5	40753.5	40357.6	36189.2	3.28621	12956.3	14959.2
Run 9	1.0149	0.94735	2400.95	46662.398	44756.6	42440.8	31851.7	41434.8	40711.3	36359.8	3.29238	12904.9	14810.7
Run 10	0.98553	0.9318	2428.82	46447.883	44796.7	42636.6	30881	41723.4	40706.7	36337.4	3.31997	13915.7	15566.9
Run 11	0.9913	0.93699	2420.03	46563.387	44931.3	42721.2	31248.9	42027.3	40080.3	36445.8	3.31128	13682.4	15314.5
Run 12	1.04406	0.94451	2418.76	46181.117	43446.1	42167.2	31121.2	41617.3	40528.1	36256.9	3.31002	12325	15060
Mean	**1.008**	**0.9317**											
Stdev	**0.0184**	**0.0112**											
uncertai	**0.0365**	**0.0241**											

Run 14	0.97155	0.95565	1536.04	43290.355	43042.6	39202.7	35661.1	41419	40162.3	35832.6	2.38369	7381.47	7629.26
Run 15	0.97502	0.96049	1535.48	43334.582	43111.4	41437.3	35786.1	41133.5	39923	36085.4	2.38306	7325.29	7548.49
Run 16	0.98547	0.93016	1508.04	43600.297	42744.9	40425.7	35758.7	42275.9	40648.5	37926	2.35219	6986.21	7841.61
Run 17	0.95728	0.92428	1543.23	43637.992	43081.7	41035.2	35426.9	40045.9	38767.8	37348.8	2.39175	7654.82	8211.1
Run 18	1.03785	0.93133	1519.11	43442.422	41903.1	43175.3	35537.3	40960.1	40284.2	36533.7	2.36467	6365.79	7905.13
Run 19	1.04095	0.93181	1570.5	43516.523	41870	40071.8	35230.3	40490.1	39214	36249.4	2.42224	6639.71	8286.18
Run 20	1.05592	0.931	1520.46	43419.41	41656.1	41569.1	35498.5	41519	40152	36725.3	2.36618	6157.56	7920.87
Run 21	1.05716	0.92715	1526.17	43675.152	41821.5	40484	35644.9	40500.1	40253.1	36446.4	2.3726	6176.6	8030.27
Run 22	1.04371	0.9305	1545.37	43526.027	41860.6	41548.2	35408.1	41719.5	40108.8	36401.1	2.39415	6452.43	8117.88
Run 23	1.03427	0.90827	1509.5	43860.273	41975.8	40160.1	35624.5	41505	40136	37770	2.35383	6351.28	8235.76
Mean	**1.0159**	**0.9331**											
Stdev	**0.0388**	**0.015**											
Uncertai	**0.0763**	**0.0321**											
Run 26	1.04681	0.86359	774.633	38324.93	37216.1	36684.2	34853.4	36021.8	35665.6	33682.8	1.45304	2362.64	3471.5
Run 27	1.0086	0.8613	768.182	38218.992	37285.4	36947.3	34770.9	36454.5	36293.8	34259.5	1.44428	2514.47	3448.07
Run 28	1.04143	0.86529	783.187	38447.797	37359.9	36465.9	34934.5	36583.6	36180.8	33813.7	1.46462	2425.32	3513.27
Run 29	1.10794	0.88977	789.95	37992.988	36798.6	35906.1	34628.9	36031.6	35464.8	33510.9	1.47376	2169.7	3364.13
Run 30	1.13805	0.85968	790.559	38004.898	36455.8	35882.4	34397.1	35968.1	35731	33623.2	1.47458	2058.71	3607.81
Run 31	1.05097	0.86151	795.762	37513.785	36324.1	35795.5	33887.1	35644.1	35156.4	32948.5	1.48159	2436.99	3626.72
Run 32	1.08103	0.85624	807.333	37479.645	36082.6	35201.7	33730.7	35385.3	34934.4	32653.6	1.49714	2351.94	3748.93
Run 33	1.11045	0.90357	812.075	36861.719	35714.5	35055.2	33466.6	34982.8	34551.1	32319	1.50349	2247.91	3395.14
Run 34	1.04597	0.88208	809.073	36972.297	35948.9	35141.5	33428.8	35089.7	34581.6	32361.8	1.49947	2520.06	3543.5
Run 35	0.99377	0.86307	807.132	36788.563	35882.1	35421.4	33100.1	34894.1	34596.5	32285.4	1.49687	2782.08	3688.5
Mean	**1.0625**	**0.8706**											
stdev	**0.0461**	**0.0157**											
uncertai	**0.0868**	**0.036**											
Run 37	0.87898	0.76313	365.913	35205.484	34835.4	34283.1	33702.7	34181.1	34148.6	32401.9	0.84482	1132.77	1502.83
Run 38	1.0646	0.75232	355.709	35482.945	34739.9	34098.4	33998.6	34430.8	34415.4	32691	0.82771	741.258	1484.33
Run 39	1.7126	0.75988	301.624	35807.254	34886.7	34385.2	34661	35069.4	34545	33593.1	0.73466	225.652	1146.22
Run 40	1.3467	0.77375	328.823	35846.918	35007.9	34610.2	34594.4	35798.7	35643.9	34173.6	0.78199	413.465	1252.5
Run 41	1.70946	0.75918	305.22	37566.461	36628.7	35996.5	36398.3	36569.5	36446.1	35017.7	0.74099	230.398	1168.16
Run 42	1.54742	0.76867	312.165	37665.879	36779.2	36023.7	36488.7	36560.6	36505.1	35119.2	0.75314	290.477	1177.2
Run 43	1.2589	0.77331	321.898	37808.711	37051.6	36377.7	36592.8	36776.6	36678.5	35125.3	0.77004	458.805	1215.9
Run 44	3.17916	0.78276	312.405	37326.016	36258.5	35356.5	36189.6	36727.1	36507.8	35139.9	0.75356	68.8945	1136.45
Run 45	1.67041	0.76785	313.382	37961.379	37025.7	36083.5	36775	37282.1	37135.1	35422	0.75526	250.684	1186.38
Run 46	1.74344	0.7556	313.657	38144.27	37148	36856.8	36917.6	37184.6	36925.2	35436.1	0.75574	230.414	1226.71
Mean	**1.6112**	**0.7656**											
stdev	**0.6265**	**0.0094**											
uncertai	**0.7777**	**0.0245**											

Table B.16: C-D 0.6(15-15) with CMC 6%

			Date:	15/07/2013	Test done by LUc								
			Venturi angle [°]:	15									
			Venturi length [m]:	0.14	Area[m2]								
			Throat diameter[m]:	0.0276	0.0006								
			Pipe Diameter [m]:	0.046	0.00167								
			Diameter ratio	0.6	0.28364								
			Material Type:	CMC									
			Density[kg/m3]:	1031									
			Concentration:	0.06									
			ty:	0		**1/n**	**n/(n+1)**	**(n+1)/n**	**K1/n**				
			K:	2.2025369		1.68235	0.37281	2.68235	3.775				
			n:	0.5944064									
					Contracting		**Throat**	**Expanding**					
	Axial distances			-0.025	-0.07	-0.035	0	0.035	0.07	2.4			
	Venturi plane												
	Non-dimensionalised dista			-0.543478	-1.5217	-0.7609	0	0.76087	1.52174	52.1739			
	Distances[m]:			5.17	5.215	5.25	5.285	5.32	5.355	7.685			
Run #	**Cd(D&D**	**Cd(Flan**	**Re3**	**Pod 3**	**Pod 4**	**Pod 5**	**Pod 6**	**Pod 7**	**Pod 8**	**Pod 9**	**Average**	**DPcont**	**ΔPFlang**
Run 8	0.98068	0.97873	448.579	121624.32	121570	111034	107860	108392	106722	84942.5	3.25353	13709.7	13764.3
Run 9	1.00273	0.98649	449.294	120954.55	120518	106763	107375	107481	105401	84534.5	3.25722	13143.1	13579.3
Run 10	0.97859	0.98641	450.058	120501.58	120720	110953	106887	107053	102889	84204.5	3.26116	13832.8	13614.5
Run 11	1.01244	1.01027	451.919	119523.56	119468	112856	106468	107632	105134	84930.4	3.27075	12999.6	13055.5
Run 12	0.97618	0.96973	452.319	119158.56	118972	111408	104971	106518	102554	84473.6	3.27281	14000.8	14187.6
Run 13	0.99171	0.99836	454.15	117284.57	117466	110054	103822	105021	103048	84421.7	3.28223	13643.8	13462.8
Run 14	1.01161	1.00334	455.357	117327.3	117109	103666	103947	104298	101763	84308.6	3.28843	13161.9	13380
Run 15	0.96038	0.93624	456.033	117111.86	116348	98588.6	101713	102492	100898	84056.4	3.29191	14634.6	15398.9
Run 16	1.01051	1.004	457.147	116433.34	116261	105919	102996	104917	101914	84847.9	3.29762	13264.6	13437.2
Run 17	1.00984	1.00482	457.889	116361.86	116229	107357	102916	103040	100948	84516.6	3.30143	13313	13446.2
Mean	**0.9935**	**0.9878**											
Stdev	**0.0186**	**0.0223**											
Uncertai	**0.0375**	**0.0452**											
Run 19	0.97097	0.97511	311.091	98028.477	98098.8	91689.5	89790.8	90981	88926.5	74909	2.50767	8308.09	8237.73
Run 20	0.91938	0.90918	312.133	98208.352	97998.2	88566.5	88687.4	89076	86525.2	72881.8	2.51364	9310.77	9520.92
Run 21	0.92785	0.91901	312.485	98041.188	97864.3	88548.8	88708	88856.4	87070.6	73085.8	2.51566	9156.31	9333.21
Run 22	0.92356	0.89794	312.863	97794.695	97258.8	87798	88001.4	88150.8	86361	72888.8	2.51782	9257.39	9793.33
Run 23	0.90598	0.88272	313.463	97724.969	97210	87684.4	87563.5	87477.3	85346.9	72784.5	2.52126	9646.46	10161.5
Run 24	0.94265	0.95521	313.831	97402.516	97635.8	93039.8	88710.3	89820.2	88095.3	72559.6	2.52336	8925.48	8692.22
Run 25	0.95094	0.94657	314.476	97370.227	97288.6	89659.4	88492.6	88653.3	85468.6	72421.8	2.52705	8796.06	8877.64
Run 26	0.95016	0.92757	314.136	97159.938	96726.3	87601.5	87929.2	87903	85503.7	72383.5	2.52511	8797.1	9230.75
Run 27	0.87884	0.88346	315.427	96943.828	97051.8	86476.1	86708.9	86775.1	83558.9	72127.7	2.53248	10343	10235
Run 28	1.00777	0.96731	316.006	95945.391	95271.9	91753.8	87385.5	87998.1	86206	71564.8	2.53579	7886.41	8559.89
Run 29	0.97041	0.92364	316.117	96366.266	95482.8	86321.7	86973.2	87189.2	85552.9	72001.8	2.53643	8509.58	9393.07
Mean	**0.9408**	**0.9262**											
Stdev	**0.0353**	**0.0319**											
Uncertai	**0.075**	**0.069**											
Run 31	0.88854	0.87832	183.461	83465.375	83355.9	80723.1	78676	79047.3	78226.1	62342.7	1.72228	4679.84	4789.35
Run 32	0.91896	0.90296	183.046	83120.641	82964.7	79200.6	78603.7	78531.6	77088.5	62358.4	1.71951	4361.03	4516.93
Run 33	0.93154	0.89884	183.639	83288.461	82972.6	78805.2	78709	78590.3	77133.5	62534.6	1.72347	4263.59	4579.48
Run 34	0.93338	0.90378	183.368	83612.008	83329.9	80140	79092	79433.3	78365.6	62866.6	1.72167	4237.91	4520.02
Run 35	0.92455	0.88887	183.339	83711.055	83357.4	78736.4	79039.1	78984.2	77600.3	63089.8	1.72147	4318.3	4671.91
Run 36	0.87352	0.86238	182.772	84037.813	83912.6	78996.3	79096.3	79163.5	78076.7	63359.3	1.71768	4816.26	4941.5
Run 37	0.94654	0.9029	183.051	84318.914	83912	82356	79801.2	80192.2	79221.2	63600	1.71955	4110.78	4517.72
Run 38	0.87482	0.89529	183.06	84445.82	84663.4	80340.7	79850.6	79828.3	78320.7	63759.1	1.71961	4812.77	4595.17
Run 39	0.83177	0.80126	183.064	84686.766	84273.7	78403.2	78949.7	79068.5	77597.6	64002.8	1.71964	5324.02	5737.09
Run 40	0.88544	0.90051	183.076	85005.68	85161.7	81170.8	80463.1	80843.1	79926.8	64340.7	1.71971	4698.59	4542.56
Run 41	0.81344	0.80737	183.089	85063.523	84979.6	78183.4	79411.9	79827	78944.1	64451	1.7198	5567.72	5651.67
Run 42	0.84169	0.79926	182.747	85173.391	84608.1	79514.8	79421.7	79417.4	77988.6	64564	1.71751	5186.44	5751.69
Mean	**0.8887**	**0.8701**											
Stdev	**0.0436**	**0.0425**											
Uncertai	**0.0982**	**0.0976**											

Run 44	0.84976	0.80181	89.1475	78424.656	78198.9	75930.4	76366.6	76556.5	74953.7	66064.1	1.03066	1832.33	2058.05
Run 45	0.57292	0.55944	89.3781	78401.938	78204.6	73544.9	74158.8	74763.6	73644.8	66064.7	1.03255	4045.77	4243.13
Run 46	0.54905	0.51428	89.3855	78422.367	77806.5	73295.6	73400.7	73674.9	72503.8	66037	1.03261	4405.77	5021.68
Run 47	0.49367	0.48387	89.3727	78466.281	78243.2	72798	72794.7	72923.1	71896.1	66048.9	1.03251	5448.5	5671.55
Run 48	0.87149	0.76444	89.1311	78207.359	77685.4	75169.8	75943.8	76343.2	75508.3	66076.2	1.03052	1741.65	2263.61
Run 49	0.5556	0.58988	88.9829	78471.156	78953.6	74684.1	74678.6	74866	73596.9	66333.6	1.0293	4275.03	3792.57
Run 50	0.60129	0.5509	89.0012	78716.547	78018.1	74484.1	74367.1	74371.1	73046.1	66374.1	1.02945	3650.98	4349.46
Run 51	0.56598	0.55471	89.153	78776.289	78606.7	74691.1	74475.9	74296.8	72872.4	66459.8	1.0307	4130.86	4300.42
Run 52	0.57058	0.53423	89.1292	78761.688	78190	74357.9	74127.1	73998.2	72894.1	66480.2	1.03051	4062.92	4634.62
Run 53	0.98092	0.95036	89.1457	78149.633	78059.8	77014.6	76684.7	76807.8	75911.9	66397	1.03064	1375.05	1464.91
Mean	**0.6611**	**0.6304**											
Stdev	**0.1708**	**0.1537**											
Uncertai	**0.5166**	**0.4877**											
Run 55	0.42348	0.25732	15.9804	57311.004	56218.8	54770.3	55579.5	56076.7	55831.4	52113.1	0.30339	639.332	1731.52
Run 56	0.20743	0.19635	15.7725	57313.477	57009.8	54291.1	54394.4	54657.3	54132	52051.8	0.30058	2615.34	2919.03
Run 57	0.18295	0.16706	15.7858	57470.781	56800.1	53411.7	53433.7	53556.6	53039	52122.6	0.30076	3366.32	4037.04
Run 58	0.21075	0.19382	15.7813	57524.57	57062.4	54690.1	54526.6	54420.4	53630.7	52183.5	0.3007	2535.73	2997.95
Run 59	0.17903	0.16746	15.808	57542.68	57039.4	53791.2	53517	53357.1	52705.9	52148.1	0.30106	3522.38	4025.68
Run 60	0.17724	0.17079	15.8291	57607.551	57330.5	54003.4	53730	53587.8	52849.3	52204.7	0.30135	3600.52	3877.59
Run 61	0.53249	0.51404	15.957	57000.898	56971.4	56167.4	56567.9	56737.6	56356.3	52086.7	0.30308	403.512	433
Run 62	0.23041	0.22338	15.8435	57546.188	57409.8	55164.9	55276.4	55507.6	55016.9	52279.6	0.30154	2133.39	2269.8
Run 63	0.19623	0.19224	15.8335	57671.203	57547.9	54660.7	54609.2	54670.2	54177.5	52321.6	0.30141	2938.71	3061.99
Run 64	0.216	0.20285	15.8091	57737.672	57413.7	55250.8	54993.7	54836.6	54144.6	52351.5	0.30108	2420.05	2744
Mean	**0.2556**	**0.2285**											
Stdev	**0.1212**	**0.104**											
Uncertai	**0.9483**	**0.9106**											

Table B.17: C-D 0.6(15-15) with water Experimental 2013

			Date:	10/07/2013	Test done by Luc								
			Venturi angle [°]:	15									
			Venturi length [m]:	0.14	Area[m2]								
			Throat diameter[m]:	0.0276	0.0006								
			Pipe Diameter [m]:	0.046	0.00167								
			Diameter ratio	0.6	0.28364								
			Material Type:	Water									
			Density[kg/m3]:	999.87									
			Concentration:	1									
			ty:	0									
			K:	0.001		**1/n**	**n/(n+1)**	**(n+1)/n**	**K1/n**				
			n:	1		1	0.5	2	0.001				
					Contracting		**Throat**	**Expanding**					
	Axial distances			-0.025	-0.07	-0.035	0	0.035	0.07	2.4			
	Venturi plane												
	Non-dimensionalised dista			-0.5434783	-1.5217	-0.7609	0	0.76087	1.52174	52.1739			
	Distances[m]:			5.17	5.215	5.25	5.285	5.32	5.355	7.685			
Run #	**Cd(D&D**	**Cd(Flan**	**Re3**	**Pod 3**	**Pod 4**	**Pod 5**	**Pod 6**	**Pod 7**	**Pod 8**	**Pod 9**	**Average [l/s]**	**DPcont**	**ΔPFlang**
Run 4	0.9993	0.99738	139295	37453.832	37336	32149.3	6692.33	17500.1	31029.5	27816.9	5.03313	30643.7	30761.5
Run 5	0.99898	0.99703	139233	37482.203	37362.2	32819.2	6726.1	19199.5	31883.6	27150.2	5.03089	30636.1	30756.1
Run 6	1.00165	1.0001	139338	37524.91	37430.5	32489.7	6910.95	19738.6	31149.7	27183.7	5.03471	30519.5	30614
Run 7	1.00058	1.00134	139655	37410.727	37457.3	33374.5	6733.66	22604.6	31488.9	27073.7	5.04615	30723.7	30677.1
Run 8	1.00067	0.99955	139603	37515.313	37446.3	32793.7	6751.09	18762.8	32261.6	27042.3	5.04428	30695.2	30764.2
Run 9	0.99282	0.9953	139669	37478.164	37633.7	32289.3	6421.62	22013.5	31073.7	27098.3	5.04665	31212.1	31056.5
Run 10	0.9996	1.00382	140134	37435.18	37695.6	32379.5	6699.88	21622.3	30886.3	27180.3	5.06347	30995.7	30735.3
Run 11	0.99861	1.00106	139998	37546.66	37698	32666.8	6701.24	21705.3	31491.6	27181	5.05855	30996.8	30845.4
Run 12	0.99694	0.99604	140206	37685.059	37628.7	33109.6	6435.66	20873.8	32008.2	27024.5	5.06606	31193	31249.4
Run 13	1.00096	1.0009	140079	37613.965	37609.8	32375.3	6722.85	17472.7	31138.7	27104.6	5.06149	30886.9	30891.1
Mean	**0.999**	**0.9993**	**139721**										
stdev	**0.0026**	**0.0027**											
uncert	**0.0051**	**0.0054**											

Run 15	0.99895	0.99546	116019	28176.455	28027.1	24592	6753.8	15151.5	23769.5	22786	4.1921	21273.3	21422.7
Run 16	0.99854	0.99636	116098	28140.766	28047.2	24511.5	6727.44	16303.2	23970	22889.8	4.19497	21319.8	21413.3
Run 17	0.99908	0.99789	116130	28079.557	28029	24892.8	6720.28	16728.5	24105.5	22822.6	4.19613	21308.7	21359.3
Run 18	0.99894	0.99879	116133	28075.506	28069.3	24459	6753.55	15309.8	23793.9	22779.1	4.19625	21315.7	21322
Run 19	1.00332	0.99917	116290	28136.422	27960	23404.1	6773.27	20617.3	24603.2	22498.4	4.2019	21186.7	21363.1
Run 20	1.00399	1.00222	116288	27992.383	27917.8	24683.9	6759.5	17121.5	23950.1	22544.7	4.20185	21158.3	21232.9
Run 21	0.99861	0.99747	116130	28079.947	28031.2	24687.8	6702.74	15938.4	23358.2	22795.3	4.19613	21328.4	21377.2
Run 22	0.9983	0.99768	116149	28109.012	28082.2	24534.7	6733.54	15767.2	24103.9	22850	4.19682	21348.7	21375.5
Run 23	0.9988	0.99788	116091	28084.135	28044.9	24457.5	6739.08	16147.1	24099.4	22922.6	4.1947	21305.9	21345.1
Run 24	0.99985	0.99804	116181	28087.922	28010.6	24611.2	6716.36	15128.9	23986.7	22966.5	4.19795	21294.3	21371.6
Run 25	1.00046	1.00082	116290	28014.428	28029.8	23899.1	6721.37	15929.4	23501.7	22491.3	4.20193	21308.5	21293.1
Mean	**0.9999**	**0.9983**	**116164**										
stdev	**0.002**	**0.0019**											
uncet	**0.0039**	**0.0038**											
Run 28	0.99866	0.96761	95864.5	22498.387	21550.5	19542.9	7018.01	12184.4	18884.5	17208	3.46387	14532.5	15480.4
Run 29	0.99075	0.99166	95772.4	21660.414	21687.4	19286.1	6950.31	15253.8	19309.8	17206.9	3.46055	14737.1	14710.1
Run 30	0.99779	0.99589	96037.7	21602.016	21546.5	19291.4	6935.7	14735.2	18563	17052.2	3.47013	14610.8	14666.3
Run 31	0.99801	0.99955	95724.5	21440.811	21485.5	19251	6976.51	11239.2	18422.7	17007	3.45882	14509	14464.3
Run 32	0.9984	0.99787	95792.8	21484.193	21468.7	19376.1	6950.16	10930.2	18049.7	17060	3.46128	14518.5	14534
Run 33	0.99885	0.99846	95869.9	21509.467	21498.1	18903.4	6969.5	14298.4	18750.7	17091.3	3.46407	14528.6	14540
Run 34	1.00644	1.00576	95926.1	21339.309	21319.9	18932.6	6992.59	14400.3	18365.3	17052.2	3.4661	14327.3	14346.7
Run 35	1.00297	1.003	96039	21388.504	21389.5	19224.1	6928.82	13843.6	18863.3	16907.8	3.47018	14460.6	14459.7
Run 36	1.00163	1.00063	95782.4	21387.432	21358.6	19221.5	6936.8	11437.5	18555.8	16925.5	3.46091	14421.8	14450.6
Run 37	1.00383	1.00375	95992.8	21411.076	21408.9	19394.2	6987.08	14400.6	18435.6	17084.7	3.46851	14421.8	14424
Run 38	1.00182	1.00274	95861.5	21397.295	21424	19708.7	6983.69	14191.6	18786.5	16994.9	3.46377	14440.4	14413.6
Mean	**0.9999**	**0.997**	**95879**										
Stdev	**0.0041**	**0.0105**											
Uncert	**0.0083**	**0.0211**											
Run 40	0.99457	0.9952	76132.7	16337.383	16349.1	14979.2	7107.73	11485.5	14576.9	13666.3	2.75091	9241.41	9229.65
Run 41	0.99889	0.99216	76179.4	16390.35	16265.5	14996.1	7092.61	10039.1	14217	13646.6	2.75259	9172.88	9297.74
Run 42	0.99282	0.98884	76095.3	16366.163	16291.3	15091	7026.53	12150.9	14184.5	13668.1	2.74955	9264.77	9339.64
Run 43	0.9944	0.99196	76236	16334.139	16288.4	14972.7	7018.83	12841.6	14525.4	13624.1	2.75464	9269.61	9315.31
Run 44	0.99802	0.9952	76276.4	16368.6	16316.3	15341.9	7104.1	11008.3	14393.1	13517.7	2.7561	9212.19	9264.5
Run 45	0.9973	0.99114	76216	16337.764	16222.9	14956.8	7011.92	11643.1	14507	13590.8	2.75392	9210.99	9325.84
Run 46	1.00155	0.99411	76125.7	16355.757	16218.7	15092.5	7107.46	12657	14261.1	13685	2.75065	9111.26	9248.29
Run 47	1.00179	0.99948	76114	16253.741	16211.6	15223.8	7107.46	11295.2	14155.4	13655.9	2.75023	9104.1	9146.28
Run 48	1.00246	1.00266	76246.9	16223.86	16227.5	15069.5	7103.67	12062.5	14328.9	13633	2.75503	9123.83	9120.19
Run 49	1.00491	1.00201	76272.3	16188.989	16136.3	15018.3	7050.97	13415.3	14391.2	13567.4	2.75595	9085.33	9138.02
Run 50	1.00854	1.00209	76209.8	16157.111	16040.8	15432.5	7035.44	8914.4	14008.5	13509.3	2.75369	9005.32	9121.67
Mean	**0.9996**	**0.9959**	**76191**										
Stdev	**0.0048**	**0.0049**											
Uncert	**0.0096**	**0.0098**											
Run 53	0.99731	0.99716	56036.6	13404.572	13403.1	12339.8	8423.99	11819.9	12553	12072.4	2.02477	4979.07	4980.59
Run 54	0.98338	0.99276	56189	13036.839	13133.6	11959.8	7984.66	11298.8	12161.7	11715.6	2.03028	5148.97	5052.18
Run 55	0.99628	0.99309	56244.8	12741.726	12709.4	11687.2	7682.88	10577.8	11867.8	11442.6	2.0323	5026.52	5058.84
Run 56	1.00038	0.99713	56502.2	12596.429	12563.6	11431	7532.47	10910	11645.3	11243.7	2.0416	5031.13	5063.96
Run 57	0.9981	0.99727	56458.9	12348.719	12340.3	11199.9	7293.96	10558.8	11526.7	11000.3	2.04003	5046.38	5054.76
Run 58	0.99473	0.99911	56457.3	12148.165	12192.6	11128.8	7112.31	10193.8	11274.1	10899.4	2.03997	5080.34	5035.86
Run 59	1.00811	1.00038	56615.9	11991.01	11913.9	10862.1	6939.63	10334.9	11052.9	10692.8	2.0457	4974.23	5051.38
Run 60	1.0088	0.99613	56404.8	11924.247	11798	10715.2	6867.59	10173.1	11018.8	10592	2.03807	4930.44	5056.65
Run 61	0.99996	1.00043	56564.3	11722.211	11727	10629.5	6680.57	9964.72	10801	10430.8	2.04384	5046.38	5041.64
Run 62	1.00812	1.00189	56303.1	11597.211	11535.8	10490.3	6616.51	9820.8	10734.1	10338.5	2.0344	4919.34	4980.7
Mean	**0.9995**	**0.9975**	**56378**										
Stdev	**0.0077**	**0.003**											
Uncert	**0.0154**	**0.0061**											
Run 64	0.99409	0.99041	30916.7	10080.136	10068.8	9847.69	8543.31	9283.07	9715.66	9441.6	1.11711	1525.46	1536.82
Run 65	0.99909	0.9944	30810.9	10071.213	10057	9847.28	8557.12	9234.42	9729.57	9439.16	1.11329	1499.9	1514.09
Run 66	1.01656	1.01035	30789.7	10030.133	10012.3	9787.28	8565.5	9184.98	9681.61	9419.58	1.11252	1446.8	1464.64
Run 67	1.00066	0.99889	30685.1	9936.3506	9931.07	9735.81	8448.06	9222.81	9677.41	9392.82	1.10875	1483.01	1488.29
Run 68	0.98752	0.97591	30711	9961.8877	9925.4	9649.85	8400.08	9103.74	9556.19	9356.33	1.10968	1525.33	1561.81
Run 69	1.03315	1.00585	30809.3	9895.4033	9818.23	9607.42	8415.75	9025.9	9573.49	9309.42	1.11323	1402.48	1479.65
Run 70	0.98913	0.99341	30876.3	9788.9111	9802.15	9559.03	8265.37	9305.25	9499.3	9167.54	1.11565	1536.78	1523.54
Run 71	0.98507	0.97847	30763.4	9808.915	9788.09	9504.58	8249.94	9002.12	9436.85	9185.38	1.11158	1538.15	1558.97
Run 72	1.00602	1.00256	30863.4	9748.0811	9737.81	9488.22	8253.45	8908.06	9369.84	9164.97	1.11519	1484.36	1494.63
Run 73	0.9821	0.97812	30704.3	9770.5313	9757.95	9419.58	8216.42	8933.35	9341.6	9110.23	1.10944	1541.54	1554.11
Mean	**0.9993**	**0.9928**	**30793**										
Stdev	**0.0158**	**0.0121**											
Uncert	**0.0317**	**0.0244**											

Table B.18: C-D 0.6(15-15) with CMC 0.7 %

			Date:	17/10/2013	Test done by Luc								
			Venturi angle [°]:	15									
			Venturi length [m]:	0.14	Area[m2]								
			Throat diameter[m]:	0.0276	0.0006								
			Pipe Diameter [m]:	0.046	0.00167								
			Diameter ratio	0.6	0.28364								
			Material Type:	CMC									
			Density [kg/m3]:	1000.4									
			Concentration:	0.7%									
			ty:	0		1/n	n/(n+1)	(n+1)/n	K1/n				
			K:	0.0735		1.35135	0.42529	2.35135	0.02937				
			n:	0.74									
					Contracting		**Throat**	**Expanding**					
	Axial distances			-0.025	-0.07	-0.035	0	0.035	0.07	4.67			
	Venturi plane												
	Non-dimensionalised dista			-0.5434783	-1.5217	-0.7609	0	0.76087	1.52174	101.522			
	Distances[m]:			4.6	4.645	4.68	4.715	4.75	4.785	9.385			
Run #	**Cd(D&D**	**Cd(Flan**	**Re3**	**Pod 3**	**Pod 4**	**Pod 5**	**Pod 6**	**Pod 7**	**Pod 8**	**Pod 9**	**Average [l/s]**	**DPcont**	**ΔPFlang**
Run 1	0.96191	0.95423	9290.38	53236.0508	52734.4	46582.4	21688.9	33690.2	44834.6	37619.4	4.87516	31045.5	31547.1
Run 2	0.96359	0.95364	9293.73	53285.3633	52635.9	46475.9	21681.1	31520.4	44957.6	37699.1	4.87655	30954.8	31604.2
Run 3	0.97695	0.95132	1207.35	11566.9336	11502.5	11318.6	10322.6	10329.2	10829.1	10294.6	0.96528	1179.91	1244.36
Run 4	0.9653	0.95442	5125.64	28423.6172	28148.5	25849.9	16154.5	19902.8	24665.4	21297.2	3.04089	11993.9	12269.1
Run 5	0.96546	0.95451	7947.87	44692.9023	44138.2	39440.8	20083.1	27891.6	38027.8	31913.5	4.30718	24055.1	24609.8
Run 6	0.96675	0.95658	6375.73	35327.1094	34965.6	31658.8	18057.2	24235.1	29989.2	25796.8	3.61597	16908.4	17269.9
Run 7	0.97245	0.95575	1686.16	13129.0068	13057.7	12698.3	11034.1	11650.9	12266	11281.4	1.2583	2023.58	2094.92
Run 8	0.97021	0.95567	3842.73	22003.1387	21772.6	20502	14256.9	16201.8	19332.2	17027.5	2.4194	7515.67	7746.22
Run 9	0.97262	0.95578	2643.66	16779.6875	16632.8	15925.9	12502.5	13456.5	14909.4	13643.4	1.79801	4130.29	4277.18
Run 10	0.96728	0.95545	9913.15	57173.2148	56324.8	49715	22293	32994.6	48284.9	40173.9	5.13278	34031.8	34880.3
Run 12	0.9649	0.95606	9906.06	57045.4844	56410.6	49837.7	22249.7	36705	48666.7	40234.1	5.12986	34160.9	34795.8
Run 13	0.96172	0.95621	7740.03	43264.8398	42996	38209.8	19752.3	27781.6	37093.9	31045.6	4.21755	23243.7	23512.5
Run 14	0.96101	0.95622	9294.95	53262.793	52950.1	46525.5	21822.6	33668.9	45058.6	37586.8	4.87706	31127.5	31440.2
Run 15	0.97368	0.95602	1186.49	11422.6055	11379.5	11198.9	10224.1	10288.1	10678.1	10200.8	0.95203	1155.45	1198.54
Run 16	0.97829	0.95607	1700.42	13169.9697	13074.7	12727.2	11048.3	11246.1	12047.5	11314.8	1.26675	2026.43	2121.7
Run 17	0.96352	0.95489	2726.2	17089.9609	17009.7	16163.2	12590.5	13413.1	15181.4	13836.2	1.84242	4419.19	4499.45
Run 18	0.96729	0.95617	5123.49	28403.4805	28124.3	25758	16187.6	19897.4	24400.3	21250.9	3.03987	11936.7	12215.9
Run 19	0.96527	0.95516	6525.66	36186.8867	35812.4	32347.2	18214.6	23027.7	30521.7	26281.8	3.68329	17597.8	17972.3
Run 20	0.9697	0.95499	3789.78	21788.9355	21560.4	20061.8	14200.7	16344.5	19310.1	16867	2.39291	7359.74	7588.25
Run 21	0.96798	0.95569	3311.36	19608.1914	19454	18331.5	13492.1	14869.2	17269.7	15431.8	2.14987	5961.85	6116.06
Run 23	0.97163	0.95783	3300.78	19587.2324	19416.4	18292.2	13529.3	15019.4	17040.9	15483.3	2.14442	5887.1	6057.92
Run 24	0.96854	0.95829	6512.36	36018.2266	35643.4	32168.8	18220.8	23960.8	30373.6	26219.5	3.67733	17422.5	17797.4
Run 25	0.9668	0.95674	9872.44	57061.8516	56346.3	49527.9	22502.6	32804.2	47691.6	40058.2	5.11604	33843.7	34559.2
Run 26	0.96514	0.9558	9203.1	52598.7422	52001.8	45926.7	21622.8	30547.1	44160.3	37215.3	4.83877	30379	30976
Run 27	0.97884	0.95736	1401.42	12188.4521	12120.9	11850.3	10631.8	10663.8	11270.2	10679.1	1.0865	1489.1	1556.67
Run 28	0.96705	0.95689	1882.51	13829.3232	13777.3	13330.3	11340	11640.6	12563.2	11729.4	1.37327	2437.24	2489.28
Run 29	0.97994	0.95734	2654.32	16868.625	16672.9	15918.2	12578.1	13313.9	14987.3	13662.8	1.80376	4094.87	4290.57
Run 30	0.96815	0.95471	4995.39	27830.7754	27506.4	25302.7	16060.2	19425.9	23528.7	20867.4	2.9794	11446.2	11770.6
Run 31	0.96921	0.95813	3981.01	22746.3828	22561.1	21005.3	14595.2	16242.6	19563.7	17469.8	2.48825	7965.96	8151.22
Run 32	0.96915	0.9572	3986.63	22741.541	22541	21048.5	14556.2	16649.3	19483.9	17523.5	2.49104	7984.75	8185.32
Run 34	0.95732	0.95488	3989.19	22558.9805	22517.1	21336.3	14325.4	15494.4	18180.7	17715.8	2.4923	8191.66	8233.58
Run 35	0.96976	0.95599	9825.61	56736.2813	55767.2	51097.2	22382.7	28394.4	43190.3	40355.4	5.09677	33384.6	34353.6
Run 36	0.96353	0.95548	9830.54	56384.9414	55812.2	50334.3	21967.6	28721.1	43294.2	40164.6	5.0988	33844.6	34417.3
Run 37	0.96299	0.95574	8909.07	50316.332	49874.8	45424.9	20892.8	25486.3	38424	35466.7	4.71567	28982	29423.5
Run 38	0.96768	0.95739	7726.55	43226.4609	42731.6	39344	19836.7	23988.2	32354.9	31165.2	4.21171	22894.8	23389.7
Run 39	0.95865	0.9541	6217.01	34051.5352	33893.8	31249.6	17372.8	19407.9	25551	25087.7	3.54434	16521.1	16678.7
Run 40	0.97172	0.9557	5137.76	28401.1914	27999.7	26312.5	16119.1	18033.6	21852.5	21533.4	3.04659	11880.5	12282
Run 41	0.96733	0.9582	3832.33	21755.1504	21611.1	20670.2	14083	14996.5	17624.5	17139.4	2.41421	7528.13	7672.2
Run 42	1.0072	0.95731	2714.22	17136.8535	16707.4	16361	12691.3	13064.2	14182.7	13836.2	1.83599	4016.03	4445.51
Run 43	0.98265	0.9562	1698.23	13038.3506	12925.9	12795.4	10921.5	11146.5	11635.1	11427.3	1.26545	2004.37	2116.8
Run 44	0.96704	0.95517	1255.19	11555.8682	11523.8	11392.9	10243	10314.9	10504.9	10358.8	0.99552	1280.84	1312.88

Table B.19: C-D 0.6(15-15) with CMC 1%

			Date:	12/09/2013	Test done by Luc								
			Venturi angle [°]:	15									
			Venturi length [m]:	0.14	Area[m2]								
			Throat diameter[m]:	0.0276	0.0006								
			Pipe Diameter [m]:	0.046	0.00167								
			Diameter ratio	0.6	0.28364								
			Material Type:	CMC									
			Density[kg/m3]:	1007									
			Concentration:	1%									
			ty:	0		**1/n**	**n/(n+1)**	**(n+1)/n**	**K1/n**				
			K:	0.082		1.31752	0.4315	2.31752	0.00263				
			n:	0.726									
					Contracting		**Throat**	**Expanding**					
	Axial distances			-0.025	-0.07	-0.035	0	0.035	0.07	4.67			
	Venturi plane												
	Non-dimensionalised dista			-0.543478	-1.5217	-0.7609	0	0.76087	1.52174	101.522			
	Distances[m]:			4.6	4.645	4.68	4.715	4.75	4.785	9.385			
Run #	**Cd(D&D**	**Cd(Flan**	**Re3**	**Pod 3**	**Pod 4**	**Pod 5**	**Pod 6**	**Pod 7**	**Pod 8**	**Pod 9**	**Average [l/s]**	**DPcont**	**ΔPFlang**
Run 1	0.93173	0.84948	56250.3	63676.527	56767.4	50143.3	22737.4	36915.4	46284.7	40242.1	4.92779	34030	40939.2
Run 2	1.04298	0.94044	56102.8	63752.344	57533.8	50840	30490.7	31868.1	44492.7	40189.3	4.91738	27043	33261.6
Run 3	0.97881	0.88408	56144.1	63852.484	56911.9	50543.7	26170	33503.3	44254.5	40272.3	4.92029	30741.8	37682.5
Run 4	0.90698	0.83419	56158.5	63948.32	57424.7	50593.4	21605.8	33074.9	44212.3	40320.1	4.92131	35818.9	42342.5
Run 5	0.98248	0.88871	56102.8	63999.129	57228.5	50544.4	26752.5	34014.1	43292	40320.8	4.91738	30476	37246.6
Run 6	0.98114	0.88726	56264.4	64008.699	57167.8	50572.8	26466.3	33784.2	45603.8	40359.1	4.92879	30701.6	37542.4
Run 7	0.92916	0.84989	56183.6	64020.602	57352.8	50553.9	23199.2	33627.6	44958.8	40323.2	4.92308	34153.6	40821.4
Run 8	0.96734	0.87733	56260.8	64072.102	57259.4	50563.1	25678.9	34194.6	43836.5	40448.9	4.92853	31580.5	38393.2
Run 9	0.91451	0.84009	56241.1	64038.156	57503.8	50731	22189.2	33589.9	43706.5	40403.1	4.92714	35314.6	41848.9
Run 10	0.97263	0.88196	56246.4	64108.586	57358.5	50638.4	26133.7	34705.8	43965	40426.4	4.92752	31224.8	37974.9
Run 12	0.952	0.85889	39122.3	42683.742	38534	34870.8	20377.8	25715.4	30209.9	27948.6	3.67771	18156.2	22305.9
Run 13	0.98266	0.88335	39050.4	42594.965	38560.4	34836.8	21569.9	25175.3	29738.9	27920.3	3.67226	16990.5	21025.1
Run 14	0.96603	0.87148	39008.6	42554.148	38539.4	34878.9	20989.3	24998.4	29615	27988.6	3.66909	17550.1	21564.8
Run 15	0.96895	0.87284	38938.3	42629.82	38588.5	34665.2	21194.6	25209	29941.6	27910.8	3.66376	17393.9	21435.2
Run 16	0.98884	0.88572	39010.2	42507.652	38380.3	34744.3	21629.5	24917.1	29630.8	27874	3.66921	16750.9	20878.2
Run 17	0.97273	0.87417	38938.3	42531.988	38420.8	34744.4	21161.9	25035.5	29781.9	27886.6	3.66376	17258.9	21370.1
Run 18	0.98644	0.8857	39008.6	42506.977	38460.4	34786.3	21629.2	25275.4	29871.7	27892.9	3.66909	16831.2	20877.8
Run 19	0.98116	0.88108	39010.2	42516.035	38431	34711.7	21417	25478.7	30160.6	27855.8	3.66921	17014	21099
Run 20	0.96547	0.87437	39006.9	42483.863	38632.1	34730.5	21063	23969.8	30307.1	27890.2	3.66896	17569.1	21420.9
Run 21	0.97453	0.87891	39050.4	42492.508	38529.5	34709.7	21254.5	25271.5	30079	27900.8	3.67226	17275.1	21238
Run 23	0.91842	0.8096	25583	29822.707	27000.3	23640.1	17162.1	18504.6	20506.2	19522.1	2.61173	9838.2	12660.6
Run 24	0.99361	0.88157	25496.7	27917.924	25657.9	23808.4	17298	18511.2	20689.7	19524.8	2.60463	8359.9	10620
Run 25	0.96555	0.86968	25378.2	27889.818	25845.8	23913.5	17059.2	18522.7	22564.4	19448.6	2.59487	8786.67	10830.7
Run 26	0.98183	0.87377	25447.4	27903.205	25661.6	23764.1	17126.6	18496.1	20466.9	19500.2	2.60057	8535.03	10776.6
Run 27	0.98229	0.87538	25544.5	27969.014	25745.4	23840.1	17165.8	18627.5	20603.8	19527.9	2.60856	8579.62	10803.2
Run 28	0.98897	0.88195	25516.7	27879.957	25704.9	23767.6	17255.7	18423.8	20282.3	19505.1	2.60628	8449.23	10624.3
Run 29	0.97309	0.86961	25495.2	27952.797	25755.1	23773.9	17039.8	18537.5	20653.6	19471.6	2.60451	8715.32	10913
Run 30	0.98119	0.87539	25507.5	27936.447	25737.5	23811.2	17158.8	18439.3	20526.3	19500.1	2.60552	8578.71	10777.7
Run 31	0.97939	0.87502	25544.5	27943.477	25761.9	23749.7	17131.5	18009.1	21420.5	19478.3	2.60856	8630.46	10812
Run 32	0.98085	0.87313	25498.3	27903.732	25656.2	23739.5	17076.6	18522.7	20566.3	19500.1	2.60476	8579.63	10827.1

Table B.20: Venturi with Water

			Date:	28/09/2012	Test done by Luc					
			Venturi angle [°]:	Classical						
			Venturi length [m]:	0.28	Area[m2]					
			Throat diameter[m]:	0.0276	0.0006					
			Pipe Diameter [m]:	0.046	0.00167					
			Diameter ratio	0.6	0.28364					
			Material Type:	Water						
			Density[kg/m3]:	999.87						
			Concentration:	1						
			ty:	0		**1/n**	**n/(n+1)**	**(n+1)/n**	**K1/n**	
			K:	0.001		1	0.5	2	0.001	
			n:	1						
				Contracting		**Throat**	**Expanding**			
Axial distances				-0.158	-0.085	0	0.63	2.46		
Venturi plane										
Non-dimensionalised dista				-3.434783	-1.8478	0	13.6957	53.4783		
Distances[m]:				6.85	6.923	7.008	7.638	9.468		
Run #	**Cd(D&D**	**Re3**		**Pod 4**	**Pod 5**	**Pod 6**	**Pod 7**	**Pod 8**	**Average**	**Dpcont**
									[l/s]	
Run 2	0.98433	156073		59818.148	59297.1	19647.7	53643.6	48673	5.63939	39649.4
Run 3	0.98192	156017		60694.906	59596.1	19780.3	53700.1	48663	5.63738	39815.8
Run 4	0.98858	156108		60571.074	59927.4	20600.4	53673.7	48872.9	5.64065	39327
Run 5	0.98413	156352		61356.441	59837.5	20029.9	53850.6	48825.2	5.64947	39807.6
Run 6	0.98589	156272		61350.629	59669.9	20045.2	53830.8	48604.9	5.64657	39624.7
Run 7	0.97992	156425		61364.227	60090.8	19902.4	53841.4	48729	5.65211	40188.4
Run 8	0.98527	156383		60835.223	59431.6	19700.2	53905.1	48771.2	5.6506	39731.3
Run 9	0.98745	156802		61121.566	59470.9	19702.4	53762.1	48717.5	5.66572	39768.5
Run 10	0.9804	156342		60773.391	59603.8	19497.9	53643.2	48745.2	5.64909	40105.9
Run 11	0.98686	156554		60880.281	59512.7	19822.6	53880.3	48725	5.65678	39690
Mean	**0.9845**									
Stdev	**0.0029**									
uncertai	**0.006**									
Run 13	0.97437	105797		39010.215	38023.9	19430.4	35484.9	33077.3	3.82276	18593.6
Run 14	0.9886	106114		39951.168	39450.6	21280.1	36332.4	33765.2	3.83422	18170.5
Run 15	0.9647	105922		40713.391	39925.1	20912	36499.3	34104.1	3.82729	19013.1
Run 16	0.97802	105762		40530.078	39489.6	21046.9	36468.8	33884.9	3.8215	18442.7
Run 17	0.9644	105919		40266.336	39678.5	20654.8	36103.4	33854.2	3.82717	19023.8
Run 18	0.97273	105650		40846.074	39478.3	20873.7	36337.1	34020.5	3.81747	18604.6
Run 21	0.98378	105957		40267.57	39537.5	21242.7	36314.1	33690	3.82855	18294.8
Run 24	0.97132	105790		40105.207	39576.5	20868.6	36297	33668.7	3.82251	18707.9
Run 25	0.98151	105800		40023.258	39425.1	21099.7	36470.5	34048.5	3.82288	18325.3
Run 26	0.97885	105598		40193.934	39466.1	21111.5	36317.7	34089.8	3.81558	18354.6
Mean	**0.9758**									
Stdev	**0.0079**									
uncertai	**0.0162**									

Run 30	0.95977	62183.4	27105.693	26537	19916.7	25528.5	24567.1	2.24688	6620.36
Run 31	0.96159	62218.3	27128.717	26526.6	19924	25546.7	24584.3	2.24814	6602.62
Run 32	0.96622	62117.2	27106.807	26493.1	19974.8	25522	24609.1	2.24448	6518.32
Run 33	0.96426	62110.2	27144.801	26511.4	19968	25585.5	24594.8	2.24423	6543.43
Run 34	0.96456	62256.7	27176.666	26504.6	19934.4	25538.1	24573	2.24952	6570.17
Run 35	0.95876	62256.7	27116.234	26514.5	19864.5	25555.9	24615.6	2.24952	6649.92
Run 36	0.96081	62103.2	27125.375	26458.3	19869.2	25490.2	24504.7	2.24398	6589.04
Run 37	0.96178	62263.6	27030.82	26398.9	19789.2	25410.2	24472.2	2.24977	6609.69
Run 38	0.95888	62221.8	27041.902	26401.4	19760.7	25445.1	24503.4	2.24826	6640.75
Run 39	0.96591	62218.3	27006.139	26350.5	19806.7	25456.9	24483.6	2.24814	6543.82
Run 40	0.96274	62253.1	27087.396	26438.8	19844.4	25457.2	24495.8	2.24939	6594.34
Mean	**0.9623**								
Stdev	**0.0027**								
uncertai	**0.0055**								
Run 42	0.95498	43044.5	27112.063	26535.9	23331.8	26067.1	25578.1	1.55533	3204.17
Run 44	0.95615	43294.8	26997.133	26446.4	23212.8	25967	25463.5	1.56437	3233.59
Run 45	0.95386	43191	26970.51	26430	23196.4	25953.4	25467.8	1.56062	3233.58
Run 47	0.95587	43161.6	26985.885	26484.9	23269.3	26034.8	25528.6	1.55956	3215.57
Run 48	0.95459	43147.1	26935.15	26470.1	23248	25982.8	25487.7	1.55904	3222.09
Run 49	0.95885	43276.2	26874.555	26422.9	23210.3	25983.9	25481.8	1.5637	3212.65
Run 50	0.95579	43163.3	26825.732	26398.8	23182.4	25956.8	25451.7	1.55962	3216.38
Run 52	0.95758	43162	26775.256	26370.4	23166.2	25901	25402.9	1.55957	3204.18
Run 53	0.95832	43366	26716.33	26355.4	23125.8	25912.7	25393.5	1.56694	3229.57
Run 54	0.95638	43270.8	26716.195	26361.2	23132.8	25896.4	25396	1.56351	3228.46
Mean	**0.9562**								
Stdev	**0.0016**								
uncertai	**0.0034**								

Table B.21:Venturi with CMC 2%

			Date:	06/10/2012	Test done by Luc					
			Venturi angle [°]:	Classical						
			Venturi length [m]:	0.28	Area[m2]					
			Throat diameter[m]:	0.0276	0.0006					
			Pipe Diameter [m]:	0.046	0.00167					
			Diameter ratio	0.6	0.28364					
			Material Type:	CMC						
			Density[kg/m3]:	1012						
			Concentration:	2%						
			ty:	0						
			K:	0.096		**1/n**	**n/(n+1)**	**(n+1)/n**	**K1/n**	
			n:	0.716		1.26582	0.44134	2.26582	0.00517	
				Contracting		**Throat**	**Expanding**			
Axial distances				-0.158	-0.085	0	0.63	2.46		
Venturi plane										
Non-dimensionalised dista				-3.434783	-1.8478	0	13.6957	53.4783		
Distances[m]:				6.85	6.923	7.008	7.638	9.468		
Run #	**Cd(D&D**	**Re3**		**Pod 4**	**Pod 5**	**Pod 6**	**Pod 7**	**Pod 8**	**Average**	**DPcont**
									[l/s]	
Run 1	0.95324	34067.1		89494.32	89394	54653.4	82095.3	38458.5	5.07954	34740.6
Run 2	0.96044	34201		89029.516	89010.3	54565.7	82202.1	45298.2	5.09604	34444.6
Run 3	0.95965	34042.5		88733.094	88700.3	54462.8	83059.7	57283.8	5.07651	34237.5
Run 4	0.95343	34007.8		89155.172	89002.5	54375.7	83438.6	54644.1	5.07223	34626.8
Run 5	0.95977	34243		88758.68	88659.7	54097.5	83496.6	60354.6	5.10121	34562.1
Run 6	0.94687	34041.5		89535.633	89529.8	54363.6	83303.9	60415.1	5.07639	35166.2
Run 7	0.95239	34135.6		89314.953	89252.3	54334.2	82599.7	75623.8	5.08798	34918
Run 9	0.96065	34020.1		89565.922	89560.3	55431.9	83465.1	42460.8	5.07374	34128.5
Run 10	0.95472	34100.8		89823.258	89643.1	54953.2	83042.7	39979.2	5.08369	34689.9
Run 11	0.95809	34066.1		89222.797	89174.6	54786.5	83152.7	40082	5.07941	34388.1
Mean	**0.9559**									
stdev	**0.0045**									
uncertai	**0.0095**									
Run 12										
Run 13	0.94437	19825.6		50438.234	50446.6	35980.7	47251.4	28172.6	3.24728	14466
Run 14	0.95821	19805.2		50583.953	50481.9	36454.8	47444.4	29996	3.24451	14027.1
Run 15	0.95892	19808		50634.945	50686.5	36676.9	47553.6	27831	3.24489	14009.6
Run 16	0.94802	19804.2		50656.82	50652.3	36322.9	47765	27758.8	3.24439	14329.4
Run 17	0.95821	19754		50465.594	50453.9	36486.7	47739.2	31600.4	3.23758	13967.2
Run 18	0.95843	19806.1		50626.148	50589.7	36568	47533.3	30155.1	3.24464	14021.7
Run 19	0.95462	19785.6		50520.09	50595.7	36485.7	47601.3	28833.3	3.24187	14109.9
Run 20	0.96166	19805.2		50647.863	50345.4	36418.8	47395.8	31748.9	3.24451	13926.6
Run 21	0.95036	19767		50450.758	50628.6	36414.2	47585.7	31290.8	3.23935	14214.4
Mean	**0.9548**									
stdev	**0.0059**									
uncertai	**0.0123**									

Run 25	0.94922	9732.55	30510.582	30571.8	26154.5	29520.2	19497.2	1.80363	4417.32
Run 26	0.94489	9778.93	30298.506	30209.1	25716	29243.7	20136.9	1.81073	4493.06
Run 27	0.95049	9729.92	30153.188	30042.4	25638.9	29083.3	17708.6	1.80323	4403.47
Run 28	0.94905	9745.83	30022.145	30019.7	25590.8	29050.1	19203.8	1.80567	4428.83
Run 29	0.94402	9705.91	30021.604	29967.7	25521.8	28963.5	19800.3	1.79955	4445.91
Run 30	0.94919	9745.14	29991.229	29942.8	25515.8	28966.9	19578.8	1.80556	4427.04
Run 31	0.94371	9738.12	29951.158	29939.7	25466.4	28960.1	19874.8	1.80448	4473.21
Run 32	0.94755	9714.99	29954.906	29914.4	25494.7	28922.4	19377.1	1.80094	4419.69
Run 33	0.94146	9711.96	29930.227	29922.9	25448.1	28917.3	20284.5	1.80048	4474.74
Run 34	0.94696	9707.96	29925.648	29891.8	25472	28933.4	19460.7	1.79987	4419.84
Mean	**0.9467**								
stdev	**0.003**								
uncertai	**0.0063**								
Run 36	0.92697	3982.41	24851.891	24846.6	23789.1	24470.6	18005.6	0.86183	1057.55
Run 37	0.9286	3991.94	24849.391	24838.6	23780.6	24510.9	18318.9	0.86353	1058.02
Run 38	0.92341	4015.28	24830.959	24864.1	23783.8	24500.8	18353.4	0.8677	1080.29
Run 39	0.92691	4016.45	24843.037	24861.5	23788.8	24496.1	18629.2	0.86791	1072.67
Run 40	0.92759	4015.61	24837.193	24860.2	23789.5	24494	17915.1	0.86776	1070.73
Run 42	0.9289	4005.48	24853.969	24854.9	23791.7	24510.5	18681.9	0.86595	1063.26
Run 43	0.93408	4005.74	24881.707	24856.6	23805	24504	18986.4	0.866	1051.62
Run 44	0.94955	3993.52	24841.787	24830.4	23817.9	24517.3	19427.7	0.86381	1012.5
Run 45	0.93114	3983.41	24838.309	24859.1	23810.6	24504	19215.2	0.86201	1048.53
Run 46	0.91597	3994.03	24834.287	24886.4	23798.1	24499.8	19838.5	0.8639	1088.34
Mean	**0.9293**								
stdev	**0.0086**								
uncertai	**0.0185**								

Table B.22: Venturi with CMC 2% +XG

			Date:	18/10/2012	Test done by Luc				
			Venturi angle [°]:	Classical					
			Venturi length [m]:	0.28	Area[m2]				
			Throat diameter[m]:	0.0276	0.0006				
			Pipe Diameter [m]:	0.046	0.00167				
			Diameter ratio	0.6	0.28364				
			Material Type:	CMC+XG					
			Density[kg/m3]:	1015					
			Concentration:	2%					
			ty:	0					
			K:	0.323		**1/n**	**n/(n+1)**	**(n+1)/n**	**K1/n**
			n:	0.675		1.40449	0.41589	2.40449	0.04678
				Contracting		**Throat**	**Expanding**		
Axial distances				-0.158	-0.085	0	0.63	2.46	
Venturi plane									
Non-dimensionalised dista				-3.434783	-1.8478	0	13.6957	53.4783	
Distances[m]:				5.14	5.213	5.298	5.928	7.758	
Run #	**Cd(D&D**	**Re3**		**Pod 4**	**Pod 5**	**Pod 6**	**Pod 7**	**Pod 8**	**Average [l/s]**	**DPcont**
Run 3	0.94535	3175.87		39898.207	39236.8	30282	36565.3	36811.4	2.55464	8954.79
Run 4	0.89063	3131.96		43741.73	42966.9	33093.8	37707.2	37517.8	2.52718	9873.1
Run 5	0.91827	3016.62		41579.59	41995.6	33233.5	39502.6	39570.8	2.45462	8762.1
Run 6	0.90001	3200.9		39961.965	40351.2	30350.4	37448.6	37424.1	2.57026	10000.8
Run 7	0.93434	3094.21		41837.641	40892.9	32089.3	37624	37886.2	2.5035	8803.6
Run 9	0.90707	3176.68		39612.961	40883.6	31153.4	36427.2	36713.6	2.55515	9730.25
Run 10	0.90765	3120.91		41841.102	41926.2	32471.9	37431.5	37239.6	2.52025	9454.31
Run 12	0.93418	3119.9		39229.426	40240.3	31319.8	37749.4	38367.8	2.51962	8920.52
Run 13	0.94222	3122.92		40043.918	39300.4	30518.4	36693	37264.3	2.52151	8781.97
Mean	**0.92**									
Stdev	**0.0198**									
uncertai	**0.043**									
Run 16	0.90115	1765.31		34767.406	34212.8	30253.5	32544	34572.9	1.61926	3959.28
Run 17	0.90904	1776.89		33560.527	33081	29150.5	32005.9	32525.9	1.6275	3930.53
Run 18	0.9128	1795.55		33519.207	33179.9	29217.9	32060.2	32111.4	1.64076	3962.01
Run 19	0.90235	1786.69		33295.133	33037.4	29014.1	31840.2	32060.1	1.63446	4023.26
Run 20	0.90278	1767.29		33327.461	33035.7	29083.8	31776.1	31920.3	1.62067	3951.9
Run 21	0.86128	1762.82		33595.48	33365	29040.2	32098.6	32107	1.61748	4324.85
Run 22	0.9332	1744.66		33681.875	33396.4	29771.2	31871.9	32206.8	1.60454	3625.18
Run 23	0.91083	1775.67		34153.863	33759	29848	32310.1	32362.5	1.62663	3910.96
Run 24	0.91918	1719.4		33956.969	33523	29870.1	32012.3	32273.9	1.58647	3652.91
Run 25	0.88214	1713.7		33993.848	33798.5	29852.7	32881.6	32801.5	1.58238	3945.76
Mean	**0.9035**									
Stdev	**0.0198**									
uncertai	**0.0439**									

Run 29	0.87656	700.055	29944.23	33018.4	32023.2	32502.6	32637.5	0.78967	995.205
Run 30	0.89873	710.946	30470.869	33342	32372.3	32843	32860.3	0.79919	969.672
Run 31	0.86735	690.546	30793.672	33752.4	32757.4	33369.2	33314.3	0.78133	995.078
Run 32	0.89227	687.008	30933.719	33885.4	32952.6	33505.2	33532.9	0.77822	932.813
Run 33	0.88097	689.134	30760.949	33773.2	32811.7	33282.2	33287.2	0.78009	961.488
Run 34	0.8851	682.609	30530.773	33547.5	32608.9	33033.6	33042.2	0.77435	938.574
Run 35	0.90775	686.957	30545.199	33781.3	32880.1	33198.6	33396.9	0.77818	901.152
Run 36	0.90788	680.404	30703.258	33664	32776.4	33279.1	33320.5	0.77241	887.594
Run 37	0.85166	661.047	31125.207	34125.9	33161.4	33729	33664	0.75529	964.434
Mean	**0.8854**								
Stdev	**0.0187**								
uncertai	**0.0422**								
Run 39	0.81766	198.306	31339.842	34385.8	34224.4	34248.3	34190.9	0.29658	161.328
Run 40	0.82048	190.794	31716.887	34606.7	34455.9	34441.7	34396.4	0.28782	150.895
Run 41	0.82562	185.172	31951.805	34739.2	34596.9	34568.3	34541.8	0.28121	142.262
Run 42	0.83938	186.072	32134.965	34827.4	34688.7	34694.9	34691.2	0.28227	138.676
Run 43	0.82809	182.817	32265.857	34939.5	34800.9	34759.1	34725.2	0.27843	138.629
Run 44	0.80782	178.694	32387.879	34947.3	34806.7	34785.2	34759.7	0.27354	140.605
Run 45	0.80562	173.179	32489.527	35042.7	34908	34869.6	34837.3	0.26697	134.656
Run 46	0.79044	176.408	32599.471	35007.2	34863.2	34834.8	34850.5	0.27082	143.949
Run 47	0.81447	167.716	32766.443	35174.7	35049.4	35010	35008.8	0.2604	125.348
Run 48	0.82759	165.302	32918.254	35240.8	35122.1	35052.1	35040.7	0.25749	118.703
Mean	**0.8177**								
Stdev	**0.0139**								
uncertai	**0.034**								

Table B.23: Venturi with CMC 6%

		Date:	16/07/2013	Test done by Luc						
		Venturi angle [°]:	Classical							
		Venturi length [m]:	0.28	Area[m2]						
		Throat diameter[m]:	0.0276	0.0006						
		Pipe Diameter [m]:	0.046	0.00166						
		Diameter ratio	0.6							
		Material Type:	CMC							
		Density[kg/m3]:	1031							
		Concentration:	6%							
		ty:	0		**1/n**	**n/(n+1)**	**(n+1)/n**	**K1/n**		
		K:	2.2025369		1.68235	0.37281	2.68235	3.775		
		n:	0.5944064							
			Contracting		**Throat**	**Expanding**				
	Axial distances		-0.106	-0.085	0	0.063	1.893	4.193		
	Venturi plane									
	Non-dimensional		-2.304348	-1.8478	0	1.36957	41.1522	91.1522		
	Distances[m]:		5.03	5.051	5.136	5.199	7.029	9.329		

Run #	**Cd(D&D**	**Re3**	**Pod 4**	**Pod 5**	**Pod 6**	**Pod 7**	**Pod 8**	**Pod 9**	**Average [l/s]**	**DPcont**
Run 1	0.91679	524.572	133951.66	133941	114371	122224	108963	92373.4	3.63671	19581.1
Run 2	0.91483	529.243	132748.14	132742	112834	120963	107727	91214	3.65972	19914.5
Run 3	0.91177	530.384	132403.8	132420	112293	120473	107497	90368.9	3.66533	20110.4
Run 4	0.9208	533.052	131721.88	131869	111863	120286	107088	90795.3	3.67844	19858.7
Run 5	0.9217	533.601	131322.81	131507	111474	119836	106674	90441.8	3.68114	19849.1
Run 6	0.92228	537.044	131019.84	131121	111013	119396	106421	90249.3	3.69802	20006.5
Run 7	0.91957	538.068	130716.15	129687	110537	118923	106107	90052.6	3.70303	20179
Run 8	0.93043	538.418	129913.59	130226	110185	118781	105849	89748.8	3.70475	19729
Run 9	0.91596	539.922	130193.44	129983	109755	117919	105466	89561.9	3.71211	20438.6
Run 10	0.92843	540.907	129541.77	129656	109597	118367	105313	89467.6	3.71692	19944.5
Mean	**0.9203**	**534.52**								
Stdev	**0.0059**	**5.2815**								
uncertai	**0.0127**	**0.0198**								
Run 12	0.88565	386.839	109309.03	109191	95705.8	100252	90106.3	76825.8	2.92821	13603.3
Run 13	0.89061	387.462	109404.3	109365	95921.5	100260	90224	76942	2.93157	13482.8
Run 14	0.89377	387.082	109569.44	109548	96200.3	100609	90591.2	77338.4	2.92952	13369.1
Run 15	0.8824	388.279	109666.32	109606	95890	99871.3	89884.1	76651.7	2.93596	13776.3
Run 16	0.89606	388.525	109051.3	108969	95679.9	99971.4	90119.5	76831.6	2.93729	13371.4
Run 17	0.90028	388.172	108690.35	108919	95461.1	99875.2	90060.1	76976.5	2.93539	13229.3
Run 18	0.9017	389.241	108973.87	109043	95734.6	100004	90244	77145	2.94114	13239.3
Run 19	0.89631	389.222	109099.03	109061	95700.9	100024	90292.2	77288.9	2.94104	13398.1
Run 20	0.89557	387.73	109025.65	108960	95678.6	99912.2	90291.6	77360.3	2.93301	13347
Run 21	0.89861	387.817	109043.34	108964	95782.1	100360	90689.9	77788.3	2.93348	13261.2
Mean	**0.8941**	**388.04**								
Stdev	**0.0062**	**0.8158**								
Uncertai	**0.0139**	**0.0042**								

Run 23	0.82429	254.866	90736.422	90888.7	82063.8	83344.3	75173.2	64465.6	2.17609	8672.59
Run 24	0.85353	255.186	89613.703	89576.4	81510.7	82633.7	74630.6	64234.4	2.17803	8103
Run 25	0.8513	254.829	89636.938	89524.9	81507.6	82476.7	74768	64228.7	2.17586	8129.34
Run 26	0.83955	254.715	89816.406	89821.1	81463.3	82790.3	75162.5	64961.2	2.17517	8353.13
Run 27	0.82573	254.237	90905.891	90858.6	82293.7	83939.6	75941.9	65348.7	2.17227	8612.16
Run 28	0.83338	253.658	91065.531	90757.3	82638.3	84083.1	76772.3	66263.6	2.16875	8427.22
Run 29	0.85005	254.255	91058.883	90980.6	82931.7	83820	76400.5	65876.6	2.17237	8127.19
Run 30	0.85061	254.185	91186.711	91066.6	83073.5	83946.5	76542.2	66673	2.17195	8113.23
Run 31	0.83921	254.245	91321.328	91244.3	82983.3	83777.1	76689.3	65961.6	2.17231	8337.98
Run 32	0.85537	254.235	91471.609	91374.2	83446.1	83967.7	76879.5	66313.6	2.17225	8025.55
Mean	**0.8423**	**254.44**								
Stdev	**0.0116**	**0.4469**								
Uncertai	**0.0274**	**0.0035**								
Run 34	0.7654	133.118	73080.023	72982.5	69088.2	68781.3	62526.1	54822.6	1.37087	3991.82
Run 35	0.7743	133.01	73257.195	73223.8	69361.1	69077.9	62855.2	55230.8	1.37007	3896.13
Run 36	0.77493	132.786	73492.313	73497.3	69611.9	69350.6	63140.9	55505	1.36843	3880.42
Run 37	0.78219	132.529	73686.516	73666.3	69888.2	69616.1	63457.6	55875.6	1.36655	3798.28
Run 38	0.77433	132.525	73909.773	73857.2	70034.2	69785.9	63605.2	56033.6	1.36652	3875.59
Run 39	0.78339	132.271	74109.766	74072.8	70333.6	70058.7	63872.5	56334	1.36466	3776.19
Run 40	0.77276	132.745	74102.602	74018.4	70202	69986.2	63823.7	56310.2	1.36813	3900.55
Run 41	0.7791	132.324	74269.523	74262.6	70449.5	70186.9	64007	56485.2	1.36505	3820.02
Run 42	0.77234	132.261	74555.313	74525.3	70670.7	70413	64249.3	56770.1	1.36458	3884.58
Run 43	0.77036	132.263	75098.344	75038.3	71193.7	70945.1	64776.1	57276.5	1.3646	3904.63
Mean	**0.7749**	**132.58**								
Stdev	**0.0054**	**0.3185**								
Uncertai	**0.014**	**0.0048**								
Run 45	0.64798	46.8203	66823.688	66937.6	65564.4	64442.5	60482.9	55801.9	0.65184	1259.26
Run 46	0.63074	47.6215	66260.813	66247.8	64899.3	63854.1	59956	55216.2	0.65976	1361.52
Run 47	0.65798	47.6322	66085.141	66165.5	64833.6	63797.9	59899.5	55186.4	0.65986	1251.54
Run 48	0.64584	47.5604	66161.07	66210.6	64864.8	63842.6	59916.4	55248.4	0.65915	1296.25
Run 49	0.71369	47.7483	65349.027	65529	64281.6	63370.2	59539.8	54950.7	0.66101	1067.46
Run 50	0.6685	47.8751	66008.922	66096.9	64787.7	63769	59851.1	55199.3	0.66225	1221.25
Run 51	0.64981	47.6627	66081.766	66157.8	64797.4	63818.3	59863.6	55218.4	0.66016	1284.38
Run 52	0.69473	47.5803	65587.695	65750.5	64466.8	63547	59688.2	55104.7	0.65935	1120.87
Run 53	0.6616	47.9639	66109.703	66185	64859.5	63819.7	59943.8	55248	0.66313	1250.17
Run 54	0.64776	47.9654	66126.742	66165.4	64822.5	63809.4	59924.6	55267.9	0.66314	1304.22
Mean	**0.6619**	**47.643**								
Stdev	**0.0249**	**0.3267**								
Uncertai	**0.0753**	**0.0137**								

Table B.24: Venturi with CMC 0.7%

			Date:	20/10/2013	Test done by Luc						
			Venturi	Short							
			Venturi	0.28	Area[m2]						
			Throat d	0.0276	0.0006						
			Pipe Dia	0.046	0.00166						
			Diamete	0.6							
			Material	CMC							
			Density[	1000.4							
			Concent	0.0007							
			ty:	0		**1/n**	**n/(n+1)**	**(n+1)/n**	**K1/n**		
			K:	0.0735		1.35135	0.42529	2.35135	0.02937		
			n:	0.74							
				Contracting		**Throat**	**Expanding**				
	Axial distances		-0.106	-0.085	0	0.63	2.46	4.76			
	Venturi plane										
	Non-dimensional		-2.3043	-1.8478261	0	13.6957	53.4783	103.478			
	Distances[m]:		5.03	5.051	5.136	5.766	7.596	9.896			
Run #	**Cd(D&D**	**Re3**	**Pod 4**	**Pod 5**	**Pod 6**	**Pod 7**	**Pod 8**	**Pod 9**	**Average**	**Dpcont**	
									[l/s]		
Run 1	0.97002	11021.6	65324.2	64683.4492	24681.3	57512.8	51317.9	44410.7	5.58323	40002.1	
Run 2	0.97296	11071.9	65357	64755.7578	24706.3	57585	51384.1	44419.6	5.60346	40049.4	
Run 3	0.96761	9347.95	53816.3	53305.9102	22352.5	47472.3	42518.8	37018.8	4.89912	30953.5	
Run 4	0.96082	6531.32	35999.2	35719.8516	17951.2	32144.3	29130.3	25609.6	3.68582	17768.6	
Run 5	0.9579	5164.71	28382.3	28189.4238	15873.6	25553.9	23334.1	20719.2	3.05927	12315.8	
Run 6	0.94808	3645.89	20712.3	20572.5371	13339	18863.8	17463.1	15855.7	2.32051	7233.52	
Run 7	0.93544	2556.92	15892.4	15862.6436	11631.8	14721.8	13875.7	12826.3	1.75103	4230.84	
Run 8	0.91965	1552.44	12090.7	12088.3145	10105.7	11483.1	11040	10475.1	1.17844	1982.64	
Run 9	0.95077	4374.11	24307.3	24212.5313	14609.2	22009.3	20301	18159.9	2.68133	9603.32	
Run 10	0.97596	12231.4	73614.2	72999.1875	26377.9	64798.1	57856.9	50063.1	6.06437	46621.3	
Run 12	0.97483	12229.5	73777.7	73033.6484	26316.3	64977.3	57873.4	50106.3	6.06361	46717.4	
Run 13	0.96773	10696.5	63009.8	62461.7734	24135.6	55635.9	49660.6	42991.3	5.45214	38326.1	
Run 14	0.96967	9358.93	53803.4	53318.6211	22438.8	47554.8	42650.8	37084.9	4.90369	30879.8	
Run 15	0.96209	7440.46	41599.5	41272.7461	19478	37003.9	33344.9	29234.3	4.08746	21794.7	
Run 16	0.95284	5045.8	27995.8	27879.8105	15884.5	25305.9	23132.2	20599.2	3.00323	11995.3	
Run 17	0.93699	2735.57	16913.2	16888.4824	12194.4	15661.5	14716	13627.2	1.84745	4694.09	
Run 18	0.91912	1539.64	12306.4	12313.584	10354.6	11710.7	11295.9	10725.3	1.17072	1958.98	
Run 19	0.94918	3835.12	21907.9	21795.0117	13974.6	19946.4	18481	16721.6	2.4156	7820.41	
Run 20	0.95698	6147.04	34038.7	33848.0313	17580	30454.8	27736	24458.8	3.51264	16268.1	
Run 21	0.95187	4541.54	25359.7	25224.459	15054.5	22954.2	21126.9	18897.7	2.76248	10170	

Run 23	0.95271	4541.54	25366.5	25202.8242	15051	22929.5	21083.8	18934.6	2.76248	10151.8
Run 24	0.97894	12285.3	73742.3	73034.8672	26373.7	64784	58042.6	50332.3	6.08554	46661.2
Run 25	0.98027	12288.8	73891	72995.2656	26439.1	64961.3	58022.2	50399.7	6.08693	46556.2
Run 26	0.97384	10716.3	62852.9	62321.2148	24362.8	55632.8	49790.4	43097.4	5.46013	37958.4
Run 27	0.9756	10743.5	62832.3	62285.2578	24311.3	55542.2	49764	43223.3	5.47116	37973.9
Run 28	0.96442	7675.3	43022.9	42640.6211	19854.4	38177.8	34471.2	30151.3	4.18953	22786.2
Run 29	0.96219	6707.31	37130.7	36959.6328	18477.6	33217.1	30114.1	26451.6	3.76443	18482
Run 30	0.95991	6147.32	33972.6	33689.6445	17519.7	30331.9	27628.3	24338.6	3.51277	16169.9
Run 31	0.9486	3823.97	21697	21658.373	13864.6	19857.3	18407.8	16636.9	2.41002	7793.78
Run 32	0.93808	2683.14	16569.7	16557.3828	12015.9	15343.3	14497	13402.4	1.81929	4541.5
Run 34	0.93816	2678.36	16621.9	16563.4727	12035.6	15326.9	14510.8	13398.6	1.81672	4527.86
Run 35	0.98023	13970.6	86644.1	85627.2188	28553.4	76102.3	67740.5	58494.6	6.73923	57073.8
Run 36	0.96934	10509.4	61692.3	61158.8711	24014.5	54322.2	48691.8	42164.8	5.37633	37144.3
Run 37	0.96851	10066.7	58496.4	58081.4805	23330.6	51609.5	46244.6	40122.3	5.19579	34750.9
Run 38	0.96212	7540.04	42106.2	41745.5938	19487.6	37386.4	33742.8	29588.9	4.13083	22258
Run 39	0.95735	5571.91	30665	30381.2637	16472.7	27459.1	25103.5	22177.3	3.24919	13908.6
Run 40	0.94836	3673.52	20954.2	20833.6445	13517.1	19113.8	17694.7	16059.8	2.33446	7316.5
Run 41	0.92545	2068.9	14049.2	14016.6094	10928	13134.8	12520.6	11762.2	1.48011	3088.6
Run 42	0.9564	5645.42	31037.2	30855.1973	16626.1	27750.1	25437.2	22505.2	3.28317	14229.1

Table B.25: Venturi with CMC 1%

				Date:	12/09/2013	Test done by Luc				
				Venturi angle [°]:	Short					
				Venturi length [m]:	0.28	Area[m2]				
				Throat diameter[m]:	0.0276	0.0006				
				Pipe Diameter [m]:	0.046	0.00166				
				Diameter ratio	0.6					
				Material Type:	CMC					
				Density[kg/m3]:	1007					
				Concentration:	1%					
				ty:	0		**1/n**	**n/(n+1)**	**(n+1)/n**	**K1/n**
				K:	0.082		1.31752	0.4315	2.31752	0.00263
				n:	0.726					
				Contracting		**Throat**	**Expanding**			
	Axial distances			-0.106	-0.085	0	0.63	2.46	4.76	
	Venturi plane									
	Non-dimensional			-2.3043	-1.8478261	0	13.6957	53.4783	103.478	
	Distances[m]:			5.03	5.051	5.136	5.766	7.596	9.896	
Run #	**Cd(D&D**	**Re3**		**Pod 4**	**Pod 5**	**Pod 6**	**Pod 7**	**Pod 8**	**Pod 9**	**Average [l/s]**	**DPcont**
Run 1	0.97391	60573.7		61901.6	62642.9805	26840.7	55760.6	49914.4	43089.3	5.23078	35060.9
Run 2	0.97313	60581		61973.1	62690.5469	26849	55841.3	49841.2	43160	5.23129	35124.1
Run 3	0.9762	60715.9		62078.8	62615.5508	27049.7	55697.3	49854	43169.7	5.24067	35029.1
Run 4	0.97207	60570.1		62248.5	62785.9609	27057.8	55799.4	50008.6	43288.2	5.23053	35190.7
Run 5	0.97651	60655.7		62019.2	62743.25	27068.7	55868.1	50047.9	43286.6	5.23649	34950.5
Run 6	0.97892	60714		62007.4	62776.9336	27174.7	55839.6	50089.4	43362	5.24054	34832.8
Run 7	0.97669	60730.5		62086.6	63020.1523	27079.7	55904.9	50038.5	43335	5.24168	35006.9
Run 8	0.97592	60794.2		62304	62775.1563	27182.4	56084	50117.1	43406.6	5.24612	35121.7
Run 9	0.96317	60652.1		62819.7	62885.1719	26897.3	55957.4	50148.6	43476.2	5.23623	35922.4
Run 10	0.96128	60816.1		63227	62845.1484	27006.2	56020.7	50197.6	43394.8	5.24764	36220.9
Run 11	0.96125	60907.3		63391.8	63044.7656	27080.9	55902.4	50150.3	43445.3	5.25398	36311

Run 13	0.95282	38499	37875.2	37701.5391	20230.4	33967.5	30881.7	27099.4	3.63042	17644.8
Run 14	0.95411	38492.3	37918.6	37763.8438	20326.1	33876.1	30829.4	27137.9	3.62991	17592.5
Run 15	0.95652	38525.7	37851.7	37746.6875	20323.2	33861.4	30802.6	27136.3	3.63245	17528.5
Run 16	0.9553	38497.3	37878.4	37744.7773	20326.2	33882.2	30806.8	27104	3.63029	17552.3
Run 17	0.95516	38514	37863.8	37732.2148	20294.3	33803.2	30806.4	27124.7	3.63156	17569.5
Run 18	0.95363	38494	37915.6	37750.0469	20304.4	33858.8	30789.4	27006.9	3.63004	17611.2
Run 19	0.95141	38495.7	37976	37753.7148	20281	33881.9	30768.3	27158	3.63017	17695
Run 20	0.95552	38530.7	37924.2	37756.9609	20355.4	33824.1	30845.7	27034.7	3.63283	17568.9
Run 21	0.94908	38417.3	37993.7	37793.0352	20270.4	33883.3	30806	27037.6	3.62421	17723.3
Run 22	0.94965	38459	38000.7	37670.9844	20267.5	33811	30797.8	27125.6	3.62738	17733.2
Run 24	0.94259	23422.1	23672.2	23600.2012	15578	21477.8	19994.5	18062.3	2.43246	8094.21
Run 25	0.94049	23387.3	23676	23618.8691	15565.1	21511.3	19990	18040.1	2.42955	8110.97
Run 26	0.9391	23388.8	23697.8	23587.7852	15562	21438.8	19995.5	18043.5	2.42967	8135.83
Run 27	0.94269	23422.1	23674.9	23610.0781	15582.5	21494.1	19992.9	18006.8	2.43246	8092.46
Run 28	0.94295	23455.5	23669.4	23629.8184	15562.8	21412.8	19949	18028.4	2.43525	8106.64
Run 29	0.93988	23358.5	23652.1	23614.2754	15546.8	21490	19969	18062.4	2.42714	8105.31
Run 30	0.93718	23357	23666.8	23563.4512	15515.6	21308.7	19942.4	18046.1	2.42701	8151.24
Run 31	0.93873	23400.9	23685.9	23597.6328	15536.9	21342.2	19987.9	18036.2	2.43069	8148.95
Run 32	0.93839	23405.5	23680.2	23623.4473	15522.8	21428	19983.5	18049.7	2.43107	8157.42
Run 33	0.9424	23419.1	23671.2	23618.1934	15575.3	21510.1	19976.8	18019.2	2.43221	8095.83